



HAL
open science

Synthesis and valorisation of furan derivatives from biomass by selective oxidations

Nadim Ayoub

► **To cite this version:**

Nadim Ayoub. Synthesis and valorisation of furan derivatives from biomass by selective oxidations. Chemical and Process Engineering. Université de Technologie de Compiègne, 2022. English. NNT : 2022COMP2677 . tel-04503557

HAL Id: tel-04503557

<https://theses.hal.science/tel-04503557>

Submitted on 13 Mar 2024

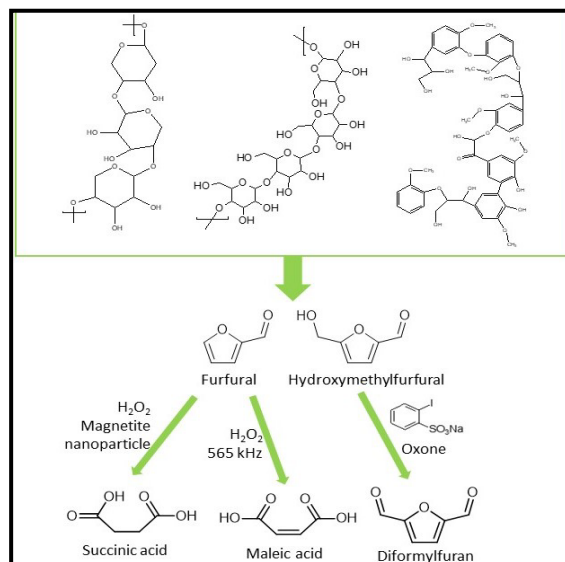
HAL is a multi-disciplinary open access archive for the deposit and dissemination of scientific research documents, whether they are published or not. The documents may come from teaching and research institutions in France or abroad, or from public or private research centers.

L'archive ouverte pluridisciplinaire **HAL**, est destinée au dépôt et à la diffusion de documents scientifiques de niveau recherche, publiés ou non, émanant des établissements d'enseignement et de recherche français ou étrangers, des laboratoires publics ou privés.

Par Nadim AYOUB

Synthèse et valorisation des dérivés furaniques issus de la biomasse par oxydations sélectives

Thèse présentée
pour l'obtention du grade
de Docteur de l'UTC



Soutenue le 4 mai 2022

Spécialité : Chimie et Génie des Procédés : Transformations intégrées de la matière renouvelable (EA-4297)

D2677

Ecole Doctorale Sciences pour l'Ingénieur ED71

**Thèse présentée pour l'obtention du grade de Docteur
de l'Université de Technologie de Compiègne**

Par Nadim AYOUB

*Synthèse et valorisation des dérivés
furaniques issus de la biomasse
par oxydations sélectives*

Spécialité : Chimie et Génie des Procédés

Soutenue le 4 mai 2022

Jury composé de :

Anne Wadouachi	Professeur, Université de Picardie Jules Verne	Rapporteur
Nicolas Brosse	Professeur, Université de Lorraine	Rapporteur
Arnaud Haudrechy	Professeur, Université de Reims Champagne-Ardenne	Examineur
Edvina Lamy	Maître de conférences, Université de Technologie de Compiègne	Examineur
Erwann Guénin	Professeur, Université de Technologie de Compiègne	Membre invité
Gérald Enderlin	Enseignant-chercheur, Ecole Supérieur de Chimie Organique et Minérale	Directeur de thèse
Joumana Toufaily	Professeur, Université Libanaise	Directeur de thèse

*Synthesis and valorization of furan derivatives
from biomass by selective oxidations*

By Nadim AYOUB

Defended on May 4, 2022

Acknowledgments

Acknowledgments

Nothing in the world is worth having or worth doing comes easy, unless it means effort, pain and troubles. It is thrilling to look back at my doctoral journey knowing that a chapter of my life has now come to an end. I would like to take the time to acknowledge all of those who were there for me during this phase of personal growth and to thank every single person who was, directly or indirectly, a part of it.

First, I would like to thank the entire jury for having accepted to judge and evaluate this work. Thank you Pr. Anne Wadouachi and Pr. Nicolas Brosse for accepting to review my work. Thank you as well Pr. Arnaud Haudrechy and Dr. Edvina Lamy for judging this work

I would like to thank my PhD supervisors Gérald Enderlin and Erwann Guénin for providing guidance, support, and encouragement throughout this project. Thanks for believing in me and trusting me. Their dedication and rigor taught me to strive for excellence in everything I do and this is indeed a life-lesson I will always embrace. I feel privileged to have worked with such leaders. Words fail to express my deepest esteem to them. I will always be grateful for everything they have done. I would like to thank Joumana Toufaily as well for her assistance and contribution despite the very hard circumstances in her country of residence.

I would also like to extend my appreciation to all the members of TIMR team and Isabelle Pezron, the head of department, for hosting and welcoming me during this period. The work environment is exciting, collaborative, and positive. I truly respect all of my colleagues, not only for their work ethics, but also for their passion toward science and life itself. I also take this opportunity to thank the technical team Hervé Leclerc, Bruno Dautzat and Michael Lefebvre for their help. The time I spent in TIMR would not have been as pleasant without the company of my colleagues and friends. Special thanks go to Cristina Belda Marin, Franco Otaola, Maiqi Xiang, Ayoub Hassine and Soufiane Bakri Alaoui with whom I shared the office, conversations and laughs. I equally thank Denis Luart, Yancie Gagnon and Christa Aoude.

I am not only indebted to colleagues at work but also to many friends outside my academic circle. Their tremendous support and encouragement were an essential source of motivation and strength. As such, I am tremendously thankful to my close friends who bore my stressful days and panic attacks each in his and her own way. On that account, my deepest gratitude goes to Marc Baydoun, Moustafa Hammoud, Georgina Abi Sejaan, Anna-Maria Abi-Khattar, Ranin Atwi, Jawaher Houmani, Yaacoub Jawad, Nicole Najjoun, Ali Hamdan, Hussein Hamadi, Georges Amine, Zouheir Moukaddem, Zeinab Rida and Jean-Noel Semaan.

Last but foremost; none of my achievements would have seen the light had it not been for the support of my family. A special appreciation goes to my father who has always placed my best interest above

his, sacrificing some of his dreams only to see me fulfill mine. My deep and sincere gratitude to my mother for the continuous and unconditional love and prayers that accompanied me throughout this journey. I cannot forget my grandmother who has always been such a special support and encouragement to me. My recognition extends to my sister Hadil and her dear husband Khalil for all the affection and especially to their children Jamil, Lamar and Julia who I love the most despite the long distance between us. I offer my heartiest recognition as well to my brother Wassim for his support and for always being there for me as a friend. This journey would not have been possible if not for them, and I dedicate this milestone to them.

List of abbreviations

List of abbreviations

5-HFO	5-Hydroxy-2-(5H)-Furanone
BAIB	[Bis(acetoxy)-iodo]benzene
BHC	Betaine Hydrochloride
BHT	Butylated hydroxytoluene
CMF	5-Chloromethylfurfural
CPO	Chloroperoxidase
DCE	Dichloroethane
DCM	Dichloromethane
DFP	2,5-Diformylfuran
DMSO	Dimethylsulfoxide
FA	Furoic acid
FDCA	2,5-furandicarboxylic acid
FDMC	Furan-2,5-dimethylcarboxylate
FFCA	5-Formyl-2-furancarboxylic acid
FO	2-(5H)-Furanone
FUR	Furfural
GO	Graphene oxide
HBO	γ -hydroxymethyl- α,β -butenolide
HFUS	High Frequency Ultrasound
HMF	5-hydroxymethylfurfural
HMFA	5-hydroxymethyl-2-furancarboxylic acid
HTFA	Trifluoroacetic acid
IBS	2-iodoxybenzenesulfonic acid
IBX	2-iodoxybenzoic acid
M2F	Methyl-2-furoate
MA	Maleic acid
MaIA	Malic acid
MAN	Maleic anhydride
mCPBA	meta-Chloroperoxybenzoic acid
MIBK	Methylisobutylketone
MNP	Magnetite nanoparticles
MTHF	Methyltetrahydrofuran
NHC	N-heterocyclic carbene

OGA	2-Oxoglutaric acid
PTSA	p-Toluenesulfonic <i>acid</i>
SA	Succinic acid
TBHP	tert-Butyl hydroperoxide
TEMPO	(2,2,6,6-Tetramethylpiperidin-1-yl)oxyl
THF	Tetrahydrofuran

Table of content

<i>Acknowledgments</i>	3
<i>List of abbreviations</i>	7
<i>General introduction</i>	21
<i>Chapter 1 – Biomass Composition and valorization</i>	27
1. Introduction.....	29
2. Composition of lignocellulosic biomass	30
2.1. Cellulose	30
2.2. Hemicellulose	31
2.3. Lignin	32
3. Biomass valorization.....	33
3.1. Furfural	34
3.1.1. Furfural synthesis from xylose.....	36
3.1.2. Furfural synthesis from xylan	37
3.1.3. Furfural synthesis from lignocellulosic biomass.....	37
3.2. Hydroxymethylfurfural	39
3.2.1. Synthesis of Hydroxymethylfurfural from fructose.....	41
3.2.2. Synthesis of Hydroxymethylfurfural from glucose.....	42
<i>Chapter 2 – Oxidation methods of furanic derivatives</i>	51
1. Introduction.....	53
2. Metal catalysts for the oxidation of furan derivatives	55
2.1. Metal catalysts for the oxidation of HMF.....	55
2.2. Metal catalysts for the oxidation of furfural	61
3. Metal-free catalysts for the oxidation of furan derivatives	68
3.1. Metal-free catalysts for the oxidation of HMF	69
3.1.1. Acid catalysis	70
3.1.2. Carbon based catalyst	75
3.1.3. Organic catalysts.....	79
3.2. Metal-free catalysts for the oxidation of furfural	80
3.2.1. Acid catalysis	80
3.2.2. Basic catalysis	86
3.2.3. Oxidative amidation	87
3.2.4. Photochemical oxidation of furfural	88
4. Conclusion	89

<i>Chapter 3 – Metal-free catalyst for the selective oxidation of hydroxymethylfurfural into 2,5-diformylfuran</i>	107
1. Introduction.....	109
2. Experimental section.....	111
2.1. Materials, solvents and reagents	111
2.2. Instruments and analytical methods.....	111
2.2.1. Gas Chromatography.....	111
2.3. Catalyst synthesis and characterization	111
2.4. Catalytic experiments.....	112
2.5. Catalyst recovery	112
2.6. Gram-scale reaction procedure.....	112
2.7. Products analysis	113
3. Results and discussion.....	113
3.1. Preliminary tests.....	113
3.2. Solvent screening	114
3.3. Effect of reaction temperature	117
3.4. Effect of reaction time.....	118
3.5. Effect of the catalyst weight.....	120
3.6. Effect of Oxone® and HMF amounts	122
3.7. Catalyst recyclability.....	124
3.8. Gram-scale synthesis of DFF.....	125
4. Conclusion	125
<i>Chapter 4 – Catalyst-free oxidation of furfural into maleic acid under high frequency ultra-sound irradiations</i>	131
1. Introduction.....	133
2. Sonochemistry.....	135
3. Experimental part.....	137
3.1. Materials, solvents and reagents	137
3.2. Instruments and analytical methods.....	137
3.2.1. Gas Chromatography.....	137
3.2.2. High performance liquid chromatography.....	137
3.2.3. Evaporative Light Scattering Detector.....	138
3.2.4. NextGen Lab 1000 reactor	138
3.3. Oxidation reactions	139
3.4. Product analysis.....	140
3.5. Synthesis of 5-hydroxy-2(5H)-furanone	141

4.	Results and discussion.....	142
4.1.	Effect of frequency	142
4.2.	Effect of power	145
4.3.	Effect of reaction time.....	146
4.4.	Effect of oxygen as oxidant	147
4.5.	Effect of H ₂ O ₂ /FUR mol ratio	148
4.6.	Reaction mechanism	149
4.7.	Energy consumption.....	153
5.	Conclusion	156
	<i>Chapter 5 – Furfural oxidation using magnetic and abundant catalyst from iron oxide.....</i>	<i>163</i>
1.	Introduction.....	165
1.1.	Iron oxides	165
1.2.	Magnetite nanoparticles	167
2.	Experimental part.....	167
2.1.	Materials, solvents and reagents	167
2.2.	Instruments and analytical methods.....	167
2.2.1.	Gas Chromatography.....	167
2.2.2.	High performance liquid chromatography.....	168
2.2.3.	Transmission Electron Microscope (TEM)	168
2.2.4.	X-Ray Diffraction (XRD).....	168
2.2.5.	Ultraviolet-Visible Spectroscopy (UV)	169
2.3.	Magnetite nanoparticle synthesis.....	169
2.4.	Magnetite nanoparticle concentration	169
2.5.	Catalytic experiments.....	170
2.6.	Product analysis.....	170
3.	Results and discussions	171
3.1.	Magnetite nanoparticles	171
3.2.	Preliminary tests.....	173
3.3.	Effect of reaction time.....	173
3.4.	Effect of reaction temperature	176
3.5.	The effect of the catalyst weight.....	178
3.6.	Catalyst recyclability.....	178
3.7.	Magnetite nanoparticles Vs. Iron oxide	179
3.8.	Application of ultrasound irradiations	182
3.9.	Reaction mechanism	183
4.	Conclusion	184

<i>General conclusion and perspectives</i>	189
<i>Accomplishments</i>	197
<i>Annexes</i>	201

List of figures

Figure 1.1 - Classical representation of the structure of lignocellulosic biomass [4].....	30
Figure 1.2 – Cellobiose structure.....	31
Figure 1.3 - Galactomannan structure	31
Figure 1.4 - Primary structure of a β -(1→3)-D-xylan type X3 and b β -(1→3, 1→4)-D-xylan type Xm ..	32
Figure 1.5 - Lignin monomers.....	32
Figure 1.6 - Main approaches for lignocellulosic biomass conversion.....	34
Figure 1.7 - Biofuels and chemicals from furfural [86].....	35
Figure 1.8 - The two ways of biomass valorization	38
Figure 1.9 - 5-HMF as a platform chemical [86]	40
Figure 1.10 - Glucose isomerization mechanism [74]	42
Figure 2.1 - Summary of furfural, HMF, LGO derived chemicals.....	54
Figure 2. 2 - Main products obtained by oxidation of HMF by metallic catalysis	56
Figure 2.3 - Structures of common products after oxidation of furfural.	62
Figure 2. 4 - Furfural oxidation to afford dicarboxylic acids and acid anhydrides	62
Figure 2.5 - Some examples of structure of TEMPO and TEMPO derivatives.	72
Figure 2.6 - Structural model of graphene oxide (GO) on the basis of proposed structure of ref [153].	76
Figure 2.7 - Schematic representation of HMF oxidation over polymeric carbon nitride (g-C ₃ N ₄) catalyst in presence of oxygen. [164] And the solar pilot plant for continuous flow oxidation. [166]	78
Figure 2.8 - Furfural evolution with time by autoxidation	81
Figure 2. 9 - Recapitulation of furfural oxidation in biphasic systems	83
Figure 2.10 - Betaine Hydrochloride (BHC) structure.....	84
Figure 3.1 - Effect of solvent on HMF conversion, selectivity and yield of DFF. 1.6 mmol of HMF, 1.17 g Oxone® (KHSO ₅ /HMF mol ratio=1.2), 30 mg of catalyst (0.36 wt%), 70°C, 4h.....	117
Figure 3.2 - Effect of temperature on HMF conversion, selectivity and yield of DFF. 1.6 mmol of HMF, 1.17 g Oxone® (KHSO ₅ /HMF mol ratio=1.2), 30 mg of catalyst (0.36 wt%), 6 ml nitromethane, 4h. .	118
Figure 3.3 - Effect of reaction time on DFF yield and selectivity, and the HMF conversion at T=70 °C	118
Figure 3.4 - Effect of reaction time on DFF yield and selectivity, and the HMF conversion at T=80 °C	119
Figure 3.5 - Effect of reaction time on DFF yield and selectivity, and the HMF conversion at T=90 °C	119
Figure 3.6 - Effect of temperature as a function of time on the conversion of HMF at 70°C and the yield of DFF at 70 °C, 80 °C and 90 °C. HMF 1.6 mmol, Oxone® 1.17g (KHSO ₅ /HMF mol ratio=1.2), catalyst 30mg (0.098mmol, 0.36 wt%), 6 ml nitromethane.	120
Figure 3.7 - Effect of the catalyst weight sodium 2-iodobenzenesulfonate (wt%) on HMF conversion and DFF selectivity. HMF 1.6 mmol, Oxone® 1.17g, sodium 2-iodobenzenesulfonate 0 to 1.44 wt%, 6 ml nitromethane, 70 °C, 4h.	121
Figure 3.8 - Effect of the amount of catalyst on DFF yield as a function of time. HMF 1.6 mmol, Oxone® 1.17g, sodium 2-iodobenzenesulfonate 0.36wt% (red) and 0.73wt% (green), 6 ml of nitromethane, 70°C.	122

Figure 3.9 - Effect of the amount HMF on DFF yield and HMF conversion. Oxone® 1.17g, sodium 2-iodobenzenesulfonate 0.36wt%, 6 ml of nitromethane, 70°C.....	123
Figure 3.10 - Effect of the amount of HMF (from 100 mg to 400 mg) on the yield of DFF with various oxone® to HMF ratio and catalyst to HMF ratio, 6 ml of nitromethane, 70°C, 4 h. (□): Oxone®/HMF ratio= 2.4 (100 mg of HMF), 1.2 (200 mg of HMF), 0.8 (300 mg of HMF) and 0.6 (400 mg of HMF), (Δ): catalyst/HMF ratio = 0.12 (100 mg of HMF), 0.06 (200 mg of HMF), 0.04 (300 mg of HMF) and 0.03 (400 mg of HMF).....	124
Figure 4.1 - Cavitation bubble in a homogeneous medium	136
Figure 4.2 - NextGen Lab 1000 reactor	138
Figure 4.3 - Installation Synoptic.....	139
Figure 4.4 - The experimental setup	140
Figure 4.5 - The experimental setup for the synthesis of hydroxyfuranone.....	141
Figure 4.6 - Effect of the frequency (kHz); Furfural 10 mL (0.12 mol); H ₂ O ₂ 40 mL (0.46 mol), 2 h, 42 °C, 80 W, after boiling	143
Figure 4.7 - Effect of the frequency (kHz); Furfural 10 mL (0.12 mol); H ₂ O ₂ 40 mL (0.46 mol), 2 h, 42 °C, 80 W.....	144
Figure 4.8 - Conversion and yields before and after boiling; Furfural 10 mL (0.12 mol); H ₂ O ₂ 40 mL (1.7 mol), 2 h, 42 °C, 80 W, after boiling.	145
Figure 4.9 - Effect of power variation; Furfural 10 mL (0.12 mol), H ₂ O ₂ 40 mL (0.46 mol), 42 °C, 565 kHz, 2 h, after boiling.....	146
Figure 4.10 - kinetic profile of the reaction; FUR 10 mL (0.12 mol), H ₂ O ₂ 40 mL (0.46 mol), 42 °C, 565 kHz, 80 W.....	147
Figure 4.11 - kinetic profile of the reaction; Furfural 10 mL (0.12 mol), H ₂ O ₂ 40 mL (0.46 mol), 42 °C, 565 kHz, 80 W.....	149
Figure 4.12 - Representation of an oil bath and a heating plate.....	154
Figure 4.13 - Oil bath	155
Figure 4.14 – Power consumed by the plate in function of time	155
Figure 5.1 - TEM images for the three different samples of magnetite nanoparticles.....	171
Figure 5.2 - Diameter distribution of the three different samples of magnetite nanoparticles.....	172
Figure 5.3 - Nanoparticle size using XRD technique.....	172
Figure 5.4 – Products of furfural oxidation; 0.04 mol of furfural, 0.3 mol (20.4 mL) of H ₂ O ₂ , 5.4 mL of H ₂ O, 80 μmol (0.615 mL) of magnetite nanoparticles, 40 °C, 12 h.	173
Figure 5.5 - Effect of time on furfural conversion and products' yields; 0.04 mol of furfural, 0.3 mol (20.4 mL) of H ₂ O ₂ , 5.4 mL of H ₂ O, 80 μmol (0.615 mL) of magnetite nanoparticles, 40 °C.	175
Figure 5.6 - Effect of time on furfural conversion and products' yields; 0.04 mol of furfural, 0.3 mol (20.4 mL) of H ₂ O ₂ , 5.4 mL of H ₂ O, 80 μmol (0.615 mL) of magnetite nanoparticles, 50 °C.	175
Figure 5.7 - Effect of temperature on furfural conversion and succinic acid yield; 0.04 mol of furfural, 0.3 mol (20.4 mL) of H ₂ O ₂ , 5.4 mL of H ₂ O, 80 μmol (0.615 mL) of magnetite nanoparticles, 24 h.....	177
Figure 5.8 - Yields of the obtained by-products; 0.04 mol of furfural, 0.3 mol (20.4 mL) of H ₂ O ₂ , 5.4 mL of H ₂ O, 80 μmol (0.615 mL) of magnetite nanoparticles, 24 h.	177
Figure 5.9 - Effect of the catalyst weight on furfural conversion and succinic acid yield; 0.04 mol of furfural, 0.3 mol (20.4 mL) of H ₂ O ₂ , 5.4 mL of H ₂ O, 40°C, 24 h.	178

Figure 5.10 - Reusability of MNP catalyst in the oxidation of furfural into succinic acid ; 0.04 mol of furfural, 0.3 mol (20.4 mL) of H ₂ O ₂ , 5.4 mL of H ₂ O, 80 μmol (0.615 mL) of magnetite nanoparticles, 40 °C, 24 h.	179
Figure 5.11 - Effect of temperature on furfural conversion and succinic acid yield; 0.04 mol of furfural, 0.3 mol (20.4 mL) of H ₂ O ₂ , 5.4 mL of H ₂ O, 18.5 mg of iron oxide, 24 h.	181
Figure 5.12 - Yields of the obtained by-products; 0.04 mol of furfural, 0.3 mol (20.4 mL) of H ₂ O ₂ , 5.4 mL of H ₂ O, 18.5 mg of iron oxide, 24 h.	181
Figure 5.13 - Effect of time on furfural conversion and products' yields; 0.04 mol of furfural, 0.3 mol (20.4 mL) of H ₂ O ₂ , 5.4 mL of H ₂ O, 18.5 mg of iron oxide, 50 °C.	182
Figure 5.14 - Effect of US irradiations on the yields of different products; 2 h, 40 °C.	183
Figure A.1 - 1H spectrum of DFF after filtration and evaporation	203
Figure A.2 - 13C spectrum of DFF after filtration and evaporation.....	203
Figure A.3 -1H spectrum of over-oxidation of HMF	204
Figure A.4 - 13C spectrum of over-oxidation of HMF	204
Figure A.5 - 1H spectrum of IBS catalyst	205
Figure A.6 - 13C spectrum of IBS catalyst.....	205
Figure A.7 - 1H spectrum of the gram scale of HMF oxidation	206
Figure A.8 - 13C spectrum of the gram scale of HMF oxidation	206
Figure A.9 - Chromatogram of DFF after filtration and evaporation	207
Figure A.10 - chromatogram of HMF oxidation without catalyst	207
Figure A.11 - chromatogram of HMF oxidation without solvent	208
Figure A.12 - 1H spectrum; Furfural 10 mL (0.12 mol), H ₂ O ₂ 40 mL (1.7 mol), 42 °C, 2 h, 565 kHz, 80 W	209
Figure A.13 - 13C spectrum; Furfural 10 mL (0.12 mol), H ₂ O ₂ 40 mL (1.7 mol), 42 °C, 2 h, 565 kHz, 80 W	210
Figure A.14 - HPLC chromatogram; Furfural 10 mL (0.12 mol), H ₂ O ₂ 40 mL (1.7 mol), 42 °C, 2 h, 565 kHz, 80 W.....	210
Figure A.15 - HPLC chromatogram before (a) and after (b) boiling at 565 kHz, Furfural 10 mL (0.12 mol); H ₂ O ₂ 40 mL (1.7 mol), 2 h, 42 °C, 80 W.....	211
Figure A.16 - GC chromatogram before (a) and after (b) boiling at 565 kHz, Furfural 10 mL (0.12 mol); H ₂ O ₂ 40 mL (1.7 mol), 2 h, 42 °C, 80 W.	212
Figure A.17 - The used reactor with thermal shell.....	215
Figure A.18 - The synthesis process	215
Figure A.19 - The magnetic separator	216

List of tables

Table 1.1 - Furfural synthesis from xylose.....	37
Table 1.2 - Furfural synthesis from lignocellulosic biomass.....	38
Table 1.3 - Synthesis of HMF from fructose.....	41
Table 1.4 - Glucose isomerization into fructose.....	43
Table 1.5 - HMF synthesis from glucose.....	44
Table 2.1 - Some examples of HMF oxidation using metallic catalysts.....	60
Table 2. 2 - Furfural oxidation using metallic catalysts.....	68
Table 2.3 - HMF oxidation using acid catalysts.....	74
Table 2.4 - HMF oxidation methods using carbon-based catalysts.....	78
Table 2.5 - HMF oxidation methods using organic catalysts.....	80
Table 2.6 - Furfural oxidation using acid catalysis.....	85
Table 2.7 - Furfural oxidation using basic catalysis.....	88
Table 3.1 - Comparison of the effectiveness of IBX and IBS formed in situ for the selective oxidation of HMF to DFF.....	114
Table 3.2 - Catalytic oxidation of HMF into DFF using different solvents. ^a	115
Table 4.1 - Different methods of MA production highlighting the concentration of FUR.....	134
Table 4.2 - Energy consumption to produce 1 g of MA from furfural.....	156
Table A.1 - Molar relations for the different reagents.....	213
Table A. 2 - Weights and volumes of reagents fixing FeCl ₂ ·4H ₂ O to 1.5 g.....	214

List of schemes

Scheme 2.1 - The two-oxidation route of HMF to FDCA.....	58
Scheme 2.2 - Avantium's Process to polyethylene furandioate via 5-methoxymethylfurfural [20].....	59
Scheme 2.3 - General representation of oxidative esterification of furfural in presence of gold nanoparticles catalyst.....	63
Scheme 2.4 - Schematic representation of oxidation of HMF to DFF with TEMPO	75
Scheme 2.5 - Furfural autoxidation in presence of air.	81
Scheme 3.1 - Hypervalent Iodine derivatives used to oxidize selectively primary alcohols to aldehydes.	110
Scheme 3.2 - One step preparation of hypervalent iodine compounds from 2-iodobenzoic acid or 2-iodosulfonic acid and Oxone [®] , leading to highly selective oxidant species of primary alcohol, IBX and IBS.....	110
Scheme 3.3 - Different iodine derivatives and supposed catalytic cycle during the selective oxidation of HMF to DFF [43]	116
Scheme 3.4 - Synthesis of DFF by selective oxidation of HMF in gram scale.....	125
Scheme 4.1 - Examples of radical formation under HFUS.....	150
Scheme 4.2 - Proposal for the first step of oxidation of furfural under HFUS.	151
Scheme 4.3 - Structures of potential intermediates leading to 5-Hydroxyfuranone.....	151
Scheme 4.4 - Structures of potential intermediates leading to 2-(5H)-Furanone.	151
Scheme 4.5 - Proposal reaction pathway leading to maleic acid from 5-hydroxyfuranone and 2-(5H)-Furanone via non-radical mechanism.	152
Scheme 4.6 - Proposal pathway leading to Succinic acid.....	152
Scheme 5.1 – Mechanistic aspect for Fenton reaction [28].....	166
Scheme 5.2 - Proposal for the first step of oxidation of furfural and the structures of potential intermediates leading to 2-(5H)-Furanone	184
Scheme 5.3 - Proposal reaction pathway leading to succinic acid from 2-(5H)-Furanone via non-radical mechanism.....	184

General introduction

In the past century, fossil resources, petroleum, natural gas, and coal, have been the main source for the production of transportation fuels and chemicals and have played an important role in accelerating economic growth as well.[1] In 2016, about 85.5% of the energy consumed worldwide came from fossil resources. However, these resources are exhaustible, and the associated release of CO₂ in the atmosphere has been the source of climate change and global warming.[2,3]

Biomass is one of the renewable and green resources that can sustainably meet our needs for the production of fuels, chemicals and materials. An average of 1466 Mt of total terrestrial biomass (dry matter) was produced annually from 2006 to 2015 and 1.5 Mt (dry weight) from fisheries and aquaculture in the European Union (EU). [4,5] Lignocellulosic biomass refers typically to plant-based biomass (such as corn stover, straw, forestry and agricultural residues) and it is the most abundant (after atmospheric CO₂) and inexpensive carbon source. Thus, it has been found to be a valuable commodity due to its scalability, economic viability and its potential carbon neutrality. These convenient aspects converge in the production of renewable biofuels and value-added products via appropriate technologies. These plant biomass resources are diverse, and only a small part of these raw materials is efficiently used. Hence, there exists a need to establish innovative, ecofriendly processes and cost-effective perspectives to benefit from these resources.[6]

For these reasons, nonedible biomass such as lignocellulose has attracted attention of researchers and scientists in the last decades as a renewable alternative. It is an abundant, sustainable, renewable, and a cost-efficient source of organic chemicals and liquid biofuels.

Furfural, the first bio-sourced derivative that have been produced industrially, is derived from the dehydration of pentoses, such as xylose, treated in acidic medium under heating. Historically, the industrial synthesis of furfural from pentoses in the presence of dilute sulfuric acid began with the Quaker Oats company for the recovery of waste from the grain industry.[7,8] Since then, the industrial synthesis of furfural has been extensively modified and exploited, and new processes have emerged such as Suprayield, Vedernikovs and Huaxia/WestPro processes. [9,10] The global furfural market held a market value of USD 457.4 Million in 2022 and is projected to reach USD 840.7 Million by the year 2030. The market is anticipated to grow at a compound annual growth rate (CAGR) of 8.7% from 2022 to 2030. Around 390.31 kilo tons of furfural was sold in 2022. [11]

On the other hand, HMF is produced by dehydration from the transformation of hexoses, such as fructose and glucose, contained in cellulose and starch. One of the major limitations of HMF synthesis is related to its polarity and the need of D-Fructose, which is the best starting materials. The global 5-Hydroxymethylfurfural market is valued at 55,8 Million USD in 2018 and is expected to reach 62,7 Million USD by the end of 2025, growing at a CAGR of 1.45% between 2018 and 2025. [12]

The traditional valorization processes of these bio-sourced molecules used metal catalysis, usually with noble metals to obtain good conversion, yields and selectivity. Though catalysis is one of the pillars of green chemistry, the use of expensive, toxic and critical metals is often detrimental to this appellation. Therefore, recently, cheap and nontoxic metals and metal-free catalysis have attracted the attention of scientists and researchers and such catalyst can be considered as green catalytic materials, because they can be highly efficient, easy to handle, environmentally friendly and economical in various industrial sectors. This dynamic was motivated by the desire to overcome the disadvantages of metallic catalysis and by the interests that can be gained from their substitution.

Previous studies have already been conducted on the development of more eco-friendly catalytic oxidation of furanic derivatives within the Integrated Transformations of Renewable Matter (TIMR) laboratory a joint research laboratory of the Université de Technologie de Compiègne (UTC) and the Ecole Supérieure de Chimie Organique et Minérale (ESCOM). Therefore, in the frame of the chair for “Green Chemistry and Processes” (financed by UTC/ESCOM/Région Hauts de France and FEDER) this work was continued and this PhD project has been settled over these preliminary studies in collaboration with laboratory of Materials, Catalysis, Environment and Analytical Methods (MCEMA) at the Lebanese University, financed by both Région Hauts-de-France and Lebanon.

This project proposes to develop new methods for the oxidation of the platform molecules furfural and HMF by proposing whether the use of metal free catalysis, new activation technologies or using nontoxic and non-critical metal catalysts. We focused in this project on the methodological development and the optimization of operating conditions.

This manuscript is divided in five chapters. Chapter 1 introduces the composition of the lignocellulosic biomass and some examples of the synthesis of furfural from xylose, xylan and of HMF from fructose and glucose.

In chapter 2, we propose to review the state of art of the traditional catalytic methods for the oxidation of the two platform molecules furfural and HMF. The literature is divided in two main parts: metal catalysis and metal-free (acid, basic, carbon based, organic, photochemical ...) catalysis for the oxidation of these molecules into value-added products.

In chapter 3, an alternative system for HMF oxidation is studied in attempt to avoid the use of expensive and toxic metal catalysts. The selective oxidation of the hydroxyl group on the HMF molecule leading to the corresponding aldehyde, 2,5-diformylfuran (DFF), was catalyzed by 2-iodobenzenesulfonic acid in the presence of Oxone®. An optimization of the catalytic system and scale up of the process are presented as well.

In chapter 4, we demonstrate a catalyst-free process for the gram-scale synthesis of maleic acid from furfural using high frequency ultrasound irradiations. Selectivity towards maleic acid and furfural conversion are studied under mild conditions using only H₂O₂ as an oxidant.

In chapter 5, a novel metallic-catalyst process is developed using magnetite nanoparticles (MNP) under mild conditions for the synthesis of succinic acid from furfural. Selectivity towards another bio-sourced diacid: succinic acid is described and recyclability is evaluated.

In the last part, a general conclusion will provide the summary of the results from the developed oxidation methods of furfural and HMF, and their advantages. Finally, several perspectives of this work are presented.

1. Serrano-Ruiz, J.C., West, R.M., and Dumesic, J.A. (2010) Catalytic conversion of renewable biomass resources to fuels and chemicals. *Annu. Rev. Chem. Biomol. Eng.*, **1**, 79–100.
2. Ravishankara, A.R., Rudich, Y., and Pyle, J.A. (2015) Role of Chemistry in Earth's Climate. *Chem. Rev.*, **115** (10), 3679–3681.
3. Huber, G.W., Iborra, S., and Corma, A. (2006) Synthesis of transportation fuels from biomass: Chemistry, catalysts, and engineering. *Chem. Rev.*, **106** (9), 4044–4098.
4. Klaas, M.R.G., and Schöne, H. (2009) Direct, high-yield conversions of cellulose into biofuel and platform chemicals - On the way to a sustainable biobased economy. *ChemSusChem*, **2** (2), 127–128.
5. CAMIA A., G.J.. J.R.. R.N.. C.N.E.. J.G.. A.V.. G.G.. B.J.I.. M.S. (2021) *The use of Woody biomass for energy purposes in the EU*.
6. Liu, C., Wang, H., Karim, A.M., Sun, J., and Wang, Y. (2014) Catalytic fast pyrolysis of lignocellulosic biomass. *Chem. Soc. Rev.*, **43** (22), 7594–7623.
7. Brownlee, H.J., and Miner, C.S. (1948) Industrial Development of Furfural. *Ind. Eng. Chem.*, **40** (2), 201–204.
8. Binder, J.B., Blank, J.J., Cefali, A. V., and Raines, R.T. (2010) Synthesis of furfural from xylose and xylan. *ChemSusChem*, **3** (11), 1268–1272.
9. Eseyin, A.E., and Steele, P.H. (2015) An overview of the applications of furfural and its derivatives. *Int. J. Adv. Chem.*, **3** (2), 42.
10. De Jong, W., and Marcotullio, G. (2010) Overview of biorefineries based on co-production of furfural, existing concepts and novel developments. *Int. J. Chem. React. Eng.*, **8**.
11. Report Ocean (2022) global furfural market, by raw material (sugarcane bagasse, corncob, rice husk, sunflower hull, others), by application (solvent, fungicides, others), by end user (paints & coatings, petroleum refineries, others), estimation & forecast, 2017 2027.
12. Business Growth Reports (2021) 2022-2029 Global 5-hydroxymethylfurfural (5-HMF) (CAS 67-47-0) Professional Market Research Report, Analysis from Perspective of Segmentation (Competitor Landscape, Type, Application, and Geography).

Chapter 1
Biomass Composition and valorization

1. Introduction

Lignocellulosic biomass is a plentiful and renewable resource for fuels and chemicals. Despite this potential, nearly all renewable fuels and chemicals are now produced from edible resources, such as starch, sugars, and oils; the challenges imposed by notoriously recalcitrant and heterogeneous lignocellulosic feedstock have made their production from nonfood biomass inefficient and uneconomical.

Lignocellulosic biomass provides access to furan derivatives such as 5-hydroxymethylfurfural (HMF) and furfural. HMF and furfural are considered as “building blocks”, so they can be used to obtain many derivatives. The industrial production of furfural is already well mastered and its derivative, furfuryl alcohol, is widely exploited. [1,2]

Hydrogenated and deoxygenated derivatives such as methyltetrahydrofuran (MTHF) are used both as solvents and as additives for fuels. 5-hydroxymethylfurfural, for its part, is not currently produced on an industrial scale. Due to poor stability in acidic media and high solubility in water, HMF is very difficult to purify and maintain for long periods. To solve this problem, HMF can be oxidized to provide added-value products such as 2,5-diformylfuran (DFF) or 2,5-furandicarboxylic acid (FDCA). These compounds can be used for the synthesis of fuels and novel polymers capable of substituting for terephthalic acid derivatives.

After presenting the composition of the lignocellulosic biomass, we will expose different synthesis of furfural and HMF. Finally, we will present some examples of valorization of these compounds in fuels and polymers.

2. Composition of lignocellulosic biomass

The term biomass includes many compounds and its definition varies according to the authors and the context of the study. In order to clearly define its use, the European Parliament has given a well-defined definition: “biomass is the biodegradable fraction of products, waste and residues of biological origin from agriculture (including plant and animal substances), forestry and related industries, including fisheries and aquaculture, as well as the biodegradable fraction of industrial and municipal waste”. [3] For the sake of clarity and in the rest of the manuscript, the use of the term biomass will refer only to lignocellulosic biomass.

This biomass is composed mainly of three biopolymers (Figure 1.1): cellulose (glucose), lignin (aromatic compounds) and hemicellulose (pentose and hexose). The distribution of these compounds varies greatly depending on the botanical origin and the culture conditions. Despite this great variation of composition from one source to another, a distribution of about 70% of saccharide compounds (cellulose and hemicellulose) and 25% of lignin will generally be retained. In addition to the carbon compounds, sulfur compounds, proteins and ashes will be found.

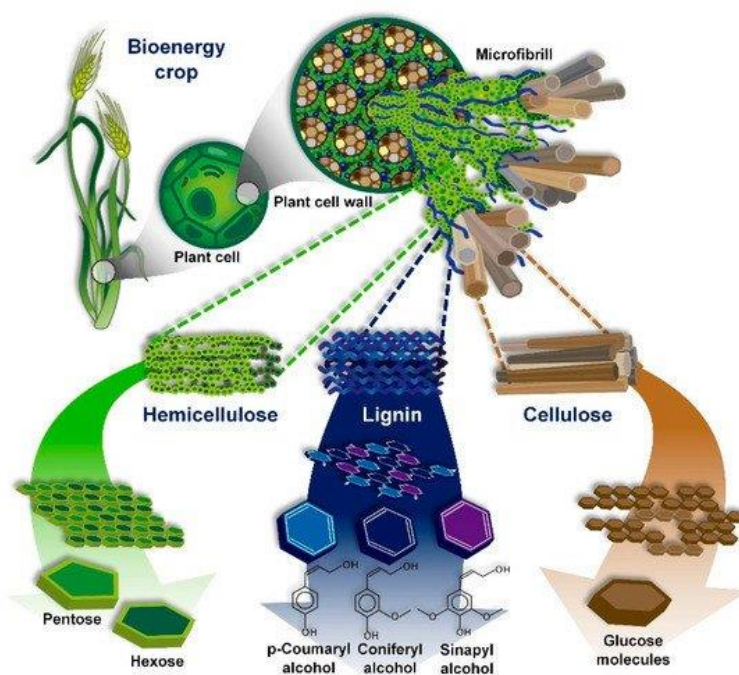


Figure 1.1 - Classical representation of the structure of lignocellulosic biomass [4]

2.1. Cellulose

Cellulose is a polymeric carbohydrate material and is the basic structural component of the cell walls of trees and other higher plants. It is the most abundant natural polymer in nature. It is estimated that

a tree can produce up to 10 g of it per day, which is equivalent to 1.3×10^{10} tons per year worldwide. [5,6]

Cellulose is composed of a sequence of glucopyranose units linked by β -1,4-glycosidic linkages [7]. In this polymer, the repeating unit is cellobiose, a glucose dimer often used as a model substrate for cellulose transformation (Figure 1.2).

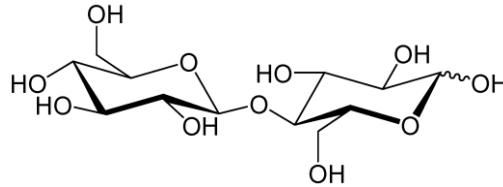


Figure 1.2 – Cellobiose structure

It serves as a chemical feedstock for several commercially important polymer industries. One of the more important of these industries is based on esterification of cellulose with a short-chain aliphatic acid: acetic, propionic, or n-butyric. The resulting thermoplastic cellulose esters are characterized by exceptional clarity and good mechanical performance. They are found in a various products, some of which are photographic films, fibers, cigarette filters, membranes, and molded articles. Historically, cellulose esters are the oldest manufactured thermoplastics, going back to the 1920's. Being plant-derived, cellulose is a renewable resource.

2.2. Hemicellulose

Hemicellulose is a mixed polymer composed of at least five different sugars with an additional large number of acetyl groups. In contrast to cellulose which is composed of 6-membered sugars, hemicellulose is mainly composed of xylan, a polymer of D-xylose. [8,9] Because of the great complexity of hemicelluloses, a general structure will not be proposed. Xylan-type polysaccharides are the main hemicellulose components of secondary cell walls constituting about 20–30% of the biomass of dicotyl plants For instance, a possible xylan-type and galactomannan hemicellulose structures are described respectively in Figure 1.3 and Figure 1.4 below. [8]

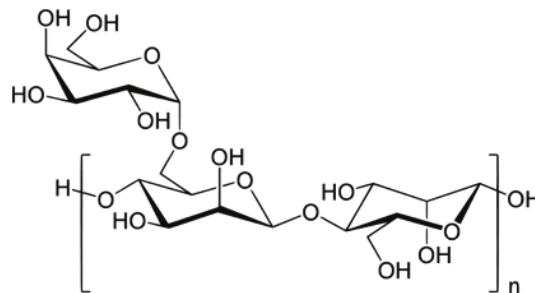


Figure 1.3 - Galactomannan structure

Hemicelluloses, the second most common polysaccharides in nature, represent about 20–35% of lignocellulosic biomass. In recent years, bioconversion of hemicellulose has received much attention because of its practical applications in various agro-industrial processes, such as efficient conversion of hemicellulosic biomass to fuels and chemicals, delignification of paper pulp, digestibility enhancement of animal feedstock, clarification of juices, and improvement in the consistency of beer. [10,11]

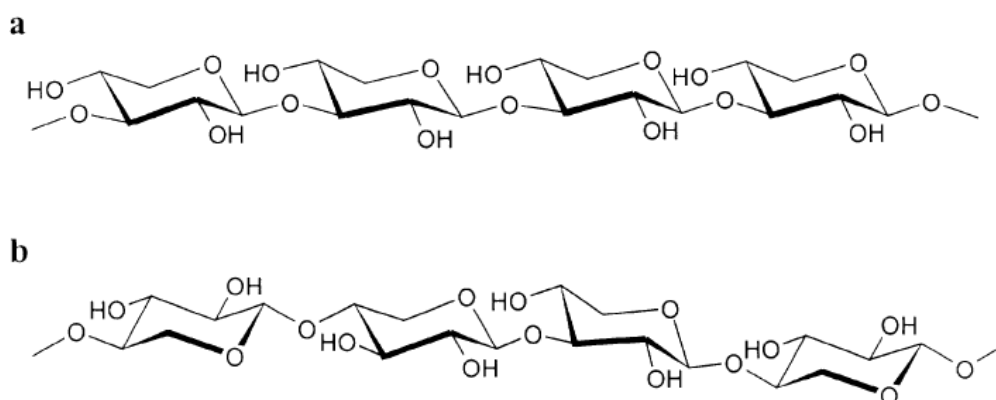


Figure 1.4 - Primary structure of a β -(1 \rightarrow 3)-D-xylan type X3 and b β -(1 \rightarrow 3, 1 \rightarrow 4)-D-xylan type Xm

2.3. Lignin

To conclude on the constituents of biomass, the last fraction is lignin. In contrast to the other two, it does not consist of sugars but aromatic monomers, including *para*-coumaryl alcohol, sinapyl alcohol and coniferyl alcohol (Figure 1.5). [12]

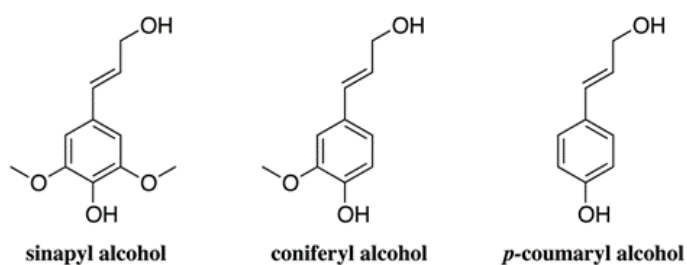


Figure 1.5 - Lignin monomers

It is immediately noticed that the polymerization of these species can lead to a great final complexity, which explains the difficulty to propose a generic structure.

As part of this work, lignin will not be considered and its valuations will not be detailed. However, it can be noted that the depolymerization of lignin is a highly researched field of research for the formation of aromatic compounds. [11,13–18]

3. Biomass valorization

Researchers and scientists have developed many biomass valorization methods since the dawn of time. Historically, the first uses of biomass are the production of energy (heating, cooking ...) and the manufacture of alcoholic beverages. Even if our societies are massively turned towards fossil resources, we cannot deny that these resources has led us to our current way of life, mainly through the development of agriculture. Currently, the valorization of biomass refers almost exclusively to transformations after the industrial revolution, such as energy production using coal and thermal power plants. Ancestral uses, such as the manufacture of furniture, fabrics and various utensils, are increasingly competing with metals and polymeric materials (PET, polyamides ...) from petrochemicals.

Today, the valorization of lignocellulosic biomass is turning away from the most obvious direct applications in order to reduce the share of chemicals derived from fossil resources. These new applications are particularly interesting since they provide access, among others, to furan derivatives, which find their utility in many areas such as biofuels [19,20] or fine chemistry [21,22].

The main approaches for converting of lignocellulosic biomass into platform molecules are gasification, pyrolysis, and hydrolysis, as summarized in Figure 1.6. [23–25] Hence, lignocellulosic biomass can be converted to bio-oil by pyrolysis and syngas by gasification. Biomass gasification means incomplete combustion of biomass resulting in production of combustible gases consisting of carbon monoxide (CO), hydrogen (H₂) and traces of methane (CH₄). [26] Biomass pyrolysis is generally defined as the thermal decomposition of the biomass organic matrix in non-oxidising atmospheres resulting in liquid bio-oil, solid biochar, and non-condensable gas products.[27] However, acid-catalyzed hydrolysis is always a more complicated process than gasification and pyrolysis. This chemical transformation consists of two steps, the first one is cracking the long carbon chains of lignocellulose into a series of C5–C6 carbohydrates, [23,28,29] and those products can be further reformed by dehydration, to form principally platform molecules such as furfural and 5-hydroxymethylfurfural (HMF). [30] In addition, further catalytic transformations of these functionalized platform compounds lead to the production of a wide range of chemicals and fuels, which are widely used in numerous fields and industries.

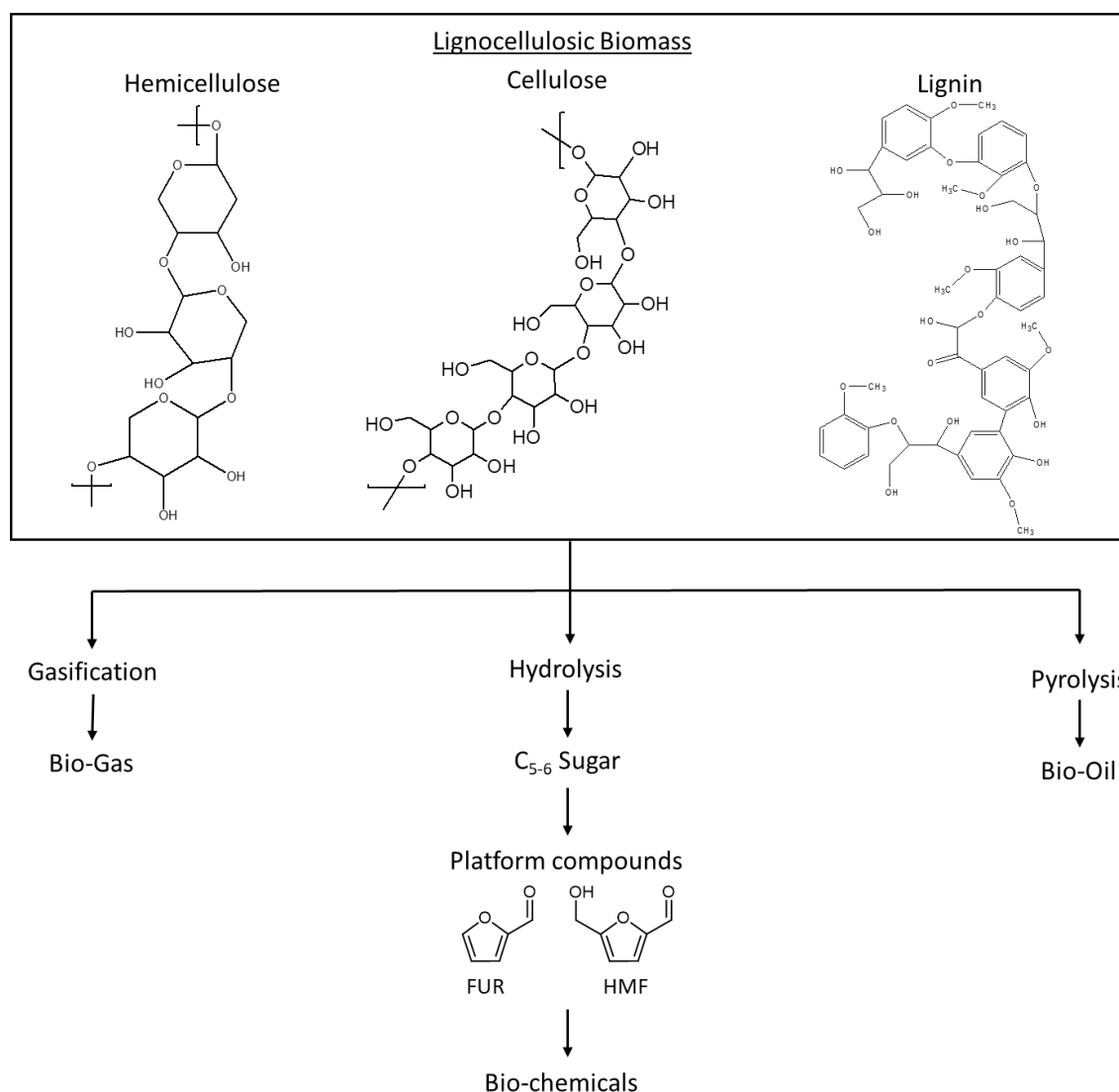


Figure 1.6 - Main approaches for lignocellulosic biomass conversion.

3.1. Furfural

Furfural is derived from the degradation of pentoses, such as xylose, in acidic medium at high temperature. Historically, the industrial synthesis of furfural from pentoses in the presence of dilute sulfuric acid began with the Quaker Oats company for the recovery of waste from the grain industry [31,32]. This process allowed to obtain up to 50% yield. The advantage of this method lies in its simplicity, so much so that this synthesis has been adapted to the requirements of the practical work of researchers. [33] Since then, the industrial synthesis of furfural has been extensively modified and exploited. [34–38]

Recently, Westpro has modified the Quaker Oats Technology process in China (Huaxia Furfural Technology) into a continuous process. This method uses fixed bed reactors and a continuous dynamic azeotropic distillation refining process, which led to 4%–12% production yield with respect to the initial

weight of dry biomass used (i.e., corn cobs, rice hulls, flax dregs, cotton hulls, sugarcane bagasse, and wood). However, no detailed information is available with regard to this technology. [31,32]

SupraYield is another modification of the Quaker Oats Technology process introduced in the late 1990s. In this technology, lignocelluloses (sugarcane bagasse) are hydrolyzed in one stage, and then pentoses are converted into furfural in aqueous solution at its boiling point with or without phosphoric acid). The solution containing furfural is then adiabatically flash-distilled, which facilitates the transfer of the furfural formed from the aqueous phase to the vapor phase. This process has a production yield of 50%– 70% and is less expensive than the traditional process described above. The high temperature of this process (240 °C) promotes the conversion of mono-sugars to furfural. [39]

Alternatively, a single-step furfural production process based on simultaneous hydrolysis and dehydration of lignocellulosic biomass to furfural in dilute sulfuric acid solution was developed by Vedernikov. [36] As a result, more pentose would be converted to furfural (furfural yield was 75% in this case). [40]

The furfural platform molecule can be derived into many compounds by reduction, oxidation, coupling, dimerization or polymerization. The applications of these products are new polymers, solvents, biofuels and bio-based carbon chemicals. [86] (figure 1.7)

Table 1. Main production processes of furfural production

Company / Process	Type of process	Temperature (°C)	Feedstock	Furfural Yield (%)*
Quaker Oats	Continuous flow	153	Bagasse sugarcane	55
SupraYield	Continuous flow	240	Rice husk Wheat straw	50-70
Vedernikovs	Continuous flow	188	Wood chips	75
Huaxia-Westpro	Continuous flow	160-200	corncob	35-50

* Furfural yield is based on the conversion of xylose

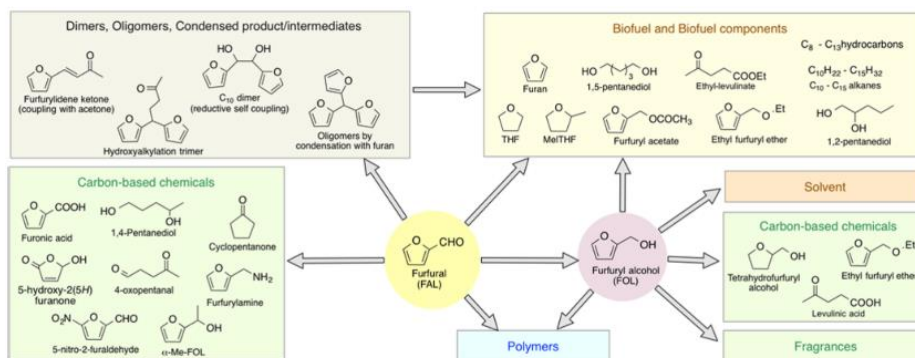


Figure 1.7 - Biofuels and chemicals from furfural [86]

3.1.1. Furfural synthesis from xylose

The transformation of xylose into furfural is the simplest process for its synthesis. As shown in Table 1.1, there are many ways to convert xylose to furfural. The simplest ones use strong acids in aqueous medium at high temperature (Table 1.1, entries 1-3). However, the use of these acids at high temperature is not compatible with the development of an environmentally friendly chemistry and can pose handling problems (chemical risks for the manipulators, corrosion of the reactors...). In addition, none of these systems makes it possible to obtain yields greater than 50% in furfural. This limitation is due to the formation of polymeric compounds resulting from the condensation of furfural on itself, as well as to the different reactions of degradation of sugars in these extreme conditions. To overcome these limitations, the use of biphasic systems can be a major asset. The addition of methyl isobutyl ketone to a dilute solution of hydrochloric acid increases the yield to 80% furfural (Table 1.1, entry 4). Other studies have shown that excellent yields can be obtained in toluene combined with a dilute solution of sulfuric acid in the presence of sodium chloride. [41]

To avoid the use of strong, corrosive and polluting acids, systems based on solid acids have been developed (Table 1.1, entries 5, 6, 8-11). The resins make it possible to obtain up to 98% yield from xylose in a water-toluene medium (Table 1.1, entry 5). The main advantage of this method is the possibility of recycling the resin with however a loss of activity (90% at the second use). [42] The loss of activity of the acid under these conditions puts forward a limitation of the heterogeneous catalysis for this type of transformation. The derivatives of graphene, a highly structured carbon compound, induce the conversion of xylose to furfural with satisfactory yields (entry 6). [43] Finally, the synthesis of furfural from xylose was carried out without catalyst in ionic liquid acids used as solvents (Table 1.1, entry 12). [44]

The comparison of the reactivity of xylose in the presence of acidic mesoporous silica in different solvent systems (Table 1.1, entries 9-11) clearly shows that it plays a preponderant role for the synthesis of furfural. Although water is a very ecofriendly solvent, it is clearly not competitive with DMSO with a furfural yield of 14% (Table 1.1, entry 10) and 75% (Table 1.1, entry 9) respectively and conversions of 25% and 91%. The addition of toluene to water (Table 1.1, entry 11) increases both the selectivity and the conversion (91%) of the xylose and provides furfural with a yield of 76%. [45]

Finally, in DMSO without catalyst addition at 150 °C (Table 1.1, entry 7), the xylose is converted to furfural with 25% yield. [46] It is important to note that to maintain liquid reaction media, some reactions are conducted at high pressure (up to 50 bar).

Table 1.1 - Furfural synthesis from xylose

Entry	Solvent	Catalyst	Temperature (°C)	Yield (%)	Ref.
1	H ₂ O	HCl	170	30	[47]
2	H ₂ O	H ₂ SO ₄	135	17	[41]
3	H ₂ O	H ₃ PO ₄	180	28	[48]
4	H ₂ O/MIBK	HCl	170	82	[47]
5	H ₂ O/toluene	H-mordenite	260	98	[42]
6	H ₂ O	SGO	200	62	[43]
7	DMSO	-	150	25	[46]
8	DMSO	Nafion 117	150	60	[49]
9	DMSO	MCM-41-SO ₃ Hc	140	75	[45]
10	H ₂ O	MCM-41-SO ₃ Hc	140	14	[45]
11	H ₂ O/toluene	MCM-41-SO ₃ Hc	140	76	[45]
12	[EMIM][HSO ₄] ^a	-	100	62	[44]

^a 1-ethyl-3-methylimidazolium hydrogen sulfate

3.1.2. Furfural synthesis from xylan

As we have shown, the synthesis of furfural from xylose is relatively simple and effective in the presence of acid catalysts. The recovery of xylan, which also involves a depolymerization step, is much more difficult. As with xylose, many methods have been developed. Metal catalysts have proved its effectiveness towards the conversion of this polymer. For example, chromium trichloride hexahydrate provides 63% furfural yield at 200 °C in ionic liquid [BMIM]Cl under microwave irradiation. [50] More conventionally, use in THF/H₂O medium of trichloride aluminum hexahydrate combined with sodium chloride leads to an 80% furfural yield at 150 °C under microwave irradiation. [51]

3.1.3. Furfural synthesis from lignocellulosic biomass

To conclude, the valorization of natural pentose contained in hemicelluloses was studied. In this context, two major strategies have been developed. The first is to separate the different constituents before their transformations. These methods will not be detailed, but mention may be made of steam explosion isolation and ethanol addition [52] precipitation and organic extraction [53].

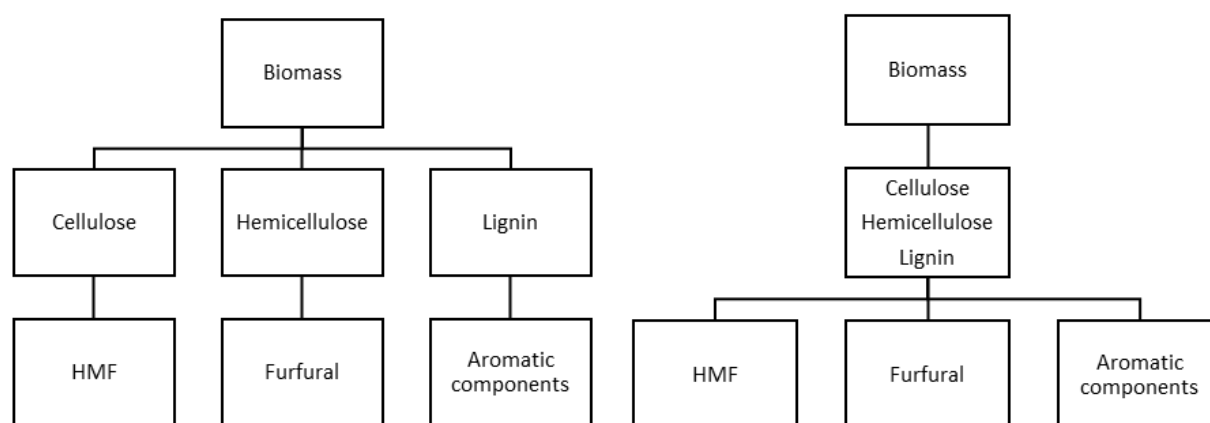


Figure 1.8 - The two ways of biomass valorization

Recently, some ionic liquids have been developed for the selective extraction of hemicelluloses but the process still needs to be improved [54]. The advantage of these techniques is that other compounds such as ash, proteins and lignin are no longer present during sugar processing. The second approach is to valorize all components of the biomass in one-step and then separate the products obtained. The undeniable advantage of this method is that it does not require pretreatment. However, the simultaneous presence of all these compounds can cause undesirable side reactions such as polymerization.

At first glance, the conversion of hemicellulose should be relatively similar to that of xylan, its main constituent.

Table 1.2 - Furfural synthesis from lignocellulosic biomass

Entry	Substrate	Solvent	Catalyst	Temperature/Power	Time (min)	Yield (%)	Ref.
1	Corn	BMIMCl ^a	CrCl ₃ , 6H ₂ O	400 W	3	23	[50]
2	Corn	THF/H ₂ O	AlCl ₃ .6H ₂ O	140 °C	60	51	[50]
3	Pine	THF/H ₂ O	AlCl ₃ .6H ₂ O	140 °C	60	29	[51]
4	Corn	H ₂ O	A1,5g-B90mLT180 ^b	180 °C	170	33	[55]
5	Corn	H ₂ O	NbOPO ₄ ^c	160 MW	30	23	[56]
6	Bagasse	H ₂ O/toluene	SAPO-44 ^d	170 °C	240	90	[57]
7	Straw	H ₂ O	BHC ^e	150 MW	30	65	[58]

^a Butylmethylimidazolium chloride, ^b Biochar catalyst, ^c Niobium phosphate, ^d Silicoaluminophosphate, ^e Betaine hydrochloride

This is the reason why most studies are conducted on this substrate. Nevertheless, in the biomass, the hemicellulose makes it possible in particular to bind cellulose and lignin because of its very trendy structure. This particular organization leads to the formation of a rigid structure, with a dense network

of hydrogen bonds, which makes the hydrolysis and the conversion of hemicelluloses much more difficult than that of pure xylan.

As expected, the $\text{CrCl}_3 \cdot 6\text{H}_2\text{O}/[\text{BMIM}]\text{Cl}$ system that yielded 63% furfural yield from xylan only yields 23% furfural from corn (Table 1.2, entry 1) [50]. Whereas the biphasic systems already described are promising with 51% yield of furfural material from corn, their effectiveness is limited by the presence of salts, essential for the good separation of the organic phase and the obtaining of the biphasic system (Table 1.2, entries 2-3) [51].

This difference clearly shows that the development of the production of products derived from biomass and associated technologies must take into account the territorial constraints and the context of local agriculture. By way of illustration, the transformation of bagasse from sugar cane into furfural is very effective (Table 1.2, entry 6) [57]. As a result, it is a substrate of choice for its production, which justifies the installation of production units near sugar cane fields as in the Dominican Republic. In the presence of solid acidic resins in water, furfural is obtained in yields of less than 35% (Table 1.2, entries 4-5). [55,56]

Interestingly, it will be noted that the addition of betaïne hydrochloride makes it possible to obtain up to 65% yield of furfural in water at 150 °C under microwave irradiation (Table 1.2, entry 7) from wheat straw [58]. This process also selectively provides xylose in place of furfural with 48% yield by decreasing the temperature from 150 °C to 120 °C. During the production of furfural at 150 °C, hexoses are not converted into HMF or levulinic acid. An increase in temperature to 180 °C after the formation of furfural provides, in two steps, yields of 65% in furfural and 87% in levulinic acid. However, whatever the conditions, HMF is not obtained by this method because of the presence of water. The use of γ -valerolactone, a solvent resulting from the conversion of levulinic acid, is noted in the presence of solid acid catalyst. The difference between boiling points makes it possible to obtain furfural directly by distillation [59]. Although this method is promising, the required high temperature (175 °C) and the low initial xylose concentration (2% by weight) strongly limit its application.

3.2. Hydroxymethylfurfural

The second bio-sourced furanic compound is the 5-hydroxymethylfurfural (HMF). Unlike furfural, which is obtained from the pentoses of hemicelluloses, HMF is produced by the transformation of hexoses, mainly from fructose and less from hexoses like glucose, contained in cellulose and starch. Just as in the case of furfural, we will first present the transformation of fructose and then that of glucose to conclude by the conversion of natural polymers. 5-HMF was identified as a high potential initial C_6 -platform chemical serving biomass-based alternatives for polymers, pharmaceuticals,

agrochemicals, flavors and fragrances, macro- and heterocycles, and natural products as well as it could be a precursor for fuel components. The most important 5-HMF-based chemicals are summarized on Figure 1.9. [86]

One of the major limitations of HMF synthesis is related to its polarity. Indeed, the HMF is hardly extracted from the aqueous phases necessary for the treatment of the reaction mixtures. Several techniques have emerged with the development of an efficient extraction system consisting of a mixture of butanol and methylisobutylketone (MIBK). [60,61] A low-pressure reactive distillation process has been specifically developed for extraction of HMF from ionic liquids. [62] However, both of these techniques require high-energy expenditure because of the vacuum required for the distillation of the solvent and the HMF respectively. Another constraint to the synthesis of HMF is its instability that makes it necessary to precisely control reaction conditions such as temperature and reaction time. Indeed, under prolonged heating or in acidic conditions, the HMF has a strong tendency to form humins, which are, for the moment, little valorized and poorly defined. [63] One can also add that, in the presence of water, the HMF can be converted to levulinic acid and formic acid. [35,58,64,65]

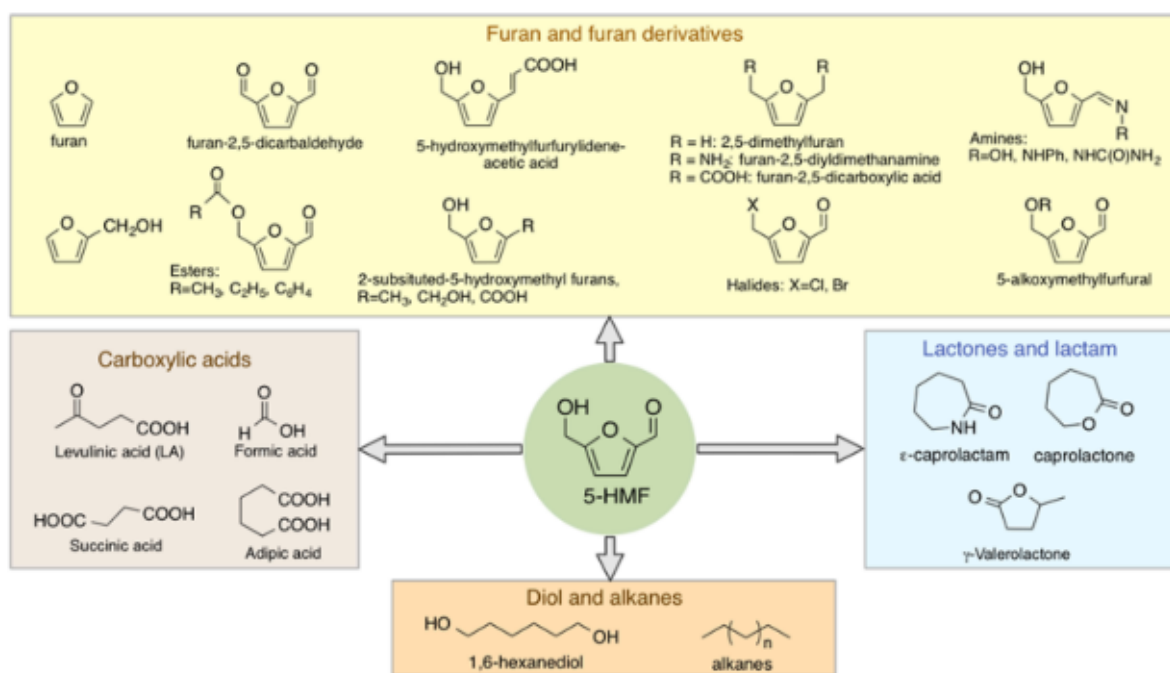


Figure 1.9 - 5-HMF as a platform chemical [86]

3.2.1. Synthesis of Hydroxymethylfurfural from fructose

Historically, HMF has been synthesized by fructose degradation in an aqueous solution of sulfuric acid. This synthesis, although effective, requires the use of a corrosive acid as in the case furfural.

Table 1.3 - Synthesis of HMF from fructose

Entry	Solvent	Catalyst	Temperature (°C)	Time (h)	Yield (%)	Ref.
1	H ₂ O/MIBK	Mordenite-H	165	1.5	74	[66]
2	H ₂ O/THF	FePO ₄	140	0.25	68	[67]
3	Choline chloride	(C ₆ H ₁₅ O ₂ N ₂) ₂ HPW ₁₂ O ₄₀ ^a	110	-	90	[68]
4	DMSO	-	150	4	90	[46]
5	[EMIM][HSO ₄] ^b	-	100	0.5	79	[44]
6	[EMIM][HSO ₄]/MIBK ^b	-	100	0.5	88	[44]
7	[EMIM]Cl ^b	-	120	3	73	[69]

^a acid-base bifunctional heteropolyacids, ^b EMIM: 1-ethyl-3-methylimidazolium ionic liquid

The development of new synthesis of HMF from fructose, similar to those used for the synthesis of furfural from xylose, provides excellent yields without acidic aqueous solution (Table 1.3). [46,70,71] The use of resins acids in an aqueous medium (Table 3, entry 1), in the presence of an organic solvent to extract and stabilize the HMF, leads to a yield of 74% [66]. According to the same principle, a biphasic system can be obtained with THF as organic solvent in the presence of a concentrated aqueous solution (Table 3, entry 2). In this configuration, an iron-based catalyst provides HMF with 68% yield. [67]

However, biphasic systems involve technical constraints such as rigorous control of the reactor shape and the stirring force. Single-phase systems, such as choline chloride at 110 °C (Table 3, entry 3), give a yield of 90%. [68] Finally, DMSO as a solvent requires the use of high temperatures (Table 3, entry 4), but induces the conversion of fructose with very high selectivity without catalyst. [46] Such a high yield despite hard conditions and without continuous extraction of HMF could be explained by the stabilizing interactions between HMF and DMSO. [72]

The preferential interactions between hydroxymethyl and aldehyde substituents of HMF with DMSO decreases its reactivity with the water responsible for the formation of levulinic and formic acid. Finally, acid ionic liquids are excellent media for fructose dehydration at moderate temperatures (Table 3, entry 5). The acidity generated by the presence of the derivatives of sulfuric acid is sufficient to induce the formation of HMF with a yield of 79%. It can be noted that, if an organic solvent is added, the yield increases up to 88% (Table 3, entry 6). [44] Other ionic liquids, preferably less acidic, also give good yields of HMF at 120 °C (Table 3, entry 7). [69]

3.2.2. Synthesis of Hydroxymethylfurfural from glucose

The literature review shows that HMF can be obtained from fructose with excellent yields. However, fructose is not accessible directly from lignocellulosic biomass. It is therefore necessary to develop methods for the formation of HMF from glucose derivatives and, ideally, from cellulose and unprocessed agro-resources. Glucose conversion involves an isomerization step to fructose prior to dehydration that leads to HMF. We will first treat the isomerization of glucose to fructose and its application to the synthesis of HMF.

3.2.2.1. Glucose isomerization

Typically, the isomerization of glucose is favored in basic medium according to the reaction mechanism of Lobry De Bruyn-Alberda Van Ekenstein (Figure 1.10). [73,74] In the presence of a base, the open form of glucose equilibrates with the 1,2-enediol intermediate which can be stabilized by the formation of a hydrogen bond with the proton of the neighboring alcohol. This intermediate can lead to the formation of the open form of fructose by displacement of a hydrogen. The open form obtained is itself in equilibrium with the pyranosic form of fructose. It is important to note that depending on the base used, the cation may also be involved in the isomerization process, which explains the failure of some heavy isotope incorporation experiments. [74]

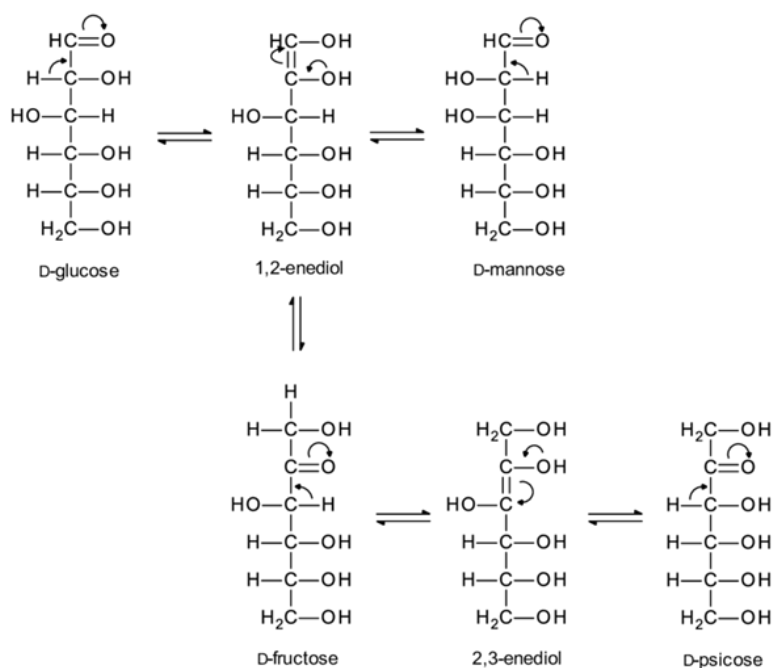


Figure 1.10 - Glucose isomerization mechanism [74]

Table 1.4 - Glucose isomerization into fructose

Entry	Solvent	Catalyst	Temperature (°C)	Time (h)	Yield (%)	Ref.
1	H ₂ O	NEt ₃ ^a	100	0.5	31	[70]
2	H ₂ O	Enzymes	55	-	42	[71]
3	H ₂ O	Sn β-zeolites	110	0.5	31	[75]
4	H ₂ O	Na ₂ B ₄ O ₇ /NaOH	90-100	-	90	[76]
5	DMSO/PEG/H ₂ O	NaAl ₂ O ₃	55	3	49	[73]

^a Triethylamine

Conventionally, the bases used for the isomerization of glucose to fructose are strong inorganic bases (NaOH, Ca(OH)₂...). Unfortunately, at the pH imposed by these bases, the monosaccharides are not stable and at least fifty degradation products have been identified. [74] It is interesting to note that the addition of borax to a dilute sodium hydroxide solution makes it possible to obtain up to 90% fructose yield (Table 1.4, entry 4). [76]

Recently, the substitution of sodium hydroxide with triethylamine at 100 °C has led to a 31% yield of fructose [70] (Table 1.4, entry 1) which is competitive with the results obtained with Sn β-zeolites (Table 4, entry 3) [75].

Industrially, isomerization is mainly used for the production of concentrated glucose syrup in fructose for example for the replacement of sucrose in sweet products such as sodas in the United States. The most efficient method involves immobilized enzymes and yields at 55 °C to 42% fructose (Table 1.4, entry 2) [71]. It is possible to further enrich the mixture by raising the temperature above 70 °C. However, these harsher conditions cause a decrease in the stability of the enzymes. Similarly, variations in pH or purity of the substrate lead to the complete replacement of the catalyst. It can also be noted that these technologies are large consumers of water.

Despite the good yields of isomerization obtained in the presence of bases or enzymes, these conditions are not suitable for the formation of HMF which is done in an acid medium at high temperature. In the case where a one-pot transformation is desired, the isomerization can be catalyzed by the addition of metals such as chromium [77,78] or tin [79–81] derivatives.

3.2.2.2. Application of glucose isomerization in the one-pot synthesis of HMF

When glucose is treated under the same conditions as fructose in DMSO or ethyl methylimidazolium hydrogen sulfate (Table 1.5, entries 1 and 6), very little HMF can be detected in the medium despite a total conversion of sugar. [44,46] In organic solvents, the addition of iron (Table 1.5, entry 3) or tin catalyst results in average yields of 23% and 48%. The addition of boric acid to an aqueous glucose solution results in the formation of HMF with 14% yield (Table 1.5, entry 4). In the ionic liquid [EMIM]Cl,

boric acid induces the conversion of glucose to HMF with a yield of 41% (Table 1.5, entry 9). These two experiments clearly show the difference in reactivity of the glucose/boric acid system as a function of the solvent.

Table 1.5 - HMF synthesis from glucose

Entry	Solvent	Catalyst	Temperature (°C)	Yield (%)	Ref.
1	DMSO	-	150	2	[46]
2	THF/DMSO	Sn-Mont ^a	160	48	[79]
3	H ₂ O/THF	Fe ₃ PO ₄	140	23	[67]
4	H ₂ O	B(OH) ₃	150	14	[82]
5	DMA	CrCl ₃ ·6H ₂ O/NaBr	110	65	[83]
6	[EMIM][HSO ₄]	-	100	3	[44]
7	[EMIM]Cl	CrCl ₂	100	70	[44]
8	[BMIM]Cl ^b	CrCl ₃	100	81	[44]
9	[EMIM]Cl ^c	B(OH) ₃	120	41	[84]
10	Choline chloride	CrCl ₂	110	45	[77]
11	Choline chloride	CrCl ₃	110	31	[77]

^a montmorillonite, ^b 1-ethyl-3-methylimidazolium ionic liquid, ^c 1-butyl-3-methylimidazolium

A simulation shows that boric acid catalyzes the isomerization of glucose to fructose by binding with the oxygen atoms of sugar. The formation of borates would lower the energy of the various reaction intermediates and promote isomerization [84]. A similar mechanism has been proposed for the same isomerization in the presence of boronic acids. [85]

In contrast to boric acid, the effect of which depends on the solvent, the chromium chloride catalysts make it possible to obtain good yields of HMF from glucose in both organic solvents (Table 1.5, entry 5) and in ionic liquids (Table 1.5, entries 7, 8). The various studies of chromium dichloride catalysis in chlorinated ionic liquids suggest that the active species is in fact a chromium trichloride formed by the association between the ionic liquid and the catalyst. [69]

References

1. Barr, J.B., and Wallon, S.B. (1971) The chemistry of furfuryl alcohol resins. *J. Appl. Polym. Sci.*, **15** (5), 1079–1090.
2. Alamos, L. (1968) Investigation of the Polymerization of Furfuryl Alcohol with Gel Permeation Chromatography. 1671–1681.
3. European Commission (2009) DIR2009/28/CE-Directive relative à la promotion de l'utilisation de l'énergie produite à partir de sources renouvelables et modifiant puis abrogeant les directives 2001/77/CE et 2003/30/CE. *J. Off. l'Union Eur.*, **2008** (5), 16–62.
4. Hernández-Beltrán, J.U., Hernández-De Lira, I., Cruz-Santos, M., Saucedo-Luevanos, A., Hernández-Terán, F., and Balagurusamy, N. (2019) Insight into pretreatment methods of lignocellulosic. *Appl. Sci.*
5. Alder, E. (1976) Lignin Chemistry: Past, Present, and Future. *Wood Sci. anci Technol.*, **8**, 1–25.
6. Lichtenthaler, F.W., and Peters, S. (2004) Carbohydrates as green raw materials for the chemical industry. *Comptes Rendus Chim.*, **7** (2), 65–90.
7. Wilson, J.D., and Kelvin Hamilton, J. (1986) Wood cellulose as a chemical feedstock for the cellulose esters industry. *J. Chem. Educ.*, **63** (1), 49–53.
8. D. Fengel, and Wegener, G. (1989) Wood: chemistry, ultrastructure, reactions. *Walter de Gruyter*.
9. Ebringerová, A., Hromádková, Z., and Heinze, T. (2005) Hemicellulose. *Adv Polym Sci*, **186**, 1–67.
10. Wong, K.K., Tan, L.U., and Saddler, J.N. (1988) Multiplicity of beta-1,4-xylanase in microorganisms: functions and applications. *Microbiol. Rev.*, **52** (3), 305–317.
11. Amarasekara, A.S. (2013) Acid Hydrolysis of Cellulose and Hemicellulose. *Handb. Cellul. Ethanol*, 247–281.
12. Vanholme, R., Demedts, B., Morreel, K., Ralph, J., and Boerjan, W. (2010) Lignin biosynthesis and structure. *Plant Physiol.*, **153** (3), 895–905.
13. Nguyen, J.D., Matsuura, B.S., and Stephenson, C.R.J. (2014) A Photochemical Strategy for Lignin Degradation at Room Temperature. *J. Am. Chem. Soc.*, **136** (4), 1218–1221.
14. Sturgeon, M.R., O'Brien, M.H., Ciesielski, P.N., Katahira, R., Kruger, J.S., Chmely, S.C., Hamlin, J., Lawrence, K., Hunsinger, G.B., Foust, T.D., Baldwin, R.M., Bidy, M.J., and Beckham, G.T. (2014) Lignin depolymerisation by nickel supported layered-double hydroxide catalysts. *Green Chem.*, **16** (2), 824–835.
15. Deuss, P.J., Scott, M., Tran, F., Westwood, N.J., De Vries, J.G., and Barta, K. (2015) Aromatic Monomers by in Situ Conversion of Reactive Intermediates in the Acid-Catalyzed Depolymerization of Lignin. *J. Am. Chem. Soc.*, **137** (23), 7456–7467.
16. Xu, C., Arancon, R.A.D., Labidi, J., and Luque, R. (2014) Lignin depolymerisation strategies: Towards valuable chemicals and fuels. *Chem. Soc. Rev.*, **43** (22), 7485–7500.
17. Zaheer, M., and Kempe, R. (2015) Catalytic hydrogenolysis of aryl ethers: A key step in lignin valorization to valuable chemicals. *ACS Catal.*, **5** (3), 1675–1684.
18. Liao, J.J., Latif, N.H.A., Trache, D., Brosse, N., and Hussin, M.H. (2020) Current advancement on

- the isolation, characterization and application of lignin. *Int. J. Biol. Macromol.*, **162**, 985–1024.
19. Zhou, X., and Rauchfuss, T.B. (2013) Production of hybrid diesel fuel precursors from carbohydrates and petrochemicals using formic acid as a reactive solvent. *ChemSusChem*, **6** (2), 383–388.
 20. Corma, A., Delatorre, O., and Renz, M. (2011) High-quality diesel from hexose- and pentose-derived biomass platform molecules. *ChemSusChem*, **4** (11), 1574–1577.
 21. Van Putten, R.J., Van Der Waal, J.C., De Jong, E., Rasrendra, C.B., Heeres, H.J., and De Vries, J.G. (2013) Hydroxymethylfurfural, a versatile platform chemical made from renewable resources. *Chem. Rev.*, **113** (3), 1499–1597.
 22. Rosatella, A.A., Simeonov, S.P., Frade, R.F.M., and Afonso, C.A.M. (2011) 5-Hydroxymethylfurfural (HMF) as a building block platform: Biological properties, synthesis and synthetic applications. *Green Chem.*, **13** (4), 754–793.
 23. Gallezot, P. (2012) Conversion of biomass to selected chemical products. *Chem. Soc. Rev.*, **41** (4), 1538–1558.
 24. Huber, G.W., and Dumesic, J.A. (2006) An overview of aqueous-phase catalytic processes for production of hydrogen and alkanes in a biorefinery. *Catal. Today*, **111** (1–2), 119–132.
 25. Axelsson, L., Franzén, M., Ostwald, M., Berndes, G., Lakshmi, G., and Ravindranath, N.H. (2012) Perspective: Jatropha cultivation in southern India: Assessing farmers' experiences. *Biofuels, Bioprod. Biorefining*, **6** (3), 246–256.
 26. Rajvanshi, A.K. (1986) Biomass gasification. *Altern. Energy Agric.*, **2** (4), 83–102.
 27. Kan, T., Strezov, V., and Evans, T.J. (2016) Lignocellulosic biomass pyrolysis: A review of product properties and effects of pyrolysis parameters. *Renew. Sustain. Energy Rev.*, **57**, 1126–1140.
 28. Alonso, D.M., Bond, J.Q., and Dumesic, J.A. (2010) Catalytic conversion of biomass to biofuels. *Green Chem.*, **12** (9), 1493–1513.
 29. Chundawat, S.P.S., Beckham, G.T., Himmel, M.E., and Dale, B.E. (2011) Deconstruction of Lignocellulosic Biomass to Fuels and Chemicals. *Annu. Rev. Chem. Biomol. Eng.*, **2** (1), 121–145.
 30. Takagaki, A., Nishimura, S., and Ebitani, K. (2012) Catalytic Transformations of Biomass-Derived Materials into Value-Added Chemicals. *Catal. Surv. from Asia*, **16** (3), 164–182.
 31. Binder, J.B., Blank, J.J., Cefali, A. V., and Raines, R.T. (2010) Synthesis of furfural from xylose and xylan. *ChemSusChem*, **3** (11), 1268–1272.
 32. Brownlee, H.J., and Miner, C.S. (1948) Industrial Development of Furfural. *Ind. Eng. Chem.*, **40** (2), 201–204.
 33. Girka, Q. (2015) Synthèse de dérivés furaniques à partir de biomasse et leur utilisation pour la synthèse de tensioactifs gemini.
 34. De Jong, W., and Marcotullio, G. (2010) Overview of biorefineries based on co-production of furfural, existing concepts and novel developments. *Int. J. Chem. React. Eng.*, **8**.
 35. Fitzpatrick, S.W. (1990) Lignocellulose degradation to furfural and levulinic acid. US Pat. n°4897497, issued 1990.
 36. Vedernikovs, N., Kampars, V., Puke, M., and Kruma, I. (2010) Changes in the Birch Wood Lignocellulosic Composition in the Pretreatment Process. *Mater. Sci. Appl. Chem.*, **22**, 68–73.

37. Cai, C.M., Zhang, T., Kumar, R., and Wyman, C.E. (2014) Integrated furfural production as a renewable fuel and chemical platform from lignocellulosic biomass. *J. Chem. Technol. Biotechnol.*, **89** (1), 2–10.
38. Kamm, B., Kamm, M., Gruber, P.R., and Kromus, S. (2005) *Biorefineries-Industrial Processes and Products*, WILEY-VCH Verlag GmbH & Co.
39. Karl J. Zeitsch (2000) *The Chemistry and Technology of Furfural and Its Many By-products*, Elsevier.
40. AS Mamman et al. (2012) Furfural: Hemicellulose/xylose- derived biochemical. *Biofuels, Bioprod. Biorefining*, **6** (3), 246–256.
41. Rong, C., Ding, X., Zhu, Y., Li, Y., Wang, L., Qu, Y., Ma, X., and Wang, Z. (2012) Production of furfural from xylose at atmospheric pressure by dilute sulfuric acid and inorganic salts. *Carbohydr. Res.*, **350**, 77–80.
42. Lessard, J., Morin, J.F., Wehrung, J.F., Magnin, D., and Chornet, E. (2010) High yield conversion of residual pentoses into furfural via zeolite catalysis and catalytic hydrogenation of furfural to 2-methylfuran. *Top. Catal.*, **53** (15–18), 1231–1234.
43. Lam, E., Chong, J.H., Majid, E., Liu, Y., Hrapovic, S., Leung, A.C.W., and Luong, J.H.T. (2012) Carbocatalytic dehydration of xylose to furfural in water. *Carbon N. Y.*, **50** (3), 1033–1043.
44. Lima, S., Neves, P., Antunes, M.M., Pillinger, M., Ignatyev, N., and Valente, A.A. (2009) Conversion of mono/di/polysaccharides into furan compounds using 1-alkyl-3-methylimidazolium ionic liquids. *Appl. Catal. A Gen.*, **363** (1–2), 93–99.
45. Dias, A.S., Pillinger, M., and Valente, A.A. (2005) Dehydration of xylose into furfural over micro-mesoporous sulfonic acid catalysts. *J. Catal.*, **229** (2), 414–423.
46. Despax, S., Maurer, C., Estrine, B., Le Bras, J., Hoffmann, N., Marinkovic, S., and Muzart, J. (2014) Fast and efficient DMSO-mediated dehydration of carbohydrates into 5-hydroxymethylfurfural. *Catal. Commun.*, **51**, 5–9.
47. Weingarten, R., Cho, J., Conner, W.C., and Huber, G.W. (2010) Kinetics of furfural production by dehydration of xylose in a biphasic reactor with microwave heating. *Green Chem.*, **12** (8), 1423–1429.
48. Vázquez, M., Oliva, M., Téllez-Luis, S.J., and Ramírez, J.A. (2007) Hydrolysis of sorghum straw using phosphoric acid: Evaluation of furfural production. *Bioresour. Technol.*, **98** (16), 3053–3060.
49. Lam, E., Majid, E., Leung, A.C.W., Chong, J.H., Mahmoud, K.A., and Luong, J.H.T. (2011) Synthesis of furfural from xylose by heterogeneous and reusable nafion catalysts. *ChemSusChem*, **4** (4), 535–541.
50. Zhang, Z., and Zhao, Z.K. (2010) Microwave-assisted conversion of lignocellulosic biomass into furans in ionic liquid. *Bioresour. Technol.*, **101** (3), 1111–1114.
51. Yang, Y., Hu, C.W., and Abu-Omar, M.M. (2012) Synthesis of furfural from xylose, xylan, and biomass using AlCl₃·3H₂O in biphasic media via xylose isomerization to xylulose. *ChemSusChem*, **5** (2), 405–410.
52. Hongzhang, C., and Liying, L. (2007) Unpolluted fractionation of wheat straw by steam explosion and ethanol extraction. *Bioresour. Technol.*, **98** (3), 666–676.
53. Puls, J., and Saake, B. (2004) Industrially isolated hemicelluloses. *ACS Symp. Ser.*, **864**, 24–37.

54. Froschauer, C., Hummel, M., Laus, G., Schottenberger, H., Sixta, H., Weber, H.K., and Zuckerstätter, G. (2012) Dialkyl phosphate-related ionic liquids as selective solvents for xylan. *Biomacromolecules*, **13** (6), 1973–1980.
55. Liu, Q. yan, Yang, F., Sun, X. feng, Liu, Z. hua, and Li, G. (2017) Preparation of biochar catalyst with saccharide and lignocellulose residues of corncob degradation for corncob hydrolysis into furfural. *J. Mater. Cycles Waste Manag.*, **19** (1), 134–143.
56. Serhan, M., Sprowls, M., Jackemeyer, D., Long, M., Perez, I.D., Maret, W., Tao, N., and Forzani, E. (2014) Furfural from corn stover hemicelluloses. A mineral acid-free approach. *Green Chem.*, **16**.
57. Bhaumik, P., and Dhepe, P.L. (2014) Exceptionally high yields of furfural from assorted raw biomass over solid acids. *RSC Adv.*, **4** (50), 26215–26221.
58. Liu, F., Boissou, F., Vignault, A., Lemée, L., Marinkovic, S., Estrine, B., De Oliveira Vigier, K., and Jérôme, F. (2014) Conversion of wheat straw to furfural and levulinic acid in a concentrated aqueous solution of betaine hydrochloride. *RSC Adv.*, **4** (55), 28836–28841.
59. Gürbüz, E.I., Gallo, J.M.R., Alonso, D.M., Wettstein, S.G., Lim, W.Y., and Dumesic, J.A. (2013) Conversion of hemicellulose into furfural using solid acid catalysts in γ -valerolactone. *Angew. Chemie - Int. Ed.*, **52** (4), 1270–1274.
60. Román-Leshkov, Y., Chheda, J.N., and Dumesic, J.A. (2006) Phase modifiers promote efficient production of hydroxymethylfurfural from fructose. *Sci. mag*, **312**.
61. Despax-Machefel, S. (2013) Développement de méthodologies de synthèse d'hydroxymethylfurfural à partir de biomasse lignocellulosique.
62. Wei, Z., Liu, Y., Thushara, D., and Ren, Q. (2012) Entrainer-intensified vacuum reactive distillation process for the separation of 5-hydroxymethylfurfural from the dehydration of carbohydrates catalyzed by a metal salt-ionic liquid. *Green Chem.*, **14** (4), 1220–1226.
63. Hoang, T.M.C., Van Eck, E.R.H., Bula, W.P., Gardeniers, J.G.E., Lefferts, L., and Seshan, K. (2015) Humin based by-products from biomass processing as a potential carbonaceous source for synthesis gas production. *Green Chem.*, **17** (2), 959–972.
64. Girisuta, B., Janssen, L.P.B.M., and Heeres, H.J. (2006) A kinetic study on the decomposition of 5-hydroxymethylfurfural into levulinic acid. *Green Chem.*, **8** (8), 701–709.
65. Kang, S., Fu, J., and Zhang, G. (2018) From lignocellulosic biomass to levulinic acid: A review on acid-catalyzed hydrolysis. *Renew. Sustain. Energy Rev.*, **94** (June), 340–362.
66. Moreau, C., Durand, R., Razigade, S., Duhamet, J., Faugeras, P., Rivalier, P., Pierre, R., and Avignon, G. (1996) Dehydration of fructose to 5-hydroxymethylfurfural over H-mordenites. *Appl. Catal. A Gen.*, **145** (1–2), 211–224.
67. Yang, L., Yan, X., Xu, S., Chen, H., Xia*, H., and Zuo, S. (2015) One-pot synthesis of 5-hydroxymethylfurfural from carbohydrates using an inexpensive FePO₄ catalyst. *RSC Adv.*, **5**, 19900–19906.
68. Zhao, Q., Sun, Z., Wang, S., Huang, G., Wang, X., and Jiang, Z. (2014) Conversion of highly concentrated fructose into 5-hydroxymethylfurfural by acid-base bifunctional HPA nanocatalysts induced by choline chloride. *RSC Adv.*, **4** (108), 63055–63061.
69. Zhao, H., Holladay, J.E., Brown, H., and Zhang, Z.C. (2007) Metal chlorides in ionic liquid solvents convert sugars to 5-hydroxymethylfurfural. *Sci. mag*, **316**.

70. Liu, C., Carraher, J.M., Swedberg, J.L., Herndon, C.R., Fleitman, C.N., and Tessonnier, J.P. (2014) Selective base-catalyzed isomerization of glucose to fructose. *ACS Catal.*, **4** (12), 4295–4298.
71. Bhosale, S.H., Rao, M.B., and Deshpande, V. V. (1996) Molecular and industrial aspects of glucose isomerase. *Microbiol. Rev.*, **60** (2), 280–300.
72. Tsilomelekis, G., Josephson, T.R., Nikolakis, V., and Caratzoulas, S. (2014) Origin of 5-hydroxymethylfurfural stability in water/dimethyl sulfoxide mixtures. *ChemSusChem*, **7** (1), 117–126.
73. Despax, S., Estrine, B., Hoffmann, N., Le Bras, J., Marinkovic, S., and Muzart, J. (2013) Isomerization of d-glucose into d-fructose with a heterogeneous catalyst in organic solvents. *Catal. Commun.*, **39**, 35–38.
74. Stutz, A.E. (2001) *Glycoscience*, Springer.
75. Moliner, M., Román-Leshkov, Y., and Davis, M.E. (2010) Tin-containing zeolites are highly active catalysts for the isomerization of glucose in water. *Proc. Natl. Acad. Sci. U. S. A.*, **107** (14), 6164–6168.
76. Mendicino, J.F. (1960) Effect of Borate on the Alkali-catalyzed Isomerization of Sugars. *J. Am. Chem. Soc.*, **82** (18), 4975–4979.
77. Zhang, Y., Pan, J., Gan, M., Ou, H., Yan, Y., Shi, W., and Yu, L. (2014) Acid-chromic chloride functionalized natural clay-particles for enhanced conversion of one-pot cellulose to 5-hydroxymethylfurfural in ionic liquids. *RSC Adv.*, **4** (23), 11664–11672.
78. Ilgen, F., Ott, D., Kralisch, D., Reil, C., Palmberger, A., and König, B. (2009) Conversion of carbohydrates into 5-hydroxymethylfurfural in highly concentrated low melting mixtures. *Green Chem.*, **11** (12), 1948–1954.
79. Wang, J., Ren, J., Liu, X., Xi, J., Xia, Q., Zu, Y., Lu, G., and Wang, Y. (2012) Direct conversion of carbohydrates to 5-hydroxymethylfurfural using Sn-Mont catalyst. *Green Chem.*, **14** (9), 2506–2512.
80. Dijkmans, J., Gabriëls, D., Dusselier, M., De Clippel, F., Vanelderden, P., Houthoofd, K., Malfliet, A., Pontikes, Y., and Sels, B.F. (2013) Productive sugar isomerization with highly active Sn in dealuminated β zeolites. *Green Chem.*, **15** (10), 2777–2785.
81. Choudhary, V., Pinar, A.B., Lobo, R.F., Vlachos, D.G., and Sandler, S.I. (2013) Comparison of homogeneous and heterogeneous catalysts for glucose-to-fructose isomerization in aqueous media. *ChemSusChem*, **6** (12), 2369–2376.
82. Hansen, T.S., Mielby, J., and Riisager, A. (2011) Synergy of boric acid and added salts in the catalytic dehydration of hexoses to 5-hydroxymethylfurfural in water. *Green Chem.*, **13** (1), 109–114.
83. Xiang, X., He, L., Yang, Y., Guo, B., Tong, D., and Hu, C. (2011) A one-pot two-step approach for the catalytic conversion of glucose into 2,5-diformylfuran. *Catal. Letters*, **141** (5), 735–741.
84. Ståhlberg, T., Rodriguez-Rodriguez, S., Fristrup, P., and Riisager, A. (2011) Metal-free dehydration of glucose to 5-(Hydroxymethyl)furfural in ionic liquids with boric acid as a promoter. *Chem. - A Eur. J.*, **17** (5), 1456–1464.
85. Lukamto, D.H., Wang, P., and Loh, T.P. (2013) Catalytic conversion of inert carbohydrates into platform chemical 5-hydroxymethylfurfural using arylboronic acids. *Asian J. Org. Chem.*, **2** (11), 947–951.

Chapter 2

Oxidation methods of furanic derivatives

1. Introduction

Nowadays, the world is facing many challenges, the increasing demand for fuels and chemicals due to the growth of global population faced by diminishing of fossil resources, energy stability and security due to political conflicts, and the resulting global warming caused by CO₂ emissions. [1,2]

Biomass, a renewable non-fossil carbon source, is found to be an ideal alternative to traditional fossil resources. The use of lignocellulosic biomass avoids the competition between food and fuel and can potentially notably reduce CO₂ emissions. It is one of the most important and promising ways to embed the concept of green industry and produce sustainable fuels and chemicals [3]. Since ever, sugars, starches and vegetable oils were the main source of biofuels. However, lignocellulose represents a more promising feedstock because it is cheaper, more abundant, and significantly more sustainable. [4,5]

As detailed in the previous chapter, furfural is derived from the dehydration of pentoses, such as xylose, treated in acidic medium under heating. Historically, the industrial synthesis of furfural from pentoses in the presence of dilute sulfuric acid began with the Quaker Oats company for the recovery of waste from the grain industry. [6,7] Since then, the industrial synthesis of furfural has been extensively modified and exploited, and new processes have emerged such as Suprayield, Vedernikovs and Huaxia/WestPro processes. [8,9]

On the other hand, HMF is produced by dehydration from the transformation of hexoses, such as fructose and glucose contained in cellulose and starch. One of the major limitations of HMF synthesis is related to its polarity. Another barrier to the synthesis of HMF is its instability that makes it necessary to precisely control reaction conditions such as temperature and reaction time. Indeed, under prolonged heating or in acidic conditions, the HMF has a strong tendency to form humins, which are, for the moment, little valorized and poorly defined [10]. One can also add that, in the presence of water, the HMF can be converted to levulinic acid and formic acid. [11–13]

Figure 2.1 outlines the most important fuel and chemical products derived from furfural and HMF, mainly by oxidation transformations in accordance with the topic covered in the thesis. Nevertheless, there is a giant number of ways to potentially transform these platform molecules into fuels and functional chemicals. Exemplary, according to the literature, there are more than 80 valuable chemicals derived directly and indirectly from furfural. [14] The oxidation of furfural can lead to the production of organic acids, esters and ketones such as maleic acid and succinic acid, which are the most important platforms for C₄ diacids molecules in chemical industries. Usually, HMF can be either reduced to a diols or oxidized to a diacids. These two compounds are used for the synthesis of

polymers. In addition, hydrogenation is used in order to upgrade HMF into fuel molecules. Furthermore, due to the furan structure, these synthons can permit to produce biologically active molecules in pharmaceutical industry. [15]

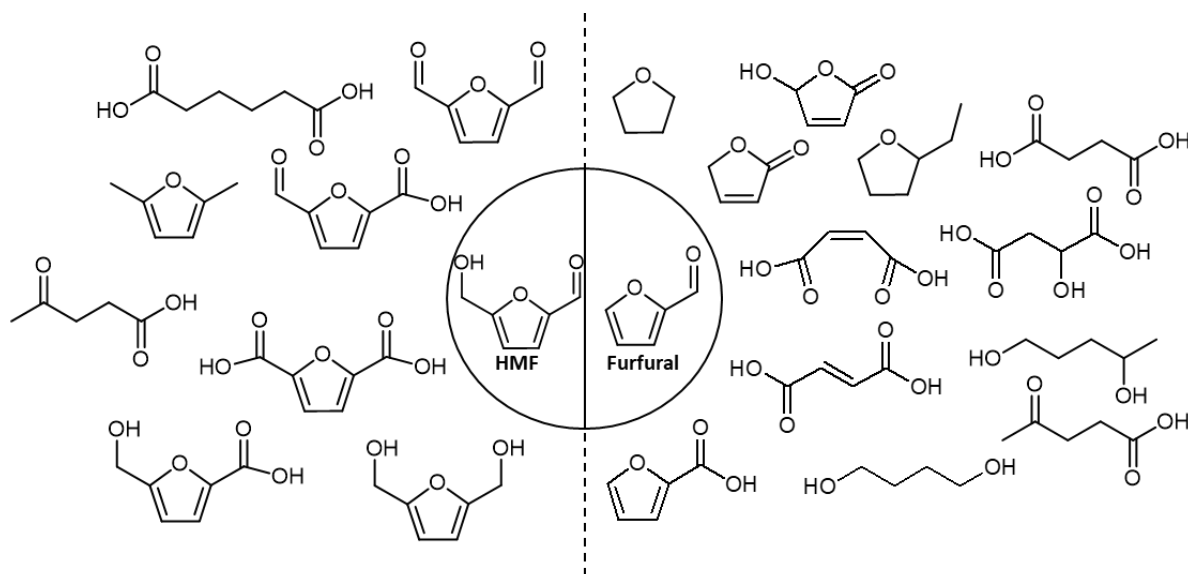


Figure 2.1 - Summary of furfural and HMF derived chemicals

The traditional valorization processes of these bio-sourced molecules used metal catalysis, usually with noble metals to obtain good conversion, yields and selectivity. Though catalysis is one of the pillars of green chemistry, the use of expensive, toxic and critical metals is often detrimental to this appellation. Therefore recently, metal-free catalysis have attracted the attention of scientists and researchers and such catalyst can be considered as green catalytic materials, because they can be highly efficient, easy to handle, environmentally friendly and economical in various industrial sectors. This dynamic was motivated by the desire to overcome the disadvantages of metallic catalysis and by the interests that can be gained from their substitution.

In this context, we propose to review, in this chapter, the catalytic methods for the oxidation of the platform molecules furfural and HMF obtained by dehydration of the oses. We will endeavor to present the benefits and disadvantages associated with oxidation methods with metallic or metal-free catalysis.

2. Metal catalysts for the oxidation of furan derivatives

Catalytic transformation of biomass-derived compounds to different platform chemicals and liquid fuel is a prominent way to reduce the global dependence on fossil resources. In past few decades, biomass-derived furans such as furfural and HMF have received outstanding attention because of their wide applications in the production of various industrially important value-added chemicals and fuel components. Various catalytic systems and methodologies have been extensively explored for the transformation of these furans to a wide range of products. This chapter is aimed to provide an extensive overview of the recent developments of several high-performing metal-based catalysts for the catalytic oxidation of the key biomass-derived furans (furfural and HMF) to value-added chemicals.

Several metallic heterogeneous and homogeneous catalysts, mainly based on Pt, Pd, Au, Ru, Ir, Re, Rh, V, Ni, Cu and Co metals, have been extensively studied in various catalytic transformations to efficiently upgrade furan derivatives.

Several recent reviews deal with the subject of oxidation by metallic catalysis, and readers may refer to them. For example, there are methods of oxidizing 5-HMF for its transformation into FDCA and DFF (figure 2.2). [16–23] In the case of furfural for its transformation into furanone, anhydrides and C4 diacids. [24–26] Noteworthy, the special case of base-free oxidation of furfural and HMF on supported gold catalysts. [27]

2.1. Metal catalysts for the oxidation of HMF

Of course, the platinum with its exceptional catalytic properties and its inertia to oxidation naturally have been studied in depth for oxidation transformations of furanic derivatives and especially HMF due to the application interest of the FDCA. As it could be predicted, HMF is oxidized very effectively in the presence of platinum. The classic conditions are to use nanoparticles of Pt dispersed on a support, to use oxygen as an oxidant and to work in a basic medium which greatly improves the kinetics of the transformation. The results obtained are generally very good, even excellent, however the separation of the FDCA from the reaction medium is a major problem due to neutralization and the presence of inorganic salts resulting from the bases used. [28] This can be illustrated by the work of Ait Rass et al. which have explored the oxidation of HMF over Pt catalysts supported on metallic oxide like TiO_2 or ZrO_2 , where the catalyst exhibited high activity towards the conversion of HMF into FDCA. (Table 2.1, Entry 2) [29]

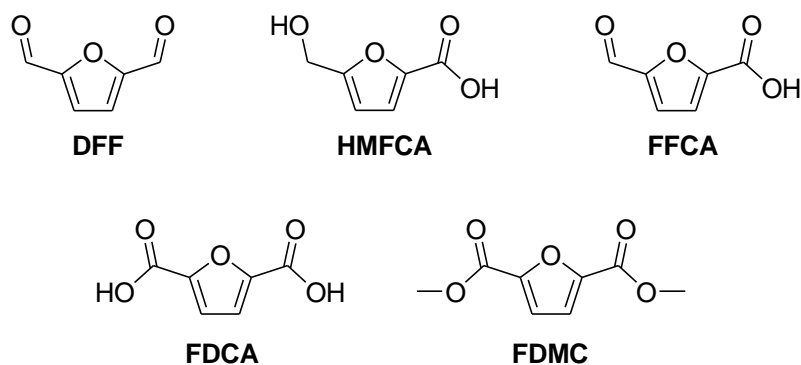


Figure 2. 2 - Main products obtained by oxidation of HMF by metallic catalysis

Several transformation improvements have been achieved, in particular by preparing bimetallic catalysts containing a fraction of other metals such as lead or bismuth, [30,31] and by working without base on zirconium oxide support or with the use of ionic polymers. [32,33] (Entries 1 and 3, Table 2.1)

From a mechanistic point of view, the significant presence of the 5-hydroxymethyl-2-furancarboxylic acid (HMFA) intermediary proves that the oxidation of the aldehyde function of HMF takes place faster than the hydroxyl function. The FDCA is, therefore, obtained through the HMFA. (Scheme 2.1)

Palladium behaves like platinum, it mainly catalyzes the oxidation of HMF towards the formation of FDCA, but under similar conditions, it is generally less active. [34,35] In order to improve its properties, the same studies and strategies of support modifications and doping have been applied to palladium. Some recent examples are reported in Table 2.1.

In some cases, the structure and size of the nanoparticles is critical and can strongly affect the yield, the smallest being the most active.[36,37] In addition, in a basic medium, nanoparticles of Pd/PVP suffer from stability and recycling problems. These problems can be partially overcome by supporting them on metallic oxide such as TiO₂, γ-Al₂O₃, ZrO₂-La₂O₃. [38] The use of magnetic iron oxide particles in combination with palladium provides the advantage of facilitating separation of the catalyst to increase its stability and recyclability. [39–41]

In order to facilitate the extraction of the FDCA and to avoid the neutralization stage of the reaction medium, many efforts were made to develop base free protocols. Effective solutions are reported using hydrotalcite (HT) support. [42] Similarly, the use of bimetallic systems improves efficiency, stability and recycling (Table 2.1, Entry11). [43]

Like platinum and palladium, gold shows a high catalytical efficiency and a very good selectivity towards various oxidation products of HMF particularly FDCA, its precursors HMFA, DFF and its ester derivatives (Table 2.1, entries 12 to 25). Many supports have been used and they influence responsiveness. Metal oxides such as CeO₂ and TiO₂ are better supports than Fe₂O₃ for example. These

supported catalysts have the advantage of being able to be separated and recycled quite easily. However, even if this phenomenon may be negligible, a decrease in catalytic activity during the cycles is sometimes reported.

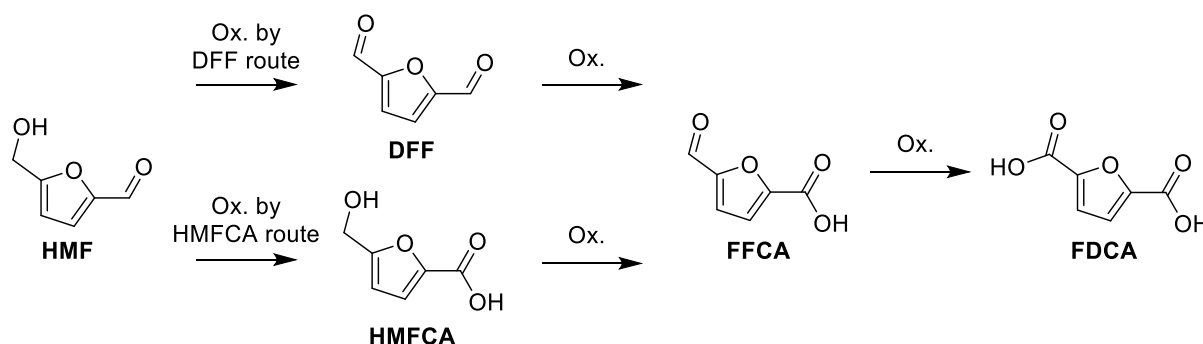
For instance, Au/TiO₂ catalyst was used for an efficient oxidative esterification of HMF to furan-2,5-dimethylcarboxylate (FDMC, 98% yield), a building block for bio-based polymers, using 4 bar O₂ in methanol at 130 °C. [44] In parallel, Casanova et al. also used oxidative esterification of HMF over Au nanoparticles supported on nanoparticulated ceria (Au/CeO₂) to obtain FDMC in more than 99% selectivity in methanol at 130 °C using 10 bar O₂. [45]

Similarly, chemical and electrochemical oxidation of HMF has also been explored over several metal catalysts (Au/TiO₂, Rh/C, Pt/C, Pd/C and Ru/C) in aqueous reaction conditions at 10 bar O₂ and 50 °C. Among these catalysts, Au/TiO₂ had the highest catalytic activity for the oxidation of HMF to FDCA. [46] Results showed that the pH of the reaction medium and the catalyst surface have a significant effect on the efficiency of the reaction and the catalytic activity. [46] It was observed that in acidic conditions, oxidation of alcoholic group of HMF was favored over the formyl group, while in highly basic medium (pH ≥ 13) the oxidation of alcoholic group was observed to be slow. Furthermore, studies also extrapolated that for Au-TiO₂ and Au-CeO₂ catalysts, base additives improved the production of FDCA by protecting the catalyst from deactivation and extending its lifetime. [47,48] In addition, the oxidation of HMF over Au/CeO₂ and Au/TiO₂ catalysts led to the formation of FFCA in 17% and 45% yields respectively, at 130 °C and 10 bar O₂. It is noteworthy that by adding 1 wt% of trifluoroacetic acid (TFA), a significant increase in the yield of FFCA to 71% and 79%, respectively was observed for Au/CeO₂ and Au/TiO₂. [49] Megías-Sayago et al. explored the Au/C catalyst and the effect of gold nanoparticle size on the oxidation of HMF. A series of gold nanoparticles in the 4-40 nm range were tested at 70 °C and 10 bar O₂. Whatever the gold nanoparticle size used, the conversion of HMF was 100%. But with 4 nm gold size, the yield of FDCA was more than 90% and this percentage decreased by increasing the gold nanoparticle size. [50] In the same direction, Au/Al₂O₃ exhibited high activity and selectivity in the oxidation of HMF in the presence of NaOH under mild conditions (70 °C for 4 h) and led to the production of FDCA with over than 99% yield. [51]

Typically, bimetallic systems of gold and palladium or copper nanoparticles show improved catalytic properties and appear superior in stability. The preparation of catalysts is not necessarily complex but generally requires several operations: the reduction of metal salts, the absorption and stabilization of nanoparticles formed on the substrate, filtration and washings and finally one or more heat treatment(s).

For example, monometallic Au and bimetallic Au-Cu catalysts have been employed and compared over TiO₂ for the oxidation of HMF. The results demonstrate that Au-Cu/TiO₂ was more efficient compared to Au/TiO₂. [52] Furthermore, using Au-Pd nanoparticles supported over functionalized carbon nanotubes to catalyze the oxidation of HMF, 94% selectivity in FDCA was achieved in water during 12 h at 100 °C and 50 bar O₂. [53] Similarly, Antonyraj et al. described the oxidation of HMF over Au-Pd alloy nano-particles supported on a basic anion-exchange resins (AER) to obtain FDCA with 93% yield at 100 °C and 10 bar O₂. [54] Interestingly, this catalyst was used 6 times without any significant loss of its catalytic activity. Xia et al. explored the oxidation of HMF over hydrotalcite-supported (HT-supported) monometallic Au or Pd and bimetallic Au-Pd. [43] The monometallic Au/HT and Pd/HT catalysts exhibited a low oxidation activity toward the hydroxyl groups of HMF, therefore a low yield of FDCA. However, the bimetallic catalyst Au-Pd/HT was able to oxidize efficiently the hydroxymethyl group of HMFCA which led to the highest yield of FDCA up to 90% at 60 °C for 6 h with a Au/Pd ratio of 4. Interestingly the selectivity of the oxidation of HMF functions can be tuned, a good example is given with the selective oxidation of HMF to DFF. As example a high catalytic activity and selectivity (98% DFF) is observed using Au-Pd nanoparticles supported on MnO₂ (Au-Pd/MnO₂) at 90 °C under O₂ atmosphere in 6 h. [55]

The comparison of some examples of catalysis involving gold alone or in the presence of other metals on various supports are shown below in table 2, entries 12 to 25. The preferred solvent is water. Apart from some examples, the O₂ pressures used for these transformations are of the order of 10 bars. The transformation is generally completed from 4 to 18 hours. The conversion of HMF is very often quantitative, and the selectivity and yield are excellent. However, too often the omission is made on the mass percentage of starting product and the resulting product is not isolated from the reaction mixture.



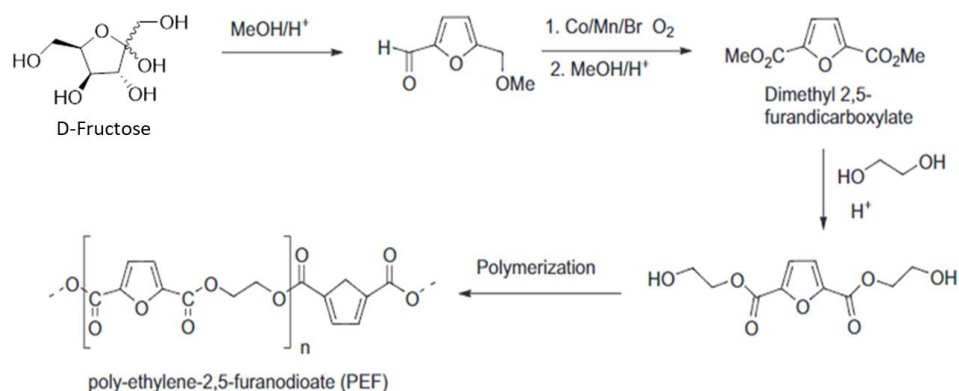
Scheme 2.1 - The two-oxidation route of HMF to FDCA

Ruthenium also has a very interesting catalytic activity. It is particularly effective for selective oxidation of the alcohol function of HMF leading to DFF. [56–61] The mechanism of the transformation and the effects of catalytic carriers have been thoroughly explored. [62,63] One example is the ruthenium

nanoparticles embedded on a mesoporous poly-melamine-formaldehyde material (Ru@mPMF) that displayed a good activity in the oxidation of HMF into DFF with 85% selectivity in toluene at 105 °C and 20 bar O₂ for 12 h. [56] This catalyst exhibited an important stability and reusability. After a simple filtration, the catalyst was used 6 times and showed a 0.0021% Ru leakage only. Wang et al. reported also the HMF oxidation over another ruthenium catalyst: the ZrP–Ru catalyst.[57] This catalyst showed a good activity towards the oxidation of HMF and afforded a total conversion at 130 °C at an oxygen flow rate of 20 ml/min after 12 h, yielding to DFF as the main oxidation product. Mishra et al. reported manganese-cobalt spinels (MnCo₂O₄) supported ruthenium (Ru) nanoparticles, Ru/MnCo₂O₄ to catalyze HMF to DFF. This catalyst afforded a high yield of DFF (98.3%) with total conversion at 130 °C in toluene and 10 bars of O₂. [58]

However it has also been shown that the oxidation with ruthenium can be pushed to FDCA with very good results.[64–68] Among the important observations, it should be noted that the use of weak bases or base free conditions will be preferred to avoid the degradation of HMF which is observed at too high pH. The support based on hydrotalcite, allows base-free protocol as in the case of catalysis with palladium or gold.

In view of the oxidation transformations reported in the literature with vanadium-based catalysts, some tests were conducted on HMF. Interesting results were obtained, particularly good selectivity in DFF. [69,70] In the field of rare metals, oxidation of HMF catalyzed by more common but less active metals has also been explored. This is the case with silver-manganese, [71] iron, [72] iron-cobalt [73,74] and manganese, [75] and cobalt-manganese. [49,76–80] Some remarkable results were obtained with good selectivity in FDCA or DFF. However, the reaction conditions are harsher, oxygen pressures and temperatures are higher, and reaction times are longer. That said, among the industrial processes for manufacturing FDCA, the cobalt/manganese-based catalysts used by Avantium in his process showed a very good performance.



Scheme 2.2 - Avantium's Process to polyethylene furandioate via 5-methoxymethylfurfural [20]

Table 2.1 - Some examples of HMF oxidation using metallic catalysts

Entry	Catalyst	Solvent	Oxidant	T (°C)	T (h)	Conversion (%)	Product	Yield (%)	Ref.
1	Pt/C 1,25M NaOH	Water	O ₂ , 1 bar	25	2	100	FDCA	81	[30]
2	Pt-Bi/TiO ₂ 2eq. Na ₂ CO ₃	Water	Air, 40 bar	100	6	99	FDCA	99	[29]
3	Pt-NP-Cl Base free	Water	O ₂ , 1 bar	80	6	100	FDCA	65	[33]
4	Pd/C 2 eq. NaOH	Water	O ₂ , 6.9 bar	65	6	100	FDCA	71	[35]
5	Pd-NCs 4eq. NaHCO ₃	Water	O ₂ , 25 mL/min	90	4	100	FDCA	92	[36]
6	PVP-Pd NP ^a 1,25 eq. NaOH	Water	O ₂ , 35 mL/min	90	7	>99	FDCA	90	[37]
7	Pd/ZrO ₂ /La ₂ O ₃ 1,25 eq. NaOH	Water	O ₂ , 35 mL/min	90	8	100	FDCA	90	[38]
8	C-Fe ₃ O ₄ -Pd 0,5eq. K ₂ CO ₃	Water	O ₂ , 30 mL/min	80	4	98.2	FDCA	82	[41]
9	γ-Fe ₂ O ₃ @HAP- Pd(0) ^b 0,5eq. K ₂ CO ₃	Water	O ₂ , 30 mL/min	100	6	97	FDCA	93	[39]
10	Pd/C@Fe ₃ O ₄ 0,5eq. K ₂ CO ₃	Water	O ₂ , 30 mL/min	80	6	100	FDCA	89	[40]
11	Pd/HT Base free	Water	O ₂ bubbling	100	8	100	FDCA	100	[42]
12	Au/TiO ₂ 4eq. NaOH	Methanol	O ₂ , 4 bar	130	3	100	FDMC	98	[44]
13	Au/CeO ₂ 2eq. NaOH	Methanol	O ₂ , 10 bar	130	5	>99	FDMC	99	[45]
14	Au/TiO ₂ pH=13	Water	O ₂ , 10 bar	50	4	100	FDCA	81	[46]
15	Au-CeO ₂ 2eq. NaOH	Water	O ₂ , 10 bar	65	8	100	FDCA	>99	[47]
16	Au-TiO ₂ 4eq. NaOH	Water	O ₂ , 10 bar	65	8	100	FDCA	>99	[47]
17	Au-Fe ₂ O ₃ 4eq. NaOH	Water	O ₂ , 10 bar	65	8	100	HMFC A	85	[47]
18	Au/TiO ₂ Base free	Acetic acid, trifluoroacetic acid	O ₂ , 10 bar	130	3	82	FFCA	79	[49]
19	Au/C 2eq. NaOH	Water	O ₂ , 10 bar	70	4	100	FDCA	>90	[50]
20	Au/Al ₂ O ₃ 4eq. NaOH	Water	O ₂ , 10 bar	70	4	100	FDCA	99	[51]
21	CNT-supported Au-Pd Base free	Water	O ₂ , 50 bar	100	12	100	FDCA	94	[53]
22	Au-Pd/ MnO ₂ Base free	Water	O ₂ , 1 bar	90	6	76	DFF	99	[55]
23	Au-Pd/IRA-743 ^g	Water	O ₂ , 10 bar	100	4	100	FDCA	>93	[54]
24	Au-Pd/HT	Water	O ₂ , 60	60	6	100	FDCA	90	[43]

25	2eq. NaOH Au-Cu/TiO ₂	Water	mL/min O ₂ , 10 bar	95	4	100	FDCA	99	[81]
26	4eq. NaOH Ru@mPMF ^c	Toluene	O ₂ , 20 bar	105	12	>99	DFF	85	[56]
27	ZrP-Ru ^g	p-chlorotoluene	O ₂ , 20 mL/min	130	12	100	DFF	55	[57]
28	Ru/MnCO ₂ O ₄ Base free	Toluene	O ₂ , 10 bar	130	3	100	DFF	>98	[58]
29	Ru/C Base free	Toluene	O ₂ , 20 bar	110	0.5	30	DFF	96	[60]
30	Ru/C Base free	Water	O ₂ , 20 bar	110	0.5	79	DFF	60	[60]
31	Ru/C Base free	Water	O ₂ , 5 bar	120	10	100	FDCA	88	[64]
32	C ₁₄ VOPO ₄ ^d	Toluene	O ₂ , 1 bar	110	6	91	DFF	87	[69]
33	V ₂ O ₅ @Cu-MOR Base free	DMSO	O ₂ balloon	120	7	100	DFF	91	[70]
30	Ag-OMS-2 ^e Base free	2-propanol	O ₂ , 15 bar	165	4	99	DFF	100	[71]
31	Fe ^{III} -POP-1 ^f Base n.r.	Water	O ₂ , 10 bar	100	10	100	FDCA	79	[72]
33	Fe-Co/C-500 1eq. Na ₂ CO ₃	Toluene	O ₂ , 10 bar	100	6	100	DFF	99	[73]
35	MnO _x -CeO ₂ 0,25eq. NaHCO ₃	Water	O ₂ , 20 bar	110	12	91	FDCA	91	[75]

[a] poly (*N*-vinyl-2-pyrrolidone) stabilized Pd nanoparticles, [b] Pd-exchanged hydroxyapatite-encapsulated magnetic γ -Fe₂O₃, [c] Ruthenium nanoparticles embedded on a mesoporous poly-melamine-formaldehyde, [d] C₁₄: length of alkyl group is 14, VOP: vanadium phosphate oxide, [e] Silver substituted manganese oxide octahedral molecular sieve, [f] Fe^{III}-porous organic polymer, [g] catalysts deposited on a basic support.

2.2. Metal catalysts for the oxidation of furfural

As a reminder, the global furfural market held a market value of USD 457.4 Million in 2022 and is projected to reach USD 840.7 Million by the year 2030. Most of the production is located in China, the Dominican Republic and South Africa, where agricultural residues rich in xylose polymers are present (sugar cane bagasse, rice bran). If the majority of furfural is reduced to furfuryl alcohol (70 to 80%), a platform molecule used in resins industry, it can be converted by oxidation into many products of interest. As stated in the introduction, Furfural oxidation is one of the most important and versatile reactions for the production of C4 chemicals, especially acid anhydrides and dicarboxylic acids [14]. Currently, the commercial processes for C4 maleic anhydride (MAN), maleic acid (MA), and succinic acid (SA) production are all derived from fossil feedstock (Figure 2.3). Commonly, MAN is produced by the oxidation of butane and benzene, knowing that butane oxidation is more preferred for environmental and economic reasons.[82] Further hydrolysis of MAN can produce MA, while SA is produced by the selective hydrogenation of MAN and MA. However, the depletion of fossil fuels and control of the carbon footprint increased the interest to produce acid anhydride and dicarboxylic acids from biomass as an alternative carbon source.

The wide variety of products resulting from the oxidation of furfural requires the use of the right reaction conditions in order to be highly selective in producing a targeted product. This selectivity requirement is linked to the constraint imposed by industrial processes to avoid complex purification steps.

Some typical studies of furfural oxidation with metal catalysts are summarized in Table 2.2.

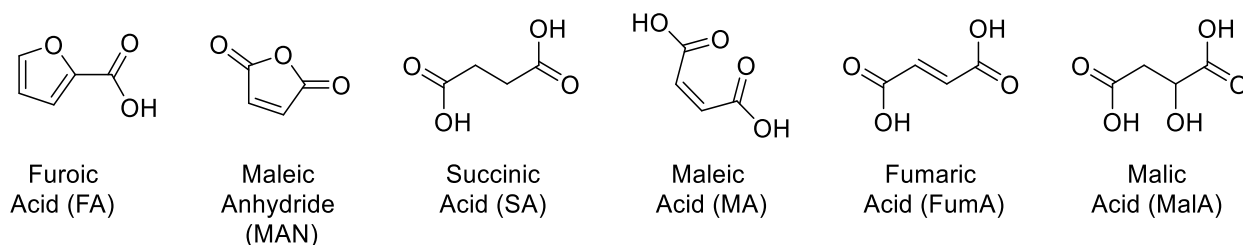


Figure 2.3 - Structures of common products after oxidation of furfural.

As for HMF the oxidation of furfural has been studied in the presence of catalysts based on noble metals, Pt, Au, Pd, V, Mo of their combinations and also other metals. Among the many parameters studied are the effect of the support, co-catalyst, synergy of polymetallic systems, conditions of pH, concentration, temperature and pressure. The transformations take place in the liquid or gaseous phase and the oxidants of choice are air, oxygen and hydrogen peroxide.

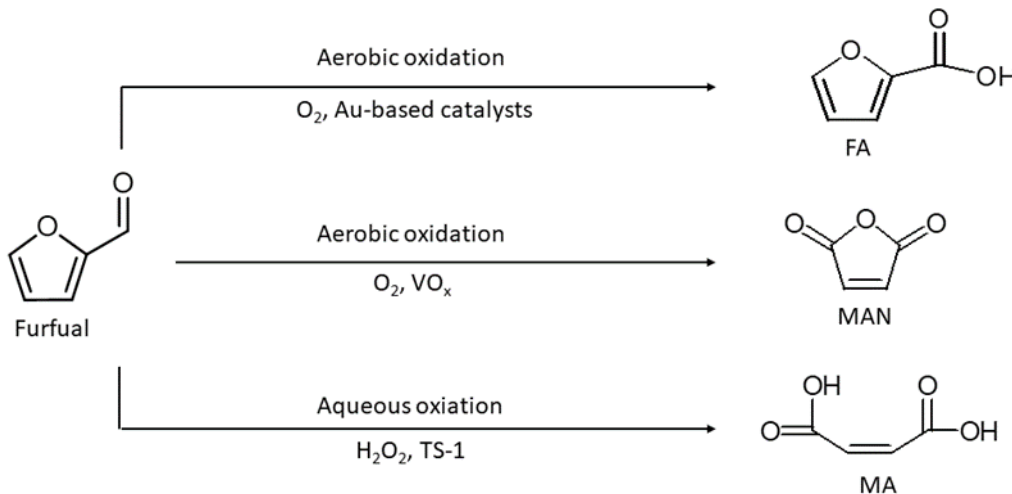


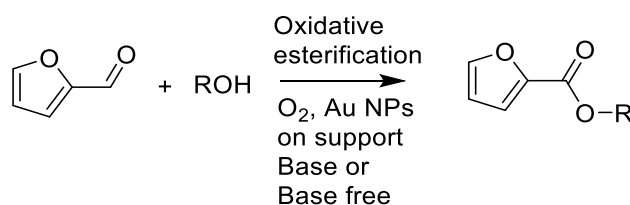
Figure 2.4 - Furfural oxidation to afford dicarboxylic acids and acid anhydrides

Compared to HMF, without surprises these catalytic systems lead to the same effects, with the difference that furfural having one less carbon and having no alcohol function, the oxidation can take place only on the furanic part and/or the carbonyl function of aldehyde. Some typical oxidation reactions and catalysts for the selective oxidation of furfural into MAN, MA, FA are summarized in figure 2.4. Noteworthy, dicarboxylic acids and maleic anhydrides present important raw materials in

chemical industries for the production of polyester resins, pharmaceuticals, plastics, lubricant additives, and vinyl copolymers. [83–85]

Compared to HMF platinum has not been used as much, however it has shown good catalytic activity for the simultaneous oxidation and esterification of furfural into methyl furoate. For example in the conditions reported by Radhakrishnan et al., but it is less active than Pd or gold.[86]

The high efficiency of gold catalysis has led to numerous researches, they have been much more explored, on many metal oxide supports in the presence or not of bases and especially by using oxygen as an oxidant. Generally under the reaction conditions used for these transformations, the solvents are often alcohols and mainly methanol, the product obtained is therefore mainly the result of oxidation of furfural and esterification, this is referred to as oxidative esterification (scheme 2.3). [87]



Scheme 2.3 - General representation of oxidative esterification of furfural in presence of gold nanoparticles catalyst.

As a first example, the conditions used on HMF with a gold catalyst deposited on cerium oxide and transposed to furfural have shown that the latter can easily be oxidized to methylfuroate under soft conditions of temperature and pressure, 22 °C and 1 bar of oxygen. However the presence of a 30% sodium methanolate solution is necessary.[44]

More recently, Metal Organic Framework (MOF) materials have been used by Ning et al. to support gold nanoparticles. Depending on the functional changes made on the MOF, a control between the oxidative condensation and oxidative esterification reactions of furfural with different aliphatic alcohols is observed. The oxidant used is the dioxygen and the base is potassium carbonate. Using methanol as a reagent and as a solvent, the Au@UiO-66 catalyst enables oxidative esterification transformation with 100% selectivity to methyl-2-furoate with complete conversion of furfural [88].

Furoic acid may also be obtained as an oxidation product. This was reported by Douthwaite et al. with the use of a 1% AuPd/Mg(OH)₂ bimetallic catalyst in the presence of NaOH for the oxidation of furfural which can selectively lead to furoic acid. Nevertheless, multiple concurrent transformations are observed, including Cannizzarro's reaction. The experimental conditions and the metal ratio AuPd can be precisely adjusted to provide good control of the selectivity of the reaction.[89]

In order to avoid the secondary reactions induced by the base, the neutralization steps or the manipulation of virulent bases, a major research effort was conducted by many researchers to develop

base free protocols. Thus, the oxidation of furfural without a base begins with the work reported by Menegazzo et al. who explored the effect of several supports like ZrO₂, CeO₂, and TiO₂. The first showing the best properties.[90]

For example, Radhakrishnan et al. working without a base obtained very good results for the preparation of 2-methylfuroate with a mesoporous carbon catalyst CMK-3 supporting gold nanoparticles. This Au/ CMK-3 catalyst, at 5 wt% Au showed a remarkable conversion of furfural (99.7%) with a very high selectivity to 2-methyl furoate (99.6%). The recyclability of the catalyst proved to be very good even after five catalytic cycles.[86] In this study, the authors impregnated several metals, Ni, Pt, Pd and gold on different supports such as SBA-15, graphite, graphene, MWCNT, active charcoal and TiO₂ and their catalytic activities were compared. In addition, different oxidizing systems were used, tertibutylperoxide, air and oxygen. Under these conditions, among the different metals, gold had the most important activity for the conversion of furfural to 2-methylfuroate. In addition, oxygen was the best oxidant, more active than air and leading to fewer secondary products compared to tertibutyl peroxide (TBHP).

Ferraz et al. investigated different Au-based catalysts supported on MnO₂ in the base-free oxidation of furfural to furoic acid. Au nanoparticles of controlled size were deposited on MnO₂ of different morphology (nanoflowers, nanowires), which allow to study the effects of the metal-support interaction on catalytic activity. The best results were obtained using MnO₂ having a nanoflower structure (MnO₂-NF) which was found to have the largest specific surface area and a large pore volume. Very good catalytic properties: furfural conversion and selectivity were observed. The superior catalytic activity of this catalyst is attributed to the presence of a significant amount of Au⁺ species on the surface, which is considered to be responsible for the most active catalytic sites in these oxidation reactions.[91] Recently the same authors reported the transformation of furfural by oxidative esterification, with the use of Au nanoparticles immobilized on alkaline earth metal oxide supports (MgO, CaO, BaO, ZrO), in the presence of oxygen between 6 and 26 bars. The reaction conditions used alcohol as both a reagent and a solvent. Substrates based on alkaline earth oxide have the advantage of being free from the use of additional bases. In fact, it has been verified that their basic properties promote the formation of esters, resulting in high selectivity, and preventing the formation of acetal as a by-product. *e.g.* the Au/MgO sample provided up to 95% yield of methyl furoate (M2F). In addition, this catalyst has been shown to be quite stable upon reuse. This method was extended to other linear and branched alcohols leading to the formation of esters up to C5 (isopentyl furoate) with high selectivity (>99%). The linear esters being obtained with better yields than the branched ones.[92] Pursuing the same goal to work base free, Ferraz et al. reported in another article the use of a catalyst based on bimetallic AuPd nanoparticles incorporated in a titanosilicate matrix under an air pressure of

6 to 26 bar. These catalysts were compared to the activity of monometallic Au and Pd, which were both less effective. Working without addition of a base, the best Au₄Pd₁@SiTi catalyst showed 50% conversion of furfural and 83% selectivity to furoic acid. It has been shown that the performance of this type of bimetallic catalyst is highly dependent on the Au-Pd ratio. Under the conditions of transformation the optimum value is 4 Au per 1 Pd with a pH always less than 3.5 so that no loss of metals was detected.[93]

Many gold-based catalysts have been reported recently for green and selective oxidation of furfural with oxygen as an oxidant. These catalysts reveal that it is important to control the size of Au particles, to choose the nature of the support and to control its morphology and the electronic properties of the material obtained. The sizes of gold nanoparticles ranging from 2 to 6 nm seem to be the most active. In general, these catalytic systems require a basis as a co-catalyst and several studies on the effect of the nature of the basis have been carried out, however more and more research reports that it is possible to achieve these transformations without a basis. These new green processes without a base are essential to be able to transform furfural into furoic acid and its esters in a perennial way by allowing easier purification as for example by simple filtration of the heterogeneous catalyst.

Huo et al. exhibited the oxidative transformation of furfural into M2F using a non-precious metal Co-N-C/MgO (cobalt N-doped carbon catalyst). This catalyst showed a high performance and catalytic activity by converting 93% of furfural into M2F with 92 % yield at 100 °C and 5 bar O₂ for 12 h (Table 2.2, entry 21). [94]

AuPd/Mg(OH)₂ is a highly effective catalyst for the oxidation of furfural into FA. This catalyst promotes the direct oxidation of the aldehyde group into the acid; furoic acid was obtained with 84% yield under O₂ pressure of 3 bar, at 30 °C for 4 hours (table 2.2, entry 8). [89] The gas-phase oxidation of furfural to maleic anhydride, MAN, over vanadium oxide-based catalysts under air or oxygen pressure has been studied for decades. For example, Alonso-Fagúndez et al. employed the oxidation of furfural to MAN at 300 °C using V₂O₅/γ-Al₂O₃ as the catalyst, and over 60% yield of MAN was obtained (table 2.2, entry 12). [95] Li et al. performed the aerobic oxidation of furfural over a Mo₄VO₁₄ catalyst at 120 °C and 20 bar O₂ for 16 hours, and a 65% yield of MAN was achieved in water solvent (table 2.2, entry 16). [96]

While catalytic systems based on gold lead essentially to the synthesis of furoic acid and its esters. Vanadium catalysis generally leads to more advanced oxidation with the loss of a carbon atom corresponding to carbonyl. In the gas phase the formation of maleic anhydride is observed and in the liquid phase the opening of the furanic cycle with formation of maleic acid or other C₄ diacides is observed. In addition, in the gaseous phase, the air or oxygen are used as an oxidant whereas in the liquid phase it is rather the hydrogen peroxide that is used. Vanadium-based catalysts are often in

combination with other metals, particularly molybdenum. Vanadium-based catalysts have long been known for their oxidizing catalytic properties. Indeed the oxidation of furfural in gaseous phase was first reported in 1928 by Session, the catalyst used was vanadium pentoxide, and air was used as oxidant, a flow of 4 L per minute of air allowed to oxidize about 0.3 g per hour of furfural in maleic acid, the best yield obtained being 12%. [97]

This work stems from preliminary results conducted in the liquid phase by Milas in 1927 relating the use of vanadium pentoxide as a catalyst used in the presence of sodium chlorate as an oxidant. The dominant diacide formed was fumaric acid obtained with a yield of 78% in 12.5 h, which is quite remarkable for the time, but according to Milas, the reaction was violent and difficult to control. [98]

Noteworthy, vanadium-based catalysts have long been known and used to oxidize petrosourced C4 fractions such as butane or butene to make anhydrides or diacides C4. [85,99–101]

Once again, numerous supports were explored to optimize catalytic activity. For example, in the gas phase, CeO₂, SiO₂, ZrO₂, TiO₂, Al₂O₃ were used as catalytic support. Among them alumina proves to be an excellent support to oxidize furfural to maleic anhydride in gaseous phase. [95,102–104] For example, Alonso-Fagúndez et al. converted furfural to maleic anhydride at 320 °C using VO_x/Al₂O₃ as a catalyst, and a 73% yield in maleic anhydride is reported. [105]

Recently Li et al. performed very well with vanadium phosphate used without support, working at 350 °C with 6 to 10 vol% of furfural in synthetic air with a flow of 40 mL.min⁻¹, 90% maleic anhydride yield was obtained. In addition, the catalyst is stable without loss of activity during 25 hours of testing. [106]

Polymetallic catalysts based on V-Mo-Fe phosphates were studied [102,104,107] as well as those based on mixed vanadium oxide and tin [108]. They are all effective in the formation of maleic anhydride, but the yield is very temperature dependent. The associated kinetic studies confirm the total oxidation of furfural if the reactive temperature is greater than 300 °C. [107,108] In the gas phase, the transformation temperatures are high, ranging from 200 to 300 °C. As a result, secondary products are formed in the form of solid residues that clog and deactivate the catalyst. To solve this problem several approaches, such as water introduction and increased oxygen concentration were proposed, but their effects were limited. [98]

Another strategy is to carry out a heat treatment at high temperature *i.e.* a pyrolysis of the catalyst, which usually allows to reactivate it and to return it its original properties. [95] Some catalysts are reported to be particularly resistant to this type of deactivation, for example the work of Li et al. [106]

Oxidation in the liquid phase leads to the formation of maleic acid rather than anhydride, which is predictable if the transformation is carried out in the presence of water. The advantage of these

transformations lies mainly in the implementation of milder reactive conditions, particularly with temperatures of the order of 70 to 90 °C. However, if the used oxidant was oxygen, pressure of several tens of bars must be managed.

In the homogeneous phase, it was demonstrated that polyoxometalates containing vanadium and/or molybdenum oxides, demonstrated a good conversion and selectivity for the transformation of furfural into maleic acid [109,110] and maleic anhydride [111] depending on the solvents used. For example Shi et al. reported the combination of copper nitrate with phosphomolybdic acid to be selective in the oxidation of furfural to maleic acid with a 49.2% yield and 51.7% selectivity, in aqueous phase under 20 bar O₂ at 98 °C for 14 hours, while the conversion of furfural is 95.2% (table 2.2, entries 18-19). [110] Guo et al. further investigated the oxidation of furfural in an aqueous/organic biphasic system with O₂ using phosphomolybdic acid catalysts and 34.5% yield of MA and 68.6% selectivity for MA are obtained (table 2.2, entry 14). [109]

In heterogeneous phase very good results were observed in the presence of mixed vanadium oxide and molybdenum Mo₄VO₁₄ [96] or modified graphene oxide supporting vanadium oxides VO-NH₂-VO or VON-GO. [112,113] The latter transformations are particularly selective and effective when carried out in acid protic polar solvents such as acetic acid or formic acid.

In the liquid phase, hydrogen peroxide is an interesting oxidant in the presence of vanadium catalysts. Many studies have been reported by Poskonin and Badovskya et al. which have helped to demonstrate the ability of vanadium at different oxidation states to transform furfural in the presence of H₂O₂, and other transition metals have been compared. In these various studies and according to the conditions, many products have been identified, including furanones and diacides C₄. [114–116] Recently vanadium pyrophosphate has also been used in the presence of H₂O₂. [117]

Many more abundant metals have been also tested to catalyze these transformations. For example and without being exhaustive, catalysts based on copper [118,119], iron [120,121] or titanium [122–125] have been used alone or in combination.

For example, Da Silva et al. reported very good results of oxidative esterification of furfural, in the presence of hydrogen peroxide catalyzed by metal silicotungstate salts, cobalt, copper, nickel, aluminum and iron were tested. The best results were obtained with copper silicotungstate, Cu₂SiW₁₂O₄₀ leading to 2-methylfuroate with a selectivity of more than 80% for 95% conversion of furfural (table 3, entry 20) [119]. Alonso-Fagúndez and co-workers reported the aqueous oxidation of furfural to obtain MA in a high yield of 78% using titanium silicalite (TS-1) as the catalyst and hydrogen peroxide as the oxidant at 50 °C for 24 hours (table 3, entry 23). [122,123] We have even demonstrated the efficiency of this catalyst by working in acetic acid in the presence of 1.8 wt% TS-1, with hydrogen

peroxide as oxidant. In 4 h, the total conversion of furfural was observed and a high yield of 62% MA was obtained as the only product without the mixing with FA. [124]

Although these methods have the great advantage of using metals that are much more economical because they are much more abundant and available, for the moment, the selectivity and yield are often lower than those obtained by vanadium catalysts.

Table 2. 2 - Furfural oxidation using metallic catalysts

Entry	Catalyst	Solvent	Oxidant	T(°C)	T(h)	Conversion (%)	Product	Yield (%)	Ref.
1	Pt/CMK-3 (0,3wt%)	CH ₃ OH	TBHP	120	3	60	M2F	53	[86]
2	Au/MgO	CH ₃ OH	O ₂ , 6 bar	110	2	100	M2F	94	[126]
3	Au/MnO ₂ -NF	-	Air, 12 bar	110	2	86	FA	62	[91]
4	Au@UiO-66	CH ₃ OH	O ₂ , 3 bar	140	4	100	M2F	100	[88]
5	Au/CMK-3	CH ₃ OH	O ₂ , 15 bar	120	3	>99	M2F	>99	[86]
6	Au/CMK-3	CH ₃ OH	TBHP	120	3	78	M2F	75	[86]
7	Au ₄ Pd ₁ @SiTi	-	Air, 26 bar	110	10	99	FA	48	[93]
8	AuPd/Mg(OH) ₂	Water	O ₂ , 3 bar	30	4	>99	FA	84	[89]
9	V-Zr/KIT-6 (VZPK2)	ACN	H ₂ O ₂	70	1	81	MA	29	[117]
10	VON-GO	AcOH AcOH	O ₂ , 20 bar	90	10	86	MAN	60	[113]
11	VPO	-	O ₂ /He, 20 mL/min	340	8	99	MAN	97	[127]
12	V ₂ O ₅ /γ-Al ₂ O ₃	-	O ₂ , 20 vol.%	300	15	100	MAN	>60	[95]
13	VO _x /Al ₂ O ₃	Vapor	O ₂ , 5.7 kPa	320	-	100	MAN	73	[105]
14	H ₃ PMo ₁₂ O ₄₀	Biphasic	O ₂ , 20 bar	110	14	50	MA	35	[109]
15	Mo ₄ VO ₁₄	Acetic anhydride	O ₂ , 20 bar	120	16	84	MAN	47	[96]
16	Mo ₄ VO ₁₄	Water	O ₂ , 20 bar	120	16	100	MAN	65	[96]
17	CaCu ₂ P ₂ O ₇	water	O ₂ , 8 bar	115	18	68	MA	37	[118]
18	Cu(NO ₃) ₂ +H ₃ PW ₁₂ O ₄₀	Water	O ₂ , 20 bar	98	14	36	MA	12	[110]
19	Cu(NO ₃) ₂ +H ₃ Mo ₁₂ O ₄₀	Water	O ₂ , 20 bar	98	14	95	MA	49	[110]
20	Cu ₂ SiW ₁₂ O ₄₀	CH ₃ OH	H ₂ O ₂	50	1	95	M2F	76	[119]
21	Co-N-C/MgO	CH ₃ OH	O ₂ , 5 bar	100	12	93	M2F	92	[94]
22	FeT(p-Cl)PPCl	Water	O ₂ , 12 bar	90	10	96	MA	44	[120]
23	TS-1	Water	H ₂ O ₂	50	24	100	MA	78	[122]
24	TS-1	AcOH	H ₂ O ₂	80	4	100	MA	62%	[124]

3. Metal-free catalysts for the oxidation of furan derivatives

Day by day, catalysis is making our life more sustainable. Nevertheless, how sustainable are catalysts themselves? Dematerializing catalysts, in using less noble and expensive materials to afford the same

or better level of functionality, has become a serious challenge for researchers and engineers. According to the Federal Register of the United States on February 2018, 35 metals and metalloids such as platinum metals, rare-earth elements group, cesium, chromium, aluminum, cobalt, titanium and many others have been listed as critical minerals [128]. Remarkably, these metals are familiar catalysts in chemical industries and lately they were widely used in nanomaterial-based catalysts, such as Co, Au, Ni, Pd and Pt, for numerous chemical reactions. This is due to the various advantageous chemical properties, such as high catalytic activity, redox properties, and acid-base sites and physical properties such as porosity, thermal stability, and high surface area. Despite all the valuable properties of nanomaterial-based catalysts, their high cost, deactivation and leakage problems and toxicity remain an important drawback. In this context, the best solution for the future industry of catalysts is to replace when possible metal catalysts by “metal-free” catalysts. This could establish a new concept or class of catalysis where metals are completely absent. The increasing use of metal-free catalysis in the recent years is not a new trend but their return to grace coincides with the development of industrial interests for more economical, eco-friendly and safer processes.

Catalytic transformation of biomass-derived compounds to different platform chemicals and liquid fuel is a leading way to reduce the global dependence on fossil resources and to establish a sustainable concept in chemical industries. However, the wide use of metallic catalysts is still, to some extent, a sustainability constraint. This is due to the use of noble and expensive metals, with their deactivation problems, toxicity and waste production.

In past few years, biomass-derived furans such as furfural and 5-hydroxymethyl-2-furfural (HMF) have received prominent attention and various metal-free catalytic systems and methodologies have been extensively explored for the transformation of these furans to a wide range of value-added chemicals and fuel components.

In the following, the metal free oxidation methods will be detailed for HMF and furfural.

3.1. Metal-free catalysts for the oxidation of HMF

As we have seen in the previous paragraph, the literature is rich in methods of oxidative transformations of HMF by metal catalysis, the advantages and disadvantages of which we have dealt with. Very briefly, we have seen that these oxidation methods or processes are rather carried out in a heterogeneous phase using catalysts based on heavy or noble metals in the presence of oxidants such as air or oxygen under pressure and sometimes under high temperatures. [34,129,130] Despite the high efficiency and excellent selectivity of these methods, they however require the preparation of catalysts often in several stages, industrial techniques which can be restrictive both on energy

consumption and on safety. Although the effects may be very small, there is deactivation and/or loss of metals by leaching, making these processes dependent on catalyst replenishment. Many academic methods are described over too short a time to estimate long-term catalytic capabilities. Management of heavy metal wastes can also be problematic under environmental regulations. These processes must now be assessed in the long term; they must be sustainable with minimal impact on the environment. For several decades, scientists have developed a new concept of HMF oxidations offering promising alternatives to metal catalysts. The trend toward green chemistry and sustainable technologies requires replacing the traditional concepts by new ones, controlling the carbon cycle and energy sobriety. Catalysis play an important role in this purpose.

In this paragraph, we will see the effects of acid-base catalysis, carbon-based catalysts and organic catalysts used to replace metal catalysts.

3.1.1. Acid catalysis

Preliminary work on transforming HMF into metal-free DFF began with the work of Morikawa, who applied the methods of oxidizing alcohols by activating DMSO with acetic anhydride or in the presence of nitroxide. This led to good DFF yields of 76% and 71%, respectively (table 2.3, entries 1 and 2) [131]. Cottier et al. then proposed the transformation of HMF to DFF in two steps by silylation of HMF followed by oxidation of the silylated intermediate in the presence of NBS and AIBN in different solvents. Carbon tetrachloride and dodecane being the best solvents 91% and 88% of DFF are obtained. [132]

Since the dehydration step of the osidic fractions leading to HMF is carried out in an acidic medium, it would be advantageous to continue the oxidative catalysis step at acidic pH. In addition, supported acid catalysis is one of the most important types of catalysis in all sectors of the chemical industries. A major reason which has led to this advance is the diversity of acid sites on the surface of solid acid catalysts and the ease of purification. [133–135]

Although many protocols for the oxidation of furfural and HMF are described in the presence of acids, no systematic studies of the source of acid had been reported prior to the work of Choudhary et al. then Lv et al. [136–138]

Before that, the oxidation of HMF in an oxidizing acid medium was reported by Descotes et al. which used 65% nitric acid and water as solvent. The energy supply by heating or by sonication were compared, under these conditions. The authors observed the formation of FDCA and formylfuran carboxylic acid (FFCA) with yields of 43% and 5% in 22 hours by heating to 100 °C and 37% and 12% by sonication at 40 °C for 5 hours. [139] Sonochemical irradiation allows to divide reaction time by four. Replacing water with acetic acid with this method does not improve yields. These results

come as a result of pioneering work carried out by the same team with many metal oxidants but also nitric acid. [140]

The strategy of HMF oxidation in an acid medium was pursued by Choudhary et al. by exploring a panel of mineral and organic acid catalysts in the presence of hydrogen peroxide. First developed for the oxidation of furfural, the method was later extended to HMF. Transformation was studied in water in the presence of an equivalent or less of acids. Under the optimized conditions, unlike furfural which leads to succinic acid as the main product in the case of HMF, 31% of 2-oxoglutaric acid are obtained as the main product, with 18% of succinic acid and 60% of formic acid. Optimum conditions are 1.5 wt% Amberlyst-15, 3 wt% HMF and four equivalents of hydrogen peroxide, at 75 °C for 24 hours (table 2.3, entry 7). Therefore, Amberlyst-15 and H₂O₂ system was found to be an effective converter of furan compound into linear di-carbonyl compounds [136]. Note that in the case of the oxidation of furfural, APTS is as effective as Amberlyst-15 but unfortunately the oxidation of HMF has not been tested under the same conditions with the APTS. This result should be compared with those described by Li et al. which also demonstrated the advantage of using aromatic acids as catalysts [137]. The beneficial effect can be attributed to a π - π stacking interaction between HMF and aromatic species. We will see a little further on how this feature will be exploited with the use of carbon catalysts with a polyaromatic structure related to graphite.

If acid catalysis is very useful for metal-free oxidation, there is a particularly interesting family of oxidants which allow working without metals, these are the oxide derivatives of 2,2,6,6 tetramethylpiperidine alias TEMPO that many researchers have used to explore the transformations of HMF without a metal catalyst. The first studies reporting the use of free radical derivatives of 2,2,6,6 tetramethylpiperidine oxide for the oxidation of HMF appeared in 1995 reported by Cottier et al. [141] A screening of four TEMPO derivatives used in catalytic amounts is described in the presence of a co-oxidant to obtain DFF. With a two-phase water/DCM system, calcium hypochlorite as a co-oxidant and 4-benzoyloxy-2,2,6,6-tetramethylpiperidine oxide, 81% DFF is obtained after only 10 min of reaction. Interestingly, the methods described were used on a gram scale. Unfortunately, in this article two structures of TEMPO derivatives have been omitted (Table 2.3, entry 8). An efficient co-oxidant was tested in this study which is p-toluenesulfonic acid (p-TsOH) [142] that gave the desired product in 81% yield. The largest disadvantage was the necessity of using more than two-fold of oxidants in respect to HMF. [143]

The very good catalytic properties of TEMPO derivatives make it a particularly interesting tool for metal-free oxidation strategies. Because yields are good and selectivity is very high, many researchers have wished to add other benefits by regulating the steric and electronic effects of various substituents

on TEMPO, from the research of co-oxidant meeting the specifications of sustainable chemistry and easy purification by heterogenisation of TEMPO.

This is for example what was proposed by Mittal et al. using bisacetoxy-iodo-benzene periodinane as a co-oxidant and then heterogenizing TEMPO on SBA-15. Using a protocol based to those proposed by Margarita, Piancatelli et al. or Epp and Widlanski. [144,145] The HMF was successfully converted to DFF using TEMPO as oxidant (0.2 eq.) and [bis(acetoxy)-iodo]benzene (BAIB) (1,5eq.) as secondary oxidant in presence of acetic acid (0.1 eq.). 66% of DFF yield was achieved rapidly (<1h) under metal-free condition at ambient temperature (table 2.3, entry 10).[146] With the use of TEMPO-functionalized mesoporous silica (TEMPO-SBA-15) and the same co-oxidants as in [146] in an oxygen-rich medium, 73% of DFF was obtained under mild reaction conditions (table 2.3, entry 11). [147]

Krystof et al. also reported the use of silica-grafted TEMPO for the transformation of HMF into DFF, with the objective of preparing FDCA under mild and sustainable conditions by continuing the oxidation without purification during a second stage by enzymatic catalysis, similarly to the work of Anelli and Cottier et al. [141,148]. The commercial silica-grafted TEMPO catalyst was used in a biphasic system with water and ethyl acetate in the presence of sodium hypochlorite as a co-oxidant. Under these conditions in 1h working at room temperature, 32% DFF was obtained.[149] Karimi et al. also developed a catalyst based on mesoporous silica doubly functionalized both by TEMPO and by imidazolium groups. This bifunctional catalyst (TEMPO @ PMO-IL-Br), showed a very good activity for the aerobic oxidation without metal of different alcohols in the presence of two co-oxidants *tert*-butylnitrite (10 mol%) and oxygen (1 atm) in 1 hour at 50 °C. In toluene, 99% of DFF were obtained. Once should note that the presence of acetic acid as a co-catalyst is required under the optimized conditions. [150]

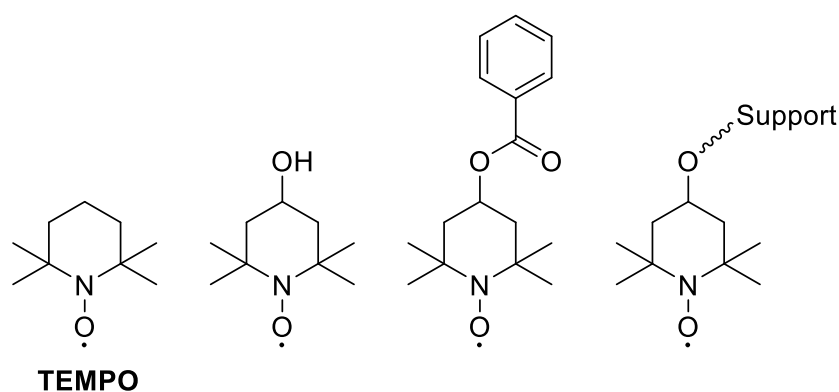


Figure 2.5 - Some examples of structure of TEMPO and TEMPO derivatives.

The use of oxygen as a co-oxidant with TEMPO was studied by Li et al. [137] This catalytic system is possible in the presence of acids and a screening was carried out by comparing mineral and organic acids. With inorganic acid, despite the high HMF conversion (95.6% to 98.2%), DFF selectivity was very

poor (less than 10%) due to the oligomerization side reactions. On the other hand, organic acids lead to good selectivity and a good conversion. It turns out that aromatic organic acids were the most effective, especially benzoic acid. Its availability and abundance makes it particularly interesting, however better results were obtained with pyrenecarboxylic acid. Finally, benzoic acid/TEMPO system was found to be effective in the catalytic aerobic oxidation of HMF and alcohols in terms of selectivity and yield and could replace the traditional metal catalysts (Table 2.3, entry 14).

These results are to be compared with the polyaromatic catalytic systems that we will describe below. Let us underline here the importance of two factors, the presence of the carboxylic acid function and that the effect of the aromatic structure which brings an undeniable advantage in these transformations. The obtained results show that the use of TEMPO as a radical initiator is particularly effective. TEMPO is often used with a very low ratio in the presence of a co-oxidant, but it is not necessarily essential.

Anthraquinone derivatives are well known for their reactivity with molecular oxygen and are applied in the global industrial preparation of hydrogen peroxide. It was therefore very wise to try this catalyst for metal-free oxidation of HMF. This was recently reported by Zhao et al.[151]. A relatively high mass percentage of HMF was implemented. The solvents used were either toluene or water with DMSO, and six different anthraquinone derivatives were tested. The best results for DFF preparation were obtained with anthraquinone-2-carboxylic acid at 130 °C for 24 hours, with 60% conversion of HMF for a selectivity of 88% to DFF or an overall yield of about 50%. In addition, for a 60% HMF conversion, 56% FDCA selectivity and 42% DFF are observed with 2,6-dihydroxyanthraquinone.

Lui et al. achieved a remarkable result with oxygen as an oxidant without radical initiator. They reported the generation of radicals by simply heating dioxygen under pressure from 1 bar to 115 °C in the presence of the solvent 1,2 diethoxyethane. The radical species formed could be identified by EPR analyses and by the use of radical scavengers such as TEMPO or butylated hydroxytoluene (BHT). Thus Lui et al. described a metal-, acid-, base-, external promotor-free oxidation of HMF for the production of FDCA. Under optimal conditions, 1,2-diethoxyethane showed the best behavior playing dual task; solvent and free-radical initiator. Using the atmospheric oxygen as the sole oxidant, the yield of FDCA was found to be 87% with 99% of HMF conversion while Bis (methoxypropyl) ether showed higher selectivity towards FFCA (Table 2.3, entries 20 and 21). [152]

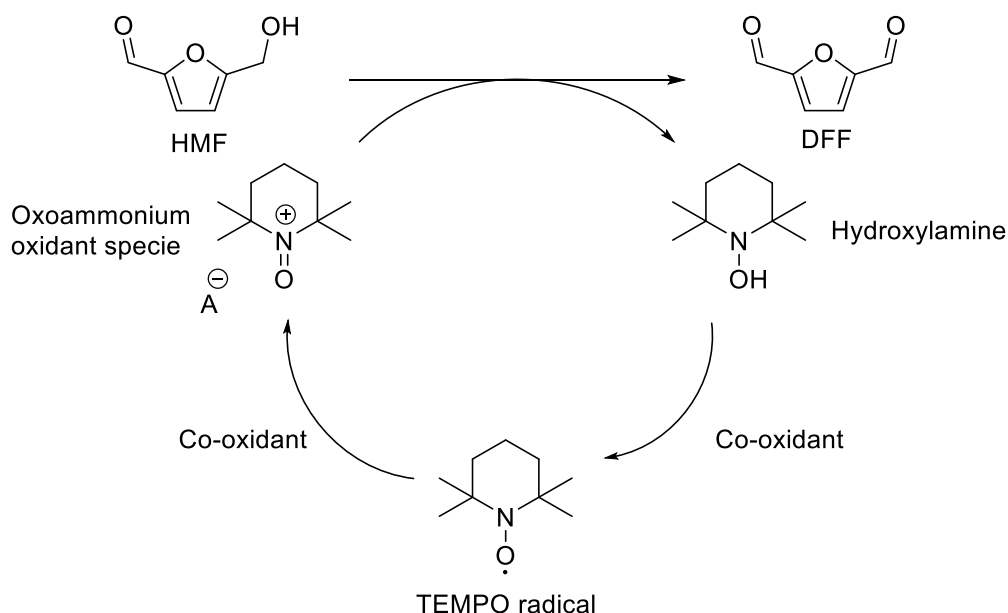
Table 2.3 - HMF oxidation using acid catalysts

Entry	Catalyst	Solvent	Oxidant	T(°C)	T(h)	Conversion (%)	Product	Yield (%)	Ref.
1	-	DMSO	Ac ₂ O DMSO	80	-	-	DFF	76	[131]
2	-	DMSO	N ₂ O ₄ DMSO	120	-	-	DFF	76	[131]
3	HNO ₃	DMSO	HNO ₃ 60%	-	-	-	DFF	31	[131]
4	HNO ₃	H ₂ O	HNO ₃ 65%	100	22	-	FDCA FFCA	67 43 5	[139]
5	HNO ₃ Ultrasounds	H ₂ O	HNO ₃ 65%	40	5	-	FDCA FFCA	37 12	[139]
6	HNO ₃	AcOH	HNO ₃ 65%	40	5	-	FDCA	11	[139]
7	Amberlyst-15	H ₂ O	H ₂ O ₂	75	24	>99	OGA	31	[136]
8	APTS/TEMPO	DCM/ H ₂ O	TEMPO der./APTS	-2 to RT	3	-	DFF	81	[143]
9	TEMPO der. (NaHCO ₃ 5%)	DCM/ H ₂ O	TEMPO der. Ca(OCl) ₂	0 to 15	0.2	-	DFF	81	[141]
10	AcOH-TEMPO	AcOEt	TEMPO/BAIB/ AcOH	30	0.75	-	DFF	66	[146]
11	TEMPO-SBA- 15	AcOEt	BAIB, AcOH/O ₂	40	1	-	DFF	73	[147]
12	TEMPO or TEMPO graft on silica	AcOEt/H ₂ O	NaOCl	RT	1	-	DFF	32	[149]
13	TEMPO@PMO -IL	Toluene	TBuNO ₂ , O ₂ , 1 bar	50	1	-	DFF	>99	[150]
14	Benzoic acid /TEMPO	AcN	O ₂ , 4 bar	100	24	79.6	DFF	77.1	[137]
15	Salicylic acid/TEMPO	AcN	O ₂ , 4 bar	100	24	80.5	DFF	76.8	[137]
16	p- Methoxybenzo ic/TEMPO	AcN	O ₂ , 4 bar	100	24	81.2	DFF	79.2	[137]
17	Pyrenecarboxy lic acid/TEMPO	AcN	O ₂ , 4 bar	100	24	87.7	DFF	87.2	[137]
18	SiO ₂ /Antraquinone 2- carboxylic acid	Toluene	O ₂ , 10 bar	130	24	60	DFF	52.8	[151]
19	2,6- dihydroxyanthraquinone	Toluene	O ₂ , 10 bar	130	24	60	DFF FDCA	25.2 34	[151]
20	-	1,2- Diethoxyethy lane	O ₂ , 1 bar	115	24	99	FDCA	87	[152]
21	-	Bis(methoxy propyl) ether	O ₂ , 1 bar	115	24	85	FFCA	63	[152]

The general mechanism of oxidation with TEMPO is now well established as shown below, in which the secondary oxidant transforms TEMPO, or a related stable radical, in an oxoammonium salt that

operates as the primary oxidant, transforming the alcohol into the corresponding aldehyde. This results in the formation of a hydroxylamine that is oxidized to a TEMPO radical, thus completing the catalytic cycle. The catalytic cycle can in fact be more complex, because TEMPO radicals can disproportionate into oxoammonium salts and hydroxylamines under acidic catalysis. Interestingly, TEMPO inhibits the oxidation of aldehydes to carboxylic acids when this oxidation proceeds via a radical mechanism, with oxygen for example. That is why Anelli's oxidation can be carried out under air and be easily stopped at the aldehyde stage with no competing overoxidation due to the presence of gaseous oxygen. [148]

Oxidation can continue in some cases, indeed the aldehyde, in the presence of water, equilibrates with the corresponding hydrate that can be oxidized via a similar mechanism to the corresponding acid (Scheme 2.4). Additionally, the co-oxidant can act as the primary oxidant for the oxidation of aldehyde to carboxylic acid.



Scheme 2.4 - Schematic representation of oxidation of HMF to DFF with TEMPO

3.1.2. Carbon based catalyst

Other oxidizing systems besides TEMPO show a strong potential in the substitution of metallic catalysts. These are based on the use of graphene materials in the form of graphene oxide or graphene doped N.

Graphene oxide (GO) is an easily available and inexpensive material, it allows to prepare chemically modified graphene. GO-based materials are of great interest because of their electronic properties. The relatively harsh conditions used in typical GO synthesis protocols (Hummers method) have introduced a variety of oxygen-containing features, for example, hydroxyl, epoxy, carboxylic acids and

others. As a result, these features give GO weak acidic properties ($\text{pH } 4.5$ to $0.1 \text{ mg}\cdot\text{mL}^{-1}$) and strong oxidizing properties. It is therefore used as a catalyst support, solid acid, and of course as oxidant [153]. (Figure 2.6)

These acidic and oxidizing properties were exploited by the team of Lv et al. in combination with TEMPO for the conversion of HMF to DFF. They were able to demonstrate the interest and effectiveness of this strategy for this oxidation under mild conditions and without metals. Thus, GO was found to be very effective with TEMPO used as co-catalyst for the selective oxidation of HMF into DFF. It has been demonstrated that GO could function as an oxidant in anaerobic oxidation of HMF by reduction of the carboxyl groups [138]. Full HMF conversion and 99.6% of DFF selectivity are obtained under optimal conditions (Table 2.4, Entries 2 and 3).

Similar to acid catalysis, metal-free carbon based materials have gained the attention of researchers and scientists due to its wide range of applications from catalysis to energy storage. [154–157] The traditional oxidation of alcohols to carbonyls can be achieved in several ways. To encourage green chemistry, organocatalytic systems have gained attention and heavy and noble metal complex systems are substituted by carbonaceous materials. Graphite, graphene oxide, and nitrogen enriched carbonaceous materials are capable of catalyzing the selective oxidation of alcohols to carbonyls. [158–160]

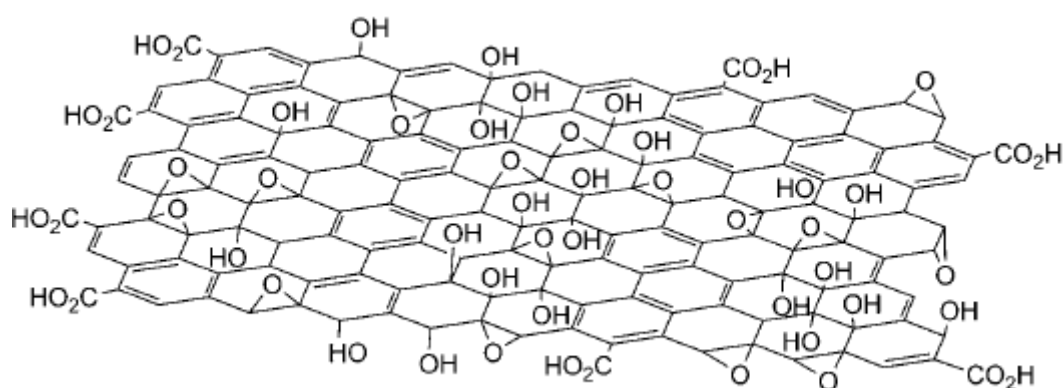


Figure 2.6 - Structural model of graphene oxide (GO) on the basis of proposed structure of ref [153].

With carbon nitride catalyst, it is very interesting to note that the presence of basic groups in these compounds can prove to be particularly beneficial. The nitrogen-enriched catalysts allow working under neutral conditions. This is the case with N-doped graphene and activated carbon which have been used successfully in the aerobic oxidation of benzyl alcohols, hydroxyl alcohol and HMF. [158,161] Indeed, in 2015 Watanabe et al. reported various nitrogen-doped carbon materials that were prepared by processing activated charcoal with ammonia and hydrogen peroxide. Their catalytic performance were tested for aerobic oxidation of several alcohols including HMF remarkably using ethanol as a

solvent. For the oxidation of HMF, a conversion of 24% was achieved at 80 °C with the nitrogen-doped activated carbon catalyst in 15 h with a selectivity of 93% (table 2.4, entry 4) [161].

Lv et al. have, for example, enriched graphene with various functions containing nitrogen by treating graphene oxide with a stream of ammonia. The resulting catalysts were then tested for the selective aerobic oxidation of HMF in the presence of TEMPO as a co-oxidant and adding a co-catalyst. Under relatively mild conditions, 6 hours at 100 °C and under a pressure of one atmosphere, a complete conversion of HMF and a selectivity to DFF close to 100% were observed. The activation of oxygen could be shown to be due to nitrogenous graphitic species [162].

In addition, several teams were able to demonstrate the efficiency of nitrogen-doped carbon catalysts. This is, for example, the case of Nguyen et al. who reported a metal-free catalysis of aerobic HMF oxidation to FDCA using zeolitic-imidazole framework (ZIF-8) derived, nitrogen-doped nanoporous carbon (NNC) as heterogeneous catalyst. NNC-900 was obtained by calcination of ZIF-8 at 900 °C. NNC-900 was found to be the best catalyst to produce FDCA with a maximum yield of 80% passing by the main intermediates HMFCa and FFCA (Table 2.4, Entry 6) [163].

Krivtsov et al. reported the use of graphitic carbon nitride ($g\text{-C}_3\text{N}_4$) which shows a good photocatalytic activity in the oxidation of HMF to DFF in aqueous medium. The conditions were mild the reaction being carried out at room temperature, in water and in the presence of air as the oxidant, but the HMF concentration was relatively low 0.5 mmol.L^{-1} . Under artificial light irradiation, 42% HMF conversion and 45% DFF selectivity were obtained. The catalyst performance was enhanced under the sunlight reaching 50% of DFF selectivity and 40% of HMF conversion [164]. Similarly, this catalyst showed a good photocatalytic behavior in another study, where 85.6% of DFF selectivity and 31.2% of HMF conversion were achieved under the irradiation of light with wavelength $> 400 \text{ nm}$ (Table 2.4, Entry 8). These catalytic systems are very interesting but, at the same time, are limited by the concentration of starting substrates here the concentration of HMF is 2 mmol.L^{-1} [165]. The same team reported a scale up of the transformation on a solar pilot with a continuous flow photoreactor, using catalysts based on PCN (N and P doped carbon) and PCN- H_2O_2 . The flow rate was 12 L.min^{-1} with a catalyst concentration of 0.1 to 0.4 g.L^{-1} and an HMF concentration of 0.5 to 4 mmol.L^{-1} , the transformation was followed for 5 hours. The authors observed a 50% conversion of HMF with a selectivity of 80 to 90% of DFF. The results are comparable to those obtained in the laboratory scale photoreactor irradiated with both artificial UV lamps and natural sunlight. The pristine PCN sample showed higher HMF conversion compared to that of the PCN- H_2O_2 adduct, but the latter was more selective for DFF formation.[166]

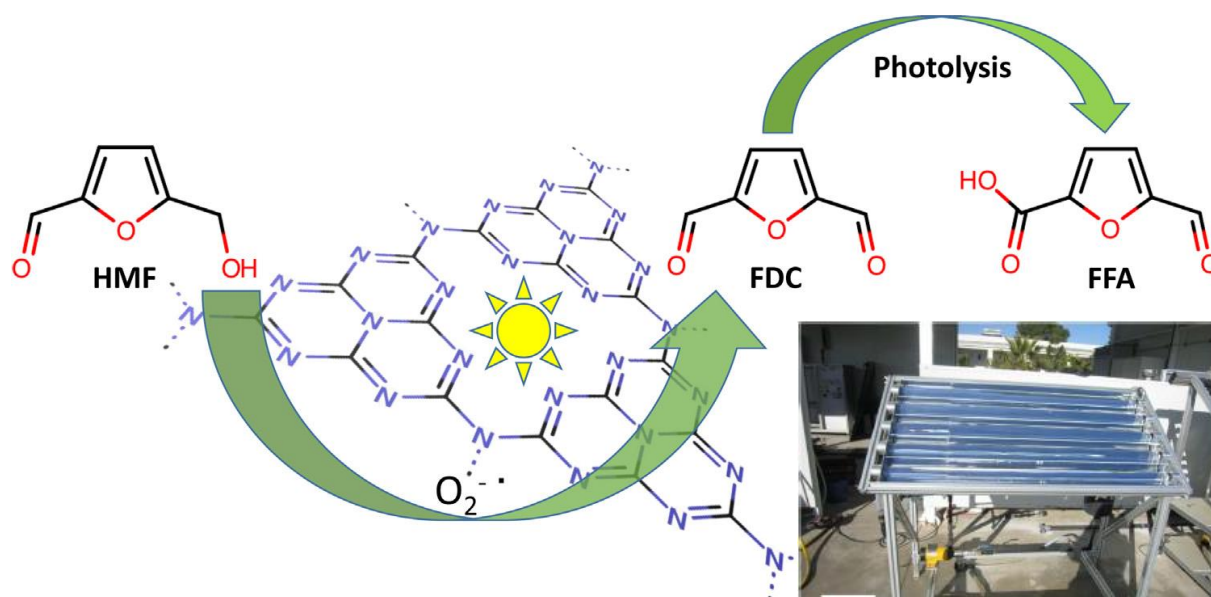


Figure 2.7 - Schematic representation of HMF oxidation over polymeric carbon nitride ($g\text{-C}_3\text{N}_4$) catalyst in presence of oxygen. [164] And the solar pilot plant for continuous flow oxidation. [166]

The natural nitrogenous osidic polymer chitosan is described as a very interesting precursor for the synthesis of carbonaceous materials enriched in nitrogen obtained by simple pyrolysis. By following this approach, Verma et al. evaluated a porous carbon nitride (PCNx) as a solid catalyst for the selective oxidation of HMF to FDCA. The PCNx with the highest catalytic activity was synthesized by calcination of chitosan under nitrogen at 300 °C. After 36 hours and at 70 °C, 83% of FDCA have been obtained from HMF oxidation under atmospheric air pressure (Table 2.4, Entry 10) [167]. The catalytic activity of this type of materials greatly depends on the surface area and the type of nitrogen atoms. In addition, following an identical strategy, Youngshen reported the preparation of the NC-950 catalyst by pyrolysis of chitosan in the presence of urea under nitrogen atmosphere at 950 °C. The as prepared nitrogen-doped carbon materials, NC-950 showed the highest stability and catalytic activity towards the oxidation of HMF due to its large surface area. The oxidation was initially promoted by HNO_3 (0,15 eq.) and oxygen was used as co-oxidant (10 bar). With an initial concentration of $0.05 \text{ mol}\cdot\text{L}^{-1}$, full HMF conversion with 95.1% of DFF yield was obtained in 14 hours at 100 °C in acetonitrile (Table 2.4, Entry 11) [168].

Table 2.4 - HMF oxidation methods using carbon-based catalysts

Entry	Catalyst	Solvent	Oxidant	T(°C)	T(h)	Conversion (%)	Product	Yield (%)	Ref.
1	GO	ACN	Air, 1 bar	100	12	9.5	DFF	86.3	[138]
2	GO/TEMPO	ACN	Air, 1 bar	100	18	100	DFF	99.6	[138]
3	GO/TEMPO	ACN	O_2 , 4 bar	100	9	100	DFF	99.5	[138]
4	N-doped activated Carbon	EtOH	Air, 1 bar	80	15	24	DFF	22%	[161]
5	NG-800/TEMPO	ACN	Air, 1 bar	100	6	100	DFF	99.5	[162]

	(no acid-base additive)								
6	NNC-900 3 eq. K ₂ CO ₃	Water	O ₂ , 1 bar 100ml/min	80	48	100	FDCA	80	[163]
7	g-C ₃ N ₄ hv	H ₂ O	Air	RT	4	40	DFF	20	[164]
8	g-C ₃ N ₄ hv	ACN and PhCF ₃	O ₂ , 10 mL/min	-	6	31.2	DFF	26.7	[165]
9	PCN hv Or PCN-H ₂ O ₂ hv	H ₂ O, 12 L/min	Air, 1 atm	42- 45	5	50	DFF	43	[166]
10	PCN _x	Water	Air, 1 bar	70	36	100	FDCA	83	[167]
11	NC-950	ACN	HNO ₃ /O ₂ , 10 bar	100	14	100	DFF	95.1	[168]

Finally, these catalysts look very promising as they allow to replace metallic catalysis by materials based on carbon very common and relatively simple to prepare. From a mechanistic point of view, it has been possible to demonstrate a strong activation of oxygen in radical superoxide species $\bullet\text{O}_2^-$, acting as a highly selective oxidant of dehydrogenation.

In the case of graphene oxide, the contribution of carboxylic acid functions as a primary oxidant has been demonstrated. With N-doped graphite-type materials, the catalytic activity is attributed to the different nitrogen species of the type pyridinic-N, pyrrolic-N and graphitic-N, giving them semi-metal properties. These doped graphitic nitrogen species have the effect of modulating the electronic structure of sp² carbon materials. Near nitrogen carbons, an electronic structure with a metal band is observed, making these materials capable of generating the formation of reactive oxygen species. As a result, excited conduction band electrons (LUMO) reduce molecular oxygen to form $\bullet\text{O}_2^-$ under mild conditions. In application to oxidation of HMF, these catalysts are very active for its selective aerobic oxidation.

3.1.3. Organic catalysts

The use of iodine and its derivatives as an oxidant or co-oxidant also offer attractive strategies for selective oxidation without metals. Iodine is used in several degrees of oxidation and depending on the conditions helps to regulate its oxidizing power. For example, hypervalent iodine derivatives are known for the selective oxidation of primary alcohols into aldehydes [169,170] particularly 2-iodoxybenzenesulfonic acid (IBS) [171]. We have been able to demonstrate the effectiveness of this catalyst in selectively converting HMF to DFF. Under optimal conditions, DFF yield was 89% with total conversion of HMF (table 2.5, entry 1) with high grade of purity using IBS catalyst and Oxone as co-oxidant. Interestingly, this method could be extended to a gram-scale production of DFF without any effect on the selectivity. [172] This method will be discussed in details in Chapter 3. Among the hypervalent iodine derivatives we have seen previously that [bis(acetoxy)-iodo] benzene has also been used with interest as a co-oxidant in combination with TEMPO for the selective oxidation of HMF to

DFF. Under these mild conditions 66 and 73% DFF yield are obtained selectively in the presence of low proportions of TEMPO.[146,147] Descotes et al. also demonstrated the benefit of using iodine as a co-oxidant in the presence of TEMPO, for a selective transformation of HMF into DFF. Only a 2/100 ratio of TEMPO/HMF was necessary to obtain at room temperature 58% of DFF.[141] Finally, Hazra and co-workers developed a metal-free synthesis of carboxylic acid from aldehyde and alcohol groups catalyzed by $I_2/NaOH$ in presence of tertibutylhydroperoxyde (TBHP) as co-oxidant. Their work indicates that IO_2^- is the most likely active catalyst, which was formed and regenerated by the oxidation of IO^- by TBHP. One of many potential applications of this technique was the oxidation of HMF to FDCA in water as the reaction medium. The use of $I_2/NaOH/TBHP$ enables a gram-scale oxidation of HMF to FDCA with a yield of 53% or in 41% by a one-pot synthesis from D-fructose (Table 2.5, entry 5). [173]

Table 2.5 - HMF oxidation methods using organic catalysts

Entry	Catalyst	Solvent	Oxidant	T(°C)	T(h)	Conversion (%)	Product	Yield (%)	Ref.
1	IBS ^a	CH ₃ NO ₂	Oxone	70	4	100	DFF	89	[172]
2	AcOH-TEMPO	AcOEt	TEMPO/BAIB/AcOH	30	0.75	-	DFF	66	[146]
3	TEMPO-SBA-15	AcOEt	BAIB, AcOH/O ₂	40	1	-	DFF	73	[147]
4	TEMPO/KOH	DCM/H ₂ O	TEMPO/ I ₂	RT	2	-	DFF	58	[143]
5	I ₂ /NaOH	Water	TBHP	70	10-16	-	FDCA	53	[173]

[a] 2-iodoxybenzenesulfonic acid

3.2. Metal-free catalysts for the oxidation of furfural

As in the case of HMF, metal catalytic oxidations of furfural showed high efficiency and excellent selectivity. Despite these advantages, they will always have a big constraint; the use of metals and heavy metals. This limitation includes the deactivation problem of metal catalysts, their high cost, treatment and recyclability efficiency and the production of toxic wastes. Under the environmental regulations, these processes must now be sustainable with minimal impact on the environment.

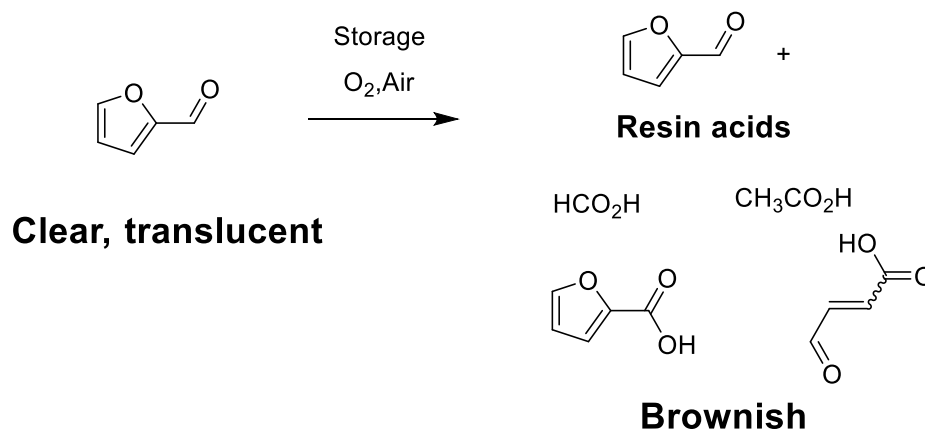
In this part, we will present all metal-free catalytic oxidations of furfural

3.2.1. Acid catalysis

The autoxidation of furan derivatives has been observed and studied since long time [174,175].

Furfural left in the open-air take on a particular brown color. The oxidation products have been identified as a complex mixture of acids, volatile or not, compounds among others, of acids, formic, acetic, furoic, β -formylacrylic, as well as acid resins resulting from the polymerization of furfural in the

presence of these acids and giving this characteristic brownish appearance to solutions of furfural in contact with oxygen. In order to prevent autoxidation and polymerization in an acidic environment, it is possible to add anti-oxidants such as hydroquinone and bases such as tertiary amines. Under these conditions, oxidation can be inhibited. Obviously, this oxidation phenomenon is faster as the surface area of furfural exposed to oxygen is larger.



Scheme 2.5 - Furfural autoxidation in presence of air.

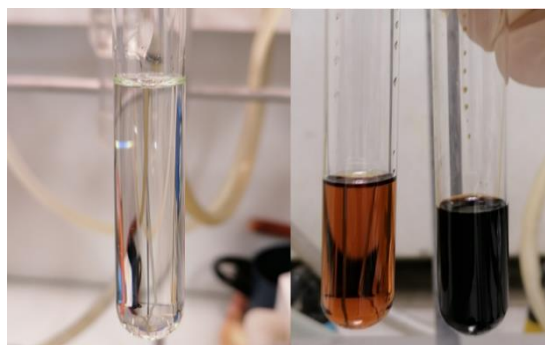


Figure 2.8 - Furfural evolution with time by autoxidation

Acid catalysis represents a large part of the oxidation methods of furfural reported in the literature. Ebitani et al. published two articles dealing with the research and optimization of a method for the oxidation of furfural and its derivatives into succinic acid. A panel of Lewis and Bronsted acids in homogeneous and heterogeneous phases were tested. The acids were used in catalytic proportions. The best results were obtained with Amberlyst-15 by working at 80 °C in water as solvent and in the presence of hydrogen peroxide as an oxidizer with a molar ratio hydrogen peroxide/furfural of four. Under these conditions, 74% of succinic acid (SA) mixed with 11% of maleic acid (MA) were obtained. Traces of fumaric and furoic acids were also reported. [136,176] Note that equivalent results were observed with APTS in the homogeneous phase, but the separation of Amberlyst-15 by filtration makes its use much more advantageous. Strong mineral acids such as H₂SO₄ or HCl then gave intermediate yields of the order of 45 to 50% of SA, and finally Lewis acids the lowest yields around 10 to 25% (Table 2.6, entry 1). The same conditions were applied by Rakshit et al. directly on a raw grade of furfural

obtained by dehydration of hemicellulose prehydrolysate. The furfural being obtained in toluene during the dehydration step, the oxidation takes place in a biphasic water-toluene medium and the final yield of succinic acid is thereby slightly affected 52%. [177,178]

Similarly, the sulfonated catalyst could be prepared directly from polystyrene waste. Granados et al. prepared several catalysts by sulfonation of different polystyrene sources recovered in different packaging and demonstrated the possibility of recycling it through several acid catalyzed reactions for biomass valorization, including the oxidation of furfural. The transformations were carried out in the aqueous phase with hydrogen peroxide as oxidizing agent. Mixtures of diacids have been obtained with a predominance for MA and SA. [179]

Smopex 101 is another polymer-supported sulfonic acid catalyst, used under identical conditions by Murzin et al. This catalyst was also very effective, depending on the protocol used in batch or semi-batch mode, the yield of succinic acid varies from 60 to 80%. Detailed kinetic studies confirmed the different mechanisms leading to succinic and maleic acids. [180,181]

A first strategy using a biphasic water/tetrachloroethane system was described in 2011 by Yin et al. which allows furfural to be selectively oxidized to maleic acid.[109] The reaction was catalyzed by phosphomolybdic acid and oxygen as the oxidizing agent. Using oxygen, or better, air as an oxidant gives at least two remarkable advantages, they are very economical oxidants and the weight percentage (wt%) of the constituents is improved. In this case, the wt% of furfural was 5.8% which is good compared to other oxidation methods. The authors demonstrated that the oxidation took place in the aqueous phase. With this method the conversion of furfural was relatively low 50.3% and the selectivity and the yield of maleic acid were 69% and 35%. However, the solubility of furfural and maleic acid being opposite for each of the two phases, the separation of the products and the recycling at the end of the reaction were all made easier.

Wang et al. also developed a protocol using a biphasic system for selectively oxidized furfural to 2(5H)-furanone.[182] Formic acid was found to be the best acid catalyst of the panel of acids tested. The oxidizing agent used was hydrogen peroxide with a relatively low molar ratio Oxidant/furfural = 2.4, which limit the oxidation of furfural to furanone without forming too many diacids. In addition, the furanone produced is extracted gradually in the organic phase avoiding overoxidation. Note that formic acid reacts with hydrogen peroxide leading to formic peracid, which is the oxidizing agent in this system. The maximum yield and the greatest selectivity to 2(5H)-furanone was obtained with 1,2 dichloroethane (1,2-DCE) as organic solvent in this study. However, small proportions of succinic acid (12%) and maleic acid (6%) were observed.

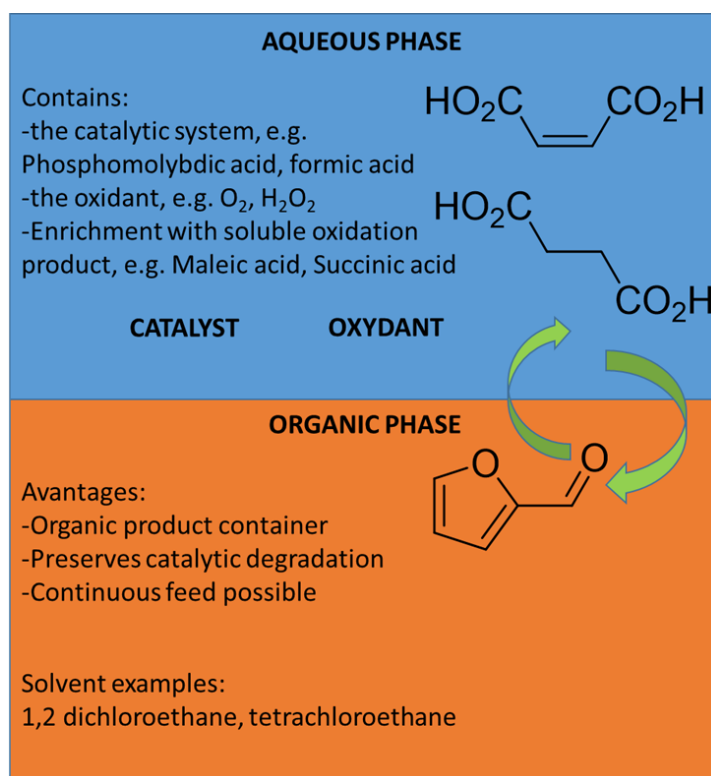


Figure 2. 9 - Recapitulation of furfural oxidation in biphasic systems

Under different conditions, maleic acid can be produced almost quantitatively from furfural. By keeping formic acid as a catalyst but also as a solvent and by considerably increasing the amount of hydrogen peroxide. Thus with a molar ratio of oxidant/furfural = 10,1, maleic acid was obtained with a yield of 95%. [183]

Among the organic acids, Betaine Hydrochloride (BHC, Figure 2.10) showed good catalytic properties for the transformation of furfural into maleic and fumaric diacids. This was recently demonstrated by Vigier et al. who used it as a catalyst in the presence of hydrogen peroxide in water as a solvent. [184] At a temperature of 100 °C and with an oxidant/furfural molar ratio equal to 10, a total conversion of the furfural was observed and yields of 61% maleic acid and 31% fumaric acid were measured, *i.e.* a 90% overall yield of C4 diacids. At 100 °C the transformation is particularly rapid since it was completed in half an hour. Note that BHC is a biobased product obtained as a co-product from the beet sugar industry. In addition, since BHC is insoluble in acetone, it was possible to precipitate it and to easily separate it by filtration after adding acetone to the reaction medium, which allows it to be recycled 6 times. The same authors having previously demonstrated the possibility of carrying out the dehydration of xylose by BHC in water at 180 °C, they carried out in one pot two steps the dehydration of xylose to furfural (48%) followed by its oxidation to diacids. The overall yield of maleic acid was 17% and 4% fumaric acid, with a starting quantity of xylose of 0.8 wt%.

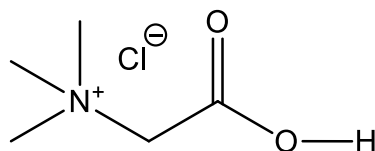


Figure 2.10 - Betaine Hydrochloride (BHC) structure

Succinic acid was obtained by catalysis with sulfonated graphene oxide at 1.2 wt% sulfur content and which proved to be remarkably effective and selective [229]. Only 0.27 wt% of this catalyst was sufficient in the presence of hydrogen peroxide to obtain more than 88% succinic acid and traces of maleic and furoic acids. This result should be compared with other sulfonated acids such as APTS, Amberlyst or sulfuric acid. All selectively and predominantly led to succinic acid, but none was used in such low proportions [160,185–187]. The sulfonated β -cyclodextrin used as another heterogeneous catalyst also effectively resulted in the conversion of furfural to succinic acid. Under optimal conditions, Maneechakr et al. reported a yield of 81% succinic acid and the advantage of being able to recycle and regenerate the catalyst many times. [230] Badovskaya et al. explored the oxidation of furfural using selenium dioxide and hydrogen peroxide at 50 °C during 2 hours. [140] When adding ethanol (EtOH) or acetamide (AcNH₂) to the reaction mixture, 70% of ethoxy-2(5H)-furanone and 60% of 5-acetamido-2(5H)-furanone were obtained respectively (Table 2.6, entries 18 and 19). Furthermore, Badovskaya et al. studied the influence of the pH medium on the oxidation reaction of furfural in water-hydrogen peroxide system.[139] It was found that the process was slow in low acidic media (pH 5-7), and the consumption of furfural was greater in more acidic media. When the pH was maintained below 3, the conversion was almost total and the reaction was more selective towards 2-(5H)-furanone but when working in higher pH medium (up to 7), the conversion decreased to around 50% and the reaction became more selective towards furoic acid (Table 2.6, entries 20 and 21).

On the other hand, furfural oxidation in more complex media have been evaluated as well. Rakshit et al. worked on a biphasic system to produce succinic acid from furfural. Toluene was found to be the best solvent to convert FUR into SA. However, the oxidant H₂O₂ is immiscible in toluene and miscible in water, therefore a 10% V/V of water was added to solubilize the mixture. 50 mg of Amberlyst-15 was enough to carry out the oxidation reaction of FUR to produce SA in a 49% yield at 80 °C (Table 8, entry 15). [188] In parallel, the oxidation of furfural, in dichloromethane (DCM) using H₂O₂ as oxidant and in the presence of sodium sulfate, afforded the production of 2(3H)-furanone and 2(5H)-furanone (Table 2.6, entry 16). This mixture was separated by distillation and 2(3H)-furanone could be converted to 2(5H)-furanone by isomerization in the presence of triethylamine (Et₃N). [189] On the other hand, according to experimental results and based on the activation parameters, the action of H₂O₂ on furan compounds involves an autocatalytic transition state complex. [190] Eventually, 2-(5H)-furanone could

be produced from furfural in a high yield (61%) by an oxidation reaction using formic acid as the catalyst, H₂O₂ as the oxidant and ethyl acetate as the solvent (Table 2.6, entry 21). [191]

Recently, interesting results were obtained by acetic acid catalysis in the presence of 1.2 hydrogen peroxide equivalents. With this low quantity of oxidant, as expected the 2-(5H)-hydroxyfuran was formed mostly with 71% yield, some secondary products being also produced, including maleic acid 11% and other acids such as succinic, Fumaric and formic, but less than 10%. Surprisingly the presence of traces of cinnamic acid was observed at 1%. Note that these results were obtained with a very high mass percentage of FUR of 16%, so this is the best method so far for a large-scale preparation of 2-(5H)-furanone. (Table 2.6, entry 22) [192] Subsequently, 2-(5H)-furanone could be further hydrogenated to obtain γ -butyrolactone, which is also an important product that has been widely used in the fields of medicine, chemicals and fine organic synthesis.

Table 2.6 - Furfural oxidation using acid catalysis

Entry	Catalyst (wt %)	Fur. wt %	Solvent	Oxidant (m.r. O/F or pressure MPa)	T(°C)	t(h)	Conversion (%)	Product	Yield (%)	Ref.
1	Amberlyst-15 (1,4%)	2,7	Water	H ₂ O ₂ (4)	80	24	>99	SA	74	[176]
								MA	11	[136]
2	Amberlyst-15 (0,5%)	1	Water-Toluene	H ₂ O ₂ (4)	80	24	>99	SA	52	[177]
										[178]
3	- PSSA ^a (3,6%) - WTC-PSSA (3,6%)	4,5	Water	H ₂ O ₂ (15)	50	24	100	SA	27,5	[179]
								MA	45,8	
								FO	17,5	
								others	6,1	
4	Smopex-101 (0,7%)	4	Water	H ₂ O ₂ (3-4)	80	8	80	SA	80	[180]
										[181]
5	Formic Acid (4%)	10	1,2 DCE-Water	H ₂ O ₂ (2,4)	60	3	>99	FO	62	[182]
								SA		
								MA	12	
									6,3	
6	Formic Acid (80%)	1,6	Formic Acid	H ₂ O ₂ (10,1)	60	4	100	MA	95	[183]
7	BHC ^b (16%)	4,0	Water	H ₂ O ₂ (10)	100	0,5	100	MA	61	[184]
								FA	31	
8	Graphene Oxide (0,27%)	2,55	Water	H ₂ O ₂ (6)	70	24	>99	SA	88,2	[193]
								MA	1,1	
								Furoic Acid	0,8	
9	SO ₃ H-cyclodextrin (2,25%)	0,6	Water	H ₂ O ₂ (4,5)	60	1,1	-	SA	81,2	[194]
10	Nafion NR50	2.7	Water	H ₂ O ₂	80	24	>99	SA	41	[136]
11	Nafion SAC13	2.7	Water	H ₂ O ₂	80	24	>99	SA	29	[136]
12	TsOH	2.7	Water	H ₂ O ₂	80	24	>99	SA	72	[136]

13	H ₂ SO ₄	2.7	Water	H ₂ O ₂	80	24	>99	SA	45	[136]
14	Amberlyst-15	1.9	Water+toluene	H ₂ O ₂	80	24	>99	SA	49	[188]
15	-	-	DCE	H ₂ O ₂ +Na ₂ SO ₄	60-70	12	100	FO	67	[189]
16	-	-	-	H ₂ O ₂	60-70	-	100	SA FO	40 40	[116]
17	- ^a	-	Water	H ₂ O ₂	60	4	100	FO SA	50 40	[115]
18	- ^b	-	Water	H ₂ O ₂	60	4	50	FA SA	65 20	[115]
19	-	-	Ethanol	H ₂ O ₂	60	3.5	70	Furfural α-hydroxy hydroperoxide	70	[195]
20	-	-	Dioxane	H ₂ O ₂	60	7.3	70	Furfural α-hydroxy hydroperoxide	98	[195]
21	Formic acid	-	Ethyl acetate	H ₂ O ₂ +Na ₂ SO ₄	60	3	100	FO	61.5	[191]
22	Acetic acid	19	Water	H ₂ O ₂	60	24h	-	FO MA	71	[192]

11

[a] pH=1, [b] pH=7.

3.2.2. Basic catalysis

In the same manner as acid catalysis described above, the oxidation of furfural in a basic medium has also been reported.

The oxidation of furfural to furoic acid was reported by disproportionation of furfural by applying the famous method described by Cannizzaro on non-enolizable aldehydes. According to this process, the maximum yield of acid can only be 50% because half of the starting material is reduced in alcohol. A step of neutralization of the residual base and of the sodium carboxylate obtained is to be expected. This method was used successfully by Wilson in 1926 by transforming 1 kg of furfural to which was added an aqueous solution of caustic soda at 33.3% [196]. The temperature of the reaction medium was maintained at less than 20 °C and the transformation lasted 2 hours. Furfuryl alcohol was separated from furoic acid in its sodium carboxylate form by liquid/liquid extraction. Then the furoic acid was precipitated and purified by successive recrystallizations. The yield of furoic acid obtained was 32%. Although this method is the oldest, and despite the yield was relatively low, no other method allows to work on quantities of furfural in such a high weight percent (wt%), with these conditions the

furfural represents 55 wt% of the reaction medium, which is remarkable and unmatched. For this reason and the fact that furfuryl alcohol is easily recoverable and desirable, this process is still in line with industrial development.

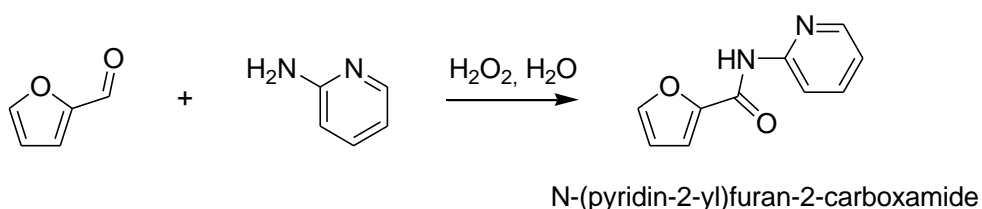
Much more recently, furoic acid was obtained by oxidation in a basic medium using salts of sodium sulphate and chloride previously mixed with hydrogen peroxide. This results in a white solid having a clathrate structure in which the Na^+ , SO_4^{2-} and Cl^- ions organize themselves in a cage having the dimensions of H_2O_2 . The hydrogen peroxide trapped in these cavities serves as a stable and easy to handle source of oxidizing agent. Water was again used as a solvent, and sodium hydroxide as the best base. The optimization of the reaction was carried out on 4-bromobenzaldehyde and then applied to furfural. According to this protocol 85% of furoic acid was isolated.[197]

The oxidation of furfural in a basic medium was reported recently in the presence of N-heterocyclic carbene (NHC) by Nakajima et al. [83] This method allowed to oxidize furfural to furoic acid quantitatively. The reaction takes place in DMSO at 40 °C over four hours and under a pressure of 0.1 MPa of oxygen in a Teflon autoclave. The same group of researchers demonstrated that it is also possible to obtain furoic acid in two relatively simple steps from xylose, keeping the same solvent. A first dehydration step was carried out in DMSO in the presence of Amberlyst-70 which was filtered, then during a second step the reaction mixture without further purification was subjected to oxidation according to the method developed, thus 57% furoic acid was obtained in the final reaction mixture. This method is remarkably efficient given the low temperature but required the use of a pressurized medium.

While the methods of oxidation of furfural without metals in a basic medium all led to furoic acid, the mixtures of KBr salts with KOH or graphitic carbon nitride ($\text{g-C}_3\text{N}_4$) led to the exclusive production of maleic acid. Indeed, Li et al. reported that with 3 wt% of these catalytic systems, using water as solvent and H_2O_2 as oxidant, maleic acid was obtained with a yield of about 70%.[198]

3.2.3. Oxidative amidation

Among the various methods of oxidation in a basic medium, let us mention the case of oxidative amidation (Scheme 2.6). The reaction medium was basic due to the use of amines as starting material.



Scheme 2.6 - Oxidative amidation of furfural

This transformation could be carried out without metal catalysis with success on furfural with the method developed and optimized on benzaldehyde by Maheswari et al. [199] Only 2-aminopyridine was specifically used for the transformation into an amide. This type of transformation is usually catalyzed by copper salts. In this case, only hydrogen peroxide was used as an oxidizer, and the solvent was water. With this method an isolated amide yield of 80% was reported. Moreover, Nguyen et al. reported the catalytic oxidation of furfural using nitrogen-doped carbon catalyst NC-900 [200]. After a parametric study (reaction conditions, solvent type, time, operating temperature, H₂O₂ concentration...), a total conversion of furfural and a high yield of MA (61%) could be achieved in 5 hours at 80 °C (table 2.7, entry 6).

Table 2.7 - Furfural oxidation using basic catalysis

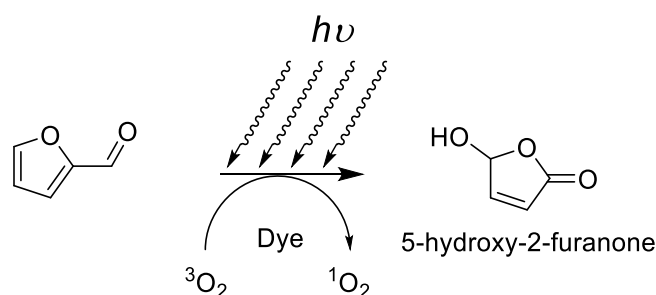
Entry	Catalyst (wt %)	Fur. wt %	Solvent	Oxidant (m.r. O/F or pressure MPa)	T(°C)	t(h)	Conversion (%)	Product	Yield (%)	Ref.
1	NaOH (13%)	55	Water	Furfural (0,5)	>20	2	-	FA	32	[196]
2	NaOH (1%)	1,5	Water	4Na ₂ SO ₄ .2H ₂ O ₂ . NaCl (1,7)	80	4	-	FA	85	[197]
3	NHC ^a : - BTIC, DBU (6,0%) - BTDIY (1,0 %)	2,0 2,1	DMSO	O ₂ (0,1 MPa)	40	4	>99	FA	99	[83]
4	- KBr/KOH (3,1%) - KBr/g-C ₃ N ₄ (3,1%)	3,0 3,0	Water	H ₂ O ₂	100	3	>99	SA SA	68,4 70,4	[198]
5	- No catalyst	3,8	Water	H ₂ O ₂ (3)	80	4	-	Amide ^d	80	[199]
6	NC-900	1.9	Water	H ₂ O ₂	80	5	100	MA	61	[200]

3.2.4. Photochemical oxidation of furfural

The photochemical excitation of oxygen from its triplet ground state to the excited singlet state using a photosensitizer under light irradiation has long been known and has been used brilliantly to oxidize furfural (scheme 2.7). It was first described by Schenck in 1953, using eosin as a photosensitizer. The generated singlet oxygen adds to the furfural leading to the formation of unstable endoperoxide which rearranges into 5-hydroxy-2-furanone. [202,203] Note that the methyl and ethyl ethers of 5-hydroxy-2-furanone were obtained when the transformation temperature is greater than 40 °C in the presence of methanol or ethanol solvents. [204,205] Since then other teams have used the same strategy with other photosensitizers such as the very effective Rose Bengal or Methylene Blue. The direct use of sunlight and a solar photoreactor have been shown to achieve this oxidation. [206,207] New custom-designed photoreactors allowed continuous flow transformation. [208] And it has been shown that relatively energy efficient light sources such as compact fluorescent lamps could be used. [209] This

transformation was selective for 5-hydroxy-2-furanone which could be formed quantitatively. A racemic mixture of two enantiomers was obtained. The latter could be separated, for example, by synthesis of intermediate diastereoisomers by coupling the racemic mixture of 5-hydroxy-2-furanone with menthol. Note that the kinetics of photo-oxidation of furfural diethyl acetal is about 140 times faster than that of furfural. Depending on the conditions, forming this intermediate in situ could significantly accelerate the transformations.

This oxidation strategy has been used for many applications; in 2013, Hoffmann et al. derived 5-hydroxy-2-furanone as a surfactant. [210] Very recently, this method was used by Gu et al. in the first step of the synthesis of quinaldic acids [211] and by Thiyagarajan et al. to obtain selectively maleic acid from furfural in two steps. By combining a first step of photochemical oxidation of furfural to 5-hydroxy-2-furanone followed by a second step of electro or biochemical oxidation. [212]



Scheme 2.7 - Photo-oxidation of furfural in the presence of singlet oxygen generated in situ

Furthermore, Schenk and others have extended the same strategy to other derivatives derived from furfural notably furoic acid and furfuryl alcohol which also lead to 5-hydroxy-2-furanone. [202,213–216]

The photochemical oxidative degradation of furfural has also been studied and reported for the purpose of pollution control, the optimum degradation conditions combine the use of hydrogen peroxide under UV irradiation. The degradation products were not described, but the pH metric degradation monitoring showed acidification of the medium. [217] In comparison with HMF, it is interesting to note that the new catalysts based on $g\text{-C}_3\text{N}_4$, which have demonstrated interesting properties for the activation of oxygen, have not yet been tested on furfural. [164,165]

4. Conclusion

To develop greener and more sustainable processes, impressive studies have been made through the last decades by employing metal-free catalysts in a wide range of chemical reactions. The aim of this chapter was to demonstrate the potential and effectiveness of metal-free catalysts, for the oxidation of biomass-derived products (furfural and HMF) into numerous value-added chemicals. Notably, metal-free catalysts are cheap and efficient for various industrially important applications. Comparing

it with main described metal catalysts, we proved that metal-free oxidation of biomass-derived products showed a competitive performance. For HMF oxidation, acid catalysts like Amberlyst-15 and IBS afforded great conversion and yield with possibility to scale-up the process to gram scale. Moreover, carbon based catalysts; especially GO with TEMPO, provided total conversion with more than 99% DFF yield. For furfural oxidation, acid catalysts showed great selectivity towards diacids (SA, MA...) while basic catalysts were more selective towards furoic acid.

In conclusion, we were able to reflect on the combination of the advantages of the different methods and move quickly towards the conditions that seemed most effective to us. We therefore explored several paths that seemed to us to be the most advantageous following different catalytic strategies in agreement with sustainable development. In the following chapters, we will develop the results obtained from this exploratory research according to the conditions of the different catalytic systems.

References

1. Alonso, D.M., Bond, J.Q., and Dumesic, J.A. (2010) Catalytic conversion of biomass to biofuels. *Green Chem.*, **12** (9), 1493–1513.
2. Clark, J.H., Budarin, V., Deswarte, F.E.I., Hardy, J.J.E., Kerton, F.M., Hunt, A.J., Luque, R., Macquarrie, D.J., Milkowski, K., Rodriguez, A., Samuel, O., Tavener, S.J., White, R.J., and Wilson, A.J. (2006) Green chemistry and the biorefinery: A partnership for a sustainable future. *Green Chem.*, **8** (10), 853–860.
3. Sun, Y., and Cheng, J. (2002) Hydrolysis of lignocellulosic materials for ethanol production: A review. *Bioresour. Technol.*, **83** (1), 1–11.
4. Yan, X., Inderwildi, O.R., and King, D.A. (2010) Biofuels and synthetic fuels in the US and China: A review of Well-to-Wheel energy use and greenhouse gas emissions with the impact of land-use change. *Energy Environ. Sci.*, **3** (2), 190–197.
5. Solomon, B.D. (2010) Biofuels and sustainability. *Ann. N. Y. Acad. Sci.*, **1185**, 119–134.
6. Brownlee, H.J., and Miner, C.S. (1948) Industrial Development of Furfural. *Ind. Eng. Chem.*, **40** (2), 201–204.
7. Binder, J.B., Blank, J.J., Cefali, A. V., and Raines, R.T. (2010) Synthesis of furfural from xylose and xylan. *ChemSusChem*, **3** (11), 1268–1272.
8. Eseyin, A.E., and Steele, P.H. (2015) An overview of the applications of furfural and its derivatives. *Int. J. Adv. Chem.*, **3** (2), 42.
9. De Jong, W., and Marcotullio, G. (2010) Overview of biorefineries based on co-production of furfural, existing concepts and novel developments. *Int. J. Chem. React. Eng.*, **8**.
10. Hoang, T.M.C., Van Eck, E.R.H., Bula, W.P., Gardeniers, J.G.E., Lefferts, L., and Seshan, K. (2015) Humin based by-products from biomass processing as a potential carbonaceous source for synthesis gas production. *Green Chem.*, **17** (2), 959–972.
11. Fitzpatrick, S.W. (1990) Lignocellulose degradation to furfural and levulinic acid. US Pat. n°4897497, issued 1990.
12. Girisuta, B., Janssen, L.P.B.M., and Heeres, H.J. (2006) A kinetic study on the decomposition of 5-hydroxymethylfurfural into levulinic acid. *Green Chem.*, **8** (8), 701–709.
13. Liu, F., Boissou, F., Vignault, A., Lemée, L., Marinkovic, S., Estrine, B., De Oliveira Vigier, K., and Jérôme, F. (2014) Conversion of wheat straw to furfural and levulinic acid in a concentrated aqueous solution of betaine hydrochloride. *RSC Adv.*, **4** (55), 28836–28841.
14. Robert Wojcieszak, Francesco Santarelli, Sébastien Paul, Franck Dumeignil, F.C., and Gonçalves, and R. V (2015) Recent developments in maleic acid synthesis from bio-based chemicals. *Sustain Chem Process*, **3** (9).
15. Krawielitzki, S., and Kläusli, T.M. (2015) Modified hydrothermal carbonization process for producing biobased 5-HMF platform chemical. *Ind. Biotechnol.*, **11** (1), 6–8.
16. Sajid, M., Zhao, X., and Liu, D. (2018) Production of 2,5-furandicarboxylic acid (FDCA) from 5-

hydroxymethylfurfural (HMF): Recent progress focusing on the chemical-catalytic routes. *Green Chem.*, **20** (24), 5427–5453.

17. Xia, H., Xu, S., Hu, H., An, J., and Li, C. (2018) Efficient conversion of 5-hydroxymethylfurfural to high-value chemicals by chemo- and bio-catalysis. *RSC Adv.*, **8** (54), 30875–30886.
18. Cavani, F., Albonetti, S., Basile, F., and Gandini, A. (2016) 2,5-Furandicarboxylic Acid Synthesis and Use, in *Chemicals and Fuels from Bio-Based Building Blocks*, John Wiley & Sons, Weinheim, Germany, pp. 191–216.
19. Zhang, Z., and Huber, G.W. (2018) Catalytic oxidation of carbohydrates into organic acids and furan chemicals. *Chem. Soc. Rev.*, **47** (4), 1351–1390.
20. de Vries, J.G. (2017) Green Syntheses of Heterocycles of Industrial Importance. 5-Hydroxymethylfurfural as a Platform Chemical, in *Advances in Heterocyclic Chemistry*, vol. 121, Elsevier Science, Cambridge, pp. 247–293.
21. Hameed, S., Lin, L., Wang, A., and Luo, W. (2020) Recent Developments in Metal-Based Catalysts for the catalytic aerobic oxidation of 5-Hydroxymethyl-Furfural to 2,5-furandicarboxylic acid. *catalysts*, **10** (120), 1–26.
22. Kucherov, F.A., Romashov, L. V., Galkin, K.I., and Ananikov, V.P. (2018) Chemical Transformations of Biomass-Derived C6-Furanic Platform Chemicals for Sustainable Energy Research, Materials Science, and Synthetic Building Blocks. *ACS Sustain. Chem. Eng.*, **6** (7), 8064–8092.
23. Gupta, K., Rai, R.K., and Singh, S.K. (2018) Metal Catalysts for the Efficient Transformation of Biomass-derived HMF and Furfural to Value Added Chemicals. *ChemCatChem*, **10** (11), 2326–2349.
24. Signoretto, M., and Menegazzo, F. (2018) On the Oxidation of Furfural to Furoic Acid, in *Furfural An Entry Point of Lignocellulose in Biorefineries to Produce Renewable Chemicals, Polymers, and Biofuels*, pp. 197–215.
25. Manuel López Granados (2018) Catalytic Oxidation of Furfural to C4 Diacids-anhydrides and Furanones, in *An Entry Point of Lignocellulose in Biorefineries to Produce Renewable Chemicals, Polymers, and Biofuels* (eds. Granados, M.L., and Alonso, D.M.), world scientific, pp. 239–261.
26. Arias, P.L., Cecilia, J.A., Gandarias, I., Iglesias, J., López Granados, M., Mariscal, R., Morales, G., Moreno-Tost, R., and Maireles-Torres, P. (2020) Oxidation of lignocellulosic platform molecules to value-added chemicals using heterogeneous catalytic technologies. *Catal. Sci. Technol.*, **10** (9), 2721–2757.
27. Wojcieszak, R., Ferraz, C.P., Sha, J., Houda, S., Rossi, L.M., and Paul, S. (2017) Advances in base-free oxidation of bio-based compounds on supported gold catalysts. *Catalysts*, **7** (11), 1–23.
28. Motagamwala, A.H., Won, W., Sener, C., Alonso, D.M., Maravelias, C.T., and Dumesic, J.A. (2018) Toward biomass-derived renewable plastics: Production of 2,5-furandicarboxylic acid from fructose. *Sci. Adv.*, **4** (1), 1–9.
29. Ait Rass, H., Essayem, N., and Besson, M. (2015) Selective aerobic oxidation of 5-HMF into 2,5-furandicarboxylic acid with Pt catalysts supported on TiO₂- and ZrO₂-based supports. *ChemSusChem*, **8** (7), 1206–1217.

30. Verdeguer, P., Merat, N., and Gaset, A. (1993) Oxydation catalytique du HMF en acide 2,5-furane dicarboxylique. *J. Mol. Catal.*, **85** (3), 327–344.
31. Ait Rass, H., Essayem, N., and Besson, M. (2013) Selective aqueous phase oxidation of 5-hydroxymethylfurfural to 2,5-furandicarboxylic acid over Pt/C catalysts: Influence of the base and effect of bismuth promotion. *Green Chem.*, **15** (8), 2240–2251.
32. Chen, H., Shen, J., Chen, K., Qin, Y., Lu, X., Ouyang, P., and Fu, J. (2018) Atomic layer deposition of Pt nanoparticles on low surface area zirconium oxide for the efficient base-free oxidation of 5-hydroxymethylfurfural to 2,5-furandicarboxylic acid. *Appl. Catal. A Gen.*, **555** (January), 98–107.
33. Siankevich, S., Mozzettini, S., Bobbink, F., Ding, S., Fei, Z., Yan, N., and Dyson, P.J. (2018) Influence of the Anion on the Oxidation of 5-Hydroxymethylfurfural by Using Ionic-Polymer-Supported Platinum Nanoparticle Catalysts. *Chempluschem*, **83** (1), 19–23.
34. Ardemani, L., Cibir, G., Dent, A.J., Isaacs, M.A., Kyriakou, G., Lee, A.F., Parlett, C.M.A., Parry, S.A., and Wilson, K. (2015) Solid base catalysed 5-HMF oxidation to 2,5-FDCA over Au/hydrotalcites: fact or fiction? *Chem. Sci.*, **6** (8), 4940–4945.
35. Davis, S.E., Houk, L.R., Tamargo, E.C., Datye, A.K., and Davis, R.J. (2011) Oxidation of 5-hydroxymethylfurfural over supported Pt, Pd and Au catalysts. *Catal. Today*, **160** (1), 55–60.
36. Lei, D., Yu, K., Li, M.R., Wang, Y., Wang, Q., Liu, T., Liu, P., Lou, L.L., Wang, G., and Liu, S. (2017) Facet Effect of Single-Crystalline Pd Nanocrystals for Aerobic Oxidation of 5-Hydroxymethyl-2-furfural. *ACS Catal.*, **7** (1), 421–432.
37. Siyo, B., Schneider, M., Pohl, M.M., Langer, P., and Steinfeldt, N. (2014) Synthesis, characterization, and application of PVP-PD NP in the aerobic oxidation of 5-hydroxymethylfurfural (HMF). *Catal. Letters*, **144** (3), 498–506.
38. Siyo, B., Schneider, M., Radnik, J., Pohl, M.M., Langer, P., and Steinfeldt, N. (2014) Influence of support on the aerobic oxidation of HMF into FDCA over preformed Pd nanoparticle based materials. *Appl. Catal. A Gen.*, **478**, 107–116.
39. Zhang, Z., Zhen, J., Liu, B., Lv, K., and Deng, K. (2015) Selective aerobic oxidation of the biomass-derived precursor 5-hydroxymethylfurfural to 2,5-furandicarboxylic acid under mild conditions over a magnetic palladium nanocatalyst. *Green Chem.*, **17** (2), 1308–1317.
40. Liu, B., Ren, Y., and Zhang, Z. (2015) Aerobic oxidation of 5-hydroxymethylfurfural into 2,5-furandicarboxylic acid in water under mild conditions. *Green Chem.*, **17** (3), 1610–1617.
41. Mei, N., Liu, B., Zheng, J., Lv, K., Tang, D., and Zhang, Z. (2015) A novel magnetic palladium catalyst for the mild aerobic oxidation of 5-hydroxymethylfurfural into 2,5-furandicarboxylic acid in water. *Catal. Sci. Technol.*, **5** (6), 3194–3202.
42. Wang, Y., Yu, K., Lei, D., Si, W., Feng, Y., Lou, L.L., and Liu, S. (2016) Basicity-Tuned Hydrotalcite-Supported Pd Catalysts for Aerobic Oxidation of 5-Hydroxymethyl-2-furfural under Mild Conditions. *ACS Sustain. Chem. Eng.*, **4** (9), 4752–4761.
43. Xia, H., An, J., Hong, M., Xu, S., Zhang, L., and Zuo, S. (2019) Aerobic oxidation of 5-hydroxymethylfurfural to 2,5-difurancarboxylic acid over Pd-Au nanoparticles supported on Mg-Al hydrotalcite. *Catal. Today*, **319** (December 2017), 113–120.

44. Taarning, E., Nielsen, I.S., Egeblad, K., Madsen, R., and Christensen, C.H. (2008) Chemicals from renewables: Aerobic oxidation of furfural and hydroxymethylfurfural over gold catalysts. *ChemSusChem*, **1** (1–2), 75–78.
45. Casanova, O., Iborra, S., and Corma, A. (2009) Biomass into chemicals: One pot-base free oxidative esterification of 5-hydroxymethyl-2-furfural into 2,5-dimethylfuroate with gold on nanoparticulated ceria. *J. Catal.*, **265** (1), 109–116.
46. Vuyyuru, K.R., and Strasser, P. (2012) Oxidation of biomass derived 5-hydroxymethylfurfural using heterogeneous and electrochemical catalysis. *Catal. Today*, **195** (1), 144–154.
47. Casanova, O., Iborra, S., and Corma, A. (2009) Biomass into chemicals: Aerobic oxidation of 5-hydroxymethyl-2-furfural into 2,5-furandicarboxylic acid with gold nanoparticle catalysts. *ChemSusChem*, **2** (12), 1138–1144.
48. Gorbanev, Y.Y., Klitgaard, S.K., Woodley, J.M., Christensen, C.H., and Riisager, A. (2009) Gold-catalyzed aerobic oxidation of 5-hydroxymethylfurfural in water at ambient temperature. *ChemSusChem*, **2** (7), 672–675.
49. Saha, B., Dutta, S., and Abu-Omar, M.M. (2012) Aerobic oxidation of 5-hydroxymethylfurfural with homogeneous and nanoparticulate catalysts. *Catal. Sci. Technol.*, **2** (1), 79–81.
50. Megías-Sayago, C., Lolli, A., Bonincontro, D., Penkova, A., Albonetti, S., Cavani, F., Odriozola, J.A., and Ivanova, S. (2020) Effect of Gold Particles Size over Au/C Catalyst Selectivity in HMF Oxidation Reaction. *ChemCatChem*, **12** (4), 1177–1183.
51. Megías-Sayago, C., Lolli, A., Ivanova, S., Albonetti, S., Cavani, F., and Odriozola, J.A. (2019) Au/Al₂O₃ – Efficient catalyst for 5-hydroxymethylfurfural oxidation to 2,5-furandicarboxylic acid. *Catal. Today*, **333** (March 2018), 169–175.
52. Pasini, T., Piccinini, M., Blosi, M., Bonelli, R., Albonetti, S., Dimitratos, N., Lopez-Sanchez, J.A., Sankar, M., He, Q., Kiely, C.J., Hutchings, G.J., and Cavani, F. (2011) Selective oxidation of 5-hydroxymethyl-2-furfural using supported gold-copper nanoparticles. *Green Chem.*, **13** (8), 2091–2099.
53. Wan, X., Zhou, C., Chen, J., Deng, W., Zhang, Q., Yang, Y., and Wang, Y. (2014) Base-free aerobic oxidation of 5-hydroxymethyl-furfural to 2,5-furandicarboxylic acid in water catalyzed by functionalized carbon nanotube-supported Au-Pd alloy nanoparticles. *ACS Catal.*, **4** (7), 2175–2185.
54. Antonyraj, C.A., Huynh, N.T.T., Park, S.K., Shin, S., Kim, Y.J., Kim, S., Lee, K.Y., and Cho, J.K. (2017) Basic anion-exchange resin (AER)-supported Au-Pd alloy nanoparticles for the oxidation of 5-hydroxymethyl-2-furfural (HMF) into 2,5-furan dicarboxylic acid (FDCA). *Appl. Catal. A Gen.*, **547** (June), 230–236.
55. Zhu, Y., and Lu, M. (2015) Plant-mediated synthesis of Au-Pd alloy nanoparticles supported on MnO₂ nanostructures and their application toward oxidation of 5-(hydroxymethyl)furfural. *RSC Adv.*, **5** (104), 85579–85585.
56. Ghosh, K., Molla, R.A., Iqbal, M.A., Islam, S.S., and Islam, S.M. (2016) Ruthenium nanoparticles supported on N-containing mesoporous polymer catalyzed aerobic oxidation of biomass-derived 5-hydroxymethylfurfural (HMF) to 2,5-diformylfuran (DFF). *Appl. Catal. A Gen.*, **520**, 44–52.

57. Wang, F., Yuan, Z., Liu, B., Chen, S., and Zhang, Z. (2016) Catalytic oxidation of biomass derived 5-hydroxymethylfurfural (HMF) over RuIII-incorporated zirconium phosphate catalyst. *J. Ind. Eng. Chem.*, **38**, 181–185.
58. Mishra, D.K., Cho, J.K., and Kim, Y.J. (2018) Facile production of 2,5-diformylfuran from base-free oxidation of 5-hydroxymethyl furfural over manganese–cobalt spinels supported ruthenium nanoparticles. *J. Ind. Eng. Chem.*, **60**, 513–519.
59. Artz, J., Mallmann, S., and Palkovits, R. (2015) Selective aerobic oxidation of hmf to 2,5-diformylfuran on covalent triazine frameworks-supported ru catalysts. *ChemSusChem*, **8** (4), 772–789.
60. Nie, J., Xie, J., and Liu, H. (2013) Efficient aerobic oxidation of 5-hydroxymethylfurfural to 2,5-diformylfuran on supported Ru catalysts. *J. Catal.*, **301**, 83–91.
61. Wang, S., Zhang, Z., Liu, B., and Li, J. (2014) Environmentally friendly oxidation of biomass derived 5-hydroxymethylfurfural into 2,5-diformylfuran catalyzed by magnetic separation of ruthenium catalyst. *Ind. Eng. Chem. Res.*, **53** (14), 5820–5827.
62. Gorbanev, Y.Y., Kegnaes, S., and Riisager, A. (2011) Effect of support in heterogeneous ruthenium catalysts used for the selective aerobic oxidation of HMF in water. *Top. Catal.*, **54** (16–18), 1318–1324.
63. Gorbanev, Y.Y., Kegnaes, S., and Riisager, A. (2011) Selective aerobic oxidation of 5-hydroxymethylfurfural in water over solid ruthenium hydroxide catalysts with magnesium-based supports. *Catal. Letters*, **141** (12), 1752–1760.
64. Yi, G., Teong, S.P., and Zhang, Y. (2016) Base-free conversion of 5-hydroxymethylfurfural to 2,5-furandicarboxylic acid over a Ru/C catalyst. *Green Chem.*, **18** (4), 979–983.
65. Ståhlberg, T., Eyjólfsdóttir, E., Gorbanev, Y.Y., Sádaba, I., and Riisager, A. (2012) Aerobic oxidation of 5-(Hydroxymethyl)furfural in ionic liquids with solid ruthenium hydroxide catalysts. *Catal. Letters*, **142** (9), 1089–1097.
66. Mishra, D.K., Lee, H.J., Kim, J., Lee, H.S., Cho, J.K., Suh, Y.W., Yi, Y., and Kim, Y.J. (2017) MnCo₂O₄ spinel supported ruthenium catalyst for air-oxidation of HMF to FDCA under aqueous phase and base-free conditions. *Green Chem.*, **19** (7), 1619–1623.
67. Gao, T., Yin, Y., Fang, W., and Cao, Q. (2018) Highly dispersed ruthenium nanoparticles on hydroxyapatite as selective and reusable catalyst for aerobic oxidation of 5-hydroxymethylfurfural to 2,5-furandicarboxylic acid under base-free conditions. *Mol. Catal.*, **450** (February), 55–64.
68. Kerdi, F., Ait Rass, H., Pinel, C., Besson, M., Peru, G., Leger, B., Rio, S., Monflier, E., and Ponchel, A. (2015) Evaluation of surface properties and pore structure of carbon on the activity of supported Ru catalysts in the aqueous-phase aerobic oxidation of HMF to FDCA. *Appl. Catal. A Gen.*, **506**, 206–219.
69. Grasset, F.L., Katryniok, B., Paul, S., Nardello-Rataj, V., Pera-Titus, M., Clacens, J.M., De Campo, F., and Dumeignil, F. (2013) Selective oxidation of 5-hydroxymethylfurfural to 2,5-diformylfuran over intercalated vanadium phosphate oxides. *RSC Adv.*, **3** (25), 9942–9948.
70. Zhang, W., Hou, W., Meng, T., Zhuang, W., Xie, J., Zhou, Y., and Wang, J. (2017) Direct synthesis

of V-containing all-silica beta-zeolite for efficient one-pot, one-step conversion of carbohydrates into 2,5-diformylfuran. *Catal. Sci. Technol.*, **7** (24), 6050–6058.

71. Yadav, G.D., and Sharma, R. V. (2014) Biomass derived chemicals: Environmentally benign process for oxidation of 5-hydroxymethylfurfural to 2,5-diformylfuran by using nano-fibrous Ag-OMS-2-catalyst. *Appl. Catal. B Environ.*, **147**, 293–301.
72. Saha, B., Gupta, D., Abu-Omar, M.M., Modak, A., and Bhaumik, A. (2013) Porphyrin-based porous organic polymer-supported iron(III) catalyst for efficient aerobic oxidation of 5-hydroxymethyl-furfural into 2,5-furandicarboxylic acid. *J. Catal.*, **299**, 316–320.
73. Fang, R., Luque, R., and Li, Y. (2016) Selective aerobic oxidation of biomass-derived HMF to 2,5-diformylfuran using a MOF-derived magnetic hollow Fe-Co nanocatalyst. *Green Chem.*, **18** (10), 3152–3157.
74. Wang, S., Zhang, Z., and Liu, B. (2015) Catalytic conversion of fructose and 5-hydroxymethylfurfural into 2,5-furandicarboxylic acid over a recyclable Fe₃O₄-CoOx magnetite nanocatalyst. *ACS Sustain. Chem. Eng.*, **3** (3), 406–412.
75. Han, X., Li, C., Liu, X., Xia, Q., and Wang, Y. (2017) Selective oxidation of 5-hydroxymethylfurfural to 2,5-furandicarboxylic acid over MnOX-CeO₂ composite catalysts. *Green Chem.*, **19** (4), 996–1004.
76. Partenheimer, W., and Grushin, V. V (2001) Synthesis of 2,5-Diformylfuran and Furan-2,5-Dicarboxylic Acid by Catalytic Air-Oxidation of 5-Hydroxymethylfurfural. Unexpectedly Selective Aerobic Oxidation of Benzyl Alcohol to Benzaldehyde with Metal-Bromide Catalysts. *Adv-Synth. Catal.*, **343** (1), 102–111.
77. Janka, M.E., Parker, K.R., Shalkh, A.S., and Partin, L.R. (2014) Oxidation process to produce a crude dry carboxylic acid product (Eastman Chemical Company). US Patent 2014/0256964 A1, issued 2014.
78. Yutaka, K., Miura, T., Eritate, S., and Komuro, T. (2012) Method of producing 2,5-furandicarboxylic acid (Canon Kabushiki Kaisha). US Patent 8,242,292 B2, issued 2012.
79. Zuo, X., Subramaniam, B., Busch, D., and Venkitasubramaniam, P. (2013) Spray oxidation process for producing 2,5-furandicarboxylic acid from hydroxymethylfurfural (ARCHER DANIELS MIDLAND CO). WO 2013/033058 A1., issued 2013.
80. Ebihara, Y., and R., F. (2009) Process for producing 2,5-furandicarboxylic acid (AIR WATER INC). JP5252969B2-2, issued 2009.
81. Pasini, T., Piccinini, M., Blosi, M., Bonelli, R., Albonetti, S., Dimitratos, N., Lopez-Sanchez, J.A., Sankar, M., He, Q., Kiely, C.J., Hutchings, G.J., and Cavani, F. (2011) Selective oxidation of 5-hydroxymethyl-2-furfural using supported gold-copper nanoparticles. *Green Chem.*, **13** (8), 2091–2099.
82. Hodnett, B.K. (1985) *Science and Engineering Vanadium-Phosphorus Oxide Catalysts for the Selective Oxidation of C 4 Hydrocarbons to Maleic Anhydride*.
83. Gupta, N.K., Fukuoka, A., and Nakajima, K. (2018) Metal-Free and Selective Oxidation of Furfural to Furoic Acid with an N-Heterocyclic Carbene Catalyst. *ACS Sustain. Chem. Eng.*, **6** (3), 3434–3442.

84. Felthouse, T.R., Burnett, J.C., Horrell, B., Mummey, M.J., and Kuo, Y.-J. (2001) Maleic Anhydride, Maleic Acid, and Fumaric Acid. *Kirk-Othmer Encycl. Chem. Technol.*, (10).
85. Centi, G., Trifirò, F., Ebner, J.R., and Franchetti, V.M. (1988) Mechanistic Aspects of Maleic Anhydride Synthesis from C4 Hydrocarbons Over Phosphorus Vanadium Oxide. *Chem. Rev.*, **88** (1), 55–80.
86. Radhakrishnan, R., Thiripuranthagan, S., Devarajan, A., Kumaravel, S., Erusappan, E., and Kannan, K. (2017) Oxidative esterification of furfural by Au nanoparticles supported CMK-3 mesoporous catalysts. *Appl. Catal. A Gen.*, **545** (April), 33–43.
87. Manzoli, M., Menegazzo, F., Signoretto, M., and Marchese, D. (2016) Biomass derived chemicals: Furfural oxidative esterification to methyl-2-furoate over gold catalysts. *Catalysts*, **6** (7).
88. Ning, L., Liao, S., Liu, X., Guo, P., Zhang, Z., Zhang, H., and Tong, X. (2018) A regulatable oxidative valorization of furfural with aliphatic alcohols catalyzed by functionalized metal-organic frameworks-supported Au nanoparticles. *J. Catal.*, **364**, 1–13.
89. Douthwaite, M., Huang, X., Iqbal, S., Miedziak, P.J., Brett, G.L., Kondrat, S.A., Edwards, J.K., Sankar, M., Knight, D.W., Bethell, D., and Hutchings, G.J. (2017) The controlled catalytic oxidation of furfural to furoic acid using AuPd/Mg(OH)₂. *Catal. Sci. Technol.*, **7**, 5284–5293.
90. Menegazzo, F., Signoretto, M., Pinna, F., Manzoli, M., Aina, V., Cerrato, G., and Boccuzzi, F. (2014) Oxidative esterification of renewable furfural on gold-based catalysts: Which is the best support? *J. Catal.*, **309** (January), 241–247.
91. Ferraz, C.P., Gabriel, A., Da, M., Rodrigues, T.S., Henrique, P., Camargo, C., Id, P., and Wojcieszak, R. (2018) applied sciences Furfural Oxidation on Gold Supported on MnO₂ : Influence of the Support Structure on the Catalytic Performances. *Appl. Sci.*
92. Camila P. Ferraz, Adriano H. Braga, Mohamed Nawfal Ghazzal, M.Z. ński, Mariusz Pietrowski, Ivaldo Itabaiana Jr., Franck Dumeignil, L.M.R., Wojcieszak, and R., Ferraz, C.P., Braga, A.H., Ghazzal, M.N., Zieliński, M., Pietrowski, M., Itabaiana, I., Dumeignil, F., Rossi, L.M., Wojcieszak, R., Camila P. Ferraz, Adriano H. Braga, Mohamed Nawfal Ghazzal, M.Z. ński, Mariusz Pietrowski, Ivaldo Itabaiana Jr., Franck Dumeignil, L.M.R., and Wojcieszak, and R. (2020) Efficient oxidative esterification of furfural using au nanoparticles supported on group 2 alkaline earth metal oxides. *Catalysts*, **10** (4), 1–14.
93. Ferraz, C.P., Costa, N.J.S., Teixeira-neto, E., Teixeira-neto, Â.A., Liria, C.W., Thuriot-roukos, J., Machini, M.T., Froidevaux, R., Dumeignil, F., Rossi, L.M., and Wojcieszak, R. (2020) 5-Hydroxymethylfurfural and Furfural Base-Free Oxidation over AuPd Embedded Bimetallic Nanoparticles. *Catalysts*, **10** (75).
94. Huo, N., Ma, H., Wang, X., Wang, T., Wang, G., Wang, T., Hou, L., Gao, J., and Xu, J. (2017) High - efficiency oxidative esterification of furfural to methylfuroate with a non - precious metal Co - N - C / MgO catalyst. *Chinese J. Catal.*, **38** (7), 1148–1154.
95. Ojeda, M., Mariscal, R., Fierro, J.L.G., and Granados, M.L. (2017) Gas phase oxidation of furfural to maleic anhydride on 2O 5 / c -Al₂ O₃ catalysts : Reaction conditions to slow down the deactivation. *J. Catal.*, **348**, 265–275.
96. Li, X., Ho, B., and Zhang, Y. (2016) Selective aerobic oxidation of furfural to maleic anhydride

with heterogeneous Mo-V-O catalysts. *Green Chem.*, **18** (10), 2976–2980.

97. Session, W. V. (1928) Catalytic oxidation of furfural in the vapor phase. *J. Am. Chem. Soc.*, **50** (6), 1696–1698.
98. Milas, N.A. (1927) Catalytic oxidations in aqueous solutions I. The oxidation of furfural. *J. Am. Chem. Soc.*, **49** (8), 2005–2011.
99. Guliants, V. V, and Carreon, M.A. (2005) Vanadium-phosphorus-oxides: From fundamentals of n-Butane oxidation to synthesis of new phases. *Catalysis*, **18**, 1–45.
100. Skinner, W.A., and Tieszen, D. (1961) Production of maleic acid by oxidizing butenes. *Ind. Eng. Chem.*, **53** (7), 557–558.
101. Beach, L.K. (1951) Cis-Butene Oxidation. US 2537568 A, issued 1951.
102. Nielsen, E.R. (1949) Vapor phase oxidation of furfural. *Ind. Eng. Chem.*, **41** (February), 365–368.
103. Milas, N.A., and Walsh, W.L. (1935) Catalytic Oxidations. I. Oxidations in the Furan Series. *J. Am. Chem. Soc.*, **57** (8), 1389–1393.
104. Slavinskaya, V.A., Kreile, D.R., Dzilyuma, E.E., and Sile, D.E. (1977) Incomplete catalytic oxidation of furan. *Chem. Heterocycl. Compd.*, **13** (7), 710–721.
105. Alonso-Fagúndez, N., Granados, M.L., Mariscal, R., and Ojeda, M. (2012) Selective conversion of furfural to maleic anhydride and furan with VO_x/Al₂O₃ catalysts. *ChemSusChem*, **5** (10), 1984–1990.
106. Li, X., Ko, J., and Zhang, Y. (2018) Highly Efficient Gas-Phase Oxidation of Renewable Furfural to Maleic Anhydride over Plate Vanadium Phosphorus Oxide Catalyst. *ChemSusChem*, **11** (3), 612–618.
107. Murthy, M.S., and Rajamani, K. (1974) Kinetics of vapour phase oxidation of furfural on vanadium catalyst. *Chem. Eng. Sci.*, **29** (2), 601–609.
108. Rajamani, K., Subramanian, P., and Murthy, M.S. (1976) Kinetics and Mechanism of Vapor Phase Oxidation of Furfural over Tin Vanadate Catalyst. *Ind. Eng. Chem. Process Des. Dev.*, **15** (2), 232–234.
109. Guo, H., and Yin, G. (2011) Catalytic aerobic oxidation of renewable furfural with phosphomolybdic acid catalyst: An alternative route to maleic acid. *J. Phys. Chem. C*, **115** (35), 17516–17522.
110. Shi, S., Guo, H., and Yin, G. (2011) Synthesis of maleic acid from renewable resources: Catalytic oxidation of furfural in liquid media with dioxygen. *Catal. Commun.*, **12** (8), 731–733.
111. Lan, J., Chen, Z., Lin, J., and Yin, G. (2014) Catalytic aerobic oxidation of renewable furfural to maleic anhydride and furanone derivatives with their mechanistic studies. *Green Chem.*, **16** (10), 4351–4358.
112. Lv, G., Chen, C., Lu, B., Li, J., Yang, Y., Chen, C., Deng, T., Zhu, Y., and Hou, X. (2016) Vanadium-oxo immobilized onto Schiff base modified graphene oxide for efficient catalytic oxidation of 5-hydroxymethylfurfural and furfural into maleic anhydride. *RSC Adv.*, **6** (103), 101277–101282.

113. Lv, G., Chen, S., Zhu, H., Li, M., and Yang, Y. (2018) Determination of the crucial functional groups in graphene oxide for vanadium oxide nanosheet fabrication and its catalytic application in 5-hydroxymethylfurfural and furfural oxidation. *J. Clean. Prod.*, **196**, 32–41.
114. Badovskaya, L.A., and Poskonin, V. V. (2015) Metal Nature Effect on Catalytic Reactions in Furfural–H₂O₂–H₂O–Group V or VI d_Metal Salt Systems in Acid Media. *Kinet. Catal.*, **56** (2), 164–172.
115. Badovskaya, L.A., Poskonin, V. V., and Ponomarenko, R.I. (2014) Effect of acid-base properties of the medium on the reactions in the 2-furaldehyde-H₂O₂-H₂O system with and without VOSO₄. *Russ. J. Gen. Chem.*, **84** (6), 1133–1140.
116. Badovskaya, L.A., Poskonin, V. V., and Povarova, L. V. (2017) Synthesis of functional furan derivatives by oxidation of furans and formylfurans with hydrogen peroxide. *Russ. Chem. Bull.*, **66** (4), 593–599.
117. Rezaei, M., Naja, A., Dabbagh, H.A., Saraji, M., and Shahvar, A. (2019) Furfural oxidation to maleic acid with H₂O₂ by using vanadyl pyrophosphate and zirconium pyrophosphate supported on well-ordered mesoporous KIT-6. *J. Environ. Chem. Eng.*, **7** (December 2018).
118. Soták, T., Hronec, M., Gál, M., and Dobročka, E. (2017) Aqueous-Phase Oxidation of Furfural to Maleic Acid Catalyzed by Copper Phosphate Catalysts. *Catal. Letters*, **147** (11), 2714–2723.
119. da Silva, M.J., and Rodrigues, A.A. (2020) Metal silicotungstate salts as catalysts in furfural oxidation reactions with hydrogen peroxide. *Mol. Catal.*, **493** (June).
120. Huang, Y., Wu, C., Yuan, W., Xia, Y., Liu, X., Yang, H., and Wang, H. (2017) Catalytic Aerobic Oxidation of Biomass-based Furfural into Maleic Acid in Aqueous Phase with Metalloporphyrin Catalysts. *J. CHINESE Chem. Soc.*, 1–9.
121. Xie, Y., Huang, Y., Wu, C., Yuan, W., Xia, Y., Liu, X., and Wang, H. (2018) Iron-based metalloporphyrins as efficient catalysts for aerobic oxidation of biomass derived furfural into maleic acid. *Mol. Catal.*, **452** (January), 20–27.
122. Alonso-Fagúndez, N., Agirrezabal-Telleria, I., Arias, P.L., Fierro, J.L.G.G., Mariscal, R., Granados, M.L., Alonso-Fagundez, N., Agirrezabal-Telleria, I., Arias, P.L., Fierro, J.L.G.G., Mariscal, R., and Lopez Granados, M. (2014) Aqueous-phase catalytic oxidation of furfural with H₂O₂ : high yield of maleic acid by using titanium silicalite-1. *RSC Adv.*, **4** (98), 54960–54972.
123. Alba-Rubio, A.C., Fierro, J.L.G., León-Reina, L., Mariscal, R., Dumesic, J.A., and López Granados, M. (2017) Oxidation of furfural in aqueous H₂O₂ catalysed by titanium silicalite: Deactivation processes and role of extraframework Ti oxides. *Appl. Catal. B Environ.*, **202**, 269–280.
124. Lou, Y., Marinkovic, S., Estrine, B., Qiang, W., and Enderlin, G. (2020) Oxidation of Furfural and Furan Derivatives to Maleic Acid in the Presence of a Simple Catalyst System Based on Acetic Acid and TS-1 and Hydrogen Peroxide. *ACS Omega*, **5**, 2561–2568.
125. Rodenas, Y., Mariscal, R., Fierro, J.L.G., Martín Alonso, D., Dumesic, J.A., and López Granados, M. (2018) Improving the production of maleic acid from biomass: TS-1 catalysed aqueous phase oxidation of furfural in the presence of γ -valerolactone. *Green Chem.*, **20** (12), 2845–2856.
126. Camila P. Ferraz, Adriano H. Braga, Mohamed Nawfal Ghazzal, M.Z. ński, Mariusz Pietrowski, Ivaldo Itabaiana Jr., Franck Dumeignil, L.M.R., and Wojcieszak, and R. (2020) Efficient Oxidative

- Esterification of Furfural Using Au Metal Nanoparticles Supported on Group 2 Alkaline Earth Oxides. *Catalysts*, **10** (Scheme 1), 1–14.
127. Li, X., Ko, J., and Zhang, Y. (2018) Highly Efficient Gas Phase Oxidation of Renewable Furfural to Maleic Anhydride over Plate VPO Catalyst. *ChemSusChem*, **11** (3), 612–618.
 128. Fortier, S.M., Nassar, N.T., Lederer, G.W., Brainard, J., Gambogi, J., and McCullough, E.A. (2018) Draft Critical Mineral List—Summary of Methodology and Background Information. *U.S. Geol. Surv.*, (3359), 1–26.
 129. Giannakoudakis, D.A., Nair, V., Khan, A., Deliyanni, E.A., Colmenares, J.C., and Triantafyllidis, K.S. (2019) Additive-free photo-assisted selective partial oxidation at ambient conditions of 5-hydroxymethylfurfural by manganese (IV) oxide nanorods. *Appl. Catal. B Environ.*, **256** (March 2019), 117803.
 130. Partenheimer, W., and Grushin, V. V (2001) Synthesis of 2,5-Diformylfuran and Furan-2,5-Dicarboxylic Acid by Catalytic Air-Oxidation of 5-Hydroxymethylfurfural . Unexpectedly Selective Aerobic Oxidation of Benzyl Alcohol to Benzaldehyde with Metal / Bromide Catalysts **. *Adv- Synth. Catal.*, **343** (1), 102–111.
 131. Morikawa, S. (1979) Synthesis of 2,5-furandicarboxaldehyde from 5-hydroxymethylfurfural. *Noguchi Kenkyunsho Jiho*, **22**, 20–7.
 132. Cottier, L., Descotes, G., and Lewkowski, J. (1994) Synthesis of furan-2,5 -dicarbaldehyde by oxidation of 5-silyloxymethyl-2-furfural. *Synth. Commun.*, **24** (7), 939–944.
 133. Corma, A., and Garcá, H. (2003) Lewis Acids : From Conventional Homogeneous to Green Homogeneous and Heterogeneous Catalysis. *Chem. Rev.*, **103**, 4307–4365.
 134. Okuhara, T. (2002) Water-Tolerant Solid Acid Catalysts. *Chem. Rev.*, **102**, 3641–3666.
 135. Liu, F., Huang, K., Zheng, A., Xiao, F.-S., and Sheng Da (2018) Hydrophobic Solid Acids and Their Catalytic Applications in Green and Sustainable Chemistry. *ACS Catal.*, **8** (1), 372–391.
 136. Choudhary, H., Nishimura, S., and Ebitani, K. (2013) Metal-free oxidative synthesis of succinic acid from biomass-derived furan compounds using a solid acid catalyst with hydrogen peroxide. *Appl. Catal. A Gen.*, **458**, 55–62.
 137. Li, J., Lv, G., Lu, B., Wang, Y., Deng, T., Hou, X., and Yang, Y. (2017) Benzoic acid/TEMPO as a high efficient metal-free catalyst system for selective oxidation of 5-hydroxymethylfurfural into 2, 5-diformylfuran. *Energy Technol.*, **5** (8), 1429–1434.
 138. Lv, G., Wang, H., Yang, Y., Deng, T., Chen, C., Zhu, Y., and Hou, X. (2015) Graphene Oxide: A Convenient Metal-Free Carbocatalyst for Facilitating Aerobic Oxidation of 5-Hydroxymethylfurfural into 2, 5-Diformylfuran. *ACS Catal.*, **5** (9), 5636–5646.
 139. Cottier, L., Descotes, G., Lewkowski, J., and Skowroński, R. (1994) Oxidation of 5-Hydroxymethylfurfural under Sonochemical Conditions. *Pol. J. Chem.*, **68** (January 1994), 693–698.
 140. El Hajj, T., Masroua, A., Martin, J.C., and Descotes, G. (1987) Synthesis of 5-(hydroxymethyl) furan-2-carboxaldehyde and its derivative by acid treatment of sugars on ion-exchange resins. *Bull. Soc. Chim. Fr.*, (5), 855–860.

141. Cottier, L., Descotes, G., Viollet, E., Lewkowski, J., and Skowroński, R. (1995) Oxidation of 5-hydroxymethylfurfural and derivatives to furanaldehydes with 2,2,6,6-tetramethylpiperidine oxide radical - co-oxidant pairs. *J. Heterocycl. Chem.*, **32** (3), 927–930.
142. Ma, Z., and Bobbitt, J.M. (1991) Organic Oxoammonium Salts . 3 . 1 A New Convenient Method for the Oxidation of Alcohols to Aldehydes and Ketones. *J. Org. Chem.*, **56**, 6110–6114.
143. Cottier L, Descotes G, Viollet E, Lewkowski J, S.R. (1995) Oxidation of 5-Hydroxymethylfurfural and Derivatives to Furanaldehydes with 2,2,6,6-Tetramethylpiperidine Oxide Radical-Co-oxidant pairs. *J. Heterocycl. Chem.*, 927–930.
144. Mico, A. De, Margarita, R., Parlanti, L., Vescovi, A., and Piancatelli, G. (1997) A Versatile and Highly Selective Hypervalent Iodine (III)/ 2,2,6,6-Tetramethyl-1-piperidinyloxy-Mediated Oxidation of Alcohols to Carbonyl Compounds. *J. Org. Chem.*, **62**, 6974–6977.
145. Epp, J.B., and Widlanski, T.S. (1999) Facile Preparation of Nucleoside-5'-carboxylic Acids. *J. Org. Chem.*, **64**, 293–295.
146. Mittal, N., Nisola, G.M., Malihan, L.B., Seo, J.G., Lee, S.P., and Chung, W.J. (2014) Metal-free mild oxidation of 5-hydroxymethylfurfural to 2,5-diformylfuran. *Korean J. Chem. Eng.*, **31** (8), 1362–1367.
147. Mittal, N., Nisola, G.M., Seo, J.G., Lee, S.P., and Chung, W.J. (2015) Organic radical functionalized SBA-15 as a heterogeneous catalyst for facile oxidation of 5-hydroxymethylfurfural to 2,5-diformylfuran. *J. Mol. Catal. A Chem.*, **404–405**, 106–114.
148. Anelli, P.L., Biffi, C., Montanari, F., and Quici, S. (1987) Fast and Selective Oxidation of Primary Alcohols to Aldehydes or to Carboxylic Acids and of Secondary Alcohols to Ketones Mediated by Oxoammonium Salts under Two-Phase Conditions. *J. Org. Chem.*, **52** (12), 2559–2562.
149. Krystof, M., Pérez-Sánchez, M., and De María, P.D. (2013) Lipase-mediated selective oxidation of furfural and 5-hydroxymethylfurfural. *ChemSusChem*, **6** (5), 826–830.
150. Karimi, B., Vahdati, S., and Vali, H. (2016) Synergistic catalysis within TEMPO-functionalized periodic mesoporous organosilica with bridge imidazolium groups in the aerobic oxidation of alcohols. *RSC Adv.*, **6** (68), 63717–63723.
151. Zhao, J., Wu, D., Hernández, W.Y., Zhou, W.J., Capron, M., and Ordonsky, V. V. (2020) Non-metallic Aerobic Oxidation of Alcohols over Anthraquinone Based Compounds. *Appl. Catal. A Gen.*, **590** (October 2019), 117277.
152. Liu, K.J., Zeng, T.Y., Zeng, J. Le, Gong, S.F., He, J.Y., Lin, Y.W., Tan, J.X., Cao, Z., and He, W.M. (2019) Solvent-dependent selective oxidation of 5-hydroxymethylfurfural to 2,5-furandicarboxylic acid under neat conditions. *Chinese Chem. Lett.*, **30** (12), 2304–2308.
153. Lorf, A., He, H., Forster, M., and Klinowski, J. (1998) Structure of graphite oxide revisited. *J. Phys. Chem. B*, **102** (23), 4477–4482.
154. Wang, H., Gao, Q., and Hu, J. (2009) High hydrogen storage capacity of porous carbons prepared by using activated carbon. *J. Am. Chem. Soc.*, **131** (20), 7016–7022.
155. Zhang, P., Zhu, H., and Dai, S. (2015) Porous Carbon Supports: Recent Advances with Various Morphologies and Compositions. *ChemCatChem*, **7** (18), 2788–2805.

156. Veerakumar, P., Madhu, R., Chen, S.M., Hung, C. Te, Tang, P.H., Wang, C. Bin, and Liu, S. Bin (2014) Porous carbon-modified electrodes as highly selective and sensitive sensors for detection of dopamine. *Analyst*, **139** (19), 4994–5000.
157. Sevilla, M., and Mokaya, R. (2014) Energy storage applications of activated carbons: Super capacitors and hydrogen storage. *Energy Environ. Sci.*, **7** (4), 1250–1280.
158. Long, J., Xie, X., Xu, J., Gu, Q., Chen, L., and Wang, X. (2012) Nitrogen-doped graphene nanosheets as metal-free catalysts for aerobic selective oxidation of benzylic alcohols. *ACS Catal.*, **2** (4), 622–631.
159. Dreyer, D.R., Jia, H.P., and Bielawski, C.W. (2010) Graphene oxide: A convenient carbocatalyst for facilitating oxidation and hydration reactions. *Angew. Chemie - Int. Ed.*, **49** (38), 6813–6816.
160. Li, X.H., Chen, J.S., Wang, X., Sun, J., and Antonietti, M. (2011) Metal-free activation of dioxygen by graphene/g-C₃N₄ nanocomposites: Functional dyads for selective oxidation of saturated hydrocarbons. *J. Am. Chem. Soc.*, **133** (21), 8074–8077.
161. Watanabe, H., Asano, S., Fujita, S., Yoshida, H., and Arai, M. (2015) Nitrogen-doped Metal-free Activated Carbon Catalysts for Aerobic Oxidation of Alcohols Nitrogen-doped Metal-free Activated Carbon Catalysts for Aerobic Oxidation of Alcohols. *ACS Catal.*, **5**, 2886–2894.
162. Lv, G., Wang, H., Yang, Y., Li, X., Deng, T., Chen, C., Zhu, Y., and Hou, X. (2016) Aerobic selective oxidation of 5-hydroxymethyl-furfural over nitrogen-doped graphene materials with 2,2,6,6-tetramethylpiperidin-oxyl as co-catalyst. *Catal. Sci. Technol.*, **6** (7), 2377–2386.
163. Nguyen, C. Van, Liao, Y. Te, Kang, T.C., Chen, J.E., Yoshikawa, T., Nakasaka, Y., Masuda, T., and Wu, K.C.W. (2016) A metal-free, high nitrogen-doped nanoporous graphitic carbon catalyst for an effective aerobic HMF-to-FDCA conversion. *Green Chem.*, **18** (22), 5957–5961.
164. Krivtsov, I., García-López, E.I., Marcì, G., Palmisano, L., Amghouz, Z., García, J.R., Ordóñez, S., and Díaz, E. (2017) Selective photocatalytic oxidation of 5-hydroxymethyl-2-furfural to 2,5-furandicarboxyaldehyde in aqueous suspension of g-C₃N₄. *Appl. Catal. B Environ.*, **204**, 430–439.
165. Wu, Q., He, Y., Zhang, H., Feng, Z., Wu, Y., and Wu, T. (2017) Photocatalytic selective oxidation of biomass-derived 5-hydroxymethylfurfural to 2,5-diformylfuran on metal-free g-C₃N₄ under visible light irradiation. *Mol. Catal.*, **436**, 10–18.
166. Ilkaeva, M., Krivtsov, I., García, J.R., Díaz, E., Ordóñez, S., García-López, E.I., Marcì, G., Palmisano, L., Maldonado, M.I., and Malato, S. (2018) Selective photocatalytic oxidation of 5-hydroxymethyl-2-furfural in aqueous suspension of polymeric carbon nitride and its adduct with H₂O₂ in a solar pilot plant. *Catal. Today*, **315** (January), 138–148.
167. Verma, S., Nadagouda, M.N., and Varma, R.S. (2017) Porous nitrogen-enriched carbonaceous material from marine waste: chitosan-derived carbon nitride catalyst for aerial oxidation of 5-hydroxymethylfurfural (HMF) to 2,5-furandicarboxylic acid. *Sci. Rep.*, **7** (1), 1–6.
168. Ren, Y., Yuan, Z., Lv, K., Sun, J., Zhang, Z., and Chi, Q. (2018) Selective and metal-free oxidation of biomass-derived 5-hydroxymethylfurfural to 2,5-diformylfuran over nitrogen-doped carbon materials. *Green Chem.*, **20** (21), 4946–4956.
169. Frigerio, M., and Santagostino, M. (1994) A Mild Oxidizing Reagent for Alcohols and 1,2-Diols:

- o-Iodoxybenzoic Acid (IBX) in DMSO. *Tetrahedron Lett.*, **35** (43), 8019–8022.
170. Ballaschk, F., and Kirsch, S.F. (2019) Oxidation of secondary alcohols using solid-supported hypervalent iodine catalysts. *Green Chem.*, **21** (21), 5896–5903.
 171. Uyanik, M., Akakura, M., and Ishihara, K. (2009) 2-Iodoxybenzenesulfonic Acid As an Extremely Active Catalyst for the Selective Oxidation of Alcohols To Aldehydes, Ketones, Carboxylic Acids, and Enones With Oxone. *J. Am. Chem. Soc.*, **131** (1), 251–262.
 172. Ayoub, N., Bergère, C., Toufaily, J., Guénin, E., and Enderlin, G. (2020) A gram scale selective oxidation of 5-hydroxymethylfurfural to diformylfuran in the presence of oxone and catalyzed by 2-iodobenzenesulfonic acid. *New J. Chem.*, **44**, 11577–11583.
 173. Hazra, S., Deb, M., and Elias, A.J. (2017) Iodine catalyzed oxidation of alcohols and aldehydes to carboxylic acids in water: A metal-free route to the synthesis of furandicarboxylic acid and terephthalic acid. *Green Chem.*, **19** (23), 5548–5552.
 174. Milas, N.A., and McAlevy, A. (1934) Studies in Organic Peroxides. III. Peroxides in the Furan Series. *J. Am. Chem. Soc.*, **56** (5), 1219–1221.
 175. Dunlop, A.P., Stout, P.R., and Swadesh, S. (1946) Autoxidation of Furfural. *Ind. Eng. Chem.*, **38** (7), 705–708.
 176. Choudhary, H., Nishimura, S., and Ebitani, K. (2012) Highly Efficient Aqueous Oxidation of Furfural to Succinic Acid Using Reusable Heterogeneous Acid Catalyst with Hydrogen Peroxide. *Chem. Lett.*, **41**, 409–411.
 177. Dalli, S.S., Tilaye, T.J., and Rakshit, S.K. (2017) Conversion of Wood-Based Hemicellulose Prehydrolysate into Succinic Acid Using a Heterogeneous Acid Catalyst in a Biphasic System. *Ind. Eng. Chem. Res.*, **56** (38), 10582–10590.
 178. Dalli, S.S., and Rakshit, S.K. (2019) Conversion de prehydrolysats d’hemicellulose a base de bois dans de l’acide succinique au moyen d’un catalyseur acide heterogene dans un système biphasique. 2 991 386, issued 2019.
 179. Alonso-Fagúndez, N., Laserna, V., Alba-Rubio, A.C., Mengibar, M., Heras, A., Mariscal, R., and Granados, M.L. (2014) Poly-(styrene sulphonic acid): An acid catalyst from polystyrene waste for reactions of interest in biomass valorization. *Catal. Today*, **234**, 285–294.
 180. Saleem, F., Müller, P., Eränen, K., Warnå, J., Murzin, D.Y., and Tapio Salmi (2017) Kinetics and modelling of furfural oxidation with hydrogen peroxide over a fibrous heterogeneous catalyst: Effect of reaction parameters on yields of succinic acid. *J. Chem. Technol. Biotechnol.*, **92** (9), 2206–2220.
 181. Murzin, D.Y., Saleem, F., Warnå, J., and Salmi, T. (2020) Kinetic modelling of heterogeneous catalytic oxidation of furfural with hydrogen peroxide to succinic acid. *Chem. Eng. J.*, **382** (August 2019).
 182. Li, X., Lan, X., and Wang, T. (2016) Selective oxidation of furfural in a bi-phasic system with homogeneous acid catalyst. *Catal. Today*, **276**, 97–104.
 183. Li, X., Ho, B., Lim, D.S.W., and Zhang, Y. (2017) Highly efficient formic acid-mediated oxidation of renewable furfural to maleic acid with H₂O₂. *Green Chem.*, **19** (4), 914–918.

184. Araji, N., Madjinza, D.D., Chatel, G., Moores, A., Jérôme, F., and De Oliveira Vigier, K. (2017) Synthesis of maleic and fumaric acids from furfural in the presence of betaine hydrochloride and hydrogen peroxide. *Green Chem.*, **19** (1), 98–101.
185. Kalum, L., Morant, M.D., Lund, H., Jensen, J., Lapainaitte, I., Soerensen, N.H., Pedersen, S., Qstergaard, L.H., and Xu, F. (2014) Enzymatic oxidation of 5-Hydroxymethylfurfural and derivatives thereof (Novozymes AS). WO 2014015256-A2, issued 2014.
186. Mitsukura, K., Sato, Y., Yoshida, T., and Nagasawa, T. (2004) Oxidation of heterocyclic and aromatic aldehydes to the corresponding carboxylic acids by *Acetobacter* and *Serratia* strains. *Biotechnol. Lett.*, **26**, 1643–1648.
187. Qin, Y.Z., Li, Y.M., Zong, M.H., Wu, H., and Li, N. (2015) Enzyme-catalyzed selective oxidation of 5-hydroxymethylfurfural (HMF) and separation of HMF and 2,5-diformylfuran using deep eutectic solvents. *Green Chem.*, **17** (7), 3718–3722.
188. Rakshit, S.K., and Dalli, S.S. (2019) CONVERSION OF WOOD BASED HEMICELLULOSE PREHYDROLYSATE INTO SUCCINIC ACID USING A HETEROGENEOUS ACID CATALYST IN A BIPHASIC SYSTEM. US 2019/0382328 A1, issued 2019.
189. Cao, R., Liu, C., and Liu, L. (1996) A convenient synthesis of 2(5h)-furanone. *Org. Prep. Proced. Int.*, **28** (2), 215–216.
190. Kul'nevich, V.G., and Badovskaya, L.A. (1975) Reactions of Oxo-derivatives of Furan with Hydrogen Peroxide and Peroxy-acids. *Russ. Chem. Rev.*, **44** (7), 574–587.
191. Li, X., Lan, X., and Wang, T. (2016) Highly selective catalytic conversion of furfural to γ -butyrolactone. *Green Chem.*, **18** (3), 638–642.
192. Zvarych, V., Nakonechna, A., Marchenko, M., Khudiyi, O., Lubenets, V., Khuda, L., Kushniryk, O., and Novikov, V. (2019) Hydrogen Peroxide Oxygenation of Furan-2-carbaldehyde via an Easy, Green Method. *J. Agric. Food Chem.*, **67** (11), 3114–3117.
193. Zhu, W., Tao, F., Chen, S., Li, M., Yang, Y., and Lv, G. (2019) Efficient Oxidative Transformation of Furfural into Succinic Acid over Acidic Metal-Free Graphene Oxide. *ACS Sustain. Chem. Eng.*, **7** (1), 296–305.
194. Maneechakr, P., and Karnjanakom, S. (2017) Catalytic transformation of furfural into bio-based succinic acid via ultrasonic oxidation using B-cyclodextrin-SO₃H carbon catalyst: A liquid biofuel candidate. *Energy Convers. Manag.*, **154** (September), 299–310.
195. Badovskaya, L.A., and Poskonin, V. V. (2018) Rearrangements and Tautomeric Transformations of Heterocyclic Compounds in Homogeneous Reaction Systems Furfural–H₂O₂–Solvent. *Russ. J. Gen. Chem.*, **88** (8), 1568–1579.
196. Wilson, W.C. (1926) 2-Furancarboxylic acid and furylcarbinol. *Org. Synth.*, **6** (September), 44.
197. Gayakwad, E.M., Patil, V. V., and Shankarling, G.S. (2017) Metal-free oxidation of aldehydes to acids using the 4Na₂SO₄·2H₂O·NaCl adduct. *Environ. Chem. Lett.*, **15** (3), 459–465.
198. Yang, T., Li, W., Liu, Q., Su, M., Zhang, T., and Ma, J. (2019) Synthesis of Maleic Acid from Biomass-Derived Furfural in the Presence of KBr/Graphitic Carbon Nitride (g-C₃N₄) Catalyst and Hydrogen Peroxide. *bioresources*, **14** (3), 5025–5044.

199. Sankari Devi, E., Alanthadka, A., Tamilselvi, A., Nagarajan, S., Sridharan, V., and Maheswari, C.U. (2016) Metal-free oxidative amidation of aldehydes with aminopyridines employing aqueous hydrogen peroxide. *Org. Biomol. Chem.*, **14** (35), 8228–8231.
200. Van Nguyen, C., Boo, J.R., Liu, C.H., Ahamad, T., Alshehri, S.M., Matsagar, B.M., and Wu, K.C.W. (2020) Oxidation of biomass-derived furans to maleic acid over nitrogen-doped carbon catalysts under acid-free conditions. *Catal. Sci. Technol.*, **10** (5), 1498–1506.
201. Wilson, W.C. (1926) 2-FURANCARBOXYLIC ACID and 2-FURYL CARBINOL. *Org. Synth.*, **6**, 44.
202. Schenck, V.G.O. (1953) Photochemische Reaktionen II Über die unsensibilisierte und photosensibilisierte Autoxydation von Furanen. *Liebigs Ann. der chemie*, **584**, 156–176.
203. Grove, M.D., and Weisleder, D. (1972) Hydrolysis Products of 4-Acetamido-4-hydroxy-2-butenic Acid γ -Lactone. *J. Org. Chem.*, **38** (4), 815–816.
204. Bolz, G., and Wiersdorff, W.W. (1972) 2-hydroxy-2,5-dihydrofuran-5-one prepn - by low temp photooxidn of furan or furfural. DE-B 2111119, issued 1972.
205. Meyers, A.I., Nolen, R.L., Collington, E.W., Narwid, T.A., and Strickland, R.C. (1973) Total synthesis of camptothecin and desethyl-desoxycamptothecin. *J. Org. Chem.*, **38** (11), 1974–1982.
206. Esser, P., Pohlmann, B., and Scharf, H. (1994) The Photochemical Synthesis of Fine Chemicals with Sunlight. **33**, 2009–2023.
207. Basheer, C., and Hassan, A.A. (2017) Method of producing a furanone compound. US 9,751,849 B1, issued 2017.
208. Lee, D.S., Amara, Z., Clark, C.A., Xu, Z., Kakimpa, B., Morvan, H.P., Pickering, S.J., Poliakoff, M., and George, M.W. (2017) Continuous Photo-Oxidation in a Vortex Reactor: Efficient Operations Using Air Drawn from the Laboratory. *Org. Process Res. Dev.*, **21**, 1042–1050.
209. Stockton, K.P., May, J.P., Taylor, D.K., and Greatrex, B.W. (2014) Practical evaluation of compact fluorescent lamps for dye-sensitized photooxidation reactions. *Synlett*, **25** (8), 1168–1172.
210. Gassama, A., Ernenwein, C., Youssef, A., Agach, M., Riguët, E., Marinković, S., Estrine, B., and Hoffmann, N. (2013) Sulfonated surfactants obtained from furfural. *Green Chem.*, **15** (6), 1558–1566.
211. Li, M., Dong, X., Zhang, N., Jérôme, F., and Gu, Y. (2019) Eco-efficient synthesis of 2-quinaldic acids from furfural. *Green Chem.*, **21** (17), 4650–4655.
212. Thiyagarajan, S., Franciolus, D., Bisselink, R.J.M., Ewing, T.A., and Boeriu, C.G. (2020) Selective Production of Maleic Acid from Furfural via a Cascade Approach Combining Photochemistry and Electro- or Biochemistry. *ACS Sustain. Chem. Eng.*, **8**, 10626–10632.
213. Farina Perez, F., and Martin Ramos, Maria Victoria; Paredes Garcia, M. del C. (1976) cis- β -Formylacrylic acid. ES 431794, issued 1976.
214. Cottier, Louis; Descotes, Gerard; Nigay, Henri; Parron, Jean Claude; Gregoire, V. (1986) Photooxygenation of 5-(hydroxymethyl)-2-furfural derivatives. *Bull. Soc. Chim. Fr.*, **5**, 844–850.

215. Noutsias, D., Alexopoulou, I., Montagnon, T., and Vassilikogiannakis, G. (2012) Using water, light, air and spirulina to access a wide variety of polyoxygenated compounds. *Green Chem.*, **14** (3), 601–604.
216. Young, R.H., Martin, R.L., Chinh, N., Mallon, C., and Kayser, R.H. (1972) Substituent Effects in Dye-sensitized Photooxidation Reactions of Furans. *Can. J. Chem.*, **50** (6), 932–938.
217. Borghei, S.M., and Hosseini, S.N. (2008) Comparison of furfural degradation by different photooxidation methods. *Chem. Eng. J.*, **139** (3), 482–488.

Chapter 3

Metal-free catalyst for the selective oxidation of hydroxymethylfurfural into 2,5-diformylfuran

1. Introduction

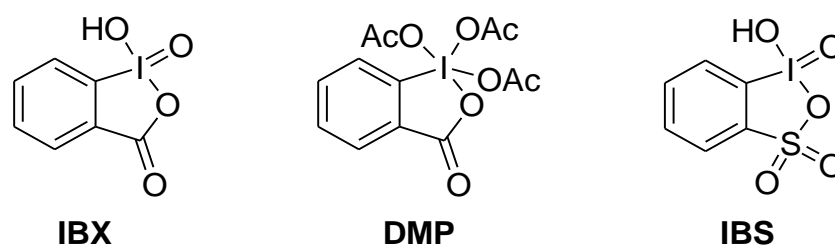
As already described in previous chapters, biomass, as a source of chemicals, represents a sustainable alternative to fossil fuel. Carbohydrates are the main carbon source in biorefineries, but must be deoxygenated to regain similar properties to those of petroleum compounds. The dehydration of C5 and C6 carbohydrates leads to the formation of furan derivatives such as furfural [1–3] and 5-hydroxymethylfurfural [4–6] (HMF). This latter compound is therefore a platform molecule that represents a major interest in the context of sustainable development. Numerous applications, towards bio-based solvents, lubricants, bio-based polymers or fine chemicals, are being developed. [7–11] Among these applications, transformations by selective oxidation of HMF is particularly studied because it leads to bifunctionalized molecules of interest like furanedicarboxylic acid (FDCA) or diformylfuran (DFF). [12,13]

Numerous oxidation methods of HMF to DFF have been reported in the literature, mainly in heterogeneous phase using noble or heavy metals in the presence of oxygen or other oxidants as detailed in the previous chapter. [14–20] However, as shown in chapter 2, metal-free catalysts predominates from the synthesis of DFF, whereas metallic catalysts predominates for the synthesis of FDCA. With metal free catalysis, much more diversity of products is observed heavily depending on operating conditions such as the type of catalyst or oxidant. However, we can still note a stronger tendency for the production of DFF. With these catalysts, oxidation selectivity over hydroxyl function is frequently well controlled.

Very often, these methods however require the presence of 2,2,6,6-tetramethylpiperidine-1-oxyl (TEMPO) or its derivatives as an oxidation mediator. These methods are sometimes very effective but may require the preparation of a complex catalyst or multi-component mixture, long reaction times, high boiling solvents and a large excess of oxidant. The old methods with conventional oxidants can also be very effective, for example, the use of barium manganate gives 93% yield of DFF. However these methods suffer from the use of dangerous compounds and the generation of significant amounts of waste. [21–24] These reactions are also often carried out in very dilute media making these methods difficult to exploit with the aim of changing the production scale from milligrams to kilos.

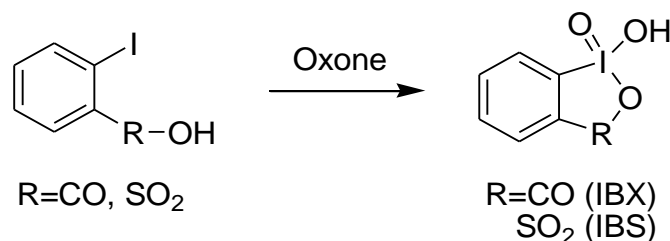
Hypervalent iodine derivatives such as 2-iodoxybenzoic acid [25][26] (IBX) or Dess-Martin reagent [27] (DMP) are well known for effective and selective oxidation of primary alcohols to aldehydes. (Scheme 3.1) These compounds offer an interesting alternative to the use of metal catalysts, which can make the processes more sustainable and less expensive, without the need of extraction, purification and recycling or treatment of metals that are often rare and/or toxic. This strategy has already been used to oxidize HMF into DFF. Lee et al. reported the use of a polymer bearing group similar to IBX, leading

under optimal conditions to quantitative yields of DFF. [28] However to use this strategy in a viable process, major constraints need to be overcome. Indeed, the polymer contains only a low concentration of oxidant 1.02 mmol.g^{-1} , and it must be prepared in its oxidative form with a large excess of tetrabutylammonium oxone (5 equivalents) in the presence of methanesulfonic acid in dichloromethane for 12 hours followed by filtration before use. Other teams have prepared IBX supported on polymer which prove to be very effective for the oxidation of alcohols (not HMF), nevertheless, the same usage constraints are encountered, in particular the numerous stages of preparation of the catalyst, the very low molar fraction of iodine hypervalent on the polymer and generally its activation in the organic phase by tetrabutylammonium oxone. [29–32] Among the iodine derivatives used for catalytic oxidation, Ishihara et al. have demonstrated that 2-iodoxybenzenesulfonic acid (IBS, scheme 3.1) is a particularly selective and effective catalyst for this type of oxidation. [33]



Scheme 3.1 - Hypervalent Iodine derivatives used to oxidize selectively primary alcohols to aldehydes.

Furthermore, it has been demonstrated that it is possible to generate the catalytic species of hypervalent iodine *in situ* from 2-iodobenzene carboxylic or sulfonic acids in the presence of Oxone[®] (2KHSO_5 , KHSO_4 , K_2SO_4) as co-oxidant (Scheme 3.2). This makes it possible to avoid the preparation of the hypervalent iodine species in stoichiometric proportions and to handle these compounds reported to be shock-sensitive. [34,35] This strategy has been reported for the selective oxidation of primary alcohols by Vinod et al., Giannis et al. and Ishihara et al. [33,36,37]



Scheme 3.2 - One step preparation of hypervalent iodine compounds from 2-iodobenzoic acid or 2-iodosulfonic acid and Oxone[®], leading to highly selective oxidant species of primary alcohol, IBX and IBS.

Compared to oxygen and hydrogen peroxide, which are well responding oxidants to the principle of atom economy, Oxone[®] provides an inert and useless mass for oxidation. However, the processes using oxygen or hydrogen peroxide require special precautions related to the management of gas

pressure or the risk of concentration and rapid decomposition of hydrogen peroxide. [38] Oxone[®] has, moreover, many advantages, it is a solid oxidant which can be easily transported and handled, it has a non-toxic nature and doesn't produce polluting by-product, and it is rather economical. [39] Considering some of these criteria, it can be classified among green oxidants. [36]

In the context of dematerializing of processes, we report, in this chapter, the metal free selective oxidation of HMF into DFF in the presence of Oxone[®] as a co-oxidant and 2-iodobenzenesulfonic acid as a catalyst. This work falls within the context of research to develop sustainable processes for the valorization of platform molecules derived from biomass.

2. Experimental section

2.1. Materials, solvents and reagents

Hydroxymethylfurfural (HMF), potassium peroxymonosulfate (Oxone[®]), nitromethane (CH₃NO₂), ethyl acetate (AcOEt), Acetone, methyl isobutyl ketone (MIBK), formic acid, acetic acid, dimethylacetamide, Acetonitrile (CH₃CN), dichloromethane (DCM), chloroform (CHCl₃), tetrahydrofuran (THF), cyclohexane and *tert*-butanol were purchased from Sigma Aldrich, Fisher Chemicals or Acros Organics and further used without any purification.

2.2. Instruments and analytical methods

2.2.1. Gas Chromatography

In this study, a PerkinElmer Autosystem XI instrument was used, and it was equipped with an auto sampler and a flame ionization detector (FID) with a 30 m length and 0.25 mm diameter AT-1HT column Part No. 16368. The different experimental parameters for the GC analyses were as follows: nitrogen as carrier gas with a flowrate of 1 mL/min, temperature of the injector (T_{injector}) set at 350 °C, temperature of the column (T_{column}) set at 40 °C for 2 min and then increased up to 250 °C with a heating rate of 20 °C/min. The injection volume is set to 1 μ L.

Q_{H_2} = 45 ml/min and Q_{air} = 450 ml/min.

2.3. Catalyst synthesis and characterization

To a stirred suspension of 2-aminobenzenesulfonic acid (5.0 g, 28.9 mmol) and crushed-ice (20 g) in concentrated HCl (10 mL) was added NaNO₂ (2.09 g, 30.3 mmol) in water (10 mL) slowly at 0 °C, and stirred for 20~30 min at below 5 °C. (Immediate precipitation of the diazonium salt was observed). A solution of NaI (4.76 g, 31.76 mmol) in water (10 mL) was then added slowly with stirring at 0 °C. After addition was complete, stirring was continued at 0 °C for 1 h, at room temperature for 1 h and at 50

°C for 12 h to remove all N₂. The mixture was then refrigerated, and the insoluble component was separated. After the solid was treated with boiling EtOH (some Et₂O and MeOH then added), the mixture was allowed to cool to separate the insoluble solid. The solid was washed with cold EtOH and Et₂O to isolate as the monohydrate of Sodium 2-Iodobenzenesulfonate. [33]

The obtained catalyst was characterized using Nuclear Magnetic Resonance (NMR)

2.4. Catalytic experiments

All the oxidation reactions were performed in a reactor (100 mL), which was coupled to a reflux condenser, oil bath heater and a magnetic stirrer (stirring speed of 600 rpm). HMF was introduced (200 mg, 1.58 mmol) in the reactor after it reached the desired temperature, and then the catalyst sodium 2-iodobenzenesulfonate (30 mg) was added with 6 mL of solvent and 1.17 g of well grinded Oxone[®]. Immediately after the given time, the reactor was cooled to room temperature, the organic phase was recovered by adding ethyl acetate, washed with water to dissolve any potassium salt traces and then filtered out.

Solvent was evaporated under reduced pressure, and the recovered product was diluted with ethyl acetate then analyzed with Gas Chromatography (GC).

2.5. Catalyst recovery

After following the typical procedure of oxidation of HMF. The resulting mixture was cooled to room temperature and filtered through a plug of tightly packed celite, which was successively washed with EtOAc, and removed of solvents in vacuum to give crude mixture which containing catalyst derivatives. To this crude mixture was added diethyl ether (2–4 mL) and iodines derivatives were precipitated. After simple filtration, pH acidic precipitates were obtained in 50%. Alternatively, the reaction mixture is basified by adding an aqueous solution of sodium hydrogencarbonate. Then the DFF is extracted with ethyl acetate. The aqueous phase containing the sulfate salts and the catalyst is then acidified and the catalyst extracted with ethyl acetate four times. The solvent is evaporated and the catalyst is recovered.

2.6. Gram-scale reaction procedure

The gram-scale oxidation reaction was performed in a three necks flask, which was coupled to a reflux condenser, an oil bath heater and a magnetic stirrer (stirring speed of 600 rpm). 60 mL of solvent, the catalyst sodium 2-iodobenzenesulfonate (300 mg) and 11.7 g of well grinded Oxone[®] were added in the reactor, as soon as the set temperature (70°C) is reached, the HMF was introduced (2 g) in the reactor for 4 hours. At the end of the reaction, about 100 mL of ethyl acetate were added in the reactor.

Then, the mixture was transferred in a separatory funnel by filtrating the residual sulphate salts that settle out at the bottom of the reactor. The insoluble sulphate salts were washed with ethyl acetate and organic phases were combined. The organic phase was washed with 3 times 40 mL of water and the aqueous phase was discarded. The organic layer was then evaporated and 1.78 g of DFF was recovered as a yellowish-white powder (Yield = 87%). The DFF was further analyzed by GC, NMR.

2.7. Products analysis

Proton nuclear magnetic resonance (^1H NMR) and Carbon-13 nuclear magnetic resonance (^{13}C NMR) were conducted on a Bruker Ascend™ 400 MHz device. The samples were prepared in deuterated water, DMSO, CD_3OD or chloroform depending on their solubility.

RMN of diformylfuran:

^1H NMR (400MHz, CDCl_3): δ /ppm 7.73 (s, 1H), 9.87 (s, 1H);

^{13}C NMR $\{^1\text{H}\}$ (100MHz, CDCl_3): δ /ppm 122.1, 153.6, 180.7.

The identification of the compounds was performed by comparison of the retention times with pure standards and by GC analysis. The solvent delay time was 3.00 min. Toluene was used as an internal standard.

The retention time of DFF: 6.9 min, HMF: 8.2 min and Toluene: 4.4 min.

HMF conversion and DFF selectivity and yield were calculated according to the following equations:

$$\text{Conversion}_{\text{HMF}} = \frac{n_{\text{HMF}_{\text{initial}}} - n_{\text{HMF}_{\text{remaining}}}}{n_{\text{HMF}_{\text{initial}}}} \times 100 \quad (1)$$

$$\text{Yield}_{\text{DFF}} = \frac{n_{\text{DFF}_{\text{obtained}}}}{n_{\text{DFF}_{\text{theoretical}}}} \times 100 \quad (2)$$

$$\text{Selectivity}_{\text{DFF}} = \frac{n_{\text{DFF}_{\text{obtained}}}}{n_{\text{HMF}_{\text{initial}}} - n_{\text{HMF}_{\text{remaining}}}} \times 100 \quad (3)$$

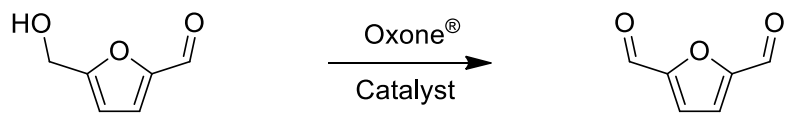
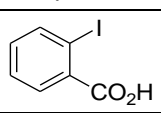
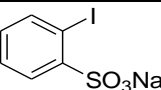
3. Results and discussion

3.1. Preliminary tests

During our preliminary tests, we evaluated the efficiency of the hypervalent iodine derivatives formed "*in situ*" during the transformation of HMF into DFF, and compared the two catalysts, 2-iodobenzenecarboxylic acid and 2-iodobenzenesulfonic acid. As we can see in table 3.1, the two catalysts lead to the formation of DFF selectively but IBS is particularly more effective.

In addition, Ishihara et al. have proved that IBS is a selective and effective catalyst for this type of oxidation and more active than IBX. [33]

Table 3.1 - Comparison of the effectiveness of IBX and IBS formed in situ for the selective oxidation of HMF to DFF

		
	Catalyst	DFF Yield
IBX		81%
IBS		89%

Reaction conditions: 200 mg (1.6 mmol) of HMF, 1.17 g Oxone®, equivalent to KHSO_5/HMF mol ratio = 1.2, 30mg of catalyst in 6 ml of nitromethane, 70°C, 4h.

3.2. Solvent screening

With these very encouraging results, we decided to explore the reaction conditions of the transformation with IBS.

Polar aprotic solvents often show good properties for the oxidation of HMF to DFF, DMSO, for example, has frequently been reported as the best solvent for this type of transformation. [12][40] However, exposure to DMSO sets problems of toxicity because of its ability to easily dissolve the chemical substances that can be absorbed through the skin, moreover it has a very high boiling point (191 °C), which complicates its separation or recycling in the processes. To this purpose, we carried out a solvent screening for this transformation in order to find an alternative to DMSO. (Table 3.2)

The same procedure was used with all solvents (same conditions of concentration, agitation speed and temperature), by mixing the Oxone® previously ground using a mortar with the hydroxymethylfurfural and the 2-iodoxybenzenesulfonic acid as catalyst. The set temperature is 70 °C. The solvents having a boiling point below this temperature (chloroform, DCM, THF and acetone) were heated under reflux (table 3.2, entries 10, 11, 13, 3).

Results are presented in table 3.2. For most of the solvents, the conversions are high and no trends can be drawn between the nature of the solvent and the HMF conversion. Among these solvents, the best selectivity of HMF to DFF is obtained digressively in nitromethane, acetonitrile, ethyl acetate and acetone. This can be interpreted by 64% and 89% of DFF yield and selectivity using, respectively, acetonitrile and nitromethane that appear to be the most effectives (entries 1 and 8).

Table 3.2 - Catalytic oxidation of HMF into DFF using different solvents. ^a

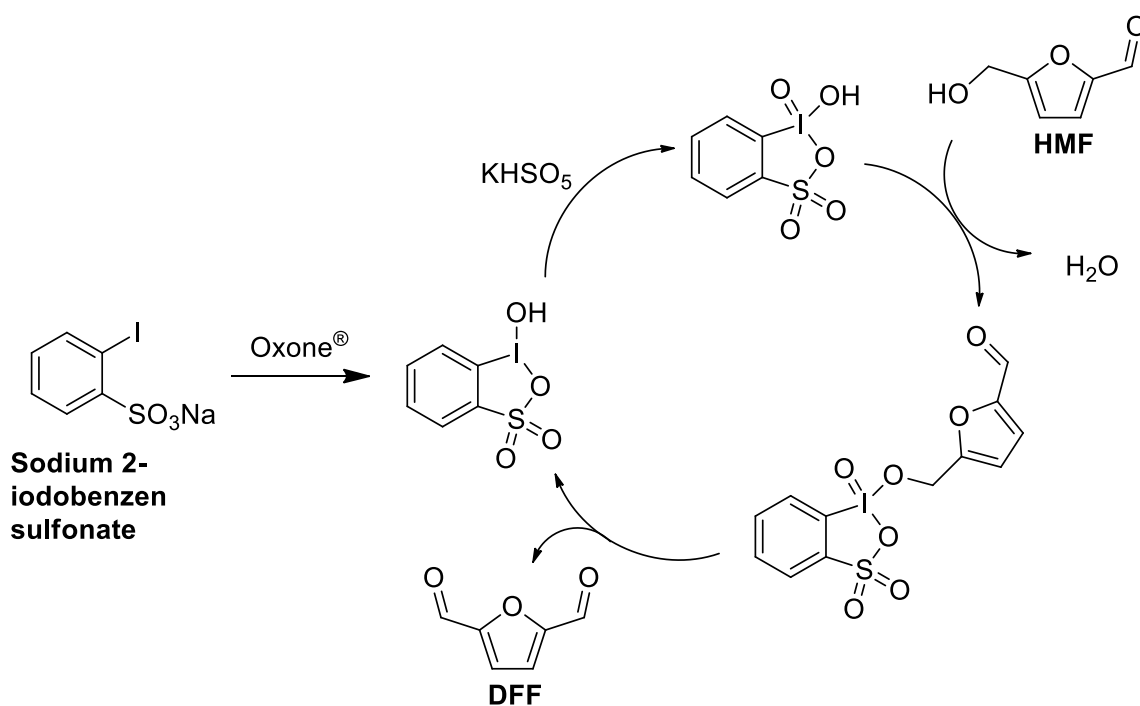
Entry	solvent	Conversion (%)	Selectivity (%)	Yield (%)	Dielectric constant (20°C)	Boiling point (°C)
1	CH ₃ NO ₂	100	89	89	36	101
2	AcOEt	87	62	54	6	77
3	Acetone	49	84	41	21	56
4	MIBK	95	39	38	13	116
5	DMA	100	0	0	37	164
6	Formic Acid	100	0	0	58	101
7	Acetic Acid	100	11	11	6	118
8	CH ₃ CN	100	64	64	38	82
9	DMSO	91	0	0	47	190
10	CHCl ₃	87	23	20	5	61
11	DCM	100	36	36	9	40
12	H ₂ O	97	0	0	80	100
13	THF	53	0	0	7	66
14	Cyclohexane	100	10	10	2	81
15	Tert-butanol	100	0	0	12	83
16	-	97	23	22	-	-

^a Reaction conditions: 200 mg (1.6 mmol) of HMF, 1.17g of Oxone® (KHSO₅/HMF mol ratio = 1.2), 30 mg of sodium 2-iodobenzenesulfonate (0.36 wt%), 6 ml solvent, 70°C with reflux for solvents having boiling point below this temperature, 4h.

Furthermore, a 50/50 mixture of acetonitrile and nitromethane leads to a DFF yield equivalent to that carried out in pure nitromethane (data not shown). One must note that DMSO in our case is inefficient. When using solvents that completely dissolve the reactant and catalyst (DMA and water), no DFF formation was detected. With acidic solvents (entries 6 and 7) the reaction medium rapidly turned dark brown which signifies the formation of humin and degradation of HMF. However, acetic acid, which is less dissociating and less acid ($\epsilon_r = 6.2$ and $pK_a = 4.7$ at 20 °C), allows to obtain a small proportion of DFF. These results corroborate the observations already reported that an excessively acidic environment is not favorable and can lead to the degradation of furan derivatives or its polymerization into humin. [41][42] Compared with the work of Yoon Sik Lee et al. which reports the best oxidation results in chloroform[28], when using chlorinated solvents (entries 10 and 11) only low yields of DFF were obtained. However, with DCM, 35% yield of DFF was obtained which relatively remarkable in view of the relatively low boiling temperature (40 °C), compared to the other solvents. Regarding the reaction without solvent, which was carried out under the same conditions, almost total HMF conversion is obtained but with a 22% yield of DFF, even though the homogenization of the reaction mixture was difficult to be achieved. This result should be compared with similar ones

obtained with non-polar solvents, justifying the hypothesis of complete insolubility of the catalytic oxidizing species of hypervalent iodine in these solvents.

In conclusion, the best solvent for this selective oxidation of HMF to DFF turns out to be nitromethane. The great diversity of results obtained demonstrates the difficulty of being able to predict the efficiency of a solvent according to its physical properties; we can simply note that for this transformation, aprotic polar solvents tend to be more selective towards DFF in the oxidation of HMF. On the base of the proposed mechanism by Santagostino [43] (Scheme 3.3), we can assume that partial solubilization of the different species produced during the oxidation is a necessary but not sufficient condition for the selective oxidation of DFF. This should be tampered by the fact that oxidation takes place under partial acid conditions in all cases (Oxone® is a salt of persulfate and hydrogen sulfate $pK_a = 1.9$) and that acidic conditions could lead to the formation of humins. Note that, the oxidation depends in particular on the dissociation of the pairs of ions and the solubility of Oxone® in different solvents.



Scheme 3.3 - Different iodine derivatives and supposed catalytic cycle during the selective oxidation of HMF to DFF [43]

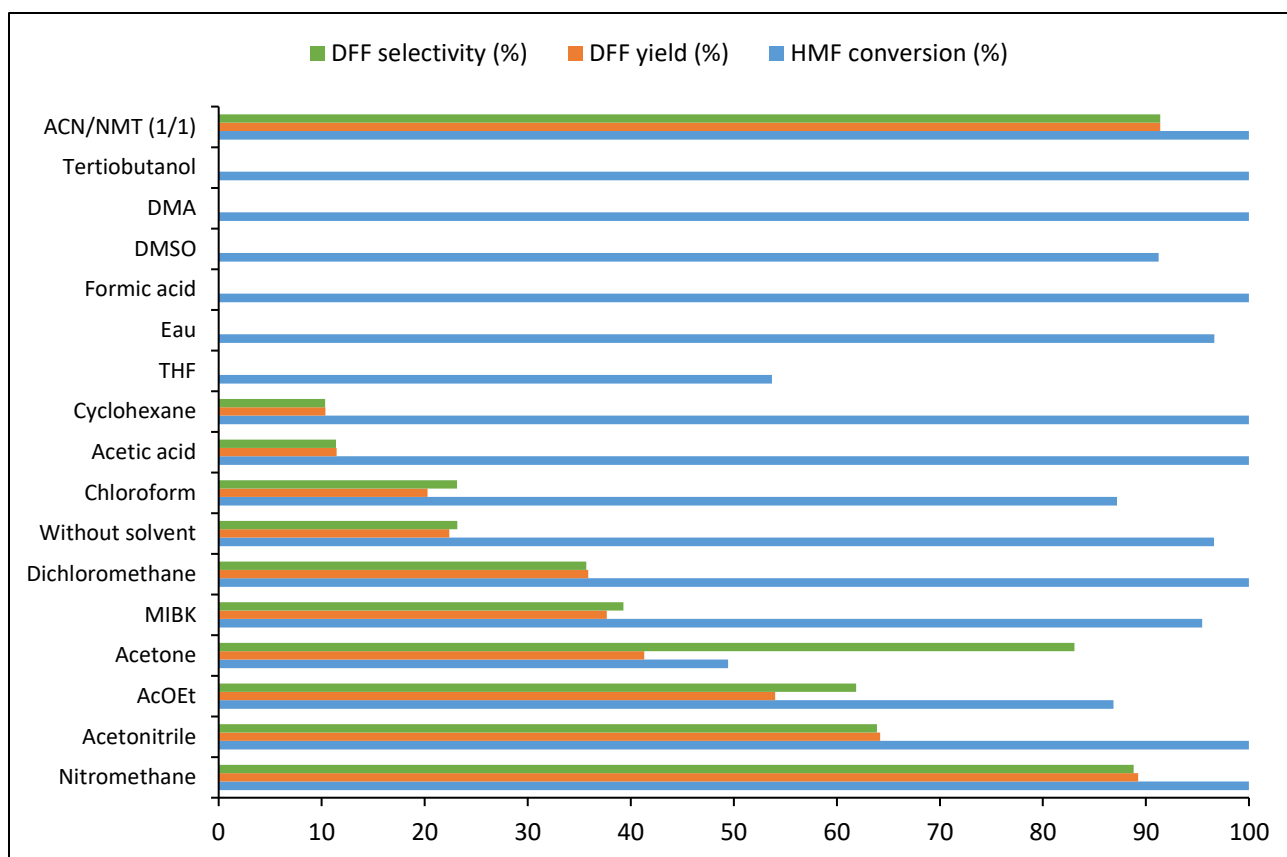


Figure 3.1 - Effect of solvent on HMF conversion, selectivity and yield of DFF. 1.6 mmol of HMF, 1.17 g Oxone® (KHSO_5/HMF mol ratio=1.2), 30 mg of catalyst (0.36 wt%), 70°C, 4h.

3.3. Effect of reaction temperature

In view of the good results obtained in nitromethane and their potential optimization, we studied, in this solvent, the effects of the various reaction parameters of the transformation. First, we evaluate the influence of the temperature over a 4 h reaction (Figure 3.2). The conversion of HMF is larger than 90% at 40 °C; however, this value is 100% at temperatures above or equal to 70 °C.

Despite the fact that there were no traces of DFF formation at room temperature (21 °C) after 4 hours of reaction, it was interesting to note that around 50% of HMF have been converted to unknown products (probably intermediate species) that could not be identified by our GC method. DFF yield and selectivity varied similarly with the reaction temperature reaching a maximum for 70 °C. Furthermore, above 70 °C, the conversion rate of HMF is total, but the yield of DFF gradually drops, demonstrating its instability at high temperatures. At 101 °C, the boiling point of nitromethane, only 18% of the DFF can be measured in GC after 4 hours of reaction. The degradation products have been identified as being mainly maleic acid (NMR analysis). Noteworthy, in other conditions, for example, by Mishra et al., the DFF is prepared at much higher temperatures (up to 130 °C) in toluene and in the presence of Ruthenium catalyst and oxygen. [44]

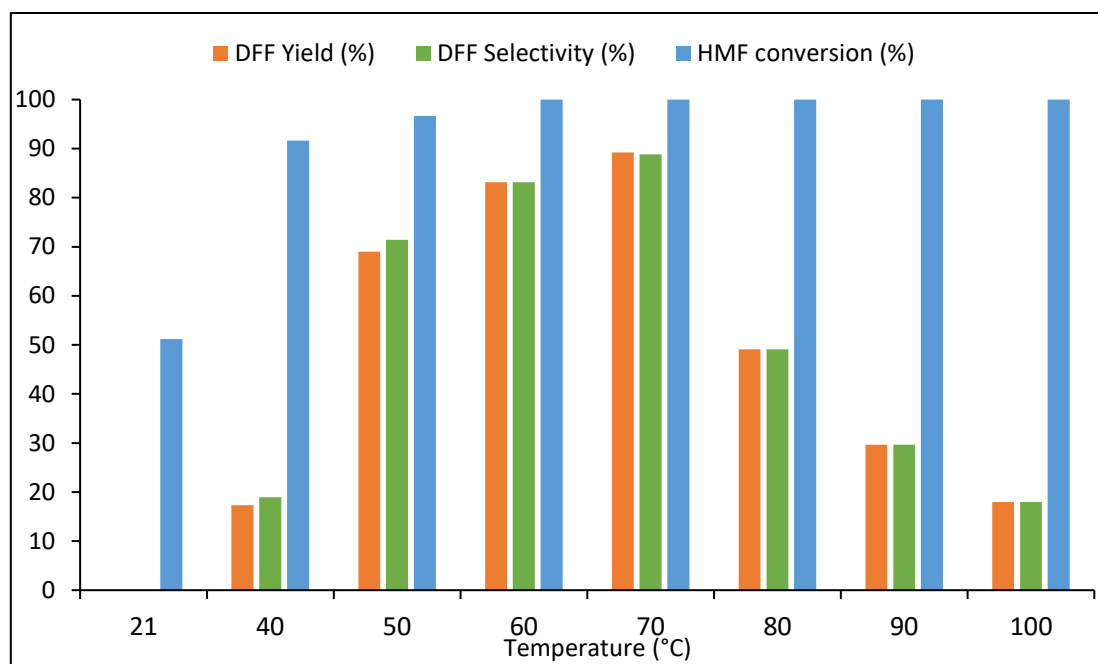


Figure 3.2 - Effect of temperature on HMF conversion, selectivity and yield of DFF. 1.6 mmol of HMF, 1.17 g Oxone® (KHSO₅/HMF mol ratio=1.2), 30 mg of catalyst (0.36 wt%), 6 ml nitromethane, 4h.

3.4. Effect of reaction time

In order to verify the hypothesis of DFF degradation at temperatures above 70 °C, we performed reaction monitoring at 70 °C, 80 °C and 90 °C as shown in the figures below.

As the temperature increases, the conversion of HMF increases and could achieve 100% of total conversion in only half-an hour at a temperature higher than 70 °C.

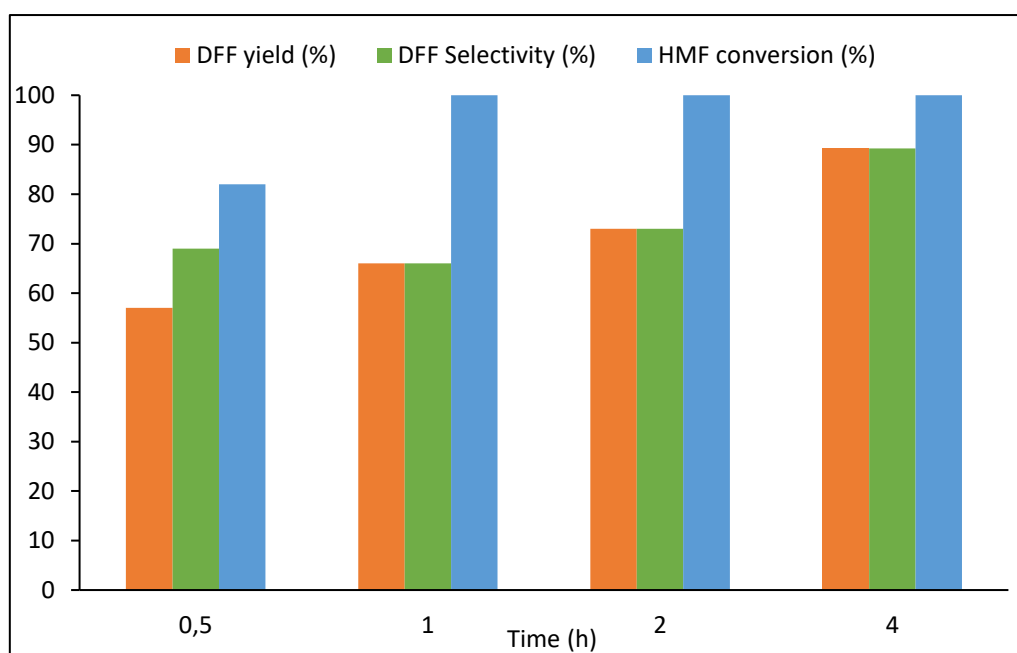


Figure 3.3 - Effect of reaction time on DFF yield and selectivity, and the HMF conversion at T=70 °C

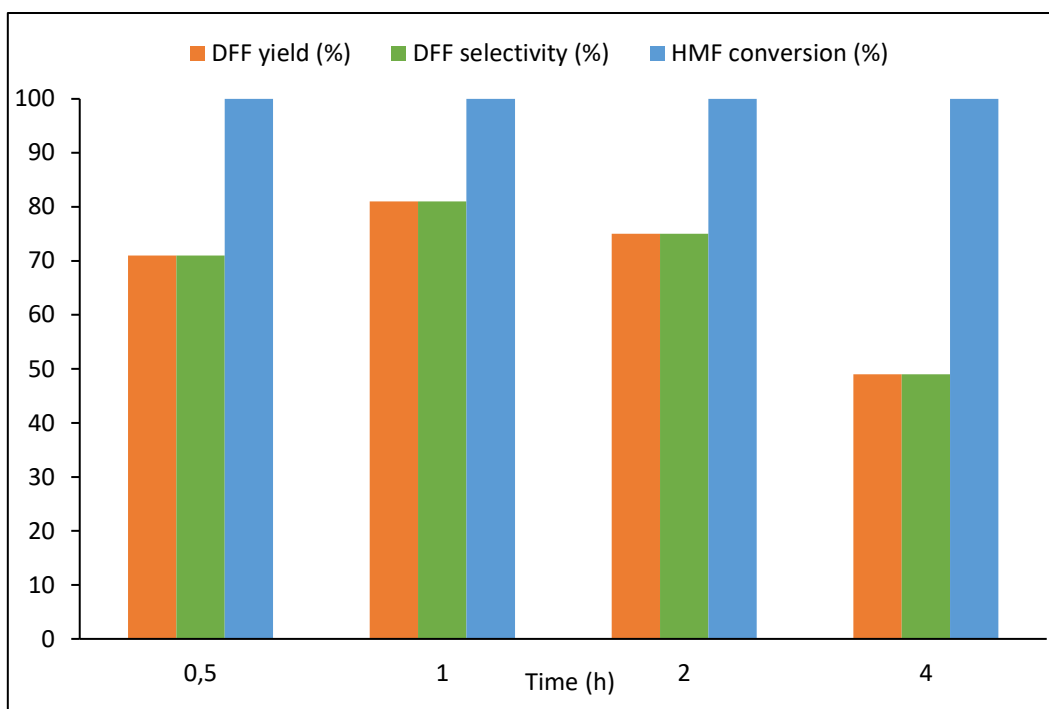


Figure 3.4 - Effect of reaction time on DFF yield and selectivity, and the HMF conversion at T=80 °C

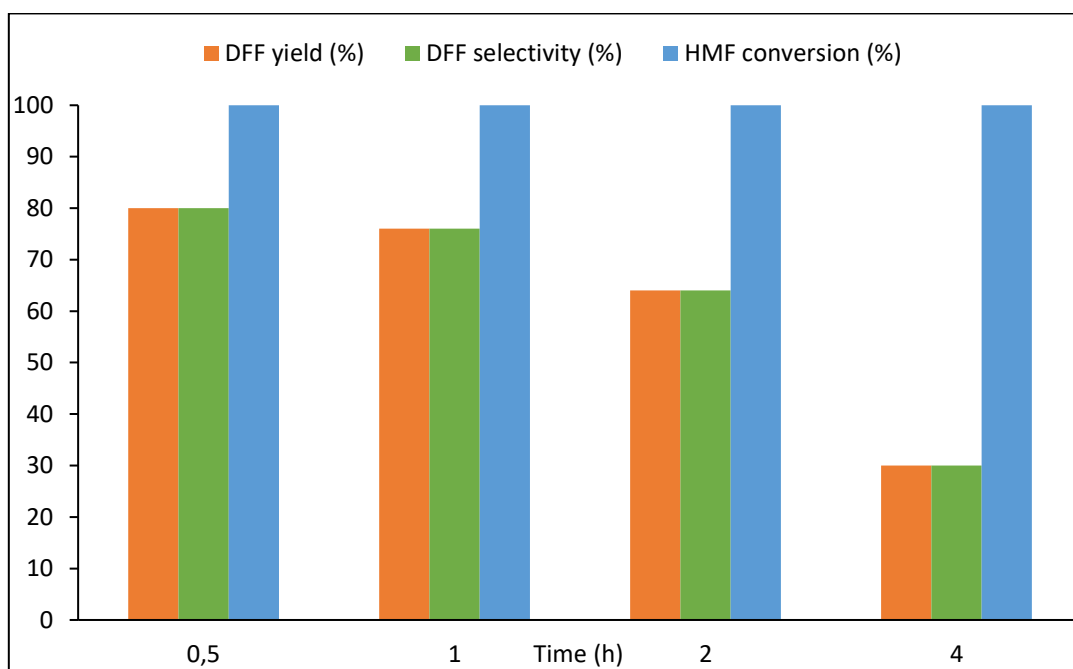


Figure 3.5 - Effect of reaction time on DFF yield and selectivity, and the HMF conversion at T=90 °C

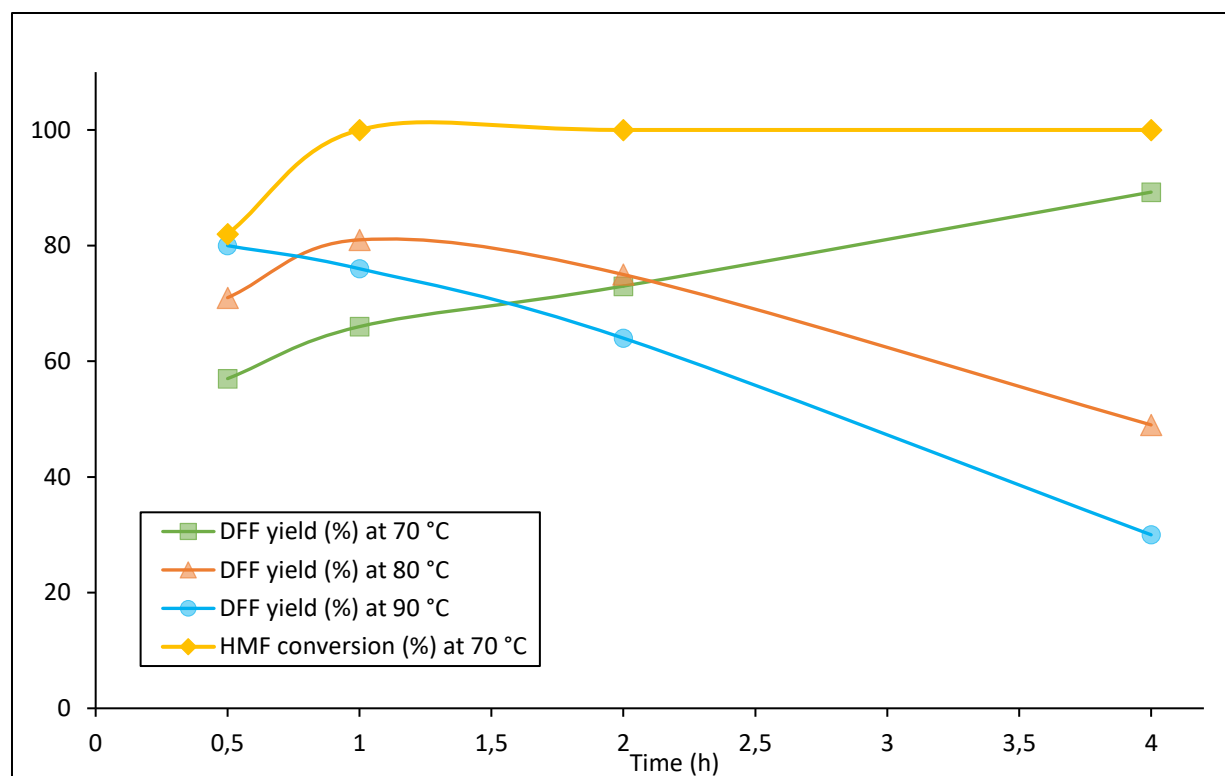


Figure 3.6 - Effect of temperature as a function of time on the conversion of HMF at 70°C and the yield of DFF at 70 °C, 80 °C and 90 °C. HMF 1.6 mmol, Oxone® 1.17g (KHSO₅/HMF mol ratio=1.2), catalyst 30mg (0.098mmol, 0.36 wt%), 6 ml nitromethane.

These experiments show that high yield of DFF could be reached rapidly at higher temperature, 80% at 90 °C in half an hour (Figure 3.6). This also indicates that the catalyst presents a good stability at higher temperature and could play its full role without inconvenience.

The catalyst's stability was also verified by preheating it at 90°C for one hour then introducing it into the reactor for 4 hours of oxidation at 70°C. Despite this, a DFF yield of 90% was still obtained.

Nevertheless, these results also demonstrate once again the instability of the formed DFF towards temperature in nitromethane. Thus, the best results are obtained for a moderate heating at 70 °C over 4 h. This is in accordance with the known instability of DFF (storage at low temperature is recommended to avoid its degradation). In conclusion, a strong acceleration of the transformation is observed by increasing the temperature as well as a more rapid degradation of the DFF formed.

3.5. Effect of the catalyst weight

For the purpose of verifying a potential acceleration of the reaction with the increase of the catalyst quantity, we investigated the effect of its concentration (Figure 3.7). It is observed that in the absence of catalyst, the HMF conversion reaches only 60% without leading to the formation of DFF. This result is indicative of one or more competitive transformations with the

selective oxidation reaction from HMF to DFF. With increasing amount of catalyst at 70 °C in 4 hours, the conversion reaches 100 % and the yield of DFF attain a maximum using 0.36 wt% of the catalyst before decreasing to values around 50 to 40%.

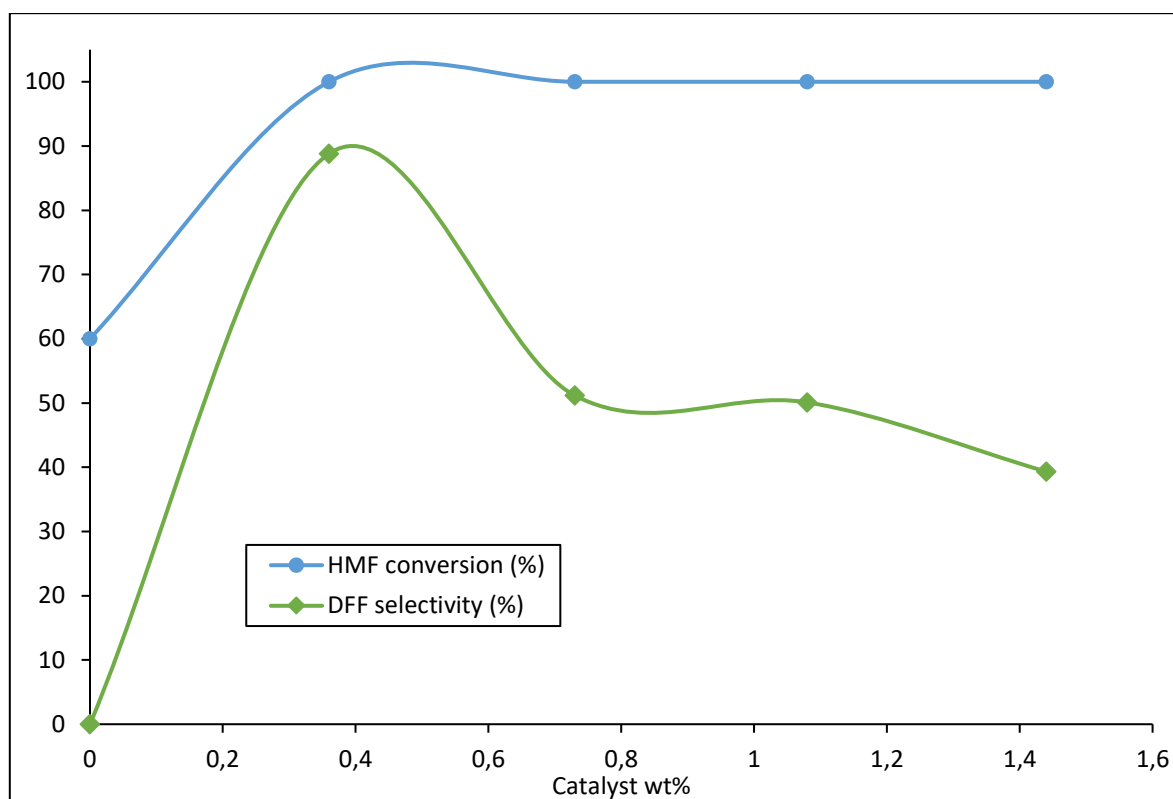


Figure 3.7 - Effect of the catalyst weight sodium 2-iodobenzenesulfonate (wt%) on HMF conversion and DFF selectivity. HMF 1.6 mmol, Oxone® 1.17g, sodium 2-iodobenzenesulfonate 0 to 1.44 wt%, 6 ml nitromethane, 70 °C, 4h.

In order to further investigate these results, we compared the formation of DFF with time at 0.36 and 0.73 wt% of catalyst (Figure 3.8). Even though an acceleration of the DFF formation is observed during the two first hours using more catalyst it quickly appears that the DFF concentration decreases with extended processing times in these conditions and over-oxidation becomes preponderant mainly into maleic acid. Therefore, it could reasonably be hypothesized that increasing the quantity of catalyst is detrimental to DFF stability and formation, probably due to the acidic nature of the catalyst leading to DFF degradation and polymerization into humins. To conclude, the best compromise is a reasonable 70 °C heating over 4h with 0.36 wt% of catalyst.

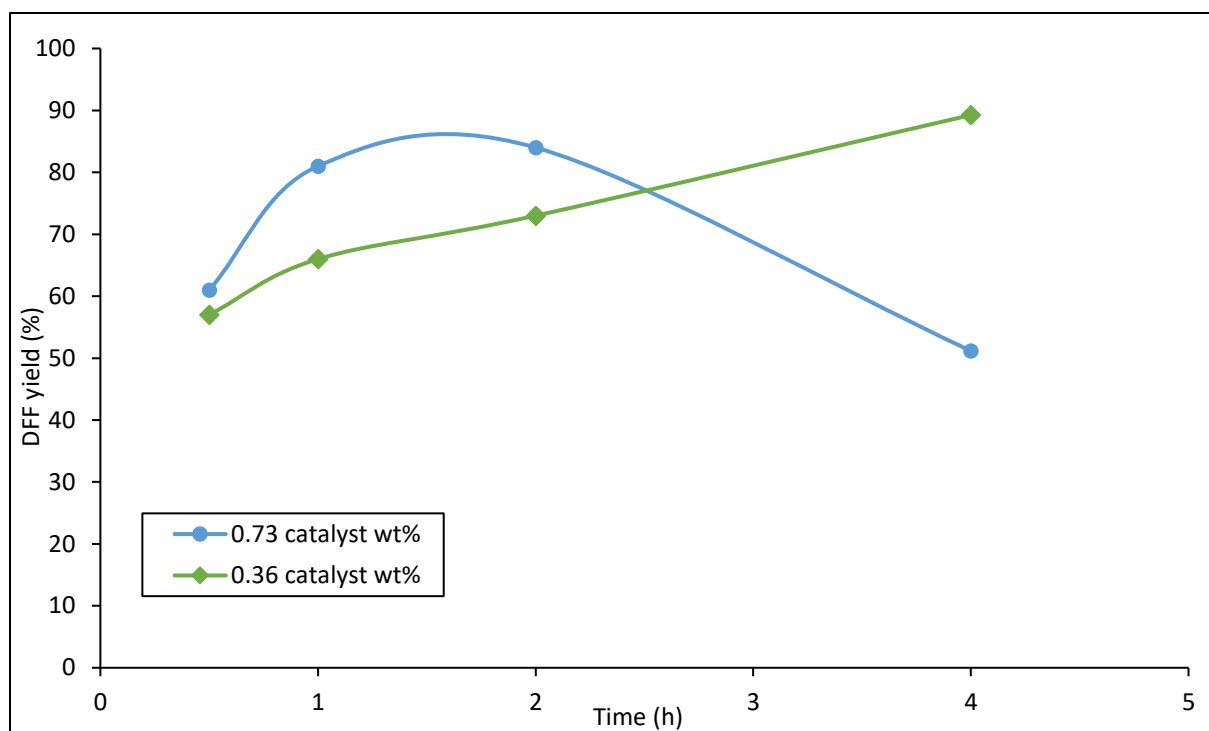


Figure 3.8 - Effect of the amount of catalyst on DFF yield as a function of time. HMF 1.6 mmol, Oxone[®] 1.17g, sodium 2-iodobenzenesulfonate 0.36wt% (green) and 0.73wt% (blue), 6 ml of nitromethane, 70°C.

3.6. Effect of Oxone[®] and HMF amounts

The effect of the introduced amount of HMF at the beginning of the reaction was examined, the corresponding results were illustrated in figure 3.9.

A total conversion could be achieved regardless the introduced amount of HMF even if the oxone[®] becomes the limiting reactant. However, we notice that the DFF yield could be affected by the mass of HMF. From 1.21 to 2.43 of HMF wt% (100 mg to 200 mg), the DFF yield increases from 55% to a maximum of 89%. Beyond this mass, the DFF yield decreases progressively. This is due to the deceleration of the reaction rate at higher amounts of HMF. This could be explained by the following, this exact amount of oxidant is sufficient for total conversion of furfural but insufficient to accelerate the reaction rate to obtain DFF in high yields, however the reaction stops at intermediate products.

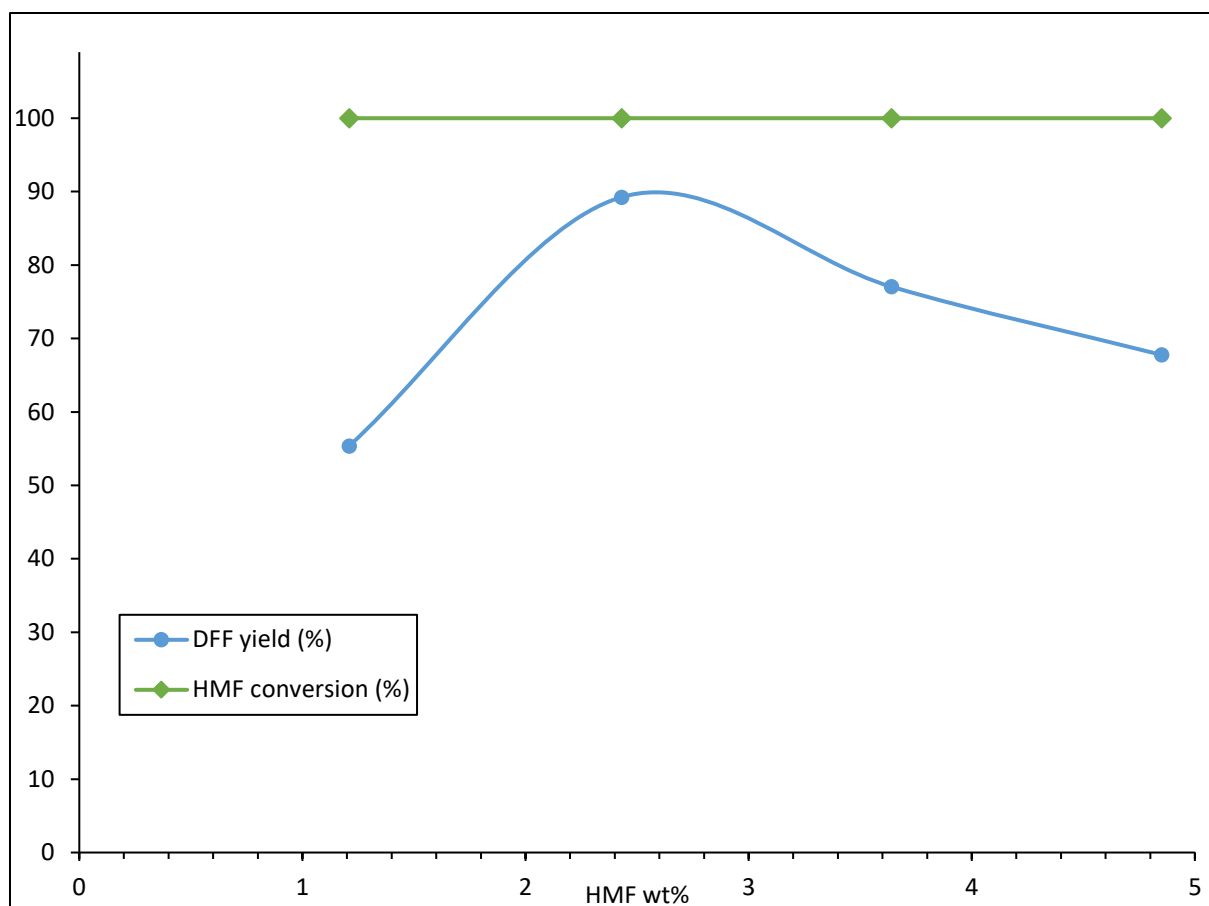


Figure 3.9 - Effect of the amount HMF on DFF yield and HMF conversion. Oxone[®] 1.17g, sodium 2-iodobenzenesulfonate 0.36wt%, 6 ml of nitromethane, 70°C.

In order to maximize the production of DFF by limiting the production of wastes, we studied the effect of the amount of co-oxidant Oxone[®] and the HMF concentration on the yield of DFF. We know that these factors can have a significant impact on the transformation.

We carried out a first series of experiments by keeping the quantities of catalyst and Oxone[®] constant and varying only the HMF mass. This, therefore, implies a variable Oxone[®]/HMF ratio ranging from 2.4 corresponding to 100 mg to 0.6 corresponding to 400 mg of HMF introduced (Figure 3.10, blue line (□)). We observe that the Oxone[®] used in excess, corresponding to 2.4 eq, leads to a loss of selectivity and yield of DFF (Figure 3.10 (□), point at 100 mg). While it is used as a limiting reagent, we observe a quantitative yield compared to the Oxone[®] which is totally consumed to oxidize the HMF to DFF (Figure 3.10 (□), points at 300 and 400 mg of HMF). Furthermore, in the latter two cases, the remaining expected HMF is no longer visible, demonstrating its transformation along unknown reaction path. During a second series of experiments, we maintained the Oxone[®]/HMF ratio at 1.2, keeping the other parameters constant (Figure 5 (Δ), Green curve). In this case, the constant amount of catalyst (30 mg) mainly affects the yield of DFF, there is a slight decrease in the yield at low HMF concentration (point

at 100 mg), and a loss of activity when the HMF concentration increases with respect to the amount of catalyst.

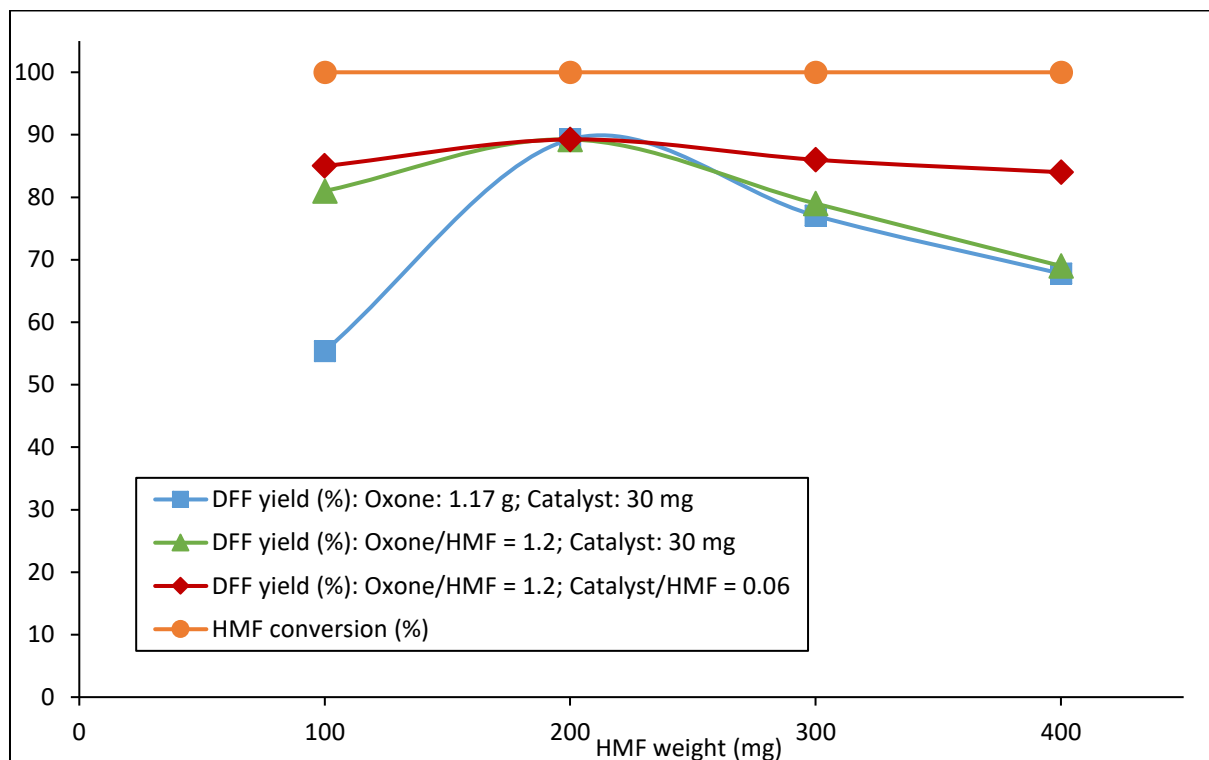


Figure 3.10 - Effect of the amount of HMF (from 100 mg to 400 mg) on the yield of DFF with various oxone[®] to HMF ratio and catalyst to HMF ratio, 6 ml of nitromethane, 70°C, 4 h. (□): Oxone[®]/HMF ratio= 2.4 (100 mg of HMF), 1.2 (200 mg of HMF), 0.8 (300 mg of HMF) and 0.6 (400 mg of HMF), (Δ): catalyst/HMF ratio = 0.12 (100 mg of HMF), 0.06 (200 mg of HMF), 0.04 (300 mg of HMF) and 0.03 (400 mg of HMF)

Finally, during a final series of experiments, the volume of solvent is kept as the only constant parameter, *i.e.* 6 ml. The Oxone[®]/HMF ratio is maintained at 1.2 and the Catalyst/HMF ratio at 0.06.

In this case, it is interesting to note that the yield obtained in DFF remains very high, close to the maximum yield under optimal conditions. Thus, with 1.3wt%, 3.4wt% and 4.2 wt% of HMF corresponding to a mass of 100 mg, 300 mg and 400 mg, the corresponding DFF yields are 85%, 86 % and 84% (Figure 3.10 (◇), red curve). These last results are very important because they confirm the possibility of working at higher HMF concentrations without significantly affecting the production of DFF.

3.7. Catalyst recyclability

For effective industrial utilizations of heterogeneous catalysts, the lifetime, stability and reusability is an important parameter.

At the end of the transformation the catalyst can be partially separated from the sulphate salts that is, recovered by filtration and extraction. This allowed us to study its recycling potential.

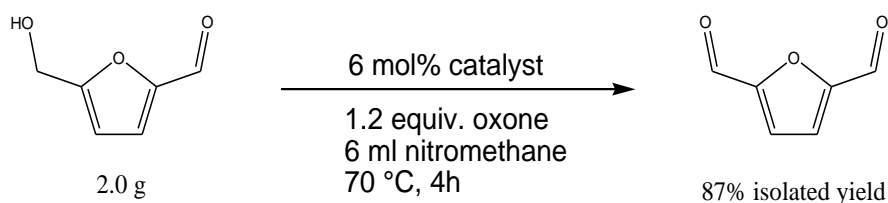
Hence, the recyclability test of 2-iodobenzenesulfonic acid was investigated on the oxidation of HMF to DFF under the optimized experimental conditions. After the catalytic test, the catalyst was recovered by simple filtration and extensively washed with ethyl acetate. After being dried under vacuum, 14 mg of catalyst precipitates were obtained (around 50% of initial mass). This exact amount was reused for the next reaction, instead of 30 mg, and a DFF yield of 50% was obtained.

Note that, at the end of the reaction, the catalyst is present in different forms with different oxidation degrees (+I, +III and +V) more or less soluble in the washing solvent. This could explain the loss of around 50% of the catalyst.

Thus, the catalyst recovery is a feature to improve, but it appears that the recovered catalyst is still active and permit to perform the reaction as efficiently.

3.8. Gram-scale synthesis of DFF

At the end of this work, we wanted to verify that this method could be adapted to the preparation of DFF on the scale of several grams. By equally multiplying the quantities of materials we obtained DFF with the same grade of selectivity and yield, with structure assigned by NMR analysis, confirming the possibility of extending our method to this first stage of scale-up. Finally, a gram scale synthesis was performed in the optimized conditions. Starting with 2 g of HMF, an 87% isolated yield of DFF (1.78 g) was achieved (Scheme 3.4), which further highlighted the interest of this catalyst in this oxidation reaction.



Scheme 3.4 - Synthesis of DFF by selective oxidation of HMF in gram scale

4. Conclusion

With this work, we demonstrated the possibility of using hypervalent iodine derivatives in the presence of persulfate (Oxone®), an economical and non-toxic oxidant with non-toxic byproducts, to carry out the oxidation of HMF to DFF with great selectivity and yields. The method is particularly simple, because only filtration or extraction of the sulfate salts and the catalyst at the end of the reaction are required to obtain the DFF with a high grade of purity. The active oxidizing species obtained "in situ" eliminate the risks associated with the use of iodine derivatives in stoichiometric proportions and reduce the costs of the catalyst. We

optimized the reaction conditions by considering the product stability and competitive reactions. The best compromise was obtained for a 4 hours of reaction at 70 °C, using nitromethane. In these conditions, 89% of DFF is obtained as the only product. In addition, very good results are also observed over much shorter times, in 30 min at 90 °C, where 80% of DFF is obtained. On the contrary to what was described in literature this method involves no metallic catalyst, uses reasonable concentration of HMF, and we have demonstrated the possibility of extending the method to a gram-scale production of DFF. Therefore, we believe that these results lay the foundation for the development of a larger scale process.

References

1. Karl J. Zeitsch (2000) *The Chemistry and Technology of Furfural and Its Many By-products*, Elsevier.
2. Cai, C.M., Zhang, T., Kumar, R., and Wyman, C.E. (2014) Integrated furfural production as a renewable fuel and chemical platform from lignocellulosic biomass. *J. Chem. Technol. Biotechnol.*, **89** (1), 2–10.
3. Mariscal, R., Maireles-Torres, P., Ojeda, M., Sádaba, I., and López Granados, M. (2016) Furfural: A renewable and versatile platform molecule for the synthesis of chemicals and fuels. *Energy Environ. Sci.*, **9** (4), 1144–1189.
4. Teong, S.P., Yi, G., and Zhang, Y. (2014) Hydroxymethylfurfural production from bioresources: Past, present and future. *Green Chem.*, **16** (4), 2015–2026.
5. Lewkowski, J. (2001) Synthesis, chemistry and applications of 5-hydroxymethyl-furfural and its derivatives. *Arkivoc*, **2001** (1), 17–54.
6. Hu, L., Lin, L., Wu, Z., Zhou, S., and Liu, S. (2017) Recent advances in catalytic transformation of biomass-derived 5-hydroxymethylfurfural into the innovative fuels and chemicals. *Renew. Sustain. Energy Rev.*, **74** (February 2016), 230–257.
7. Van Putten, R.J., Van Der Waal, J.C., De Jong, E., Rasrendra, C.B., Heeres, H.J., and De Vries, J.G. (2013) Hydroxymethylfurfural, a versatile platform chemical made from renewable resources. *Chem. Rev.*, **113** (3), 1499–1597.
8. Liu, D., and Chen, E.Y.X. (2014) Organocatalysis in biorefining for biomass conversion and upgrading. *Green Chem.*, **16** (3), 964–981.
9. Fan, W., Verrier, C., Queneau, Y., and Popowycz, F. (2019) 5-Hydroxymethylfurfural (HMF) in Organic Synthesis: A Review of its Recent Applications Towards Fine Chemicals. *Curr. Org. Synth.*, **16** (4), 583–614.
10. Kohli, K., Prajapati, R., and Sharma, B.K. (2019) Bio-based chemicals from renewable biomass for integrated biorefineries. *Energies*, **12** (2).
11. Šivec, R., Grilc, M., Huš, M., and Likozar, B. (2019) Multiscale Modeling of (Hemi)cellulose Hydrolysis and Cascade Hydrotreatment of 5-Hydroxymethylfurfural, Furfural, and Levulinic Acid. *Ind. Eng. Chem. Res.*, **58** (35), 16018–16032.
12. Pal, P., and Saravanamurugan, S. (2019) Recent Advances in the Development of 5-Hydroxymethylfurfural Oxidation with Base (Nonprecious)-Metal-Containing Catalysts. *ChemSusChem*, **12** (1), 145–163.
13. Zhang, Z., and Huber, G.W. (2018) Catalytic oxidation of carbohydrates into organic acids and furan chemicals. *Chem. Soc. Rev.*, **47** (4), 1351–1390.
14. Hong, M., Wu, S., Li, J., Wang, J., Wei, L., and Li, K. (2020) Aerobic oxidation of 5-(hydroxymethyl)furfural into 2,5-diformylfuran catalyzed by starch supported aluminum nitrate. *Catal. Commun.*, **136** (September 2019).
15. Giannakoudakis, D.A., Nair, V., Khan, A., Deliyanni, E.A., Colmenares, J.C., and Triantafyllidis,

- K.S. (2019) Additive-free photo-assisted selective partial oxidation at ambient conditions of 5-hydroxymethylfurfural by manganese (IV) oxide nanorods. *Appl. Catal. B Environ.*, **256** (March 2019), 117803.
16. Lin, J.Y., Yuan, M.H., Lin, K.Y.A., and Lin, C.H. (2019) Selective aerobic oxidation of 5-hydroxymethylfurfural to 2,5-diformylfuran catalyzed by Cu-based metal organic frameworks with 2,2,6,6-tetramethylpiperidin-oxyl. *J. Taiwan Inst. Chem. Eng.*, **102**, 242–249.
 17. Mittal, N., Nisola, G.M., Seo, J.G., Lee, S.P., and Chung, W.J. (2015) Organic radical functionalized SBA-15 as a heterogeneous catalyst for facile oxidation of 5-hydroxymethylfurfural to 2,5-diformylfuran. *J. Mol. Catal. A Chem.*, **404–405**, 106–114.
 18. Partenheimer, W., and Grushin, V. V (2001) of 5-Hydroxymethylfurfural . Unexpectedly Selective Aerobic Oxidation of Benzyl Alcohol to Benzaldehyde with Metal / Bromide Catalysts **. *Adv- Synth. Catal.*, **343** (1), 102–111.
 19. Karimi, B., Mirzaei, H.M., and Farhangi, E. (2014) Fe₃O₄@SiO₂-TEMPO as a magnetically recyclable catalyst for highly selective aerobic oxidation of 5-hydroxymethylfurfural into 2,5-diformylfuran under metal-and halogen-free conditions. *ChemCatChem*, **6** (3), 758–762.
 20. Yang, Z., Qi, W., Su, R., and He, Z. (2017) 3D Flower-like Micro/Nano Ce-Mo Composite Oxides as Effective Bifunctional Catalysts for One-Pot Conversion of Fructose to 2,5-Diformylfuran. *ACS Sustain. Chem. Eng.*, **5** (5), 4179–4187.
 21. Cottier, L., Descotes, G., Lewkowski, J., and Skowroński, R. (1995) Ultrasonically accelerated syntheses of furan-2,4-dicarbaldehyde from 5-hydroxymethyl-2-furfural. *Org. Prep. Proced. Int.*, **27** (5), 564–566.
 22. El-Hajj, T., Martin, J., and Descotes, G. (1983) Dérivés de l'hydroxyméthyl-5 furfural. I. Synthèse de dérivés du di- et terfuranne. 233–235.
 23. J. W. Van Reijendam, Heeres, G.J., and Janssen, M.J. (1970) Polyenyl-Substituted Furans. *Tetrahedron*, **26**, 1291–1301.
 24. Mittal, N., Nisola, G.M., Malihan, L.B., Seo, J.G., Lee, S.P., and Chung, W.J. (2014) Metal-free mild oxidation of 5-hydroxymethylfurfural to 2,5-diformylfuran. *Korean J. Chem. Eng.*, **31** (8), 1362–1367.
 25. Hartmann, C., and Meyer, V. (1893) Ueber Jodo- benzoësäure. *Chem. Ber.*, **26** (2), 1727–1732.
 26. Frigerio, M., and Santagostino, M. (1994) A Mild Oxidizing Reagent for Alcohols and 1,2-Diols: o-Iodoxybenzoic Acid (IBX) in DMSO. *Tetrahedron Lett.*, **35** (43), 8019–8022.
 27. Dess, D.B., and Martin, J.C. (1983) Readily Accessible 12-I-51 Oxidant for the Conversion of Primary and Secondary Alcohols to Aldehydes and Ketones. *J. Org. Chem.*, **48** (22), 4155–4156.
 28. Yoon, H.J., Choi, J.W., Jang, H.S., Cho, J.K., Byun, J.W., Chung, W.J., Lee, S.M., and Lee, Y.S. (2011) Selective oxidation of 5-Hydroxymethylfurfural to 2,5-Diformylfuran by polymer-supported IBX amide. *Synlett*, (2), 165–168.
 29. Lei, Z., Denecker, C., Jegasothy, S., Sherrington, D.C., Slater, N.K.H., and Sutherland, A.J. (2003) A facile route to a polymer-supported IBX reagent. *Tetrahedron Lett.*, **44** (8), 1635–1637.

30. Carbamates, U., Sorg, G., Mengel, A., Jung, G., and Rademann, J. (2001) Oxidizing Polymers : A Polymer-Supported , Recyclable Hypervalent Iodine (v) Reagent for the Efficient Conversion of Alcohols , Carbonyl Solution. *Angew. Chem. Int. Ed. Engl.*, **40** (20), 4395–4397.
31. Reed, N.N., Delgado, M., Hereford, K., Clapham, B., and Janda, K.D. (2002) Preparation of soluble and insoluble polymer supported IBX reagents. *Bioorganic Med. Chem. Lett.*, **12** (15), 2047–2049.
32. Mülbaier, M., and Giannis, A. (2001) The Synthesis and Oxidative Properties of Polymer-Supported IBX. *Angew. Chem. Int. Ed. Engl.*, **40** (23), 4393–4394.
33. Uyanik, M., Akakura, M., and Ishihara, K. (2009) 2-Iodoxybenzenesulfonic Acid As an Extremely Active Catalyst for the Selective Oxidation of Alcohols To Aldehydes, Ketones, Carboxylic Acids, and Enones With Oxone. *J. Am. Chem. Soc.*, **131** (1), 251–262.
34. Plumb, J. B.; Harper, D.J. (1990) 2-Iodoxybenzoic acid. *Chem. Eng. News*, **68** (29), 3.
35. Frigerio, M., Santagostino, M., and Sputore, S. (1999) A user-friendly entry to 2-iodoxybenzoic acid (IBX). *J. Org. Chem.*, **64** (12), 4537–4538.
36. Thottumkara, A.P., Bowsher, M.S., and Vinod, T.K. (2005) In situ generation of o-Iodoxybenzoic acid (IBX) and the catalytic use of it in oxidation reactions in the presence of oxone as a co-oxidant. *Org. Lett.*, **7** (14), 2933–2936.
37. Schulze, A., and Giannis, A. (2006) Oxidation of alcohols with catalytic amounts of IBX. *Synthesis (Stuttg.)*, (2), 257–260.
38. Jones, C.W., and Clark, J.H. (1999) *Applications of Hydrogen Peroxide and Derivatives*, RSC Clean Technology Monographs.
39. Travis, B.R., Sivakumar, M., Hollist, G.O., and Borhan, B. (2003) Facile oxidation of aldehydes to acids and esters with Oxone. *Org. Lett.*, **5** (7), 1031–1034.
40. Girka, Q., Estrine, B., Hoffmann, N., Le Bras, J., Marinković, S., and Muzart, J. (2016) Simple efficient one-pot synthesis of 5-hydroxymethylfurfural and 2,5-diformylfuran from carbohydrates. *React. Chem. Eng.*, **1** (2), 176–182.
41. Gao, X., Peng, L., Li, H., and Chen, K. (2015) Formation of Humin and Alkyl Levulinate in the Acid-catalyzed Conversion of Biomass-derived Furfuryl Alcohol. *BioResources*, **10** (4), 6548–6564.
42. Shen, H., Shan, H., and Liu, L. (2020) Evolution Process and Controlled Synthesis of Humins with 5-Hydroxymethylfurfural (HMF) as Model Molecule. *ChemSusChem*, **13** (3), Evolution process and controlled synthesis of humi.
43. De Munari, S., Frigerio, M., and Santagostino, M. (1996) Hypervalent Iodine Oxidants: Structure and Kinetics of the Reactive Intermediates in the Oxidation of Alcohols and 1,2-Diols by o -Iodoxybenzoic Acid (IBX) and Dess–Martin Periodinane. A Comparative 1 H-NMR Study . *J. Org. Chem.*, **61** (26), 9272–9279.
44. Mishra, D.K., Cho, J.K., and Kim, Y.J. (2018) Facile production of 2,5-diformylfuran from base-free oxidation of 5-hydroxymethyl furfural over manganese–cobalt spinels supported ruthenium nanoparticles. *J. Ind. Eng. Chem.*, **60**, 513–519.

Chapter 4

Catalyst-free oxidation of furfural into maleic acid under high frequency ultra-sound irradiations

1. Introduction

The use of biomass is increasing in order to achieve valuable compounds used in chemical industry. A variety of platform molecules can be synthesized, of which furfural and other furanic derivatives such as HMF and CMF are produced by the hydrolysis and dehydration of C5 and C6 carbohydrates contained in lignocellulose [1–3].

In chapter 3, we developed an oxidation method of HMF into DFF using an organic catalyst in the aim of dematerializing chemical processes. In the same concept, we decided to develop, in this chapter, a catalyst-free oxidation of a new furanic derivative, which is furfural. Furfural is one of the most important renewable resources obtained from corn, wheat and barley [4] and offers a rich source of derivatives that are potential biofuel components. This platform molecule is used and valued by many transformations, especially by oxidation and reduction. Selective oxidations of furfural are particularly studied due to the formation of bifunctionalized molecules like maleic anhydride and diacids such as maleic acid (MA), succinic acid (SA), fumaric acid [5–7].

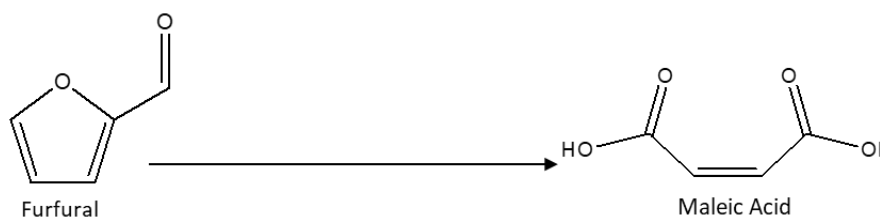
Numerous oxidation methods to convert furfural into MA have been reported in the literature. Significantly, MA is an important raw material used in the manufacture of resins, plasticizers, copolymers, surface coatings, lubricant additives, and agricultural chemicals [8–10]. Typical oxidation reactions for the selective transformation of furfural to MA necessitate the use of heavy metal catalysts, require the preparation of complex catalysts [8,11–14] and sometimes are performed at high temperatures [15,16]. Furthermore, these methods require the use of oxygen as an oxidant at high-pressure values, sometimes up to 20 bars [8,11,12,17]. Other methods present a selective oxidation towards MA. The use of TS-1/H₂O₂ catalytic system, for example, can give 78% yield of MA with total conversion of furfural. However, this method suffer from the long reaction time (24 h) to achieve this efficacy [18]. Besides, most of these methods works in low concentration mediums and are not adapted to produce MA in a gram-scale.

It should be noted that heterogeneous catalytic methods in the gas-phase rather lead to the preparation of maleic anhydride. Whereas liquid phase methods rather lead to the synthesis of maleic acid. For example, in the liquid phase in the presence of hydrogen peroxide and titanium silicalite catalyst (TS-1), MA yields oscillating between 60 and 80% are observed with total furfural conversion. [19–22] Acid catalysis also demonstrates good efficacy, particularly with Amberlyst® or formic acid (Table 4.1, entries 2-5, 7). Among these methods, the results

reported by Cao et al. in a biphasic medium are remarkable in view of the high concentration of 2-(5H)-furanone (FO) produced under optimized conditions. [23,24] (Table 4.1, entry 3) A comparison of the operating conditions of the excellent oxidation methods developed in the liquid phase are summarized in Table 4.1 and gives us an idea of the parameters which could be improved. These are the catalytic system, the nature of the oxidant, the time and temperature of transformation, the oxidant/furfural molar ratio, the mass concentration of raw material. On this last point, it is important to note that most methods are described at mass concentrations below 5 wt%, leading to the management of secondary material flows and the associated energy expenditure. Let us recall now that the solubility of maleic acid is very important in water (789 g.L^{-1}) at $25 \text{ }^{\circ}\text{C}$, [25] which is also the solvent of the majority of the methods described for its preparation. (Table 4.1) This poses a major problem for recovering MA, particularly by recrystallization, because we are forced to evaporate or freeze-dry water almost as a whole. Pure oxygen or better the direct use of air as an oxidant is ideal both economically and ecologically, the problem with its use lies in the activation of oxygen, which requires a catalytic system and / or conditions of temperature and pressure above ambient. A good alternative lies in the use of hydrogen peroxide which is also considered an ideal oxidant in terms of economics, availability, green metrics, atom economy, degradability, so particularly relevant as a green oxidant for industrial processes. [26]

The main disadvantage of hydrogen peroxide is its instability and the risk of an explosion from concentrated solutions by disproportionation. [27] Pursuing our goal of developing new methods of transformation of furfural by oxidation, we turned to high-frequency ultrasound technology.

Table 4.1 - Different methods of MA production highlighting the concentration of FUR



Entry	Catalyst Wt%	Wt% Fur. ⁽¹⁾	Solvent	m.r. O/F ⁽²⁾	Temp. ($^{\circ}\text{C}$)	Time (h)	Product(s) Sel. ⁽³⁻⁴⁾	Conv.	Products (g.L^{-1})	Ref.
1	TS-1 4.6%	4.6	H ₂ O	7.5	50	24	MA 78%	100%	45	[21,22]
2	Amberlyst-15 1.4%	2.7	H ₂ O	4	80	24	SA 74% MA 11% FA 1.9%	>99%	25.6 3.8 0.6	[28,29]

3	HCOOH 4,6%	11.5	1.2 DCE ⁽⁴⁾ / H ₂ O	2.4	60	3	FO 60.3% SA 12% MA 6.3%	>99%	110 ⁽⁶⁾ 13.3 25.6	[25,26]
4	HCOOH 80%	1.6	HCOOH	10.1	60	4	MA 95%	100%	22	[10]
5	BHC ⁽⁴⁾ 16%	4	H ₂ O	10	100	0.5	MA 61% FA 31%	100%	39 20	[16]
6	KBr/g-C ₃ N ₄ 2% (4)	2.9	H ₂ O	-	100	3	MA 70%	>99%	26	[30]
7	AcOH/TS-1 2%	4.3	AcOH	8	80	4	MA 60%	100%	32	[24]
8	1-Methylene Blue 0.1%	4.1	MeOH	O ₂ ⁽⁵⁾	R. T. ⁽⁷⁾	6	5-HFO 95%	>99%	32	[31]
	2-Electrocatal. Or enzymatic	< 0.5	H ₂ O	-	R. T.	1 Or 24	MA 90% FA 7.4% or MA 99%	>90% Or >99%	<5.8	
9	CD-SO ₃ H, US 25kHz	5.9	H ₂ O	4.5	60	1.2	SA	81%	65	[32]
10	Catalyst Free, HFUS ⁽⁴⁾ 565kHz	> 20	H ₂ O	3.9	42	2	MA 70%		180	This Work
							SA 5%		13	
							MalA 7%		21	
							FO 16%	92%	33	

(1) weight% furfural (2) Molar ratio H₂O₂/Furfural (3) Products selectivity (4) Acronyms : BHC: Betaine Hydrochloryde, 1,2 DCE : 1,2 dichloroethane, FA: fumaric acid, FO: 2-(5H)-Furanone, g-C₃N₄: graphitic carbon nitride, 5-HFO: 5-Hydroxy-2-(5H)-Furanone, MA: Maleic Acid, MalA : Malic Acid, SA: Succinic Acid, HFUS: High Frequency Ultrasound, (5) Atmospheric pressure, 250ml.min⁻¹ (6) Biphasic system, (7) Room Temperature, these concentrations could be almost multiplied by two considering each phase separately FO in DCE and MA, SA in aqueous phase

2. Sonochemistry

The use of ultrasound to promote chemical reactions is called sonochemistry. The first chemist who used intense sound waves was Alfred L. Loomis in 1927 since then, the term “sonochemistry” was born [33].

Sonochemistry has several advantages, including being able to generate oxidizing radical species such as HO• without the use of catalysts as in Fenton conditions for example, which will be discussed in the following chapter. [34] This can be of great interest in the implementation of the process by facilitating the purification steps while reducing costs. The sonolysis of water is well described. The physical phenomena of sonication such as bubble sizes and temperatures reached when they collapse have been studied extensively, as well as the generation of radical species and their concentration. These different phenomena are correlated with the frequency and power of irradiation. [35–39]

Ultrasounds, passing through a medium, consist of alternate compressions and refractions, which create regions with high and low pressure. This change of pressure gives rise to a physical process consisting of formation, growth and collapse of acoustic cavitation. This process induces high local pressure and temperature inside the cavities (bubbles) which enhance the mass transfer in the reaction medium and lead to a turbulent flow (figure 4.1). [40–42]

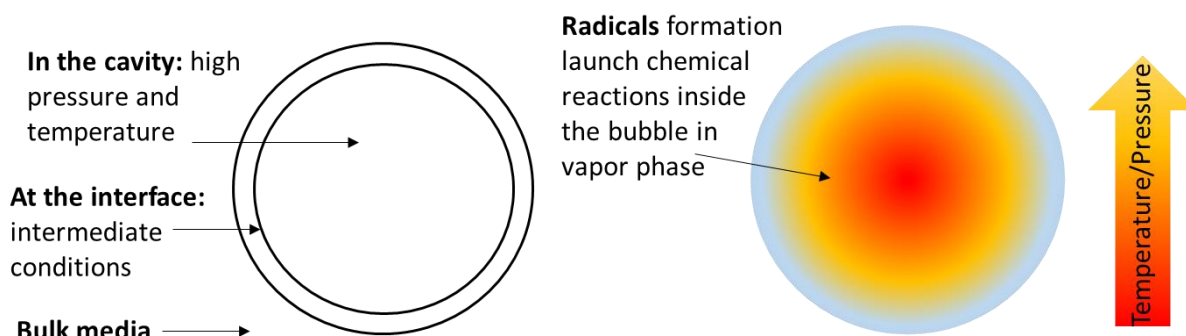


Figure 4.1 - Cavitation bubble in a homogeneous medium

On increasing frequency, the pressure cycle roughly changes, causing high turbulence in the medium. This effect is known as acoustic streaming, dominates acoustic cavitation at high frequency ultrasound (HFUS). High frequency ultrasound range can be considered from 300 to 1000 kHz where sonochemical reactions are particularly predominant. Therefore, the yield of chemical products is greater at higher frequencies. [43,44]

Sonochemistry has wide applications in chemical transformations and recently, by its advantages, finds a growing place in sustainable development and green chemistry [45–49]

Noteworthy, sonochemistry has been used also for the production of furfural. Ultrasound-assisted acid hydrolysis has shown to be efficient for lignocellulose conversion into furfural using only diluted HNO_3 with ultrasound [50,51]. Furthermore, ultrasound with the solid acid $\text{HSO}_3\text{-ZSM-5}$ have proven to be useful for the xylan conversion to furfural. Without ultrasonification, an 89% yield of furfural has obtained in 120 min at 160 °C. With ultrasound pretreatment, the same yield was achieved in 15 min at 60 °C [52].

Moreover, ultrasonic oxidation has been used for the degradation of furfural in contaminated wastewater. Sonochemical degradation of furfural conversion was found to be 83% with low ultrasound wave frequency (20 kHz) at 2 h treatment duration. [53] Free hydroxyl radicals produced in cavitation bubbles during water sonication are responsible. Aside, the degradation of furfural was clearly enhanced in acidic conditions since pH value can affect the ultrasonic decomposition rate of furfural and water as well. [54,55] In the same context, Kermani et al. studied the degradation of

furfural in aqueous solution by ultrasonic waves using the activated persulfate and peroxymonosulfate, and the main radical in the oxidation reactions was the sulfate radical.[56]

Moreover the oxidation of furfural under ultrasound has already been reported for the selective production of succinic acid (SA). [32] With this method, a yield of 81% of SA was obtained, *i.e.* the equivalent of 65g.L⁻¹ in the presence of H₂O₂ as oxidant with a Oxidant/furfural molar ratio of 4.5 and catalyzed by an acid β -cyclodextrin-SO₃H at 60°C under 25 kHz ultrasonic irradiation for 68 min (table 4.1, entry 9).

These methods, although developed at low frequencies, demonstrate the value of this activation technique for oxidation. In this project, we present the development of an effective catalyst-free method for oxidizing furfural into maleic acid in water by activation under high frequency ultrasound (HFUS, 565kHz), from a highly concentrated solution of furfural (2.4 mol.L⁻¹) is 5 to 12 times more concentrated than the methods generally reported in the literature. (Table 4.1, entry 10)

3. Experimental part

3.1. Materials, solvents and reagents

Furfural and hydrogen peroxide (H₂O₂) were purchased from Acros Organics and Fisher Chemicals respectively and further used without any purification.

3.2. Instruments and analytical methods

3.2.1. Gas Chromatography

In this study, a PerkinElmer Autosystem XI instrument was used for the detection of furfural. It was equipped with an auto sampler and a flame ionization detector (FID) with a 30 m length and 0.25 mm diameter AT-1HT column Part No. 16368. The different experimental parameters for the GC analyses were as follows: nitrogen as carrier gas with a flowrate of 1 mL/min, temperature of the injector (T_{injector}) set at 350 °C, temperature of the column (T_{column}) set at 40 °C for 2 min and then increased up to 250 °C with a heating rate of 20 °C/min. The injection volume is set to 1 μ L.

Q_{H₂}= 45 ml/min and Q_{air}=450 ml/min.

3.2.2. High performance liquid chromatography

In this study a Shimadzu HPLC equipped with a corgel 87H3 column.

Mobile phase: formic acid 8.10⁻³ M, flow 0.6 mL/min. Column Temp: 35 °C. The injection volume was 10 μ L.

3.2.3. Evaporative Light Scattering Detector

An evaporative light scattering detector ELSD-LTII from Shimadzu is used in conjunction with high-performance liquid chromatography (HPLC), to detect some diacids that could not be detected by UV lights. ELSD is related to the charged aerosol detector (CAD).

These particles are pushed through the drift tube by the carrier gas which is nitrogen (N₂) to the detection region. In this region, a beam of light crosses the column of analyte and the scattering of light is measured by a photodiode or photomultiplier tube.

Detection is done at 50 °C, with a gain of 10. The used mobile phase is formic acid 8.10⁻³ M having a flow rate of 0.6 mL/min

3.2.4. NextGen Lab 1000 reactor

The high-frequency ultrasonic reactor used was SinapTec Ultrasonic Technology, NextGen Lab 1000, 550 kHz, designed cylindrical stain steel reactor in a cup-horn configuration with a 75 mm diameter base-surface, and equipped with a double-jacket cooling system.

The sonication base integrates ultrasonic cells (piezoelectric ceramics).

Piezoelectric ceramics transform applied electrical energy into mechanical energy in the form of high frequency vibrations. These vibrations are transmitted to the solution to generate ultra-sound irradiation and create a pressure field in the fluid. If the power level is sufficient, a cavitation phenomenon is triggered in the fluid.

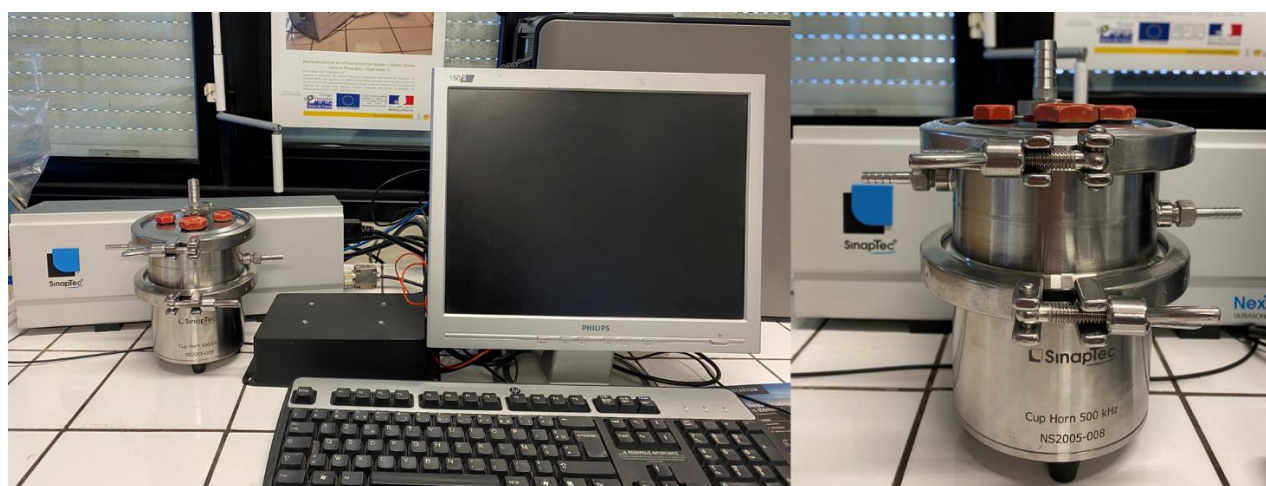


Figure 4.2 - NextGen Lab 1000 reactor

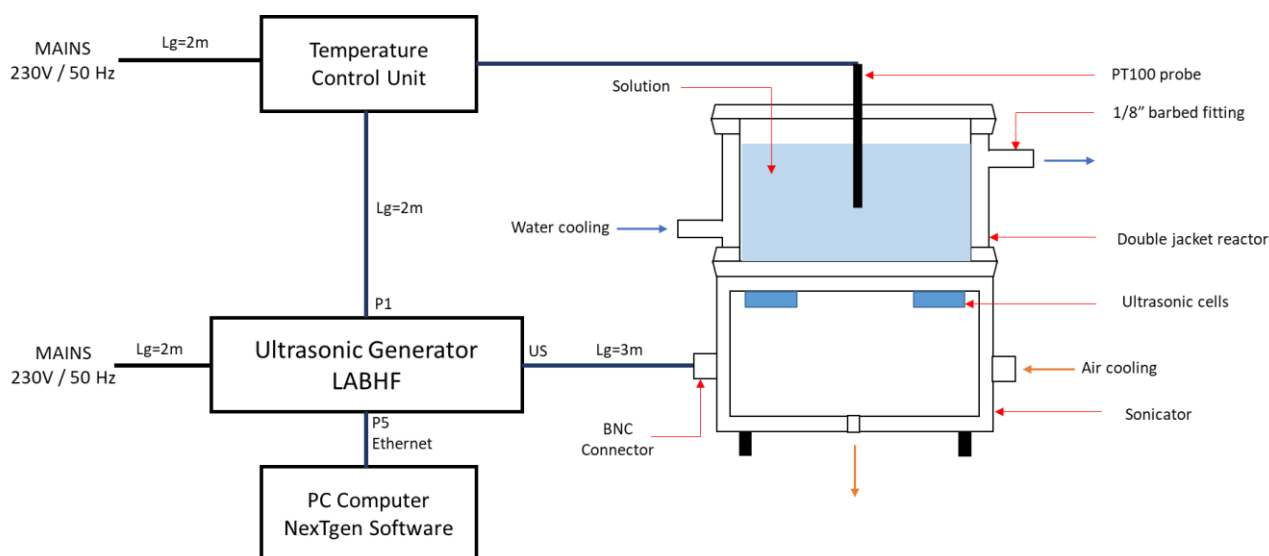


Figure 4.3 - Installation Synoptic

The solution is placed under sonication in double-jacketed reactor.

The optimum capacity of the reactor is 200ml.

The reactor is provided with a sealed double jacket allowing the circulation of a fluid (in general, water) which ensures the cooling or the temperature regulation of the solution to be insonified. The connection to the circulation pump is made via two 1/8" barbed fittings for 6 mm internal diameter tube.

A PT100 type temperature probe is placed in the reactor cover and must be immersed in the solution to be insonified.

3.3. Oxidation reactions

All oxidation reactions of furfural to maleic acid was carried out in a 250 mL high-frequency ultrasonic reactor (SinapTec Ultrasonic Technology, NextGen Lab 1000, 550 kHz, designed cylindrical stain steel reactor in a cup-horn configuration with a 75 mm diameter base-surface, and equipped with a cooling system). The total material volume introduced in the reactor was 50 mL, which is the minimum operating capacity of the reactor.

For the optimal reaction, 0.12 mol of furfural (10 mL) and 0.46 mol H₂O₂ (40 mL) were introduced in the reactor. A water-cooling stream (30 °C) circulated in the double jacket reactor since the oxidation reaction is highly exothermic and may cause the increase of temperature for above 60 °C (maximal operating temperature) in about 30 minutes. In this way, we maintained the temperature of the reaction medium at 45 °C.

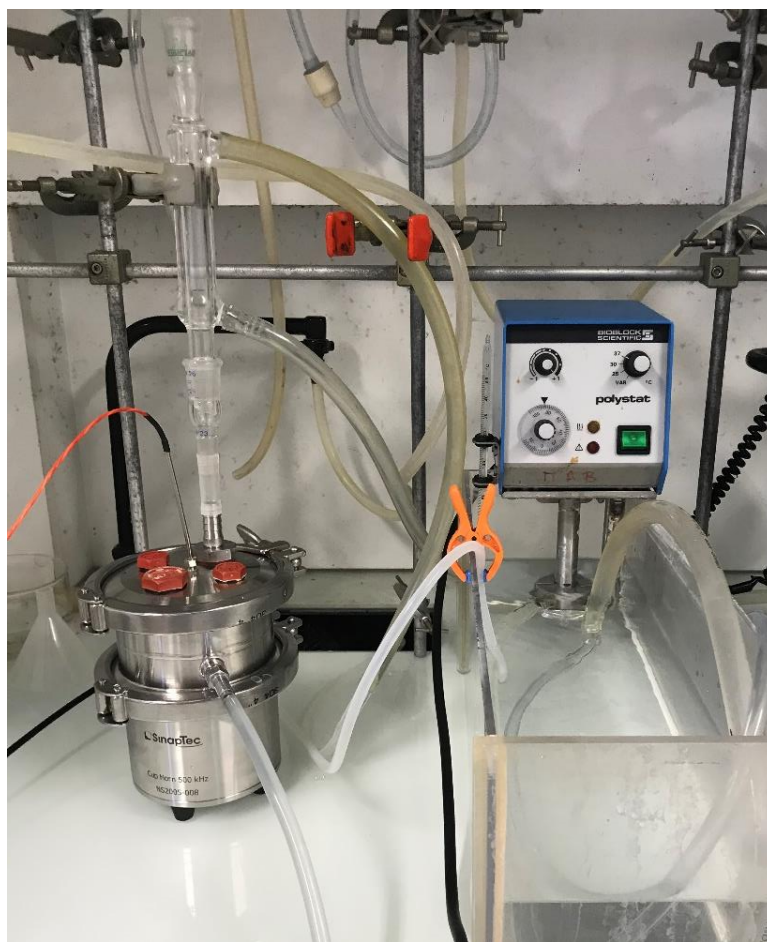


Figure 4.4 - The experimental setup

3.4. Product analysis

Preliminary tests were analyzed by NMR where maleic acid has been detected.

Proton nuclear magnetic resonance (^1H NMR) and Carbon-13 nuclear magnetic resonance (^{13}C NMR) were conducted on a Bruker Ascend™ 400 MHz device. The samples were prepared in D_2O .

^1H NMR (frequency, D_2O): Maleic acid: δ/ppm 4.79 (s, 1H), 6.28 (s, 1H)

^{13}C NMR (frequency, D_2O): Maleic acid: δ/ppm 130.5 and 169.4

Furfural was detected and quantified using by Gas Chromatography (Perkin Elmer instruments, AutoSystem XL) equipped with a Column Alltech Part No. 16368 AT-1ht 30m x 0.25mm D x 0.1 μm . The injection volume 1 μl , oven temperature 250°C, Q_{H_2} = 45 ml/min and Q_{air} = 450 ml/min.

Retention time of furfural is 4.9 min.

Maleic acid (MA), hydroxyfuranone (5-HFO) and furanone were analyzed on a Shimadzu HPLC equipped with a corgel 87H3 column, Mobile phase: formic acid 8.10^{-3} M, flow 0.6 mL/min. Column Temp: 35°C. The injection volume was 10 μL .

Retention time of MA, 5-HFO and furanone are 7.8, 19.8 and 33.4 min respectively.

Diacids such as succinic acid and malic acid were detected by an evaporative light scattering detector. Furfural conversion and products' selectivities and yields were calculated according to the following equations:

$$\text{Conversion}_{\text{furfural}} = \frac{n_{\text{furfural}_{\text{initial}}} - n_{\text{furfural}_{\text{remaining}}}}{n_{\text{furfural}_{\text{initial}}}} \times 100 \quad (1)$$

$$\text{Yield}_{\text{product}} = \frac{n_{\text{product}_{\text{obtained}}}}{n_{\text{product}_{\text{theoretical}}}} \times 100 \quad (2)$$

$$\text{Selectivity}_{\text{product}} = \frac{n_{\text{product}_{\text{obtained}}}}{n_{\text{furfural}_{\text{initial}}} - n_{\text{furfural}_{\text{remaining}}}} \times 100 \quad (3)$$

3.5. Synthesis of 5-hydroxy-2(5H)-furanone

In a 250 mL three-necked round bottom flask equipped with a cooler condenser and a thermometer was charged with freshly distilled furfural (5.0 g, 52.1 mmol) and methanol (150 mL). A catalytic amount of methylene blue indicator was added and air was bubbled in the reaction mixture while stirring at room temperature. The set-up was fenced using two 400 watt construction lamps in such a way that the light falls on the reaction mixture. During the reaction, aliquots were taken and the GC-MS analyses showed full conversion of hydroxyfuranone within 6 h. After evaporating the methanol at reduced pressure, the obtained crude product was further purified using automated column chromatography (5:1, PE:EtOAc eluents), yielding hydroxyfuranone as yellow crystalline solid in >95% purity.

NMR: ^1H NMR (400.17 MHz, D₂O): δ = 7.51 (d, H_b, H-1, J = 5.7 Hz), 6.34 (m, a+a', 2H). ^{13}C NMR (100.62 MHz, D₂O): δ = 173.8, 153.8, 123.6, 99.6.

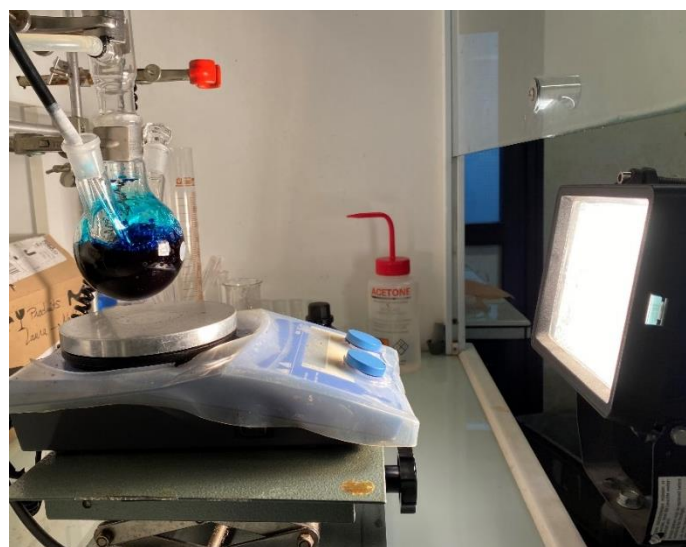


Figure 4.5 - The experimental setup for the synthesis of hydroxyfuranone

4. Results and discussion

4.1. Effect of frequency

One of the key parameters that control the effectiveness of ultrasounds is the applied frequency by affecting on the rate of radical formation [39,57]. For example, the highest rate of hydroxyl radical formation is achieved with an optimal frequency from med- to high ultrasound frequencies [58]. In homogeneous solutions, as in our case, the effects of ultrasounds are controlled by the collapse of cavitation bubbles generating a strong shear forces that activate reagents towards a particular chemical reaction.

The effectiveness of activation via high-frequency ultrasound (HFUS) on a mixture of 10 mL furfural and 40 mL of a 35% aqueous hydrogen peroxide solution was tested. Initially the system is biphasic. Under these conditions, without temperature control, the HFUS activation quickly initiates the very exothermic oxidation of furfural by hydrogen peroxide. The reaction becomes out of control and runs to the violent boiling of the reaction medium. In order to control the transformation, a maximum temperature of 42 °C was imposed. Sonication can be maintained without runaway for several hours under these conditions. After 2 h of sonication, the obtaining of a single cloudy phase demonstrates the overall transformation of furfural. Following the sonication step, the mixture was transferred to traditional glassware for analysis. Surprisingly, the reaction mixture began to boil again after only a few minutes left at rest. This translates the further transformation out of ultrasound activation. Let us immediately note that the same transformation conducted without irradiation does not lead to this phenomenon. Note that this boiling only lasts for few minutes. After allowing the reaction mixture to cool at room temperature, its analysis shows the presence of maleic acid as the majority product (Figure 4.6, results at 565 kHz).

Compared to the oxidation methods reported in the literature, the absence of catalyst, the very high concentration of furfural (20 wt%), the relatively low oxidant/furfural molar ratio (3.8), that is, close to stoichiometry, and the particularly short reaction time are so many advantages that make this result very interesting and encouraged us in the optimization of this transformation.

In order to quickly verify the effect of HFUS on this transformation, we compared it with the results of the experiments conducted at lower US frequencies 50 and 25 kHz and without US. Knowing the literature describes a production of much more important radical species in the frequency zone at 500 kHz. [38,39,50] That is, the generation of free radicals HO• by sonolysis of hydrogen peroxide is anticipated as an oxidizing species that initiates oxidation at higher concentrations.

Without irradiation, at 42 °C and after 2 h the system becomes monophasic, furfural has however not fully reacted as a conversion of 31% is observed and a selectivity to MA and 5HF less than 15%. (Figure

4.6, no US) Under these conditions a low selective mixture of maleic, fumaric, malic and succinic acid in the presence of other intermediates such as 5-HFO, or FO are obtained. These results are consistent with the work described by Muzychenko et al. [59] The transformation is catalyzed by the acids formed during oxidation which lead to the corresponding peracides which promote oxidation but without selectivity.

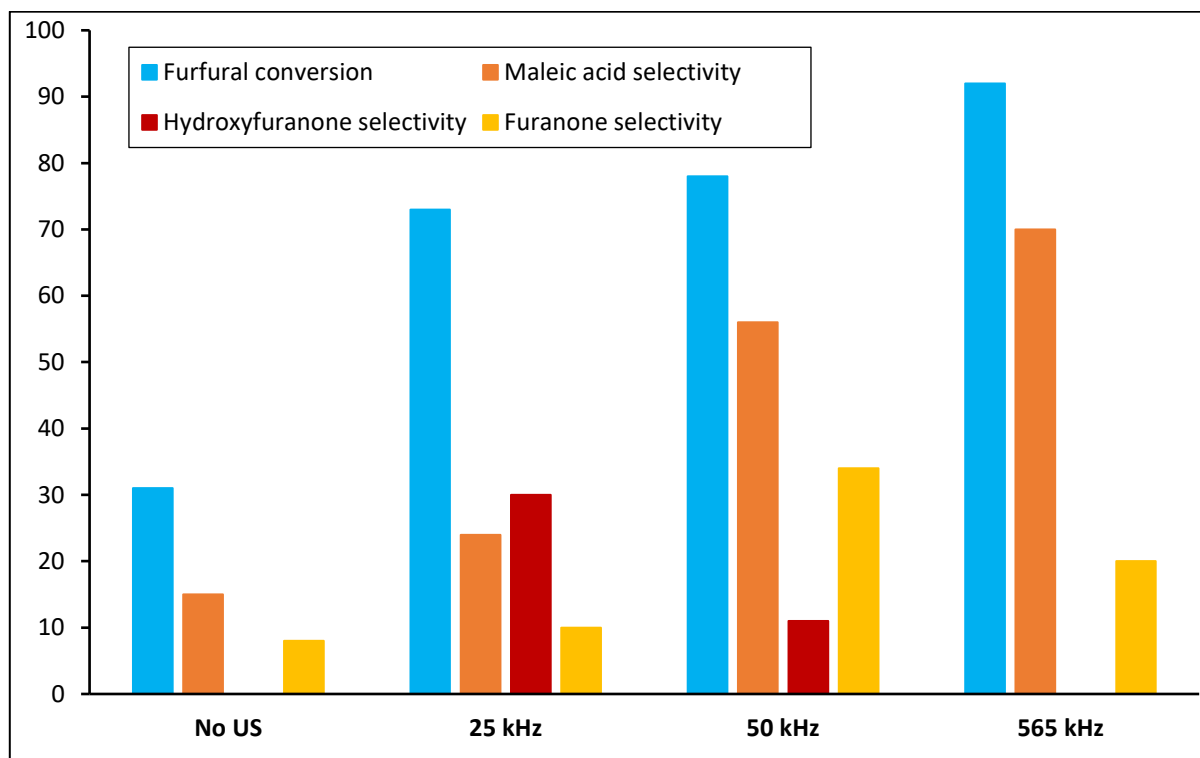


Figure 4.6 - Effect of the frequency (kHz); Furfural 10 mL (0.12 mol); H₂O₂ 40 mL (0.46 mol), 2 h, 42 °C, 80 W, after boiling

We then wanted to compare with the effects of an ultrasound probe at lower frequencies of 25 and 50 kHz, described as producing fewer radicals. In these conditions, the selectivity of the products is affected, the method is less effective under low frequency irradiations, however the effect of ultrasound still improves the conversion to furfural measured between 70 and 80%. Note that at 50 kHz the selectivity in maleic acid becomes already remarkable 54%. (Figure 4.6, 50 kHz)

Moreover, we investigated the effect of high frequency ultrasound irradiations by applying three different frequencies between 525 and 565 kHz (the frequency operating range of the reactor). As shown in figure 4.7, we have approximately the same values regardless of the applied frequency.

Thus, HFUS has the same effect on furfural conversion, nor on selectivity. Note that, 565 kHz is the maximal operating frequency, it will be interesting to explore the effect of ultra-high frequency ultrasound irradiations (> 800 kHz and even > 1 MHz) on the reaction rate and mechanism.

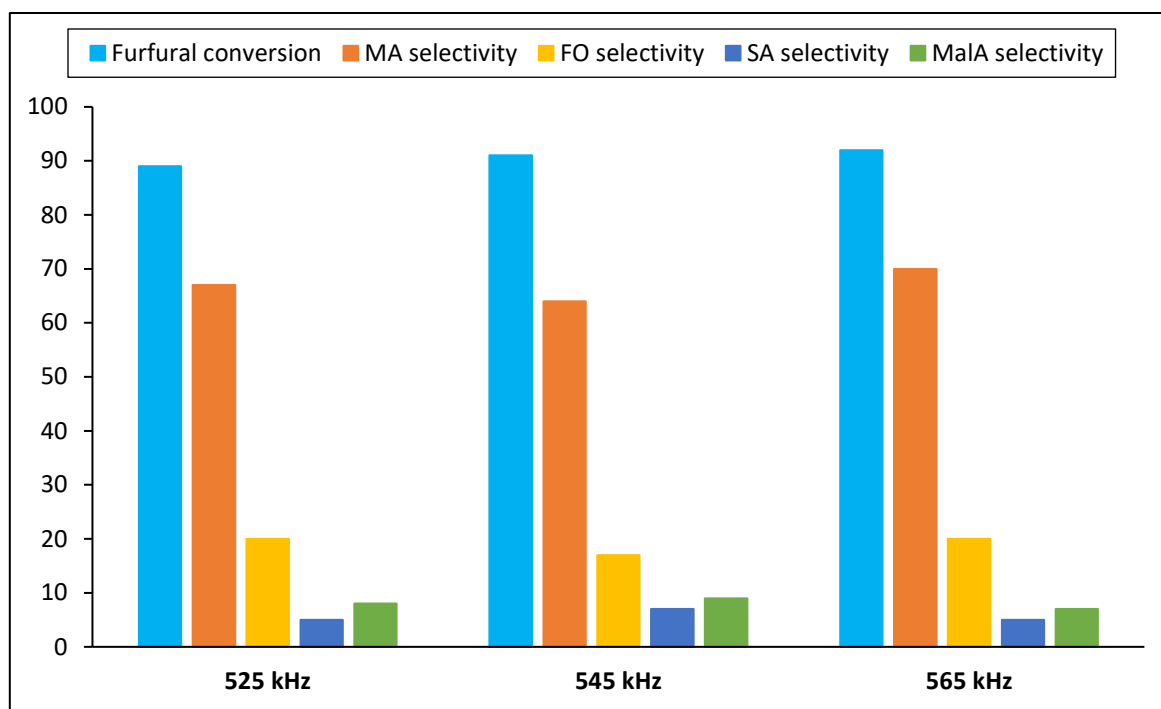


Figure 4.7 - Effect of the frequency (kHz); Furfural 10 mL (0.12 mol); H₂O₂ 40 mL (0.46 mol), 2 h, 42 °C, 80 W.

These good results observed at 50 kHz, led us to compare them with those obtained under HFUS before and after boiling especially the selectivity of the intermediate 5-HFO before boiling. (Figure 4.8)

At low frequency, furfural conversion is 54% vs 70% under HFUS, and selectivity to 5-HFO remains very good (68%) while it appears lower (52%) but with the presence of maleic acid (11%) before boiling under HFUS. Overall, after boiling, furfural conversion and maleic acid yield are better after sonication under high frequencies at 565 kHz rather than at 50 kHz. (Figure 4.8)

Note that the frequency comparison was done at identical power of 80 W. The major difference between probes is their geometry and the power per unit area of these probes. Finally, the frequency test results are well in agreement with the observations already reported in the literature, that is to say, an acceleration of the oxidation transformation by sonication by the generation of radical oxidizing species. The higher the frequency, the higher the radical concentration and the faster the rate of transformation to selective intermediate 5-HFO formation before maleic acid formation. Hasten to add, a temperature lower than 42 °C could prevent the activation of the reaction and then no transformation took place.

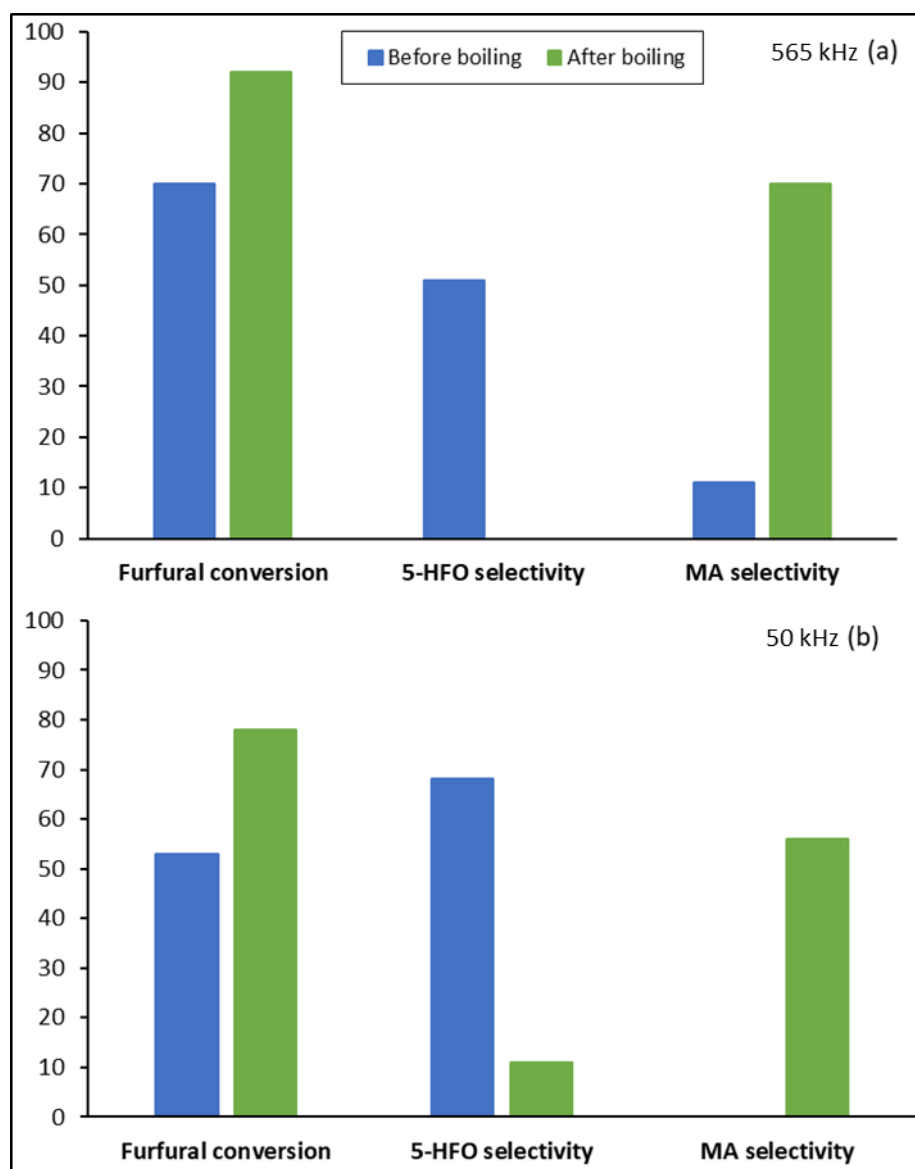


Figure 4.8 - Conversion and yields before and after boiling; Furfural 10 mL (0.12 mol); H₂O₂ 40 mL (1.7 mol), 2 h, 42 °C, 80 W, after boiling.

4.2. Effect of power

The extent of sonochemical reactions produced by acoustic cavitation depend on the applied power. The applied power reflects on the pressure amplitude and should be able to supply the pressure need for cavitation. Increasing power can however disrupt bubble dynamics as it helps bubbles grow during expansion.

In this context, we confirmed the effect of HFUS power on transformation kinetics. As expected, at increasing power, furfural conversion and maleic acid yield increase with the rate of oxidation. Thus, by going from 0.9 (40 W) to 1.8 W.cm⁻² (80 W), conversion increases after boiling from 64% to 92% and selectivity in MA increases from 25% to 70%. Intermediates are less consumed at lower power levels with a higher proportion of 5-HFO and FO remaining. All these results are consistent with the hypothesis of a first stage of oxidation corresponding mainly to the formation of HO• radicals and their

reaction with furfural leading to the selective formation of 5-HFO. This intermediate is then rapidly oxidized to maleic acid as soon as we allow the temperature of the reaction mixture to rise.

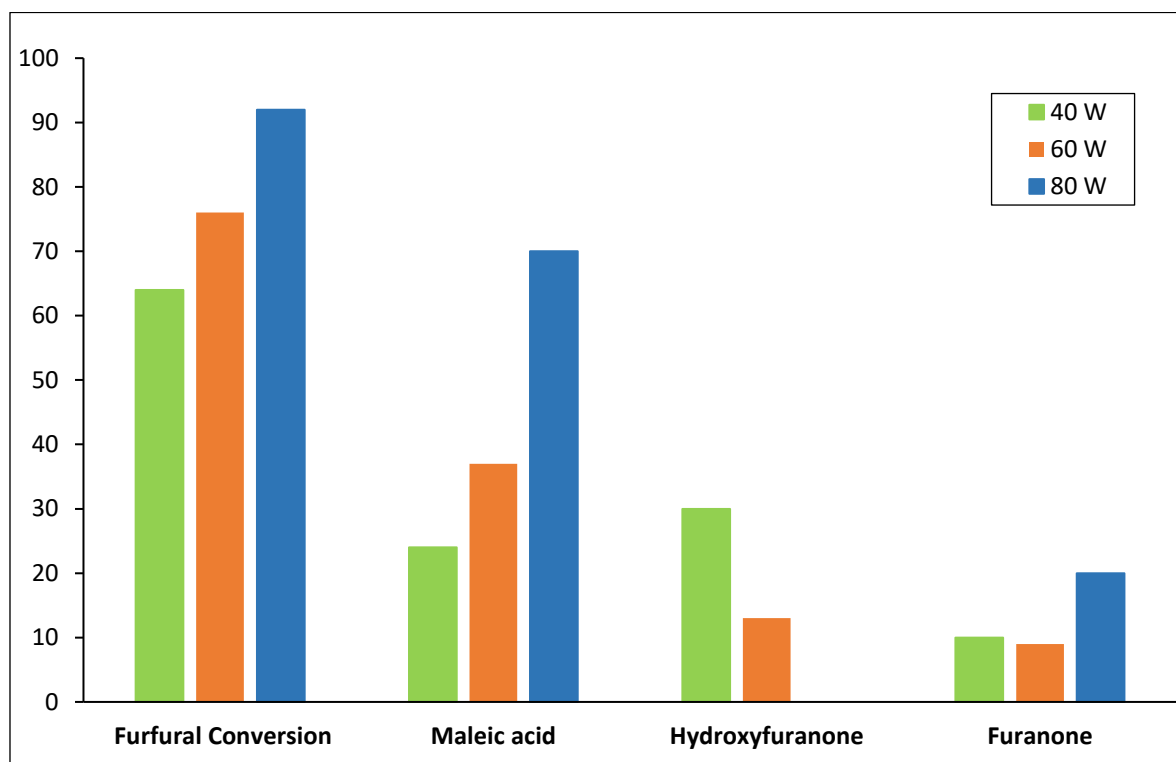


Figure 4.9 - Effect of power variation; Furfural 10 mL (0.12 mol), H₂O₂ 40 mL (0.46 mol), 42 °C, 565 kHz, 2 h, after boiling.

4.3. Effect of reaction time

In order to control the synthesis of this 5-HFO intermediate and the MA, we decided to study the effect of the HFUS irradiation time by working at full power that is 80 W or 1.8 W.cm⁻². (Figure 4.10)

At least 1 h of HFUS sonication is required to obtain a monophasic mixture, the reaction mixture behaves in the same way, that is to say boiling when the temperature is no longer maintained at 42 °C. A conversion of 90% of furfural is measured, however maleic acid is obtained with low selectivity 25% in mixture with several secondary products such as 5-HFO, SA, FO and malic acid. After 2 hours of irradiation, we observe a selectivity of 70% maleic acid, 18% FO, 7% malic acid and 5% succinic acid. After 3 h of sonication the boiling phenomenon is still observed, however maleic acid selectivity decreases to 40%. After 4h of sonication, the boiling no longer takes place, the vast majority of the oxidation process is carried out under temperature control (42 °C), all the oxidant having almost been consumed during the sonication for the oxidation of furfural or by dismutation. Note that the selectivity in maleic acid (20%) is almost obtained in equivalent proportion with succinic acid (25%) which becomes the majority product, the proportion of other remaining products is relatively low, 5-HFO (15%), malic acid (10%) FO (9%). Note that in all cases the conversion to furfural is never reached, however it almost reaches its maximum value after one hour of sonication, 88% of furfural are

converted, and after 2 h it is maximum at 92%. This last observation indicates that the amount of oxidant used is not sufficient to convert all furfural.

To achieve the overall consumption of furfural, an Ox/Fur molar ratio of 5.9 was tested with a 50% hydrogen peroxide solution. Under these conditions, under HFUS irradiation, it was not possible to maintain the temperature of the reaction medium and to avoid runaway reaction, leading very quickly to its violent boiling.

Therefore, we decided to continue our work with molar ratios below 4. We then studied the stability of hydrogen peroxide under HFUS sonication conditions. It is well described in the literature that hydrogen peroxide decomposes rapidly under the influence of temperature. Beyond 80 °C, its dismutation becomes quite fast. Similarly, sonication leads to its decomposition. Under our conditions we therefore expect a loss of hydrogen peroxide by the effect of temperature and that of sonication. This is what we were able to verify by sonication at 565 kHz of hydrogen peroxide solution (35%) maintained at 42 °C for 1 hour, and the concentration fell from 11.6 mol.l⁻¹ (35%) to 7.6 mol.l⁻¹ (23%). This result allows us to understand that only a partial conversion of furfural is observed, and confirms the activation of hydrogen peroxide under high frequency ultrasound irradiation.

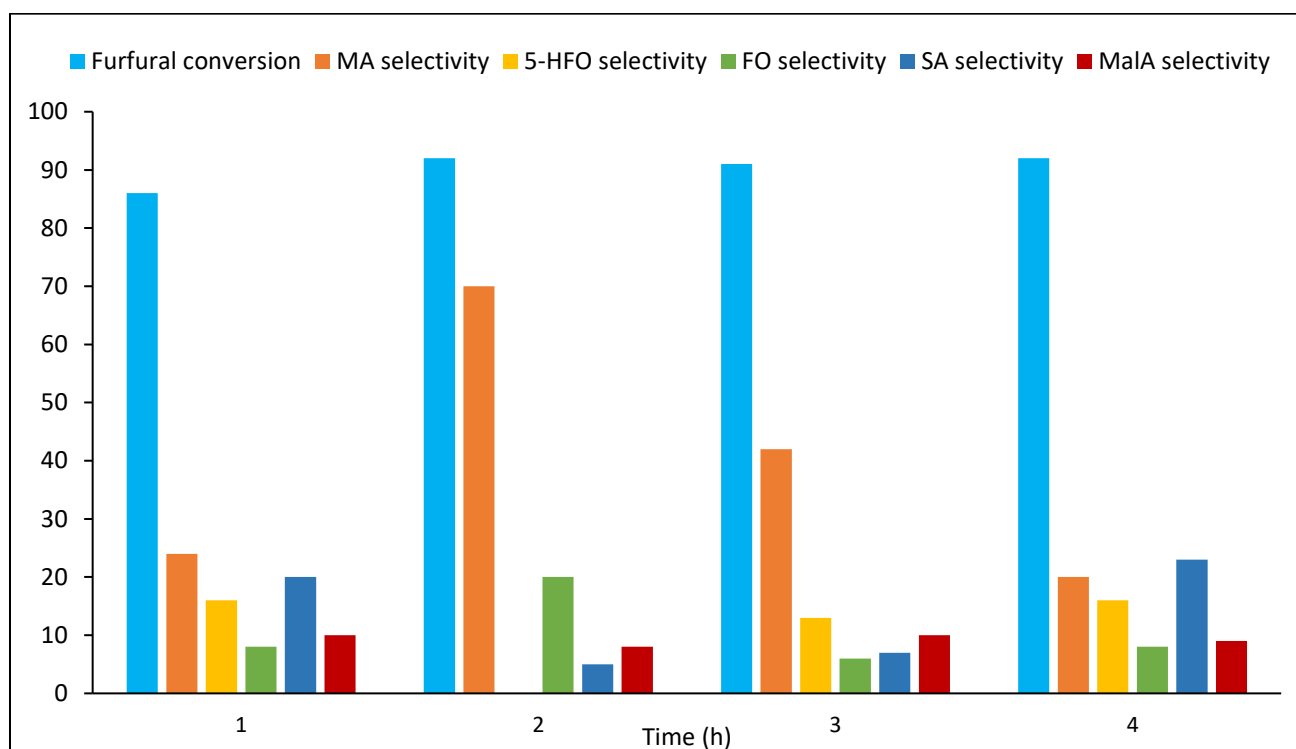


Figure 4.10 - kinetic profile of the reaction; FUR 10 mL (0.12 mol), H₂O₂ 40 mL (0.46 mol), 42 °C, 565 kHz, 80 W.

4.4. Effect of oxygen as oxidant

However, this result raises the question of the potential role of oxygen from dismutation in oxidation. Is it added in the form of an activated oxygen (singlet) on furan by cycling to form the corresponding endoperoxides in the same way as photochemical oxidations? To verify this, the same transformation

was carried out by replacing the hydrogen peroxide solution by an aqueous phase saturated in dioxygen with a continuous bubbling of 20 ml.min⁻¹ of pure dioxygen throughout the irradiation period (2 h). Under these conditions, no transformation of furfural was detected. In conclusion, dioxygen is not responsible for the first stage of the oxidation mechanism.

4.5. Effect of H₂O₂/FUR mol ratio

Based on these results, those reported in the literature and our expertise, we know that when hydrogen peroxide is used as an oxidant, selectivity is highly dependent on the furfural concentration and the H₂O₂/furfural molar ratio. We can recall the following trends for the low oxidant/furfural <3 molar ratio, 5-HFO or FO are the majority products beyond 3 < m.r. < 12 oxidation continues towards the formation of C4 diacids, an optimum is usually reached between 6 and 9 H₂O₂ equivalents, then overoxidation can be observed with the degradation of the present diacids. Lower concentrations of furfural generally allow for better selectivity control. [10,24,31,60]

This is why we decided to study the effect of the variation of the weight percentage of furfural and the H₂O₂/furfural molar ratio ranging from 1 to 3.8 corresponding to 0.48 to 0.12 mol furfural respectively. It should now be noted that following the nonradical mechanisms of oxidation of furfural by hydrogen peroxide, normally at least one equivalent of hydrogen peroxide is necessary to theoretically convert the whole furfural. Then to oxidize it until the formation of maleic acid, in theory a minimum of three equivalents of hydrogen peroxide are required. In the case of a radical mechanism, since each hydrogen peroxide molecule can potentially release two HO• radicals, in principle it is possible that only half the equivalent of hydrogen peroxide is needed for a total conversion of furfural in the first stage. Note also that a catalytic amount of radicals could be sufficient for a total conversion by considering a chain radical mechanism. Nevertheless, when the reaction is carried out without hydrogen peroxide no reaction is observed contradicting that HO• radical are formed from water by HFUS irradiation.

Moreover, when the quantity of hydrogen peroxide is only one equivalent, the conversion of furfural is the lowest (50%). (Figure 4.11) It is very interesting to note that succinic acid is very predominantly obtained under these conditions with a selectivity of 50% in the presence of 15% of 5-hydroxyfuranone and 9% of furanone, without the presence of maleic or malic acid. With two equivalents of hydrogen peroxide, the conversion increases slightly, but the selectivity for succinic acid (35%) decreases in favor of that of maleic acid (18%), 5-HFO and FO are also obtained but with selectivity below 10%. Increasing the H₂O₂/furfural molar ratio to 3 does not bring much change in products distribution, but improves furfural conversion to 70%. Finally, for a H₂O₂/furfural ratio of 3.8, the maximum conversion is

observed with high selectivity for maleic acid (70%) accompanied by FO (16%) and succinic and malic acids with selectivity of < 10%. (Figure 4.11)

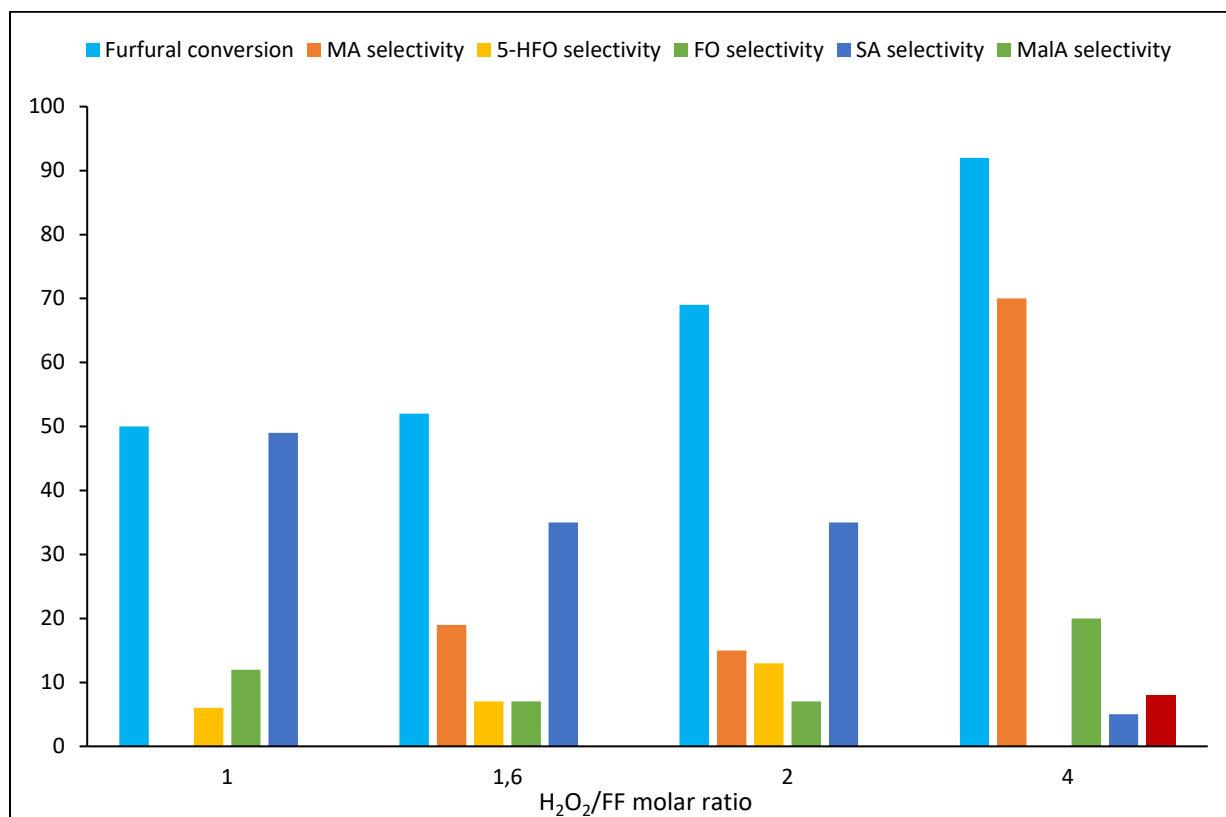
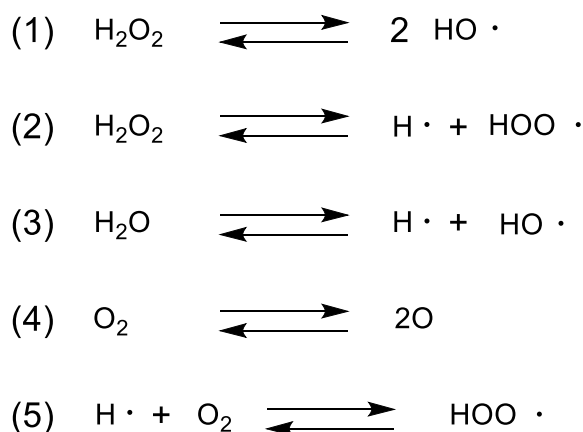


Figure 4.11 - kinetic profile of the reaction; Furfural 10 mL (0.12 mol), H₂O₂ 40 mL (0.46 mol), 42 °C, 565 kHz, 80 W.

4.6. Reaction mechanism

In view of these results and the preliminary studies of oxidation of furfural by hydrogen peroxide, among the various possible oxidation pathways in competitions, the first stage seems to be the attack of HO• radicals from the homolytic cleavage of hydrogen peroxide. Again, the formation of these radicals is very favorable due to the power and frequency used. [61] Under these extreme conditions, water molecules can be cleaved into H• and HO• radicals. Oxygen, if present in the bubble, can also decompose. [57,61] Some examples of radical formation and their equilibria under HFUS are given in scheme 4.1. As for hydrogen peroxide, the enthalpy of the O-O bond being relatively low 210 kJ.mol⁻¹ [62], the homolytic cleavage of this bond is easily done at the very high temperatures reached by the implosion of the cavitation bubbles. [35] HO• radicals cannot recombine at these very high temperatures, unlike H• radicals. Consequently, the HO• radicals persist and diffuse within the solution and then react very quickly with the molecules of furfural present. As indicated above, high frequencies are more efficient than low frequencies for the generation of radicals, which is particularly interesting for oxidation. [61]

In scheme 4.1, the formation of the radicals of equations 3, 4 and 5 most probably occur at the margin in the oxidation mechanism because the transformation carried out under optimum conditions (2 h, 42 °C) without hydrogen peroxide does not lead to oxidation, as when the transformation is conducted under a flow of oxygen (20 mL.min⁻¹). The high frequency sonication experiments under dioxygen atmosphere reported by Hart et al. show a measured concentration of hydrogen peroxide formed from aqueous phase was around 17.10⁻⁶ mol.L⁻¹.min⁻¹. [35] This is marginal compared to 9.3 mol.L⁻¹ engaged in optimum conditions.



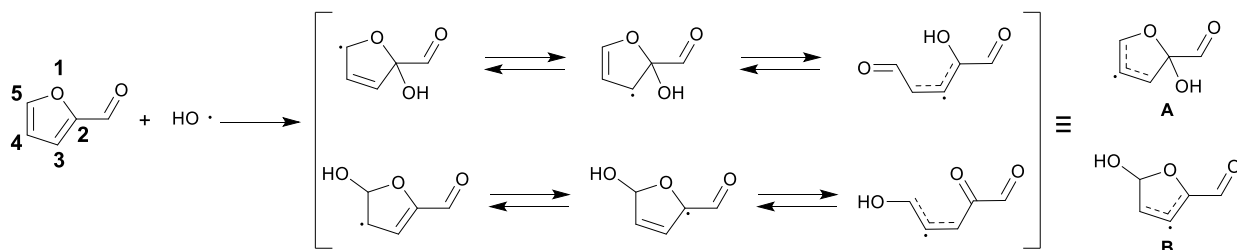
Scheme 4.1 - Examples of radical formation under HFUS

Product and kinetic study of the HO• initiated gas-phase oxidation of furan derivatives, particularly furfural, has already been reported by Bierbach et al. [63] As Zhao et al. in their study of atmospheric oxidation mechanism of furfural initiated by hydroxyl radicals. [64,65] The described intermediates agree with our experimental observations in the liquid phase, *i.e.* the formation of 5-hydroxyfuranone and 2-(5H)-furanone as main products. Based on this work, HO• radicals initiate oxidation by attacking mainly the C2 and C5 positions of furfural leading to the **A** and **B** radicals of scheme 4.2 in equilibrium with the open forms of the furan cycle. Then the radicals **A** and **B** react quickly with the surrounding species, water, hydrogen peroxide, dissolved oxygen or with other radicals. The regioselectivity of this second addition also takes place mainly in position 2 and 5. (Scheme 4.3)

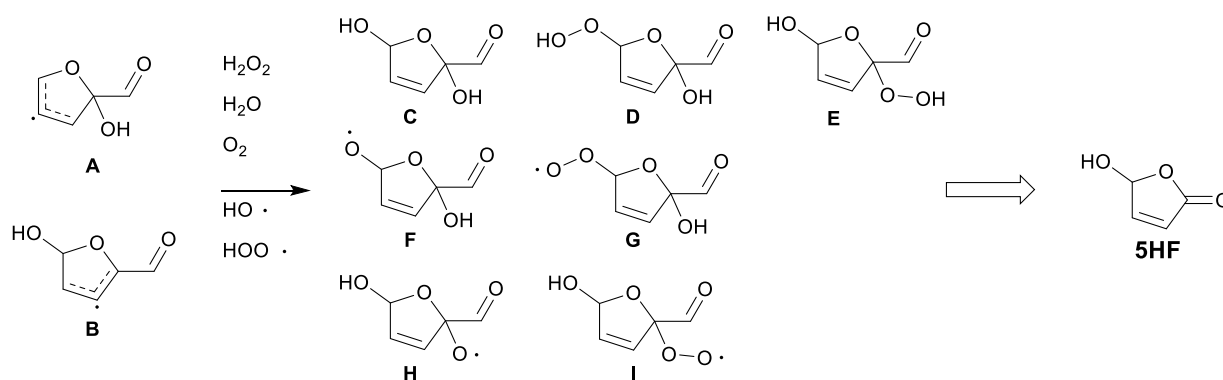
The intermediates probably formed are C, D, E, F, G, H and I in balance between the proton forms (C, D and E) and the free radicals (F, G, H and I). According to the calculations of Zhao and Wang, the rearrangement of these radical species (F, G, H and I) would lead to the elimination of carbonyl in the form of formaldehyde. The latter oxidizes rapidly into formic acid. [64]

It can be assumed that these reactions occur both in the gas phase and in the liquid phase, but mainly in the liquid phase, since it has been shown that hydroxyl radicals diffuse more predominantly in the liquid phase compared with the H• radicals which recombine faster. On the other hand, intermediates A and B can still capture hydrogen by reacting with the solvent or H• radicals present, leading to

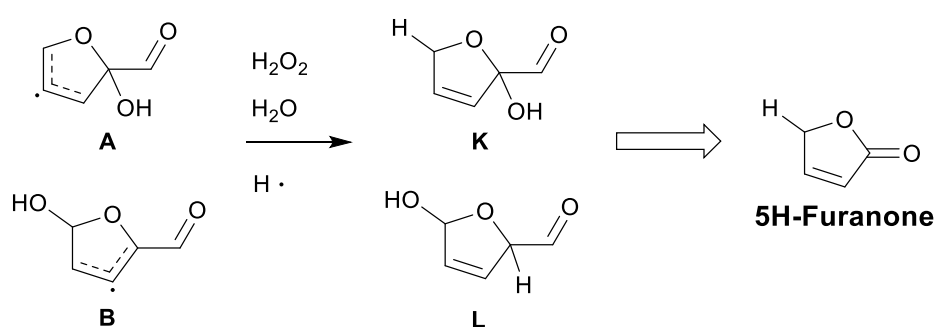
intermediates K, L and finally 2-(5H)-Furanone. (Scheme 4.4) Many other possibilities of intermediates resulting from regioselective attacks in positions 3 and 4 of furfural are possible, which can lead to the formation of secondary products. After the sonication step, we observe as the majority product the relatively stable 5-HFO under these conditions.



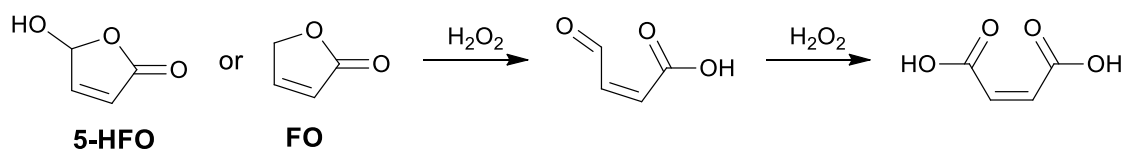
Scheme 4.2 - Proposal for the first step of oxidation of furfural under HFUS.



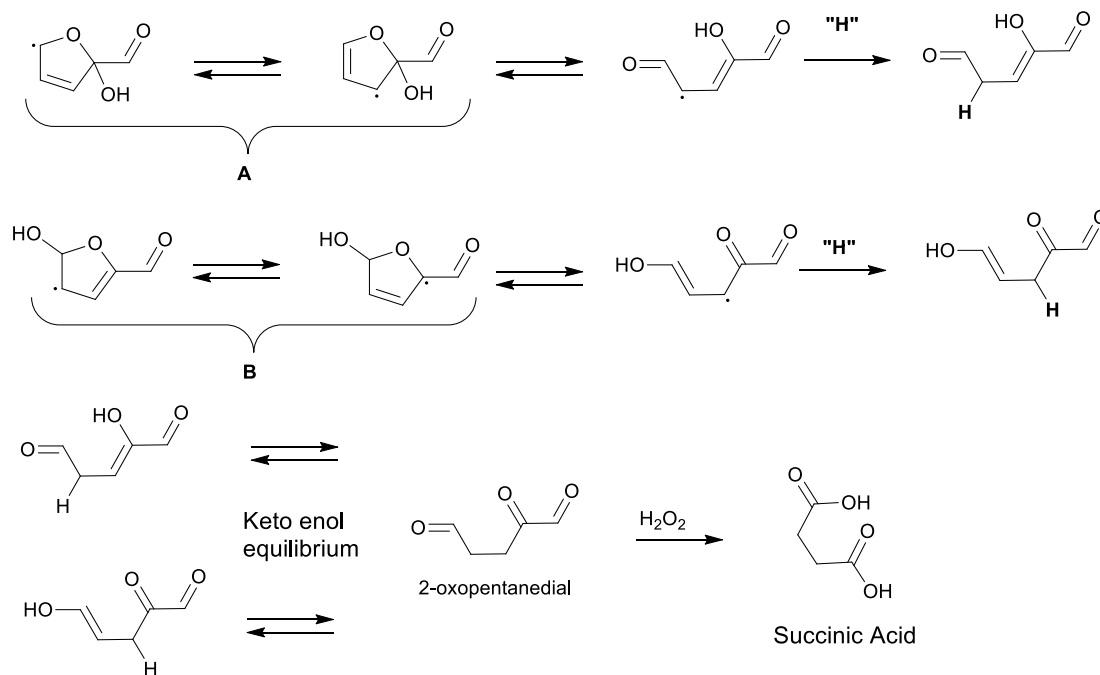
Scheme 4.3 - Structures of potential intermediates leading to 5-Hydroxyfuranone.



Scheme 4.4 - Structures of potential intermediates leading to 2-(5H)-Furanone.



Scheme 4.5 - Proposal reaction pathway leading to maleic acid from 5-hydroxyfuranone and 2-(5H)-Furanone via non-radical mechanism.



Scheme 4.6 - Proposal pathway leading to Succinic acid.

Its concentration increases during the first two hours, then after reaching its extremum decreases slowly with the continuation of HFUS irradiation over longer times (3 and 4h). (Figure 4.11)

In our case, the prolonged irradiation time eventually degrades 5-HFO and other intermediates by continuing oxidation with loss of selectivity for maleic acid. For this reason, we believe that the following oxidation steps follow a non-radical oxidation mechanism. (Scheme 4.5) This is the step corresponding to the oxidation of 5-HFO by hydrogen peroxide without temperature control and without sonication. It is well known that 5-HFO or FO are good starting compounds for maleic acid formation. This transformation being very exothermic and given the quantities of raw materials engaged the reaction mixture is quickly brought to the boil.

Finally, it should be noted that with hydrogen peroxide used as a limiting reagent, that is, with an excess of furfural of 4:1, selectivity is largely affected leading to succinic acid as the majority diacid. To explain this observation we make the hypothesis that the lack of hydroxyl radicals imposes mainly to the insertion of hydrogen on the radicals **A** and **B**. The sources of hydrogen noted ("H", Scheme 4.6) are the solvent, hydrogen peroxide, or hydrogen radicals. The intermediates obtained in keto-enol

balance with the 2-oxopentadiol would then be oxidized to succinic acid following a non-radical mechanism. [28,59,60]

To conclude, we believe that the oxidation takes place in two steps, following a radical mechanism during sonication and a non-radical mechanism on the intermediates e.g. 5-HFO, FO, 2-oxopentanedial.

4.7. Energy consumption

To approximately estimate the energy consumption using the traditional energy source, which is heating plates, we use this calculation protocol:

Heating plate adopts a 2-points regulation system: either at P=650 W or P=0 W.

The data sheet provided from the manufacturer indicates a temperature rate for the heating plate at 6.5 K/min (0.11 K/s). This accounts for the conduction from the central coil to the metallic plate.

Therefore we have: $T_{plate} = T_{0,plate} + 0.11t$

To estimate the heating energy necessary for maintaining oil bath at T_{set} , a thermal balance is done on three stages:

- 1- Warm-up
- 2- Heating stoppage
- 3- Re-heating

In all phases, the thermal balance is done by equating the sum of acting heat fluxes to the change in energy state of the system composed of oil bath, that is:

$$\rho_{oil} \times V_{oil} \times Cp_{oil} \frac{\Delta T_{oil}}{\delta t} = \Sigma Q$$

*Assumption: Due to continuous stirring, T_{oil} is uniform.

1- Warm-up phase:

In this phase, warm-up consists of heating oil from T_{amb} to T_{set} .

*Assumption: heat losses to ambient air are negligible in this phase, especially at low temperatures

→ The only heat flux acting upon the oil bath is the conductive heat from the surface of heating plate

$$\rightarrow \Sigma Q = q_{cond} = \frac{-k}{e} A \Delta T$$

$$\rightarrow \rho_{oil} \times V_{oil} \times Cp_{oil} \frac{\Delta T_{oil}}{t} = \frac{-kA}{e} (T_{oil} - T_{plate})$$

With $T_{plate} = T_{0,plate} + 0.11t$

Given:

Specific heat capacity of oil: $Cp_{oil} = 1510 \text{ J/Kg.K}$

Oil density: $\rho_{oil} = 0,96 \text{ kg/L}$

Oil Volume: $V_{oil} = 1 \text{ L}$

Convective coefficient: $h = 10 \text{ W/m}^2.\text{K}$ (Heat loss of oil through convection with air)

Thickness of the bath: $e = 3 \text{ mm}$

Ambient temperature $T_{amb} = 293 \text{ }^\circ\text{C}$

Lateral surface $A = 0.035 \text{ m}^2$

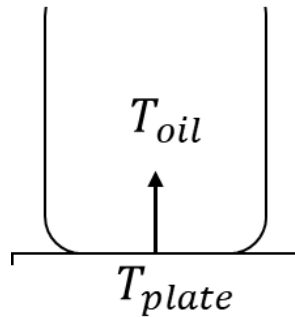


Figure 4.12 - Representation of an oil bath and a heating plate

2- Heating stoppage:

*Assumption 1: From experimental observations we will consider a threshold for lower limit of the temperature regulation.

$$T_{LI} = T_{set} - 2$$

*Assumption 2: By comparing T_{plate} at t and $T_{oil} \rightarrow T_{plate} \approx T_{oil}$

Which means that conduction is almost instantaneous \rightarrow we will consider from now on that

$$T_{plate} = T_{oil} = T_0 + 0.11t$$

Which means that $T_{int} = T_{ext}$

This is logical considering the type of bath (aluminum, a very good heat conductor) and the thickness of the bath is $e = 3 \text{ mm}$.

Heat is lost through convection with air, with a convective coefficient that has an order of magnitude of $h=10 \text{ W/m}^2\cdot\text{K}$.

In this case $\Sigma Q = h \times A_L \times \Delta T$

$$\Leftrightarrow \rho_{oil} \times V_{oil} \times Cp_{oil} \frac{\Delta T_{oil}}{t} = -h \times A_L \times (T_{oil} - T_{plate})$$

With $\Delta T_{oil} = T_{LI} - T_{set} = -2 \text{ }^\circ\text{C}$

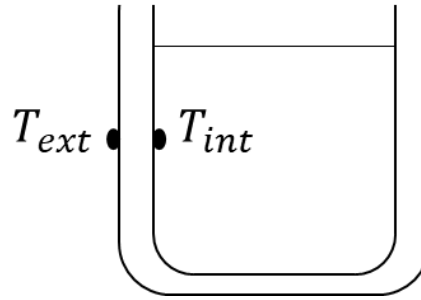


Figure 4.13 - Oil bath

3- Re-heating:

Same as first phase except that $T_0 = T_{set} - 2$

⇒ To make it even simpler, since conduction is instantaneous:

$$T_{oil} = T_0 + 0.11t$$

Since we need to heat oil to T_{set}

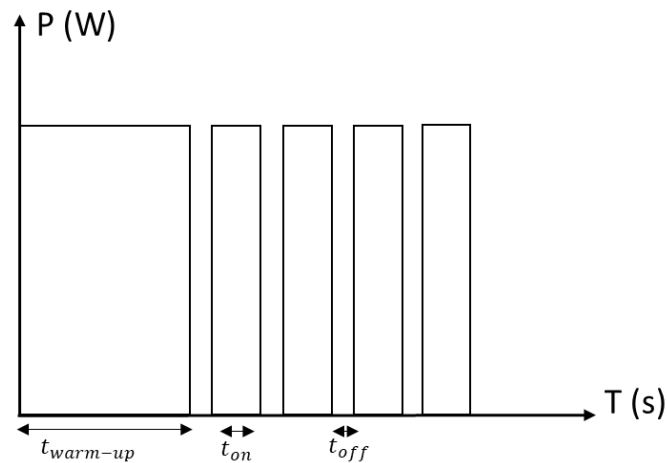


Figure 4.14 – Power consumed by the plate in function of time

At the end, we should calculate the number of times it turned off (x) and the number of times it went on (y).

$$\Delta t_{on} = \frac{T_{set} - T_{LI}}{0.11}$$

$$\Delta t_{off} = \frac{\rho_{oil} \times V_{oil} \times Cp_{oil} \times 2}{h \times A_L \times (T_{set} - T_{amb})}$$

$$t_{total} = x \cdot \Delta t_{off} + y \cdot \Delta t_{on} + t_{warm-up}$$

$$x = y + 1$$

$$y = \frac{t_{total} - t_{warm-up} - \Delta t_{on}}{\Delta t_{on} + \Delta t_{off}}$$

Hence, the consumed energy is calculated according to the following equation:

$$\Rightarrow \text{energy} = (y \cdot \Delta t_{on} + t_{warm-up}) \times \text{Power}$$

The results are presented in Table 4.2.

Note that the transformation takes place at 42 °C during the HFUS sonication step, then left at rest it continues releasing heat. This process is singularly different from those reported in the literature whose operating temperatures are generally in the order of 80 ± 20 °C with a transformation time greater than 2 h. (Table 4.2) The energy consumption of these different processes was estimated and compared to the HFUS process developed in this work. This estimate only takes into account the processing step without taking into account the energy consumption related to the purification processes, such as recrystallization, evaporation, or filtration. Thus, table 4.2 shows the consumed energy estimated in recent studies, needed to synthesize one gram of MA from furfural. This comparison materializes the advantage of the process with HFUS that needs 134 kJ.g^{-1} of MA. In the other hand, we estimated that we need at least the double of this amount of energy to produce one gram of MA by any other method.

Table 4.2 - Energy consumption to produce 1 g of MA from furfural

Method	Conversion (%)	Yield (%)	MA obtained mass (g)	Consumed energy (kJ)	Energy per gram (kJ/g)	Ref.
TS-1, Water, H ₂ O ₂ , 50 °C, 24 h	100	78	1.69	368	218	[18]
TS-1, AcOH, H ₂ O ₂ , 80 °C, 4 h	100	62	0.187	414	2216	[22]
Formic Acid, H ₂ O ₂ , 60 °C, 4 h	100	95	0.11	278	2526	[10]
BHC, Water, H ₂ O ₂ , 100 °C, 0.5 h	100	61	0.968	482	498	[16]
FeT(p-Cl)PPCl, Water, O ₂ , 90 °C, 10 h	96	44	0.123	585	4756	[12]
CaCu ₂ P ₂ O ₇ , Water, O ₂ , 115 °C, 18 h	68	37	0.076	961	12646	[13]
Cu(NO ₃) ₂ +H ₃ Mo ₁₂ O ₄₀ , Water, O ₂ , 98 °C, 14 h	95	49	0.391	724	1852	[8]
V-Zr/KIT-6, Acetonitrile, H ₂ O ₂ , 70 °C, 1 h	81	29	0.296	308	1041	[14]
H ₃ PMo ₁₂ O ₄₀ .xH ₂ O (11%), Water, O ₂ , 110 °C, 14 h	50	34	0.047	829	17639	[11]
NC-900, Water, H ₂ O ₂ , 80 °C, 5 h	100	61	0.116	429	3702	[66]
HFUS, H ₂ O ₂ , 42 °C, 2 h	92	70	8.97	1199	134	This work

5. Conclusion

Herein, we report the catalytic-free oxidation of furfural into MA using high frequency ultrasonic waves in the H₂O₂ liquid oxidant in an acid-free medium. This method shows a high selectivity of 70% towards MA with 92% of furfural conversion. SA can also be obtained with 50% selectivity when one equivalent of hydrogen peroxide was used but with 50% furfural conversion. We optimized the reaction conditions and the effect of various operating parameters such as furfural concentration, frequency, power and time were systematically

studied in details. The best compromise was obtained for 2 h of reaction, 4 H₂O₂ to furfural mol ratio, 565 kHz and 80 W.

This work shows that high-frequency ultrasound is very effective in activating hydrogen peroxide without a catalyst, which is a major advantage for the development of oxidation processes such as furfural towards the production of MA. This process combines many advantages: the solvent is water, the method is catalyst-free, under mild conditions, the temperature is low 42 °C, the transformation time is short and the molar ratio H₂O₂/Furfural is close to stoichiometry. In addition, the mass percentage of raw material is very high 20 wt% making this method appropriate for gram-scale production of MA (up to 9 g) and lay the foundation for the development of a larger scale process. Moreover, it improves energy efficiency by consuming the lowest amount of energy (134 kJ) to produce one gram of MA from furfural comparing to any other method in the literature. Therefore, we believe that this simple, green and energy-efficient process is a promising and transformative technology in chemical industries.

References

1. Ayoub, N., Bergère, C., Toufaily, J., Guénin, E., and Enderlin, G. (2020) A gram scale selective oxidation of 5-hydroxymethylfurfural to diformylfuran in the presence of oxone and catalyzed by 2-iodobenzenesulfonic acid. *New J. Chem.*, **44**, 11577–11583.
2. Mariscal, R., Maireles-Torres, P., Ojeda, M., Sádaba, I., and López Granados, M. (2016) Furfural: A renewable and versatile platform molecule for the synthesis of chemicals and fuels. *Energy Environ. Sci.*, **9** (4), 1144–1189.
3. AS Mamman et al. (2012) Furfural: Hemicellulose/xylose- derived biochemical. *Biofuels, Bioprod. Biorefining*, **6** (3), 246–256.
4. Karl J. Zeitsch (2000) *The Chemistry and Technology of Furfural and Its Many By-products*, Elsevier.
5. Li, X., Ko, J., and Zhang, Y. (2018) Highly Efficient Gas Phase Oxidation of Renewable Furfural to Maleic Anhydride over Plate VPO Catalyst. *ChemSusChem*, **11** (3), 612–618.
6. Lv, G., Chen, S., Zhu, H., Li, M., and Yang, Y. (2018) Determination of the crucial functional groups in graphene oxide for vanadium oxide nanosheet fabrication and its catalytic application in 5-hydroxymethylfurfural and furfural oxidation. *J. Clean. Prod.*, **196**, 32–41.
7. Maneechakr, P., and Karnjanakom, S. (2017) Catalytic transformation of furfural into bio-based succinic acid via ultrasonic oxidation using B-cyclodextrin-SO₃H carbon catalyst: A liquid biofuel candidate. *Energy Convers. Manag.*, **154** (October), 299–310.
8. Shi, S., Guo, H., and Yin, G. (2011) Synthesis of maleic acid from renewable resources: Catalytic oxidation of furfural in liquid media with dioxygen. *Catal. Commun.*, **12** (8), 731–733.
9. Felthouse, T.R., Burnett, J.C., Horrell, B., Mummey, M.J., and Kuo, Y.-J. (2001) Maleic Anhydride, Maleic Acid, and Fumaric Acid. *Kirk-Othmer Encycl. Chem. Technol.*, (10).
10. Li, X., Ho, B., Lim, D.S.W., and Zhang, Y. (2017) Highly efficient formic acid-mediated oxidation of renewable furfural to maleic acid with H₂O₂. *Green Chem.*, **19** (4), 914–918.
11. Guo, H., and Yin, G. (2011) Catalytic aerobic oxidation of renewable furfural with phosphomolybdic acid catalyst: An alternative route to maleic acid. *J. Phys. Chem. C*, **115** (35), 17516–17522.
12. Huang, Y., Wu, C., Yuan, W., Xia, Y., Liu, X., Yang, H., and Wang, H. (2017) Catalytic Aerobic Oxidation of Biomass-based Furfural into Maleic Acid in Aqueous Phase with Metalloporphyrin Catalysts. *J. CHINESE Chem. Soc.*, 1–9.
13. Soták, T., Hronec, M., Gál, M., and Dobročka, E. (2017) Aqueous-Phase Oxidation of Furfural to Maleic Acid Catalyzed by Copper Phosphate Catalysts. *Catal. Letters*, **147** (11), 2714–2723.
14. Rezaei, M., Naja, A., Dabbagh, H.A., Saraji, M., and Shahvar, A. (2019) Furfural oxidation to maleic acid with H₂O₂ by using vanadyl pyrophosphate and zirconium pyrophosphate supported on well-ordered mesoporous KIT-6. *J. Environ. Chem. Eng.*, **7** (December 2018).
15. Huo, N., Ma, H., Wang, X., Wang, T., Wang, G., Wang, T., Hou, L., Gao, J., and Xu, J. (2017) High - efficiency oxidative esterification of furfural to methylfuroate with a non - precious metal Co - N - C / MgO catalyst. *Chinese J. Catal.*, **38** (7), 1148–1154.
16. Araji, N., Madjinza, D.D., Chatel, G., Moores, A., Jérôme, F., and De Oliveira Vigier, K. (2017) Synthesis of maleic and fumaric acids from furfural in the presence of betaine hydrochloride and hydrogen peroxide. *Green Chem.*, **19** (1), 98–101.

17. Li, X., Ho, B., and Zhang, Y. (2016) Selective aerobic oxidation of furfural to maleic anhydride with heterogeneous Mo-V-O catalysts. *Green Chem.*, **18** (10), 2976–2980.
18. Alonso-Fagúndez, N., Agirrezabal-Telleria, I., Arias, P.L., Fierro, J.L.G., Mariscal, R., and Granados, M.L. (2014) Aqueous-phase catalytic oxidation of furfural with H₂O₂: High yield of maleic acid by using titanium silicalite-1. *RSC Adv.*, **4** (98), 54960–54972.
19. Alonso-Fagúndez, N., Agirrezabal-Telleria, I., Arias, P.L., Fierro, J.L.G.G., Mariscal, R., Granados, M.L., Alonso-Fagundez, N., Agirrezabal-Telleria, I., Arias, P.L., Fierro, J.L.G.G., Mariscal, R., and Lopez Granados, M. (2014) Aqueous-phase catalytic oxidation of furfural with H₂O₂ : high yield of maleic acid by using titanium silicalite-1. *RSC Adv.*, **4** (98), 54960–54972.
20. Alba-Rubio, A.C., Fierro, J.L.G., León-Reina, L., Mariscal, R., Dumesic, J.A., and López Granados, M. (2017) Oxidation of furfural in aqueous H₂O₂ catalysed by titanium silicalite: Deactivation processes and role of extraframework Ti oxides. *Appl. Catal. B Environ.*, **202**, 269–280.
21. Rodenas, Y., Mariscal, R., Fierro, J.L.G., Martín Alonso, D., Dumesic, J.A., and López Granados, M. (2018) Improving the production of maleic acid from biomass: TS-1 catalysed aqueous phase oxidation of furfural in the presence of γ -valerolactone. *Green Chem.*, **20** (12), 2845–2856.
22. Lou, Y., Marinkovic, S., Estrine, B., Qiang, W., and Enderlin, G. (2020) Oxidation of Furfural and Furan Derivatives to Maleic Acid in the Presence of a Simple Catalyst System Based on Acetic Acid and TS-1 and Hydrogen Peroxide. *ACS Omega*, **5**, 2561–2568.
23. Li, X., Jia, P., and Wang, T. (2016) Furfural: A Promising Platform Compound for Sustainable Production of C₄ and C₅ Chemicals. *ACS Catal.*, **6** (11), 7621–7640.
24. Cao, R., Liu, C., and Liu, L. (1996) A convenient synthesis of 2(5h)-furanone. *Org. Prep. Proced. Int.*, **28** (2), 215–216.
25. Lohbeck, K., Haferkorn, H., Fuhrmann, W., and Fedtke, N. (2000) Maleic and Fumaric Acids. *Ullmann's Encycl. Ind. Chem.*
26. Martin, B., Sedelmeier, J., Bouisseau, A., Fernandez-Rodriguez, P., Haber, J., Kleinbeck, F., Kamptmann, S., Susanne, F., Hoehn, P., Lanz, M., Pellegatti, L., Venturoni, F., Robertson, J., Willis, M.C., and Schenkel, B. (2017) Toolbox study for application of hydrogen peroxide as a versatile, safe and industrially-relevant green oxidant in continuous flow mode. *Green Chem.*, **19** (6), 1439–1448.
27. Teong, S.P., Li, X., and Zhang, Y. (2019) Hydrogen peroxide as an oxidant in biomass-to-chemical processes of industrial interest. *Green Chem.*, **21** (21), 5753–5780.
28. Choudhary, H., Nishimura, S., and Ebitani, K. (2013) Metal-free oxidative synthesis of succinic acid from biomass-derived furan compounds using a solid acid catalyst with hydrogen peroxide. *Appl. Catal. A Gen.*, **458**, 55–62.
29. Choudhary, H., Nishimura, S., and Ebitani, K. (2012) Highly Efficient Aqueous Oxidation of Furfural to Succinic Acid Using Reusable Heterogeneous Acid Catalyst with Hydrogen Peroxide. *Chem. Lett.*, **41**, 409–411.
30. Yang, T., Li, W., Liu, Q., Su, M., Zhang, T., and Ma, J. (2019) Synthesis of Maleic Acid from Biomass-Derived Furfural in the Presence of KBr/Graphitic Carbon Nitride (g-C₃N₄) Catalyst and Hydrogen Peroxide. *bioresources*, **14** (3), 5025–5044.
31. Thiyagarajan, S., Franciolus, D., Bisselink, R.J.M., Ewing, T.A., and Boeriu, C.G. (2020) Selective Production of Maleic Acid from Furfural via a Cascade Approach Combining Photochemistry and Electro- or Biochemistry. *ACS Sustain. Chem. Eng.*, **8**, 10626–10632.

32. Maneechakr, P., and Karnjanakom, S. (2017) Catalytic transformation of furfural into bio-based succinic acid via ultrasonic oxidation using B-cyclodextrin-SO₃H carbon catalyst: A liquid biofuel candidate. *Energy Convers. Manag.*, **154** (November), 299–310.
33. Suslick, K.S. (1989) The Chemical Effects of Ultrasound. *Sci. Am.*, **260** (2), 80–86.
34. Babuponnusami, A., and Muthukumar, K. (2014) A review on Fenton and improvements to the Fenton process for wastewater treatment. *J. Environ. Chem. Eng.*, **2** (1), 557–572.
35. Rae, J., Ashokkumar, M., Eulaerts, O., Von Sonntag, C., Reisse, J., and Grieser, F. (2005) Estimation of ultrasound induced cavitation bubble temperatures in aqueous solutions. *Ultrason. Sonochem.*, **12** (5), 325–329.
36. Henglein, A., and Kormann, C. (1985) Scavenging of OH radicals produced in the sonolysis of water. *Int. J. Radiat. Biol.*, **48** (2), 251–258.
37. Von Sonntag, C. (2008) Advanced oxidation processes: Mechanistic aspects. *Water Sci. Technol.*, **58** (5), 1015–1021.
38. Ashokkumar, M. (2011) The characterization of acoustic cavitation bubbles - An overview. *Ultrason. Sonochem.*, **18** (4), 864–872.
39. Brotchie, A., Grieser, F., and Ashokkumar, M. (2009) Effect of power and frequency on bubble-size distributions in acoustic cavitation. *Phys. Rev. Lett.*, **102** (8), 1–4.
40. Cravotto, G., and Cintas, P. (2006) Power ultrasound in organic synthesis: Moving cavitation chemistry from academia to innovative and large-scale applications. *Chem. Soc. Rev.*, **35** (2), 180–196.
41. Peters, D. (1996) Ultrasound in materials chemistry. *J. Mater. Chem.*, **6** (10), 1605–1618.
42. Pokhrel, N., Vabbina, P.K., and Pala, N. (2016) Sonochemistry: Science and Engineering. *Ultrason. Sonochem.*, **29**, 104–128.
43. Ji, R., Pflieger, R., Virost, M., and Nikitenko, S.I. (2018) Multibubble Sonochemistry and Sonoluminescence at 100 kHz: The Missing Link between Low- and High-Frequency Ultrasound. *J. Phys. Chem. B*, **122** (27), 6989–6994.
44. Gallipoli, A., and Braguglia, C.M. (2012) High-frequency ultrasound treatment of sludge: Combined effect of surfactants removal and floc disintegration. *Ultrason. Sonochem.*, **19** (4), 864–871.
45. Baig, R.B.N., and Varma, R.S. (2012) Alternative energy input: Mechanochemical, microwave and ultrasound-assisted organic synthesis. *Chem. Soc. Rev.*, **41** (4), 1559–1584.
46. Matsumura, S., Hlil, A.R., Lepiller, C., Gaudet, J., Guay, D., Shi, Z., Holdcroft, S., and Hay, A.S. (2008) Stability and Utility of Pyridyl Disulfide Functionality in RAFT and Conventional Radical Polymerizations. *J. Polym. Sci. Part A Polym. Chem.*, **46** (April), 7207–7224.
47. Piiskop, S., Hagu, H., Järv, J., Salmar, S., and Tuulmets, A. (2007) Sonication effects on ester hydrolysis in alcohol-water mixtures. *Proc. Est. Acad. Sci. Chem.*, **56** (4), 199–206.
48. Hofmann, J., Freier, U., and Wecks, M. (2003) Ultrasound promoted C-alkylation of benzyl cyanide - Effect of reactor and ultrasound parameters. *Ultrason. Sonochem.*, **10** (4–5), 271–275.
49. Grönroos, A., Aittokallio, N., and Kolehmainen, E. (2004) Ultrasound accelerated esterification of bile acids. *Ultrason. Sonochem.*, **11** (3–4), 161–165.
50. Santos, D., Silva, U.F., Duarte, F.A., Bizzi, C.A., Flores, E.M.M., and Mello, P.A. (2018) Ultrasound-

- assisted acid hydrolysis of cellulose to chemical building blocks: Application to furfural synthesis. *Ultrason. Sonochem.*, **40** (April 2017), 81–88.
51. Bizzi, C.A., Santos, D., Sieben, T.C., Motta, G. V., Mello, P.A., and Flores, E.M.M. (2019) Furfural production from lignocellulosic biomass by ultrasound-assisted acid hydrolysis. *Ultrason. Sonochem.*, **51** (September 2018), 332–339.
 52. Hoang, P.H., Cuong, T.D., and Dien, L.Q. (2021) Ultrasound Assisted Conversion of Corn-cob-Derived Xylan to Furfural Under HSO₃-ZSM-5 Zeolite Catalyst. *Waste and Biomass Valorization*, **12** (4), 1955–1962.
 53. Ismail, Z.Z., and Jasim, A.S. (2014) Ultrasonic treatment of wastewater contaminated with furfural. *IDA J. Desalin. Water Reuse*, **6** (3–4), 103–111.
 54. Joseph, S. (2012) Ultrasound assisted semiconductor mediated catalytic degradation of organic pollutants in water: Comparative efficacy of ZnO, TiO₂ and ZnO-TiO₂ Ultrasound assisted semiconductor mediated catalytic degradation of organic pollutants in water: Comparative ef. *Res. J. Recent Sci.*, **1** (January 2012), 191.
 55. Wu, T.N., and Shi, M.C. (2010) pH-affecting sonochemical formation of hydroxyl radicals under 20 kHz ultrasonic irradiation. *Sustain. Environ. Res.*, **20** (4), 245–250.
 56. Kermani, M., Farzadkia, M., Morovati, M., Taghavi, M., Fallahizadeh, S., Khaksefidi, R., and Norzaee, S. (2020) Degradation of furfural in aqueous solution using activated persulfate and peroxymonosulfate by ultrasound irradiation. *J. Environ. Manage.*, **266** (February), 110616.
 57. Bhangu, S.K., and Ashokkumar, M. (2016) Theory of Sonochemistry. *Top. Curr. Chem.*, **374** (4), 1–28.
 58. Ashokkumar, M., Sunartio, D., Kentish, S., Mawson, R., Simons, L., Vilku, K., and Versteeg, C. (Kees) (2008) Modification of food ingredients by ultrasound to improve functionality: A preliminary study on a model system. *Innov. Food Sci. Emerg. Technol.*, **9** (2), 155–160.
 59. Muzychenko, G.F., Badovskaya, L.A., and Kul'nevich, V.G. (1972) Role of water in the oxidation of furfural with hydrogen peroxide. *Chem. Heterocycl. Compd.*, **8**, 1311–1313.
 60. Li, X., Lan, X., and Wang, T. (2016) Selective oxidation of furfural in a bi-phasic system with homogeneous acid catalyst. *Catal. Today*, **276**, 97–104.
 61. Petrier, C., Jeunet, A., Luche, J., and Reverdyt, G. (1992) Unexpected frequency effects on the rate of oxidative processes induced by ultrasound. *J. Am. Chem. Soc.*, (114), 3148–3150.
 62. Hart, E.J., and Henglein, A. (1987) Sonochemistry of aqueous solutions: H₂O₂ combustion in cavitation bubbles. *J. Phys. Chem.*, **91** (13), 3654–3656.
 63. Bierbach, A., Barnes, I., and Becker, K.H. (1995) Product and kinetic study of the oh-initiated gas-phase oxidation of Furan, 2-methylfuran and furanaldehydes at ≈ 300 K. *Atmos. Environ.*, **29** (19), 2651–2660.
 64. Zhao, X., and Wang, L. (2017) Atmospheric Oxidation Mechanism of Furfural Initiated by Hydroxyl Radicals. *J. Phys. Chem. A*, **121** (17), 3247–3253.
 65. Yuan, Y., Zhao, X., Wang, S., and Wang, L. (2017) Atmospheric Oxidation of Furan and Methyl-Substituted Furans Initiated by Hydroxyl Radicals. *J. Phys. Chem. A*, **121** (48), 9306–9319.
 66. Van Nguyen, C., Boo, J.R., Liu, C.H., Ahamad, T., Alshehri, S.M., Matsagar, B.M., and Wu, K.C.W. (2020) Oxidation of biomass-derived furans to maleic acid over nitrogen-doped carbon catalysts under acid-free conditions. *Catal. Sci. Technol.*, **10** (5), 1498–1506.

Chapter 5

Furfural oxidation using magnetic and abundant catalyst from iron oxide

1. Introduction

Several processes have been developed for the conversion of furfural into a number of valuable chemicals and fuels such as succinic acid, maleic acid, malic acid, and so on as detailed in previous chapters.

In chapter 4, we discussed that the oxidation of furfural using hydrogen peroxide takes place in two steps. The first stage was the attack of HO• radicals from the homolytic cleavage of hydrogen peroxide. Therefore, the oxidation of furfural could be achieved following a radical mechanism.

On the other hand, numerous advanced oxidation processes has been evaluated as a pretreatment to minimize the presence of pollutants in wastewater, such as furfural. Among them, Fenton-like processes have been widely studied and showed high effectiveness for the treatment of wastewater streams resulting from the mixture of the concentrated furfural stream and other wastewater lines of the refinery. [1–5]

Usually, Fenton process lies on the interaction between H₂O₂ and Fe cations, present in iron oxides. However, magnetite nanoparticles have an important surface to volume ratio. Hence, they are used to catalyze a Fenton-like process to oxidize furfural in diacids.

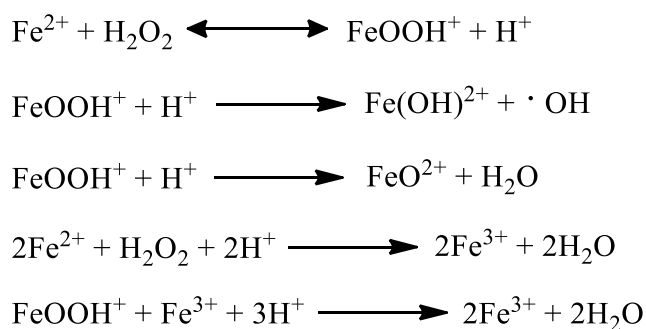
In the present work, a novel non-noble metallic catalyst process was developed using iron oxide and magnetite nanoparticles under mild conditions for the synthesis of succinic acid. Traditional applications of succinic acid include food additives, detergents, cosmetics, pigments, toners, cement additives, soldering fluxes, and pharmaceutical intermediates. [6,7] Moreover, this method could be used for the wastewater treatments contaminated by furfural pollutants.

1.1. Iron oxides

Iron oxides have been widely used as catalysts in various heterogeneous catalytic processes such as Haber-Bosch to produce ammonia [8], the Fischer-Tropsch hydrocarbon synthesis [9,10], steam reforming [11,12], water-gas shift [13,14], ethylbenzene dehydrogenation to produce styrene monomers [15,16], water splitting for hydrogen production [17,18], aerobic oxidation of organic compounds to produce new products for the fine chemical industry [19,20] and in advanced oxidation processes (AOPs) to oxidize pollutants in water and soils [21–26].

The AOPs have received special attention because of their high oxidative power towards contaminants in wastewaters and soils, which is promoted by •OH radicals. These radicals can be produced by several AOPs such as the homogeneous Fenton, heterogeneous Fenton, photo-Fenton, photocatalysis and ozonation, among others.

Fenton process lies on the interaction between Fe cations and H₂O₂ as the primary oxidant. This gives the impression of being relatively simple. However, numerous reaction mechanisms have been proposed based on different active intermediates such as FeO₂⁺, [•]OH and [•]OOH radicals. All of these can be divided into two main groups. The first is based on the [•]OH radical mechanism proposed by Haber & Weiss (1934) and is probably the most popular mechanism for describing the interactions between Fe ions (Fe²⁺ and Fe³⁺) and H₂O₂ [27].



Scheme 5.1 – Mechanistic aspect for Fenton reaction [28]

The homogeneous Fenton reaction was first reported in 1894 by H.J.H. Fenton [29]. He showed that ferrous ions strongly promote the oxidation of malic acid by H₂O₂. He subsequently suggested that the mixture of H₂O₂ and a ferrous salt, since called the “Fenton reagent”, was an effective oxidant for a variety of organic compounds. On the other hand, the reaction of H₂O₂ and other cations such as Fe³⁺, Co²⁺, Mn²⁺ and Cu²⁺ instead of Fe²⁺ is called a “Fenton-like reaction”.

The biggest advantages of classic Fenton reactions are that Fe and H₂O₂ are environmentally nontoxic, H₂O₂ activation takes place at room temperature and under atmospheric pressure, and the reaction times are relatively short. On the other hand, the reaction depends strongly on the pH, and maintenance of the pH close to the optimum of 3 requires large amounts of acid, the subsequent neutralization of which leads to sludge formation. [30,31]

Studies based on new forms of generation of reactive [•]OH radicals such as the heterogeneous Fenton-like process have therefore received increasing attention during the last decade.

Similar to the classic Fenton, the heterogeneous Fenton-like reaction is a reaction between H₂O₂ and Fe in a solid matrix to produce highly oxidizing species. The heterogeneous Fenton-like process has several advantages over the homogeneous process. Reaction can take place at neutral pH, sparing the need for the acidification and neutralization step, thereby avoiding sludge formation. The catalysts can also easily be recycled and regenerated, and all operations in the effluent treatment are significantly simplified if the solid catalyst is easy to handle. [32,33]

1.2. Magnetite nanoparticles

Magnetite is an ideal oxide support, easy to prepare, having a very active surface for adsorptions or immobilization of metals and ligands, which can be separated by magnetic decantation after the reaction, thus making it a more sustainable catalyst. [34] In the last few years, various forms of iron oxides such as FeO (wüstite), Fe₂O₃ (iron III oxides), α-Fe₂O₃ (hematite), β-Fe₂O₃ (beta phase), and γ-Fe₂O₃ (maghemite) were successfully deployed in catalysis. [35–38]

In recent years, magnetite/magnetite-supported catalysts have been successfully deployed in organic synthesis for a variety of important reactions.

Fe₃O₄ is highly soluble in aqueous medium (28 mg.mL⁻¹), financially affordable, non-toxic and readily recyclable. Accordingly, Fe₃O₄ is a valuable candidate to be used as heterogeneous catalyst in Fenton reaction. Magnetite nanoparticles were used in this study as the catalyst. It is believed that the nanostructured and well-dispersed catalyst particles offer both more number of active sites and less resistance to mass transfer. [39] A variety of chemical and hydrothermal methods have recently been utilized to generate nanostructured magnetite. [39,40] The methods, however, usually employ toxic and costly chemicals as reactants, complex devices, or high-energy cost. [40]

In this work, Fe₃O₄ were manufactured with co-precipitation method. This method was selected for its simplicity, reproducibility and low cost in terms of solvents and chemical reagents. In this method, Fe²⁺ and Fe³⁺ are generally precipitated in alkaline solutions, sodium hydroxide (NaOH) at 35 °C. The size of nanoparticles generated will have a strong impact on their magnetic properties [41].

2. Experimental part

2.1. Materials, solvents and reagents

Furfural, iron (II) chloride tetrahydrate and iron (III) chloride hexahydrate were purchased from Acros Organics, hydrogen peroxide (H₂O₂, 35%), hydrochloric acid and sodium hydroxide were purchased from Fisher Chemicals and Iron oxide from Alfa Aesar. These products were further used without any purification.

2.2. Instruments and analytical methods

2.2.1. Gas Chromatography

In this study, a PerkinElmer Autosystem XI instrument was used for the detection of furfural. It was equipped with an auto sampler and a flame ionization detector (FID) with a 30 m length and 0.25 mm diameter AT-1HT column Part No. 16368. The different experimental parameters for the GC analyses

were as follows: nitrogen as carrier gas with a flowrate of 1 mL/min, temperature of the injector (T_{injector}) set at 350 °C, temperature of the column (T_{column}) set at 40 °C for 2 min and then increased up to 250 °C with a heating rate of 20 °C/min. The injection volume is set to 1 μL .

Q_{H_2} = 45 ml/min and Q_{air} =450 ml/min.

2.2.2. High performance liquid chromatography

In this study, a Shimadzu HPLC equipped with a corgel 87H3 column, Mobile phase: formic acid $8 \cdot 10^{-3}$ M, flow 0.6 mL/min. Column Temp: 35°C. The injection volume was 10 μL .

Diacids were detected by an evaporative light scattering detector ELSD-LTII from Shimadzu in conjunction with HPLC at 50 °C, with a gain of 10. The used mobile phase is formic acid $8 \cdot 10^{-3}$ M having a flow rate of 0.6 mL/min

2.2.3. Transmission Electron Microscope (TEM)

TEM micrographs were recorded using a JEOL JEM-2100F instrument at an acceleration voltage of 200 kV and visualized with a CCD camera. Samples were diluted in deionized water, a drop was added onto a copper mesh grid coated with an amorphous carbon film and allowed to air-dry. The crystallinity and cartography of the NPs was analyzed using selected area electron diffraction (SAED) and high-resolution transmission electron microscopy (HRTEM). The solution was dried using freeze-dryer or lyophilizer before it was attached to the microscope sample holder.

2.2.3.1. Image analysis by Image J

TEM micrographs were analyzed with Image J software to determine NPs crystalline diameter. A script was created in which images were converted into 8-bit, contrast was enhanced with a fixed saturation value of 4 and normalized. A band pass filter and a color threshold were applied to the image. Scale bar was set from a previous measurement to convert pixels into nm and the scale bar from the image was removed to avoid its measurement as a particle. Particles parameter were analyzed using the Analyze particle option by setting size from 100-900 (in pixels) and circularity from 0 to 1. An overlay image was created in each case containing the counted NPs with their assigned number, the calculated values were saved in an excel file.

2.2.4. X-Ray Diffraction (XRD)

The sizing of the nanoparticles was performed by XRD powder method. Diffraction patterns (2θ) were recorded with a BRUKER D8 ADVANCE diffractometer, equipped with copper cathode ($\text{Cu K}\alpha_1$ 1.54178 Å) and Ni filter, operating at 40 kV and a current of 40 mA. A continuous scan with a step of 0.020 (1

deg/50 s) was used to collect 2θ from 10 to 80 degrees, using DIFRACT.EVA V4.2.1 software to treat the results.

2.2.5. Ultraviolet-Visible Spectroscopy (UV)

The concentration of magnetite nanoparticles was measured by UV method and was carried out using a Perkin Elmer Lambda 12 UV-vis spectrophotometer in 1 cm path length quartz cuvette at room temperature. This equipment has a double beam with deuterium and tungsten lamps, with a wavelength range (nm) 200-800. There were two analysis done: direct measure on nanoparticles sample and KSCN method.

2.3. Magnetite nanoparticle synthesis

Magnetite nanoparticles were synthesized by an alkaline co-precipitation method. 0.01 mol of $\text{FeCl}_2 \cdot 4\text{H}_2\text{O}$ were dissolved in 7.5 mL of HCl 1 M to prevent premature oxidation of Fe^{2+} to Fe^{3+} in aqueous solutions. 0.02 mol of $\text{FeCl}_3 \cdot 6\text{H}_2\text{O}$ were dissolved in 160 mL of water, and mixed with the ferrous solution in an ultrasound bath. The obtained $\text{Fe}^{2+}/\text{Fe}^{3+}$ solution was added, with a peristaltic pump set at $400 \text{ mL} \cdot \text{min}^{-1}$, into a reactor with a controlled temperature ($T = 30 \text{ }^\circ\text{C}$) containing 84 mL of 2 M NaOH solution. The addition speed will define nanoparticle size [42]. Reaction was carried under constant stirring at 2000 rpm during 2 h. At this point a 2.5 M HCl solution was used to neutralize the remaining NaOH. The dispersion was then placed at neutral pH as NPs are not charged and can easily be separated by magnetic force. Neodymium magnets were used to induce NPs precipitation. Water was added to the precipitated NPs to wash them. The procedure was repeated three times. Then, pH was set to 2 by adding 1M HCl to stabilize the obtained nanoparticles. The magnetite nanoparticles suspension was stored at $4 \text{ }^\circ\text{C}$.

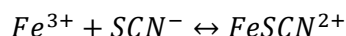
2.4. Magnetite nanoparticle concentration

The magnetite concentration dispersions were calculated by a direct and indirect method. For direct method UV-vis spectrometry was used to measure absorbance at 480 nm of a diluted iron oxide nanoparticles dispersion. The Beer-Lambert Law gives the correlation between the obtained absorbance and the dispersion concentration. Herein we used $\epsilon = 420 \text{ L} \cdot \text{mol}^{-1} \cdot \text{cm}^{-1}$.

$$[\text{Fe}] = \frac{\text{Abs} \times \text{Dilution factor}}{\epsilon \times L}$$

However, this is only and approximate concentration given that ϵ is highly dependent on the size of the obtained NPs. The exact magnetite concentration can be calculated by an indirect method using KSCN. Herein a complete oxidation is required to convert all iron ions into Fe^{3+} , which is able to form

the $FeSCN^{2+}$ complex (as described in the equation above) whose maximum absorbance is found at 475 nm.



By using the approximate concentration determined by direct method, 15 mM of nanoparticles dispersions were prepared and 10 μ L were added into a 15 mL falcon. The iron oxidation was carried out by adding 100 μ L of 20% H_2O_2 and 100 μ L of 7 M HNO_3 . Mixtures were heated at 80 °C between 2-3 h. Cooled samples were then mixed with 1 mL H_2O and 100 μ L of 2 M KSCN. The addition of KSCN results in a reddish color apparition with a specific UV-Vis maximum absorbance at 475 nm. UV-Vis absorbance at 475 nm was measured immediately after KSCN addition using a Perkin Elmer Lambda 12 UV-vis spectrophotometer in 1 cm path length quartz cuvette at room temperature. Calibration curve was obtained by preparing solutions with known iron concentrations, processing them in the same manner and plotting the absorbance as function of the iron concentrations. Experimental ϵ was determined from the calibration curve and used to determine sample iron concentration.

2.5. Catalytic experiments

The catalysts used in these oxidation reactions is the magnetite nanoparticles and iron oxides. Usually the furfural oxidation reaction is conducted in a batch reactor (Three-neck round-bottom flask) by introducing 3.34 mL of reactant, 5.4 mL of water, 20.4 mL (0.3 mol, 6 eq.) of H_2O_2 , and 0.615 ml (80 μ mol) of magnetite nanoparticles as catalyst.

The operating conditions (temperature, reaction duration, concentrations and quantities ...) were varied in order to optimize the process. At the end of each reaction, the used catalyst (Magnetite nanoparticles or iron oxides) was separated from the reaction medium using a magnet.

Solvent was evaporated under reduced pressure, and the recovered product was diluted with ethyl acetate then analyzed with GC and HPLC.

2.6. Product analysis

Furfural was detected and quantified using by Gas Chromatography (Perkin Elmer instruments, AutoSystem XL) equipped with a Column Alltech Part No. 16368 AT-1ht 30m x 0.25mm D x 0.1 μ m. The injection volume 1 μ l, oven temperature 250°C, Q_{H_2} = 45 ml/min and Q_{air} =450 ml/min.

Retention time of furfural is 4.9 min.

Maleic acid (MA), hydroxyfuranone (5-HFO) and furanone were analyzed on a Shimadzu HPLC equipped with a corgel 87H3 column, Mobile phase: formic acid $8 \cdot 10^{-3}$ M, flow 0.6 mL/min. Column Temp: 35°C. The injection volume was 10 μ L.

Retention time of MA, 5-HFO and furanone are 7.8, 19.8 and 33.4 min respectively.

Diacids such as succinic acid and malic acid were detected by an evaporative light scattering detector. Formic acid was detected by HPLC using C-18 column. Mobile phase: water, flow 1 mL/min. Column Temp: 35°C. The injection volume was 10 μ L.

Furfural conversion and products' selectivities and yields were calculated according to the following equations:

$$Conversion_{furfural} = \frac{n_{furfural_{initial}} - n_{furfural_{remaining}}}{n_{furfural_{initial}}} \times 100 \quad (1)$$

$$Yield_{product} = \frac{n_{product_{obtained}}}{n_{product_{theoretical}}} \times 100 \quad (2)$$

$$Selectivity_{product} = \frac{n_{product_{obtained}}}{n_{furfural_{initial}} - n_{furfural_{remaining}}} \times 100 \quad (3)$$

3. Results and discussions

3.1. Magnetite nanoparticles

Three samples of magnetite nanoparticles were prepared using the procedure described above. A small volume of each one was dried by freeze-dryer or lyophilizer. The dried samples are then attached to the transmission electron microscope (TEM) to be characterized. Here are the images of nanoparticles taken by the TEM and the sizes of each one is determined using ImageJ. The size distribution of each sample is shown in the graphs below.

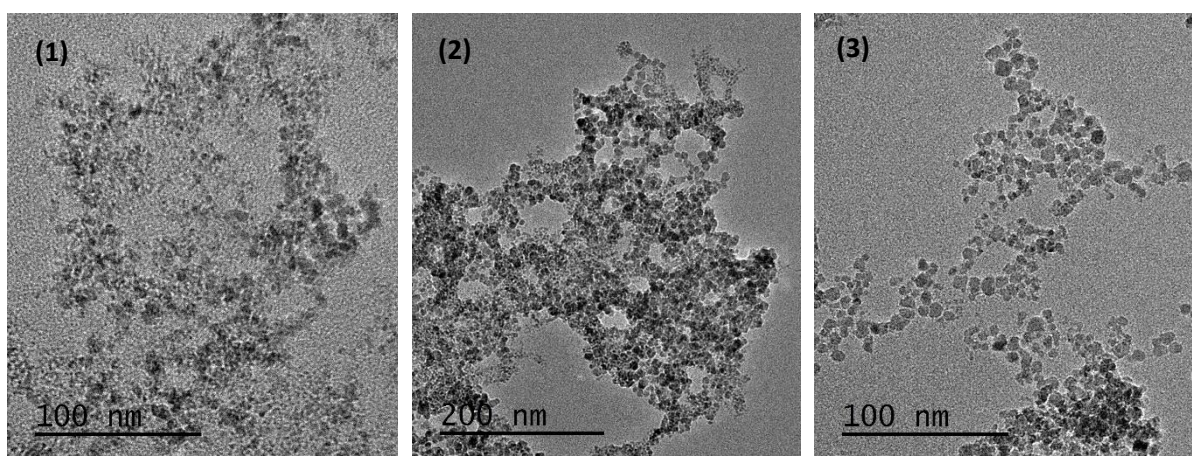


Figure 5.1 - TEM images for the three different samples of magnetite nanoparticles

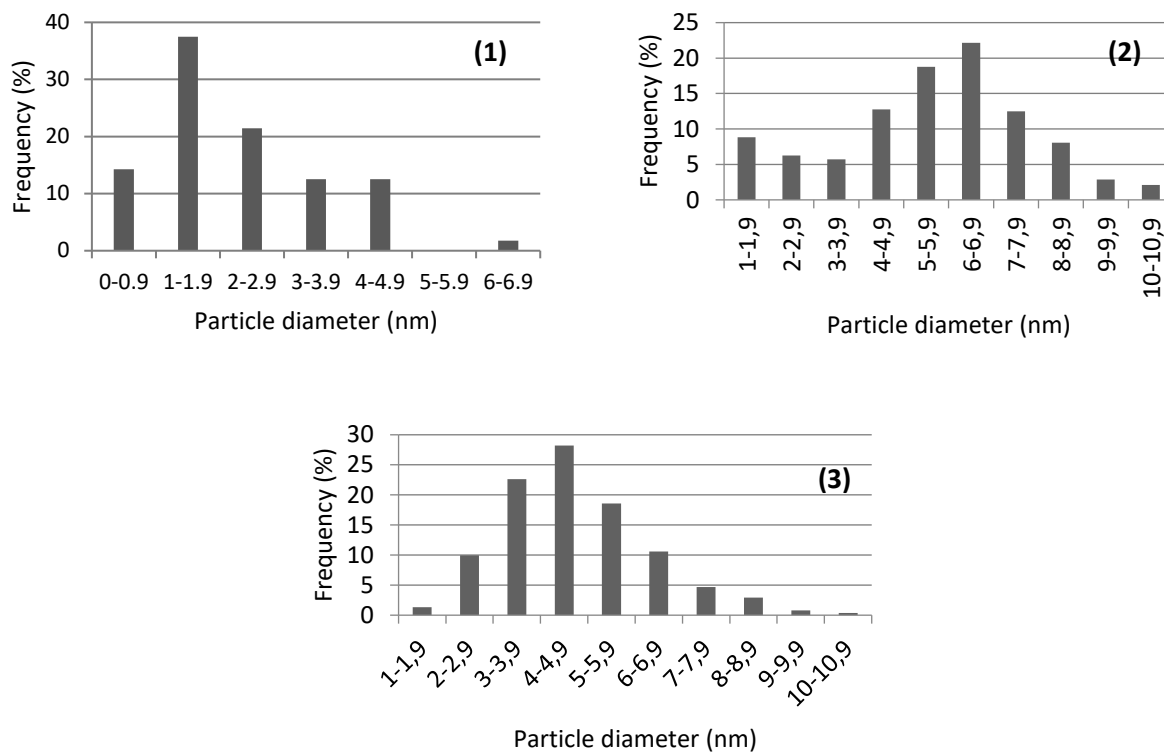


Figure 5.2 - Diameter distribution of the three different samples of magnetite nanoparticles

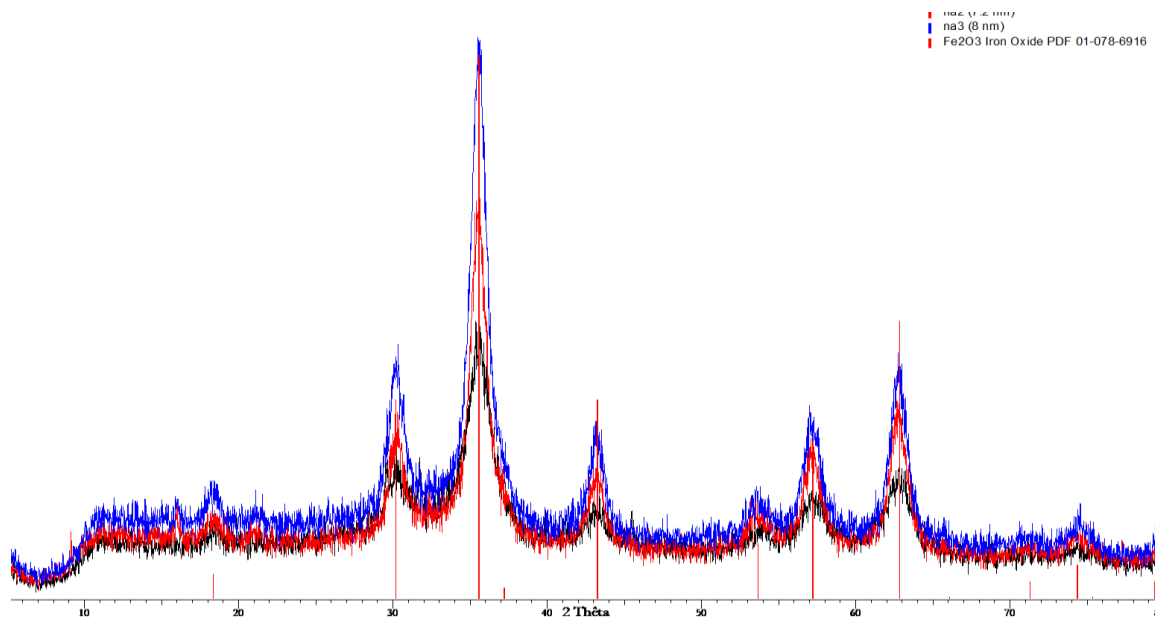


Figure 5.3 - Nanoparticle size using XRD technique

Figure 5.3 also shows the magnetite nanoparticles using the XRD technique.

Many parameters have influence on the nanoparticle size, such as the initial molar fraction X of Fe(II). According to Massart et al., the size of nanoparticles increases with X . Moreover, an increase of the pH can lead to a decrease in the nanoparticle size. [42]

Furthermore, other factors related to the operating conditions, could have a light influence on the nanoparticle size. For example, increasing the addition speed of Fe(II)-Fe(III) mixture to the reactor tends to the formation of smaller nanoparticles. [42]

The average particle diameter of samples (1), (2), and (3) are 2.9, 5.6, 6.7 nm respectively.

For the rest of experimental tests, we used sample (3) of magnetite nanoparticle, having a concentration of 0.136 mol/L, to catalyze the oxidation of furfural.

3.2. Preliminary tests

In our preliminary tests, we tested the oxidation of furfural using magnetite nanoparticles. We introduced 3.34 mL of reactant, 5.4 mL of water, 20.4 mL (0.3 mol, 6 eq.) of H₂O₂, and 0.615 mL (80 μmol) of magnetite nanoparticles. We were surprised by 95% of furfural conversion and unexpected selectivity towards succinic acid (figure 5.4). In view of these results, we decided to further investigate the operating conditions in order to obtain higher selectivity.

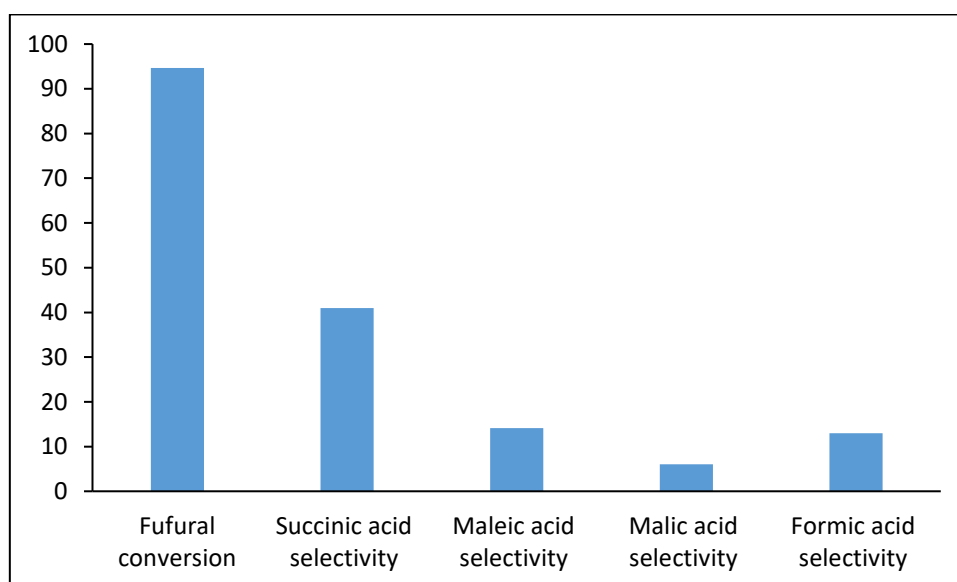


Figure 5.4 – Products of furfural oxidation; 0.04 mol of furfural, 0.3 mol (20.4 mL) of H₂O₂, 5.4 mL of H₂O, 80 μmol (0.615 mL) of magnetite nanoparticles, 40 °C, 12 h.

3.3. Effect of reaction time

In view of the good results obtained, we studied the effect of the various reaction parameters on the transformation. To do so, we evaluated the influence of time on the reaction, especially on furfural conversion and succinic acid yield.

First, we studied the reaction kinetics at 40 °C since it is the optimal temperature as demonstrated before. Figure 5.5 shows that a total conversion of furfural could be achieved after 17 h. The highest yield of succinic acid is 67% is obtained after 24 h.

Moreover, until 10 h, we obtain around 40% of succinic acid yield, which increases rapidly after longer reaction durations. The oxidation corresponds mainly to the formation of HO• radicals and their reaction with furfural leading to the selective formation of 5-HFO and furanone. These intermediates are then rapidly oxidized to succinic acid as soon as we keep heating the mixture for longer time.

Above 24 h, succinic acid yield remains the same. Strong oxidizing conditions such as high reaction duration lead to the degradation of succinic acid. Besides, the problem of catalyst dissolution when it is heated for longer times.

Despite the fact that after 24 h the yield of succinic acid slightly decreases, the yield of the other by-products decreases as well. Therefore, going further in the oxidation can reduce the impurities and decrease the yield of by-products, which can be highly interesting since it is difficult to separate the succinic acid especially from a mixture containing maleic acid. This is shown in figure 5.5, at $t = 48$ h we almost have only one pure product. Note that, the decrease of formic acid yield is due to its evaporation during the step of water evaporation using a rotary evaporator (Formic acid boiling point: 100.8 °C).

In the same context, we performed a series of reactions in function of time but at 50 °C. We see in figure 5.6 that total conversion of furfural is achieved faster than at 40 °C and this is due to a faster reaction rate at higher temperature. However, at higher temperatures, succinic acid yield decreases and reaches 43% at $t = 6$ h along with a decrease of other by-products' yields. This can be explained by the dissolution of a part of magnetite nanoparticles, which becomes more important at higher temperatures.

Hence, heating at 50 °C for long reaction time can promote the chelation of iron ions and acids, which lead to the loss of catalytic activity and then loss of selectivity.

Therefore, the best compromise was to work at 40 °C and during 24 h to guarantee a good stability and catalytic activity of magnetite nanoparticles and to obtain the highest yield of succinic acid in addition to a total conversion of furfural.

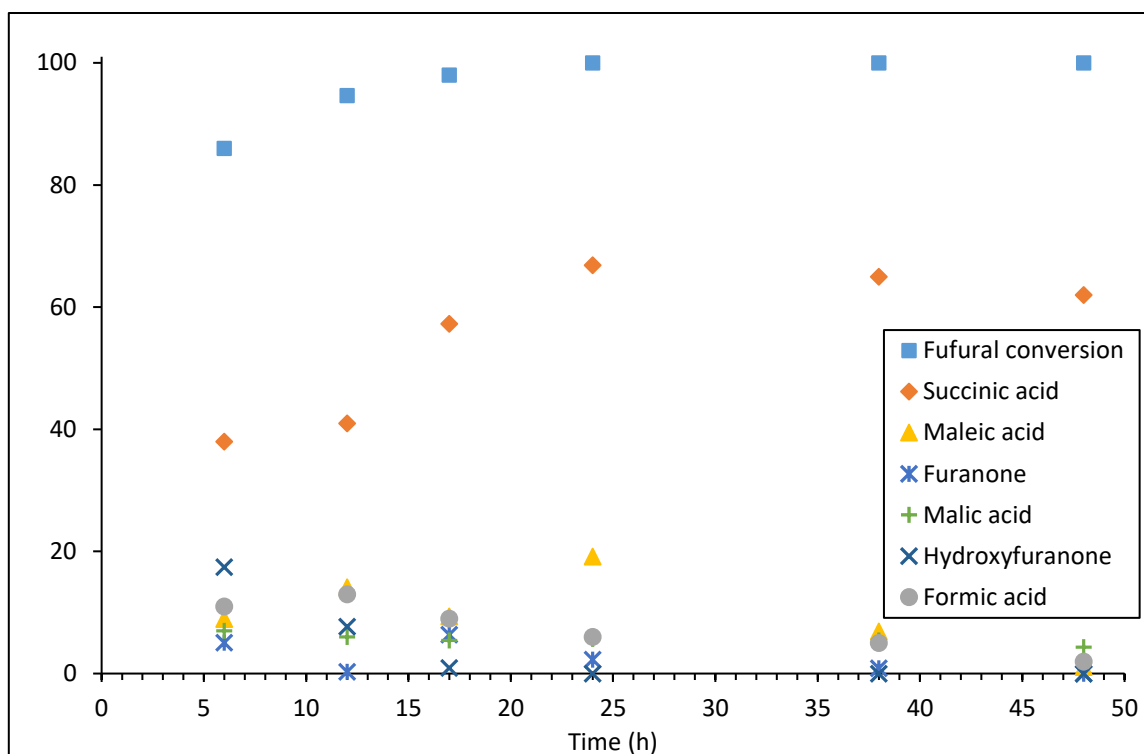


Figure 5.5 - Effect of time on furfural conversion and products' yields; 0.04 mol of furfural, 0.3 mol (20.4 mL) of H₂O₂, 5.4 mL of H₂O, 80 μmol (0.615 mL) of magnetite nanoparticles, 40 °C.

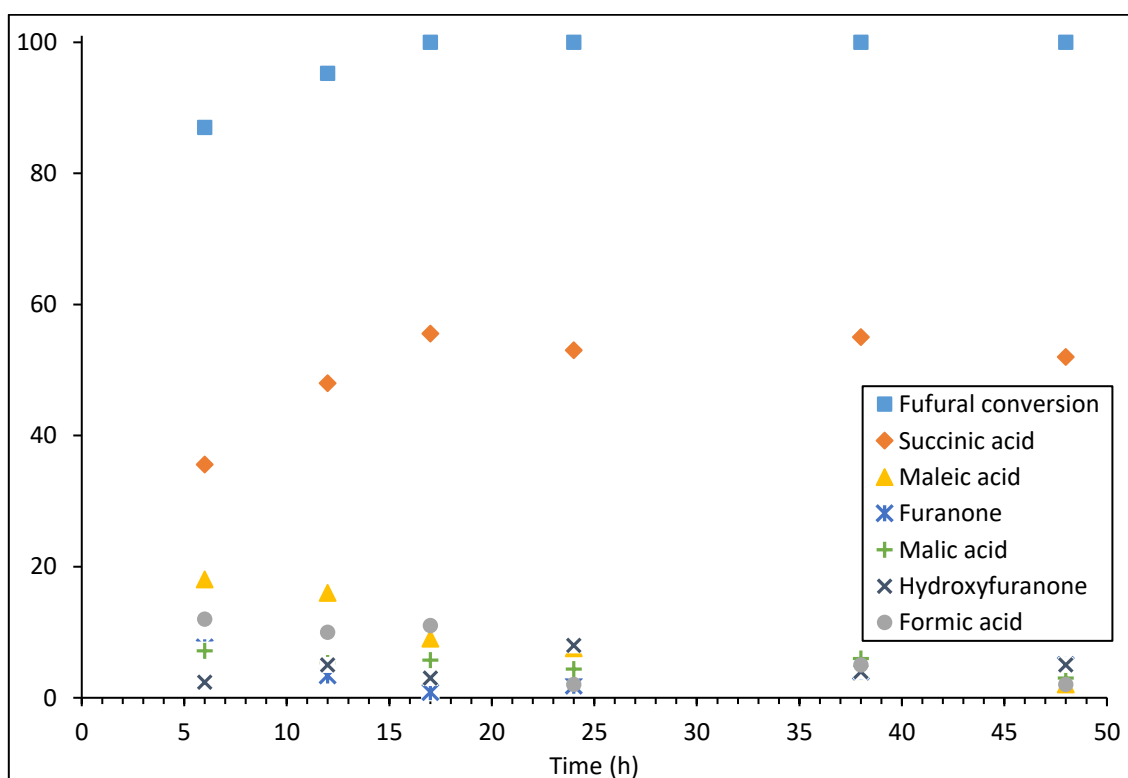


Figure 5.6 - Effect of time on furfural conversion and products' yields; 0.04 mol of furfural, 0.3 mol (20.4 mL) of H₂O₂, 5.4 mL of H₂O, 80 μmol (0.615 mL) of magnetite nanoparticles, 50 °C.

3.4. Effect of reaction temperature

We decided to figure out the optimal reaction temperature in order to further optimize the other operating conditions. To do so, we performed a reaction monitoring at three different temperatures, 30 °C, 40 °C and 50 °C. It is noteworthy to mention that magnetite nanoparticles and their activity are highly sensitive to temperature in our case. Working at 60 °C and above can lead to the deactivation of nanoparticles. Hence, there can be a dissolution as we heat the nanoparticles when we are in an acidic medium, which is the case here since there is formation of diacids. In fact, what happens is that acids and diacids are metal chelators and therefore will gradually tear ions from the surface and then gradually dissolve the nanoparticles. In addition, oxido-reduction reactions can lead to the deactivation of nanoparticles. The phenomenon, which is slow at room temperature, with these acids will therefore intensify on heating. As a result, it will not be possible to recover the catalyst and reuse it for another run.

Figure 5.7 shows the furfural conversion and the yield of succinic acid in function of time. As shown below, 40 °C is the optimal temperature where we obtained a total conversion and 67% of succinic acid yield. At 30 °C, furfural conversion and succinic acid were smaller and this is explained by lower catalytic activity at lower temperatures.

Furthermore, at higher temperature, furfural conversion and succinic acid yield decrease due to the dissolution of a part of magnetite nanoparticles when they are heated at 50 °C for 24 h. This demonstrates the fast consumption of the catalyst at high temperature.

In addition to succinic acid, other by-products were observed at the end of each reaction. Figure 5.8, shows the yields of maleic acid and malic acid. Moreover, some traces of furanone and hydroxyfuranone could be detected as well.

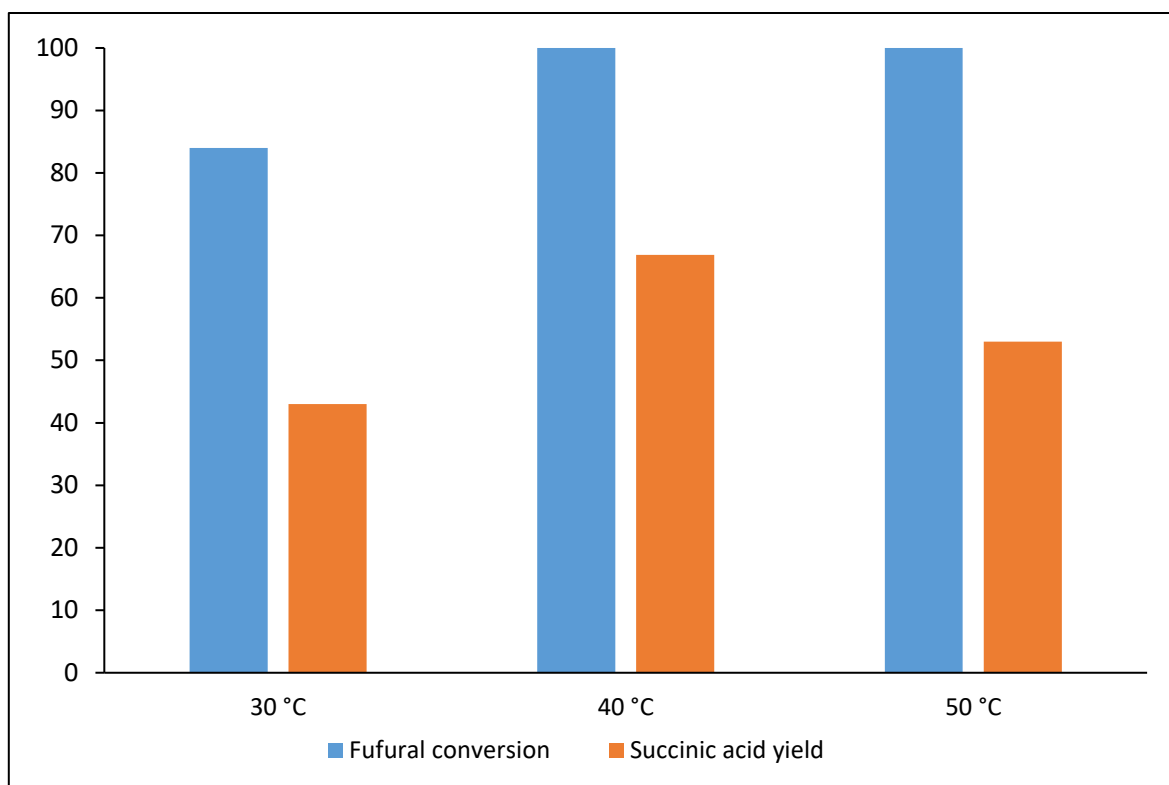


Figure 5.7 - Effect of temperature on furfural conversion and succinic acid yield; 0.04 mol of furfural, 0.3 mol (20.4 mL) of H₂O₂, 5.4 mL of H₂O, 80 μmol (0.615 mL) of magnetite nanoparticles, 24 h.

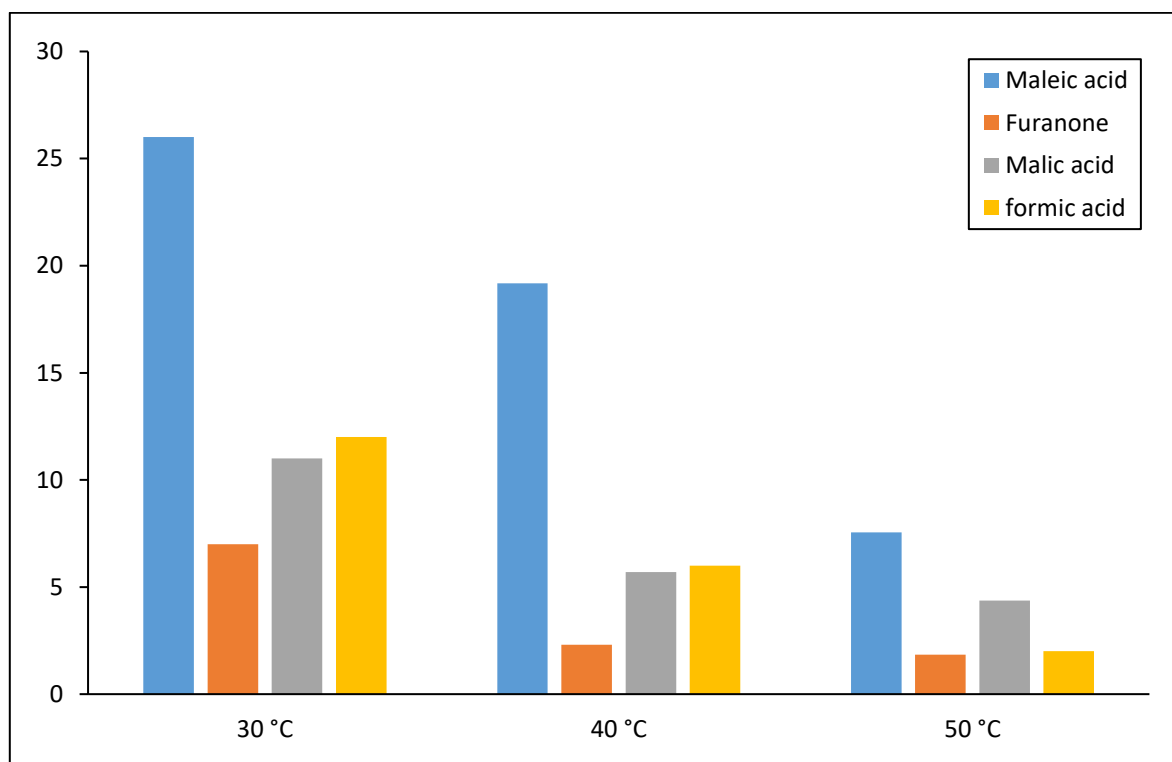


Figure 5.8 - Yields of the obtained by-products; 0.04 mol of furfural, 0.3 mol (20.4 mL) of H₂O₂, 5.4 mL of H₂O, 80 μmol (0.615 mL) of magnetite nanoparticles, 24 h.

3.5. The effect of the catalyst weight

In order to verify if there is any potential acceleration of the reaction, we investigated the effect of the catalyst weight on furfural conversion and succinic acid yield. At first, we introduced 12.8 mg of magnetite nanoparticles, which is equivalent to 0.615 ml (80 μ mol). Then we investigated the effect of introducing the double and the triple of this quantity. As shown in figure 5.9, there's an effect of the catalyst weight, the reaction rate increase but no effect on the selectivity, as the results remain the same in the three experiments. With greater quantities of catalyst, the reaction rate increases and high yields of succinic acid are obtained in a shorter time, but at longer reaction time, this yields decrease, most probably, due to over-oxidation or polymerization of SA.

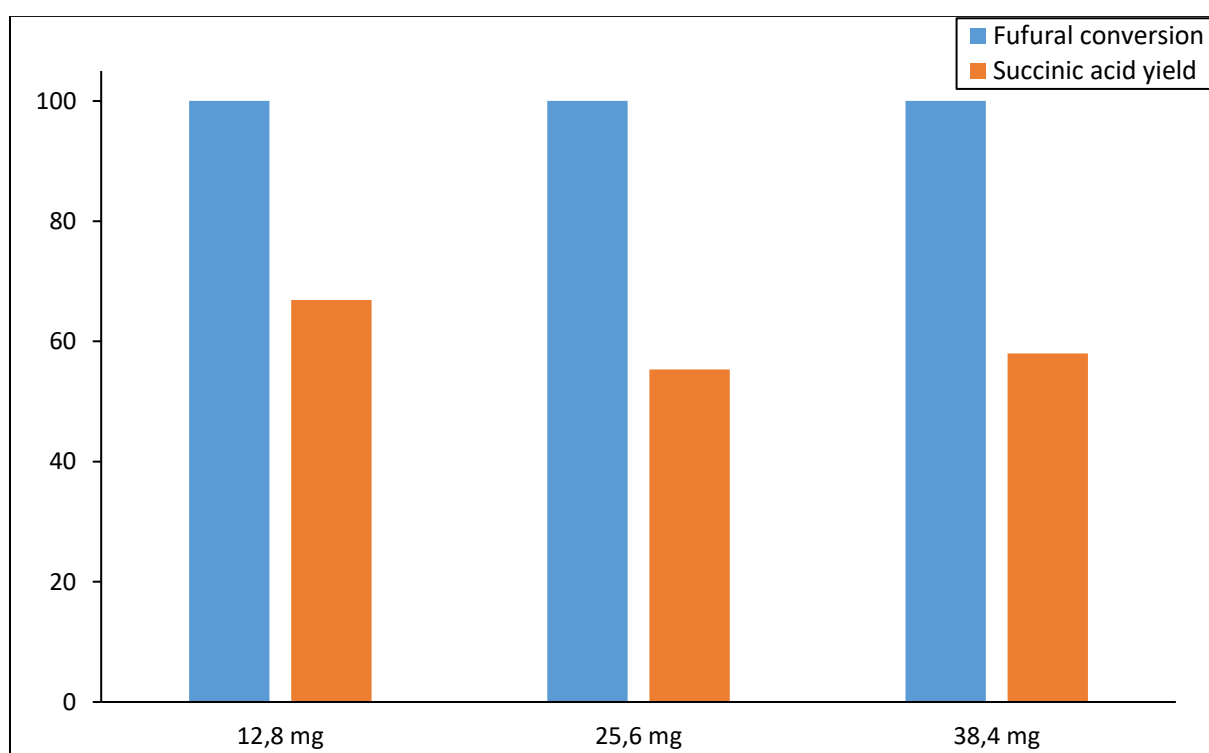


Figure 5.9 - Effect of the catalyst weight on furfural conversion and succinic acid yield; 0.04 mol of furfural, 0.3 mol (20.4 mL) of H_2O_2 , 5.4 mL of H_2O , 40°C, 24 h.

3.6. Catalyst recyclability

For green and sustainable aspects, economical reasons and effective industrial utilizations of heterogeneous catalysts, the lifetime, stability and reusability are important parameters. Hence, the recyclability test of magnetite nanoparticles was investigated on the oxidation of furfural to succinic acid under the optimized experimental conditions.

After the catalytic tests, the catalyst was quantitatively separated from the reaction mixture by employing an external magnetic field, thoroughly washed with water, and reutilized in subsequent

runs under identical reaction conditions. The results indicate that no efficiency loss was observed in furfural oxidation in up to three successive runs (Figure 5.10).

It is also noticed that at 50 °C, we cannot recover all the catalyst quantity introduced in the reaction medium. This is due to the dissolution of a part of magnetite nanoparticles when we heat at 50 °C and after 24 h of reaction time.

Thus, the catalyst recovery is a feature to improve, but it appears that the recovered catalyst is still active and permit to perform the reaction as efficiently. The catalytic properties remain quite stable for at least three runs. Therefore, the catalyst showed a good stability at 40 °C, could be reused without any loss of activity and no obvious dissolution problems were detected.

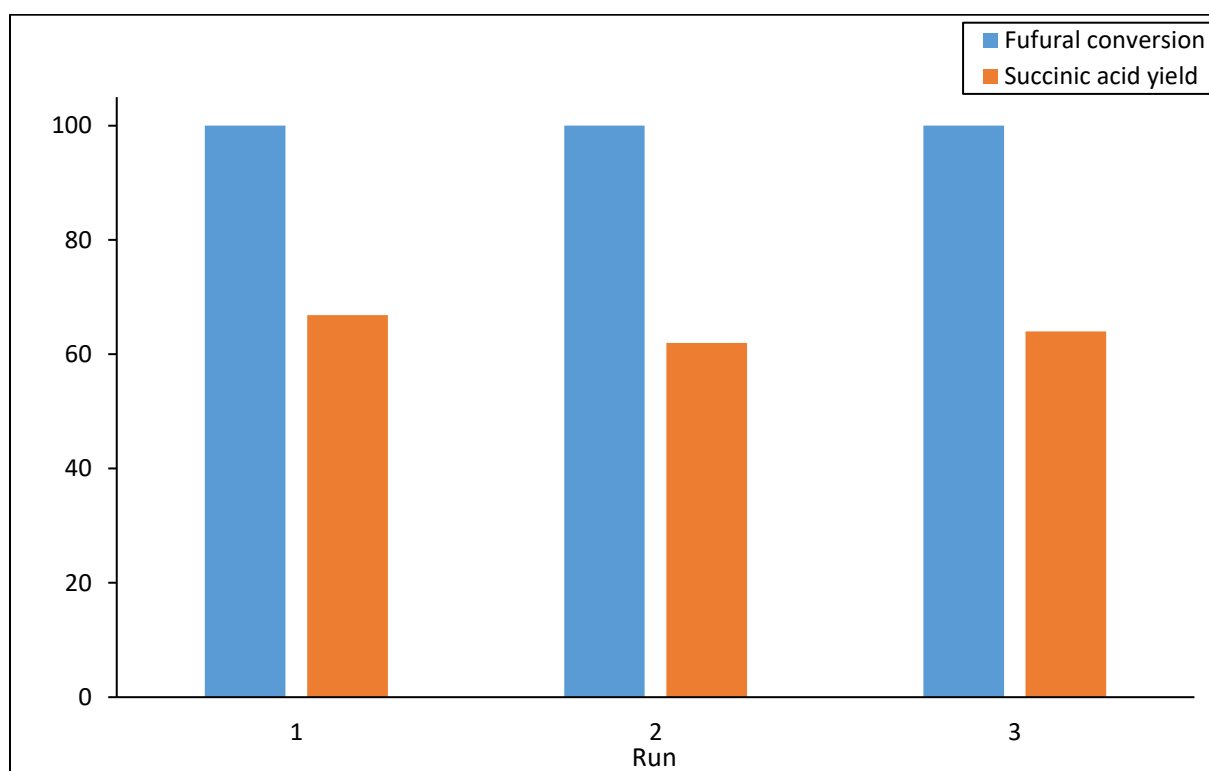


Figure 5.10 - Reusability of MNP catalyst in the oxidation of furfural into succinic acid ; 0.04 mol of furfural, 0.3 mol (20.4 mL) of H_2O_2 , 5.4 mL of H_2O , 80 μmol (0.615 mL) of magnetite nanoparticles, 40 °C, 24 h.

3.7. Magnetite nanoparticles Vs. Iron oxide

To investigate the effect of the particle size, we decided to catalyze the oxidation of furfural using iron oxide instead of magnetite nanoparticles (same molar quantity).

First, we performed a series of reactions in order to figure out the activity of iron oxide at different temperatures, from 30 °C, to 80 °C. Figure 5.11 shows the furfural conversion and the yield of succinic acid in function of time. As shown below, 50 °C is the optimal temperature where we obtained a total

conversion and 57% of succinic acid yield. Furthermore, at higher temperature, furfural conversion and succinic acid yield remain the same.

In addition to succinic acid, other by-products were observed at the end of each reaction. Figure 5.12, shows the yields of maleic acid and malic acid. Moreover, some traces of formic acid, furanone and hydroxyfuranone could be detected as well.

Moreover, we evaluated the influence of time on the reaction, especially on furfural conversion and succinic acid yield. We studied the reaction kinetics at 50 °C since it is the optimal temperature. Figure 5.13 shows that a total conversion of furfural and the highest yield of succinic acid is 57% are obtained after 24 h.

Above 24 h, succinic acid yield remains constant. Strong oxidizing conditions such as high reaction duration lead to the degradation of succinic acid. Besides, the problem of catalyst dissolution when it is heated for longer times. This can explain why there is no production of additional quantities of succinic acid.

Therefore, the best compromise was to work at 50 °C and during 24 h to guarantee a good stability and catalytic activity of iron oxide and to obtain the highest yield of succinic acid in addition to a total conversion of furfural.

By comparing the two catalysts, we can notice that a temperature of at least 50 °C is needed to achieve a total conversion with a succinic acid yield of 57% (Figure 5.11). However, a total conversion of furfural is achieved at 40 °C with higher succinic acid yield (67%) using magnetite nanoparticles.

In addition, when we change the particle size, the distribution of by-products changes as well. For instance, in the case of magnetite nanoparticles, maleic acid is the second major product while when iron oxide is used, the second major product is furanone.

Therefore, when the particle size of the used catalyst is smaller, the oxidation reaction is more efficient and economic since we could achieve total conversion of furfural at lower temperature and in shorter time. Moreover, we obtain higher succinic acid yield. Besides, with nanoparticles, we go forward to the ultimate product with less by-products, which is not the case with iron oxide.

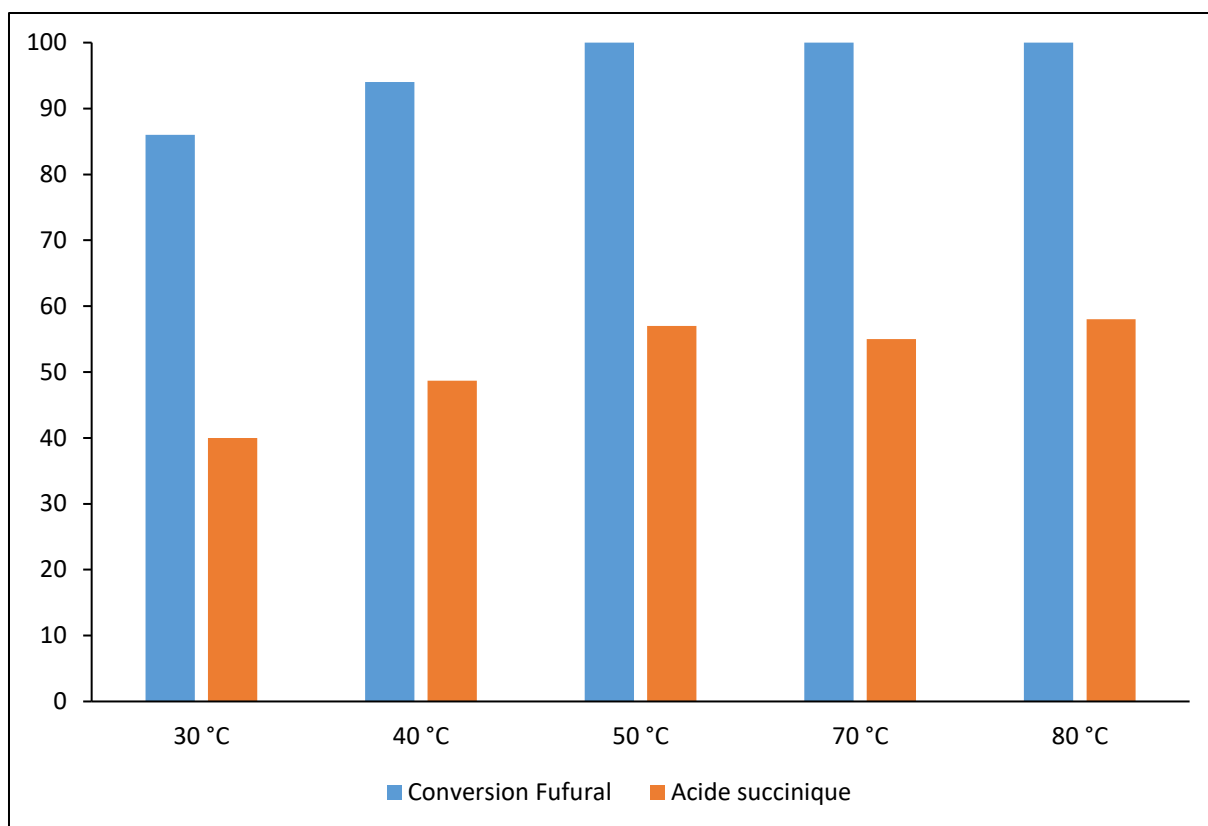


Figure 5.11 - Effect of temperature on furfural conversion and succinic acid yield; 0.04 mol of furfural, 0.3 mol (20.4 mL) of H₂O₂, 5.4 mL of H₂O, 18.5 mg of iron oxide, 24 h.

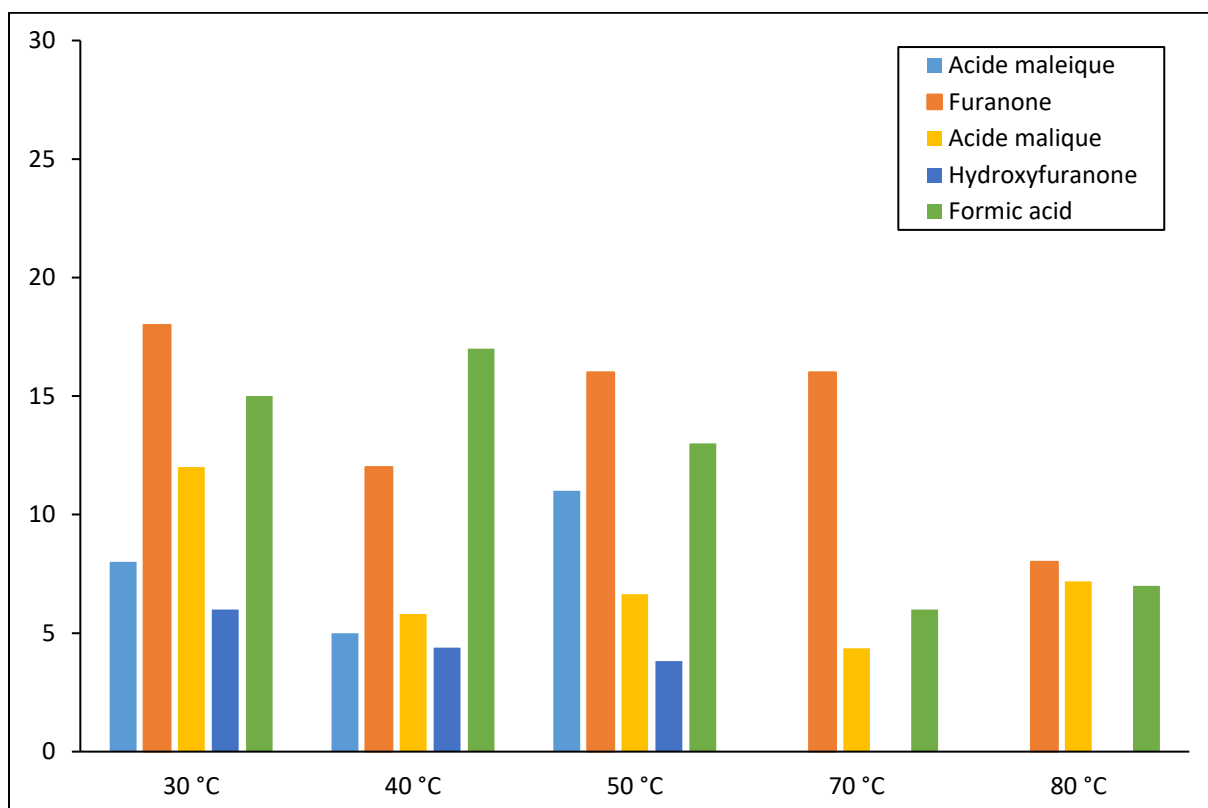


Figure 5.12 - Yields of the obtained by-products; 0.04 mol of furfural, 0.3 mol (20.4 mL) of H₂O₂, 5.4 mL of H₂O, 18.5 mg of iron oxide, 24 h.

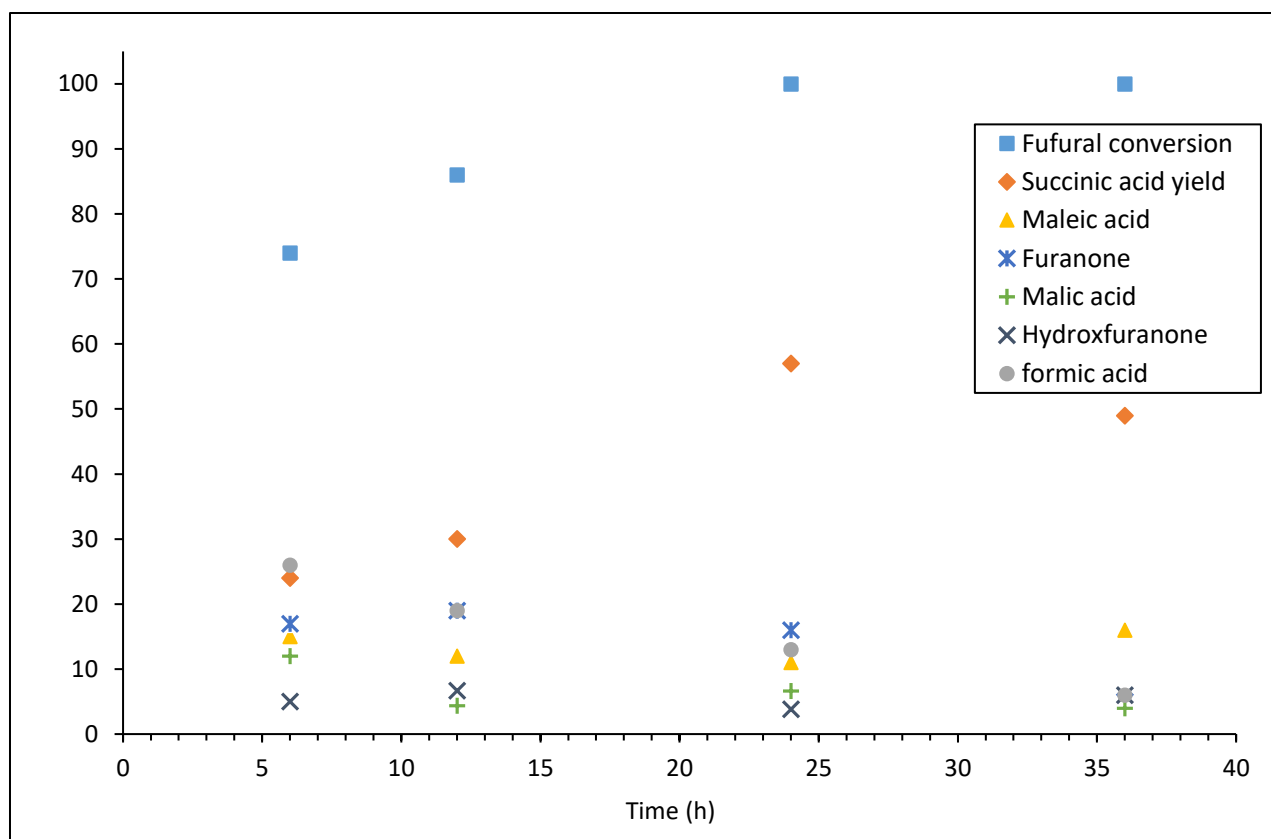


Figure 5.13 - Effect of time on furfural conversion and products' yields; 0.04 mol of furfural, 0.3 mol (20.4 mL) of H_2O_2 , 5.4 mL of H_2O , 18.5 mg of iron oxide, 50 °C.

3.8. Application of ultrasound irradiations

We investigated the effect of ultrasound irradiations on the yield of succinic acid. To do so, we performed this method under the same conditions but in the NextGen Lab 1000 reactor described in chapter 4 at a frequency of 565 kHz.

In the previous chapter, ultrasound irradiations showed a good selectivity towards maleic acid. When we added magnetite nanoparticles, we noticed a competition between two main products, maleic acid and succinic acid. As shown in figure 5.14, the succinic acid yield decreases from 67% to 36% and the maleic acid yield increases from 19% to 42% when we apply high frequency ultrasound irradiations at 565 kHz. Therefore, with the use of US, we lose selectivity and we get back to the initial major product, the maleic acid.

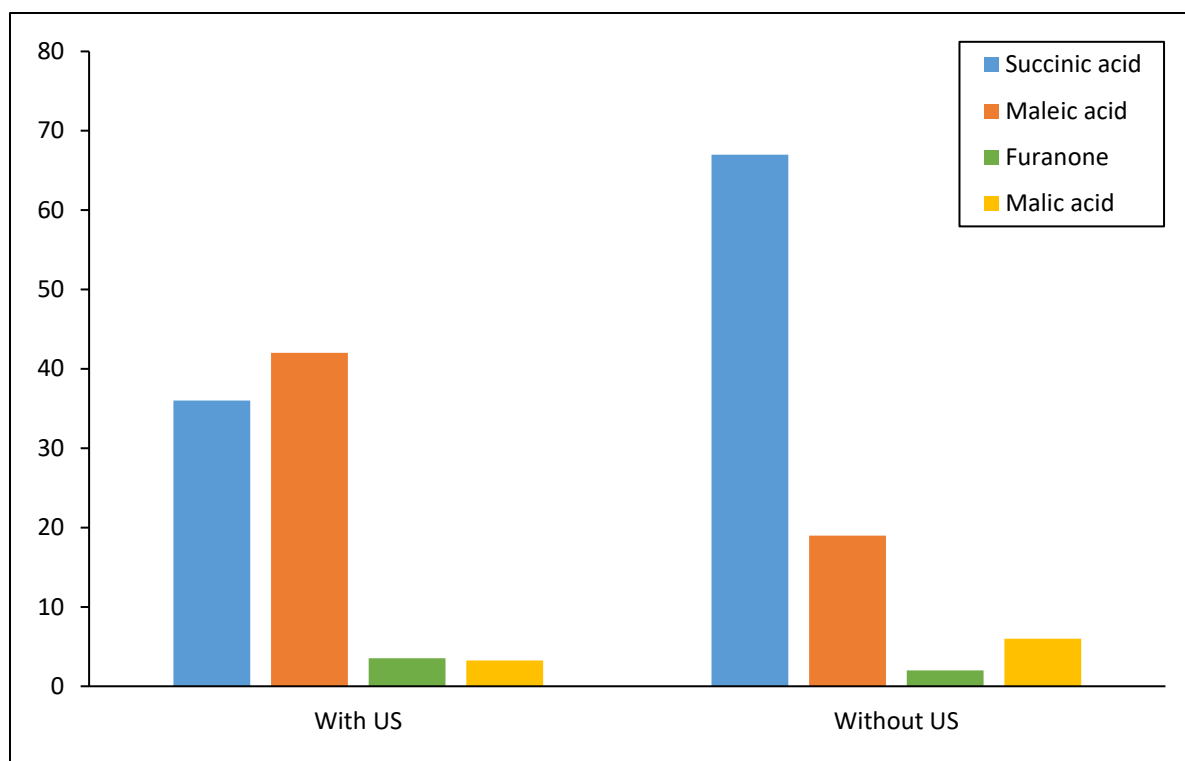


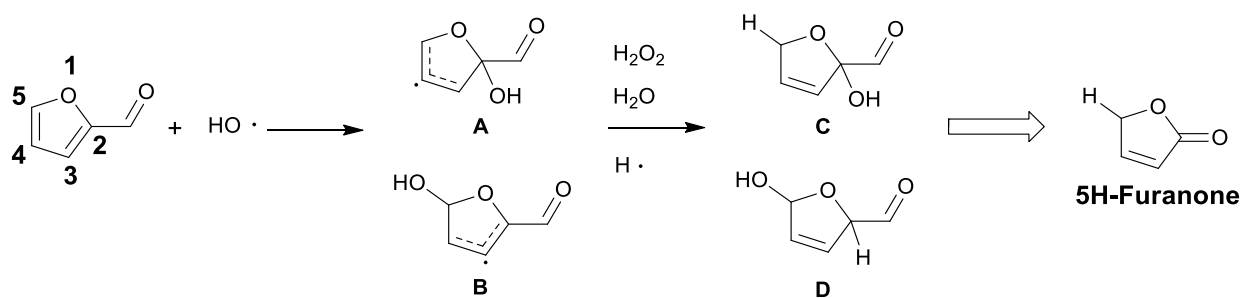
Figure 5.14 - Effect of US irradiations on the yields of different products; 2 h, 40 °C.

3.9. Reaction mechanism

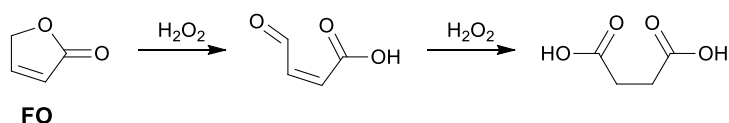
As discussed in chapter 4, the proposed mechanism is divided into two steps: first, a radical mechanism represented by the attack of radicals followed by a non-radical mechanism.

As detailed in the previous chapter, $\text{HO}\bullet$ radicals initiate oxidation by attacking mainly the C2 and C5 positions of furfural leading to the **A** and **B** radicals of scheme 5.2 in equilibrium with the open forms of the furan cycle. Then the radicals **A** and **B** react quickly with the surrounding species, water, hydrogen peroxide, dissolved oxygen or with other radicals. The regioselectivity of this second addition also takes place mainly in position 2 and 5. On the other hand, intermediates **A** and **B** can still capture hydrogen by reacting with the solvent or $\text{H}\bullet$ radicals present, leading to intermediates **C**, **D** and finally 2-(5H)-Furanone. (Scheme 5.2) Many other possibilities of intermediates resulting from regioselective attacks in positions 3 and 4 of furfural are possible, which can lead to the formation of by-products.

In our case, the prolonged reaction time eventually degrades furanone and other intermediates by continuing oxidation. For this reason, we believe that the following oxidation steps follow a non-radical oxidation mechanism. (Scheme 5.3) This is the step corresponding to the oxidation of furanone by hydrogen peroxide. It is well known that FO are good starting compounds for succinic acid formation. In our case, FO is formed in higher concentrations than 5-HFO, which explains the selectivity to succinic acid rather than to maleic acid.



Scheme 5.2 - Proposal for the first step of oxidation of furfural and the structures of potential intermediates leading to 2-(5H)-Furanone



Scheme 5.3 - Proposal reaction pathway leading to succinic acid from 2-(5H)-Furanone via non-radical mechanism

4. Conclusion

We reported in this chapter the catalytic oxidation of furfural into succinic acid. The asset of this method is the use of a metallic catalyst for the SA production. A quick revision of the literature shows that all studies reported the oxidation of furfural in metal-free catalytic conditions. A total conversion of furfural and 67% of succinic acid yield were obtained in 24 h at 40 °C. If we go further in oxidation conditions (time and temperature), succinic acid lightly decreases but without the detection of by-products. We also investigated the effect of particle size on the behavior of the catalytic system. When we use magnetite nanoparticles, the yield of succinic acid increases and the operating conditions are smoother. However, using larger particle size, the yields of by-products are negligible. Moreover, the catalyst showed a good behavior, good stability, recyclability and was easy to be separated. In addition, iron oxides is a non-toxic and cheap catalyst. Furthermore, we saw that under ultrasound irradiation we lose selectivity and we produce maleic acid rather than succinic acid. The reaction pathway and the role of iron ions in furfural- H_2O_2 -iron oxides system has been investigated as well. Therefore, we believe that this simple process is a promising technology in the production of diacids without the generation of toxic wastes.

References

1. Li, F., Bao, J., Zhang, T.C., and Lei, Y. (2015) A combined process of adsorption and Fenton-like oxidation for furfural removal using zero-valent iron residue. *Environ. Technol. (United Kingdom)*, **36** (24), 3103–3111.
2. Raid, Y.A.M., and Omran, R. (2015) Treatment of Furfural Wastewater by (AOPs) Photo-Fenton Method. *J. Eng.*, **21** (3).
3. Yang, C.W., Wang, D., and Tang, Q. (2014) Pretreatment of furfural industrial wastewater by Fenton, electro-Fenton and Fe(II)-activated peroxydisulfate processes: A comparative study. *Water Sci. Technol.*, **70** (3), 414–421.
4. González, C., Pariente, M.I., Molina, R., Masa, M.O., Espina, L.G., Melero, J.A., and Martínez, F. (2021) Study of highly furfural-containing refinery wastewater streams using a conventional homogeneous Fenton process. *J. Environ. Chem. Eng.*, **9** (1).
5. Borghei, S.M., and Hosseini, S.N. (2008) Comparison of furfural degradation by different photooxidation methods. *Chem. Eng. J.*, **139** (3), 482–488.
6. Song, H., and Lee, S.Y. (2006) Production of succinic acid by bacterial fermentation. *Enzyme Microb. Technol.*, **39** (3), 352–361.
7. Zeikus, J.G., Jain, M.K., and Elankovan, P. (1999) Biotechnology of succinic acid production and markets for derived industrial products. *Appl. Microbiol. Biotechnol.*, **51** (5), 545–552.
8. Bogdanov, S.S., Aleksić, B.D., Mitov, I.G., Klisurski, D.G., and Petranović, N.A. (1990) Comparative study of the reduction kinetics of magnetites and derived ammonia synthesis catalysts. *S.S.BogdanovB.D.AleksićI.G.MitovD.G.KlisurskiN.A.Petranović*, **173**, 71–79.
9. Dong, H., Xie, M., Xu, J., Li, M., Peng, L., Guo, X., and Ding, W. (2011) Iron oxide and alumina nanocomposites applied to Fischer-Tropsch synthesis. *Chem. Commun.*, **47** (13), 4019–4021.
10. Zhou, C., Deng, W., Wan, X., Zhang, Q., Yang, Y., and Wang, Y. (2015) Functionalized Carbon Nanotubes for Biomass Conversion: The Base-Free Aerobic Oxidation of 5-Hydroxymethylfurfural to 2,5-Furandicarboxylic Acid over Platinum Supported on a Carbon Nanotube Catalyst. *ChemCatChem*, **7** (18), 2853–2863.
11. Gong, F., Ye, T., Yuan, L., Kan, T., Torimoto, Y., Yamamoto, M., and Li, Q. (2009) Direct reduction of iron oxides based on steam reforming of bio-oil: A highly efficient approach for production of DRI from bio-oil and iron ores. *Green Chem.*, **11** (12), 2001–2012.
12. Matsuoka, K., Shimbori, T., Kuramoto, K., Hatano, H., and Suzuki, Y. (2006) Steam reforming of woody biomass in a fluidized bed of iron oxide-impregnated porous alumina. *Energy and Fuels*, **20** (6), 2727–2731.
13. Datta, P., Rihko-Struckmann, L.K., and Sundmacher, K. (2011) Influence of molybdenum on the stability of iron oxide materials for hydrogen production with cyclic water gas shift process. *Mater. Chem. Phys.*, **129** (3), 1089–1095.
14. Basińska, A., Maniecki, T.P., and Józwiak, W.K. (2006) Catalytic activity in water-gas shift reaction of platinum group metals supported on iron oxides. *React. Kinet. Catal. Lett.*, **89** (2), 319–324.
15. Schüle, A., Shekhah, O., Ranke, W., Schlögl, R., and Kolios, G. (2005) Microkinetic modelling of the dehydrogenation of ethylbenzene to styrene over unpromoted iron oxides. *J. Catal.*, **231** (1), 172–180.

16. Li, Z., and Shanks, B.H. (2011) Role of Cr and v on the stability of potassium-promoted iron oxides used as catalysts in ethylbenzene dehydrogenation. *Appl. Catal. A Gen.*, **405** (1–2), 101–107.
17. Lin, Y., Zhou, S., Sheehan, S.W., and Wang, D. (2011) Nanonet-Based hematite heteronanostructures for efficient solar water splitting. *J. Am. Chem. Soc.*, **133** (8), 2398–2401.
18. Pereira, M.C., Cavalcante, L.C.D., Magalhães, F., Fabris, J.D., Stucki, J.W., Oliveira, L.C.A., and Murad, E. (2011) Composites prepared from natural iron oxides and sucrose: A highly reactive system for the oxidation of organic contaminants in water. *Chem. Eng. J.*, **166** (3), 962–969.
19. Menini, L., Pereira, M.C., Ferreira, A.C., Fabris, J.D., and Gusevskaya, E. V. (2011) Cobalt-iron magnetic composites as heterogeneous catalysts for the aerobic oxidation of thiols under alkali free conditions. *Appl. Catal. A Gen.*, **392** (1–2), 151–157.
20. Menini, L., Pereira, M.C., Parreira, L.A., Fabris, J.D., and Gusevskaya, E. V. (2008) Cobalt- and manganese-substituted ferrites as efficient single-site heterogeneous catalysts for aerobic oxidation of monoterpenic alkenes under solvent-free conditions. *J. Catal.*, **254** (2), 355–364.
21. Botas, J.A., Melero, J.A., Martínez, F., and Pariente, M.I. (2010) Assessment of Fe₂O₃/SiO₂ catalysts for the continuous treatment of phenol aqueous solutions in a fixed bed reactor. *Catal. Today*, **149** (3–4), 334–340.
22. Hu, X., Liu, B., Deng, Y., Chen, H., Luo, S., Sun, C., Yang, P., and Yang, S. (2011) Adsorption and heterogeneous Fenton degradation of 17 α -methyltestosterone on nano Fe₃O₄/MWCNTs in aqueous solution. *Appl. Catal. B Environ.*, **107** (3–4), 274–283.
23. Rodríguez, E.M., Fernández, G., Álvarez, P.M., Hernández, R., and Beltrán, F.J. (2011) Photocatalytic degradation of organics in water in the presence of iron oxides: Effects of pH and light source. *Appl. Catal. B Environ.*, **102** (3–4), 572–583.
24. Sreethawong, T., and Chavadej, S. (2008) Color removal of distillery wastewater by ozonation in the absence and presence of immobilized iron oxide catalyst. *J. Hazard. Mater.*, **155** (3), 486–493.
25. Vicente, F., Rosas, J.M., Santos, A., and Romero, A. (2011) Improvement soil remediation by using stabilizers and chelating agents in a Fenton-like process. *Chem. Eng. J.*, **172** (2–3), 689–697.
26. Silva, A.C., Cepera, R.M., Pereira, M.C., Lima, D.Q., Fabris, J.D., and Oliveira, L.C.A. (2011) Heterogeneous catalyst based on peroxo-niobium complexes immobilized over iron oxide for organic oxidation in water. *Appl. Catal. B Environ.*, **107** (3–4), 237–244.
27. Haber, F., and Weiss, J. (1934) The catalytic decomposition of hydrogen peroxide by iron salts. *Proc. R. Soc. Lond.*, **147**, 332–351.
28. Von Sonntag, C. (2008) Advanced oxidation processes: Mechanistic aspects. *Water Sci. Technol.*, **58** (5), 1015–1021.
29. Fenton, H.J.H. (1894) OXIDATION OF TARTARIC ACID IN PRESEXE OF IRON. *J. Chem. Soc., Trans.*, **65**, 899–910.
30. Jain, B., Singh, A.K., Kim, H., Lichtfouse, E., and Sharma, V.K. (2018) Treatment of organic pollutants by homogeneous and heterogeneous Fenton reaction processes. *Environ. Chem. Lett.*, **16** (3), 947–967.
31. Poerschmann, J., Trommler, U., and Górecki, T. (2010) Aromatic intermediate formation during oxidative degradation of Bisphenol A by homogeneous sub-stoichiometric Fenton reaction.

- Chemosphere*, **79** (10), 975–986.
32. Zhang, S., Sun, M., Hedtke, T., Deshmukh, A., Zhou, X., Weon, S., Elimelech, M., and Kim, J.H. (2020) Mechanism of Heterogeneous Fenton Reaction Kinetics Enhancement under Nanoscale Spatial Confinement. *Environ. Sci. Technol.*, **54** (17), 10868–10875.
 33. Liao, Q., Sun, J., and Gao, L. (2009) Degradation of phenol by heterogeneous Fenton reaction using multi-walled carbon nanotube supported Fe₂O₃ catalysts. *Colloids Surfaces A Physicochem. Eng. Asp.*, **345** (1–3), 95–100.
 34. Ranganath, K.V.S., and Glorius, F. (2011) Superparamagnetic nanoparticles for asymmetric catalysis - A perfect match. *Catal. Sci. Technol.*, **1** (1), 13–22.
 35. Xu, L., Ma, Y., Zhang, Y., Jiang, Z., and Huang, W. (2009) Direct evidence for the interfacial oxidation of CO with hydroxyls catalyzed by Pt/oxide nanocatalysts. *J. Am. Chem. Soc.*, **131** (45), 16366–16367.
 36. Anand, N., Reddy, K.H.P., Satyanarayana, T., Rao, K.S.R., and Burri, D.R. (2012) A magnetically recoverable γ -Fe₂O₃ nanocatalyst for the synthesis of 2-phenylquinazolines under solvent-free conditions. *Catal. Sci. Technol.*, **2** (3), 570–574.
 37. Khoudiakov, M., Gupta, M.C., and Deevi, S. (2005) Au/Fe₂O₃ nanocatalysts for CO oxidation: A comparative study of deposition-precipitation and coprecipitation techniques. *Appl. Catal. A Gen.*, **291** (1–2), 151–161.
 38. Sonavane, S.U., Gawande, M.B., Deshpande, S.S., Venkataraman, A., and Jayaram, R. V. (2007) Chemoselective transfer hydrogenation reactions over nanosized γ -Fe₂O₃ catalyst prepared by novel combustion route. *Catal. Commun.*, **8** (11), 1803–1806.
 39. Acisli, O., Khataee, A., Karaca, S., Karimi, A., and Dogan, E. (2017) Combination of ultrasonic and Fenton processes in the presence of magnetite nanostructures prepared by high energy planetary ball mill. *Ultrason. Sonochem.*, **34**, 754–762.
 40. Jung, H., Kim, J.W., Choi, H., Lee, J.H., and Hur, H.G. (2008) Synthesis of nanosized biogenic magnetite and comparison of its catalytic activity in ozonation. *Appl. Catal. B Environ.*, **83** (3–4), 208–213.
 41. Mascolo, M.C., Pei, Y., and Ring, T.A. (2013) Room Temperature Co-Precipitation Synthesis of Magnetite Nanoparticles in a Large pH Window with Different Bases. *Materials (Basel)*, **6** (12), 5549–5567.
 42. MASSART, R., and CABUIL, V. (1987) Synthèse en milieu alcalin de magnetite colloïdale: contrôle du rendement et de la taille des particules. *J. Chim. Phys.*, **84**, 7–8.
 43. Kul'nevich, V.G., and Badovskaya, L.A. (1975) Reactions of Oxo-derivatives of Furan with Hydrogen Peroxide and Peroxy-acids. *Russ. Chem. Rev.*, **44** (7), 574–587.
 44. Badovskaya, L.A., Latashko, V.M., Poskonin, V. V., Grunskaya, E.P., Tyukhteneva, Z.I., Rudakova, S.G., Pestunova, S.A., and Sarkisyan, A. V. (2002) Reactions of catalytic oxidation of furan and hydrofuran compounds. 7. Preparation of 2(5H)-furanone by oxidation of furfural with hydrogen peroxide and some its conversions in aqueous solutions. *Chem. Heterocycl. Compd.*, **38** (9), 1194–1203.
 45. H. Hodgson, H., and Davies, R.R. (1939) Preparation of 2- and 3-Hydroxyfuran. *R. Ronald*, 806–809.

General conclusion and perspectives

The aim of this PhD project was to explore novel and green methods for the conversion of furfural and 2,5-hydroxymethylfurfural to produce high value-added bio-sourced products such as, diformylfuran, maleic acid and succinic acid.

Catalysis is one of the fundamental pillars of green and sustainable chemistry, however, most of the time; catalysts are neither green nor sustainable due to many reasons. Therefore, we tried to focus on the main catalysis problem in the oxidation of furanic derivatives and we suggested catalytic processes, enhanced and optimized, with good selectivity while maintaining eco-friendly as much as possible.

First, numerous catalytic conversions of furfural and HMF are catalysed by noble or heavy metals such as, Au, Pd and Pt. In addition, those methods suffer from toxicity, recyclability and deactivation problems of catalysts and most of the time using complex protocols for their synthesis.

In the notion of metal catalysis for the catalytic oxidation of furfural, we suggested a novel method using magnetite nanoparticles as the catalyst. MNP are, first, simple to synthesize, and iron is considered as a cheap and non-toxic metal. Moreover, this catalyst showed a good stability and was easy to be separated and recycled. In addition, we lied on Fenton-reaction principle since the main interaction was between Fe cations and H_2O_2 , used as primary oxidant. In terms of numbers, we achieved total conversion of furfural with 67% of succinic acid yield under mild conditions. Interestingly, the particle size had an effect on the selectivity. When we use magnetite nanoparticles, the yield of succinic acid increases and the operating conditions are smoother (lower temperature and shorter time for total conversion). However, using larger particle size, the yields of by-products become negligible. Moreover, we saw that under ultrasonic irradiations, we lose selectivity and we produce maleic acid rather than succinic acid. The reaction pathway and the role of iron ions in furfural- H_2O_2 -iron oxides system has been investigated as well.

Dematerializing catalysts, in using less noble and expensive materials to afford the same or better level of functionality, has become a serious challenge for researchers and engineers. Moreover, numerous metals and metalloids such as platinum metals, cesium, chromium, aluminum, cobalt, titanium and many others have been listed as critical minerals. Despite all the valuable properties of metallic catalysts, their high cost, deactivation and leakage problems and toxicity remain an important drawback. In this context, the best solution for the future industry of catalysts is to replace when possible metal catalysts by “metal-free” catalysts. This could establish a new concept or class of catalysis where metals are completely absent.

For this purpose, we developed a metal-free oxidation of 2,5-hydroxymethylfurfural using an organic catalyst, the 2-iodobenzenesulfonic acid. Furthermore, this catalyst is simple to be synthesized, non-toxic and cheap. We demonstrated the possibility of using hypervalent iodine derivatives of this catalyst in the presence of Oxone[®], as an economical and non-toxic oxidant with non-toxic by-products, to carry out the oxidation of HMF to DFF with great selectivity and yield.

The method is particularly simple, because only filtration or extraction of the sulfate salts and the catalyst at the end of the reaction are required to obtain the DFF with a high grade of purity. We optimized the reaction conditions by considering the product stability and competitive reactions. The best compromise was obtained for a 4 hours of reaction at 70 °C, using nitromethane as solvent. In these conditions, 89% of DFF is obtained as the only product after a simple filtration and evaporation. In addition, very good results are also observed over much shorter times, in 30 min at 90 °C, where 80% of DFF is obtained. On the contrary to what was described in literature this method involves no metallic catalyst, uses reasonable concentration of HMF, and we have demonstrated the possibility of extending the method to a gram-scale production of DFF. Therefore, we believe that these results lay the foundation for the development of a larger scale process.

In the same context of dematerializing catalysts, we reported the catalytic-free oxidation of furfural into MA using high frequency ultra-sonic waves in the H₂O₂ liquid oxidant in an acid- and catalyst free medium. This method shows a high selectivity of 70% towards MA with 92% of furfural conversion. SA can also be obtained with 50% selectivity when one equivalent of hydrogen peroxide was used but with 50% furfural conversion. We optimized the reaction conditions and the effect of various operating parameters such as furfural concentration, frequency, power and time were systematically studied in details. The best compromise was obtained for 2 h of reaction, 4 H₂O₂ to furfural mol ratio, 565 kHz and 80 W.

This work shows that high-frequency ultrasound is very effective in activating hydrogen peroxide without a catalyst, which is a major advantage for the development of oxidation processes such as furfural towards the production of MA. This process combines many advantages: the solvent is water, the method is catalyst-free, under mild conditions, the temperature is low 42 °C, the transformation time is short and the molar ratio H₂O₂/Fur is close to stoichiometry. In addition, the mass percentage of raw material is very high 20 wt% making this method appropriate for gram-scale production of MA (up to 9 g) and lay the foundation for the development of a larger scale process. Moreover, it improves energy efficiency by consuming the lowest amount of energy (134 kJ) to produce one gram of MA from furfural

comparing to any other method in the literature. Therefore, we believe that this simple, green and energy-efficient process is a promising and transformative technology in chemical industries.

The results obtained in this work pave the way for further improvements. First improvement can be done is the oxidant. Many other oxidants can be attempted instead of hydrogen peroxide such as oxygen, air bleach and percarbonate/persulfate with many organic catalysts as well. Hence, a screening of oxidants can be carried out in the aim of enhancing the yield and the selectivity of reactions.

In addition, other furanic derivatives could be exploited and investigated such as furoic acid that has been used many times to synthesize bio-based dimers [1]. Moreover, 5-chloromethylfurfural (CMF) is an appealing alternative to HMF, due to its higher stability, lower polarity and higher accessibility from glucose and cellulose [2,3]. Thus, it seems to be interesting to attempt the CMF oxidation into DFF using oxone® or transform it into other furan derivatives by inserting nitrogen.

Furthermore, since the high-frequency ultrasound irradiations showed an interesting behavior in the oxidation of furfural, it would be appealing to use this technique for the oxidation of HMF and other furanic derivatives as well. Additionally, it would be interesting to try ultra-high frequency ultra-sound irradiations (> 800 kHz).

In the same point, continuous processing is a future goal for the industry, hence, the oxidation of furanic derivatives under HFUS irradiations should be exploited in continuous flow. This transition from batch to continuous allows to, continuously, obtain higher quantities of products of interest, reduce waste and environmental impact and improve the ability to meet market demands.

From the kinetic point of view, we could use spin labels in order to make sure that we have a radical mechanism. In addition, a kinetic study will be a plus since it will provide evidence for the mechanism of each chemical process.

From eco-compatibility perspective, if we should look to the catalytic systems through their environmental impact, so in-depth study with the life-cycle analysis of the different catalysts and processes would be highly important. Nevertheless, we can recall and still propose the following. Whatever the catalytic system, in all cases the energy consumption associated with the transformation processes induces pollution. The most economical methods are preferred. Hence, it should be possible to determine the amount of energy consumed per unit of material obtained, for example, how many KJ we consumed to prepare one kg or mol from a product. This data should include the energy associated with the shaping and processing of the catalytic system. Researchers need to develop and disseminate tools that give them access to this information in order to be able to compare the catalytic systems they develop while not focusing solely on selectivity and yield criteria.

Continued efforts in metal catalysis should focus on substituting rare metals by more abundant and least toxic metals, or using metals from recycling to limit extraction.

In non-metallic catalysis, it is necessary to continue the efforts of substitution of fossil or chlorinated solvents, and continue to exploit the biphasic systems having the advantage of naturally separating the products according to their affinity for the different phases. Promote simple or heterogeneous catalytic systems facilitating separation by filtration as is the case in supported acid catalysis. For example, although this has already been partially explored we could recommend the development of heterogeneous catalytic systems with TEMPO derivatives supported with an adapted co-oxidant. [4–6]

Finally, from the point of view of keeping a balance between green chemistry and commercial economics, there are many fundamental questions remaining, which must be answered by catalysis and material scientists: how to reduce the high cost of processing? How to fix the defects in catalytic systems? How to achieve intensification processes? How can metal-free catalyst be produced in more sustainable and safer ways? How can they be scaled-up to ultimately find commercial and industrial applications? To what extent can they respect environmental and health measures? Answering such questions will require new perception in sustainable and green chemistry in order to overcome the challenges mainly synthesis and recycling problems.

For industrial applications, the main issue is to optimize reaction operating conditions for the production in large-scale with high product yield and purity, at low costs, improve the existing technologies and find new applications.

1. Cho, J.-K.; Kim, S.-Y.; Lee, D.-H.; Kim, B.; Kim, B.-J.; Jung, J.-W.; Lee, J.-S.F. (2011) Furan-based curable compound derived from biomass, solvent-free curable composition, and method for preparing same. issued 2011.
2. Mascal, M. (2015) 5-(Chloromethyl)furfural is the New HMF: Functionally Equivalent but More Practical in Terms of its Production from Biomass. *ChemSusChem*, **8** (20), 3391–3395.
3. Mascal, M., and Nikitin, E.B. (2008) Direct, high-yield conversion of cellulose into biofuel. *Angew. Chemie - Int. Ed.*, **47** (41), 7924–7926.
4. Mittal, N., Nisola, G.M., Seo, J.G., Lee, S.P., and Chung, W.J. (2015) Organic radical functionalized SBA-15 as a heterogeneous catalyst for facile oxidation of 5-hydroxymethylfurfural to 2,5-diformylfuran. *J. Mol. Catal. A Chem.*, **404–405**, 106–114.
5. Krystof, M., Pérez-Sánchez, M., and De María, P.D. (2013) Lipase-mediated selective oxidation of furfural and 5-hydroxymethylfurfural. *ChemSusChem*, **6** (5), 826–830.
6. Karimi, B., Vahdati, S., and Vali, H. (2016) Synergistic catalysis within TEMPO-functionalized periodic mesoporous organosilica with bridge imidazolium groups in the aerobic oxidation of alcohols. *RSC Adv.*, **6** (68), 63717–63723.

Accomplishments

Publications

- N. Ayoub, C. Bergère J. Toufaily, E. Guénin, G. Enderlin, A gram scale selective oxidation of 5-hydroxymethylfurfural to diformylfuran in the presence of oxone and catalyzed by 2-iodobenzenesulfonic acid, *New J. Chem.*, 2020, 44, 11577-11583
- N. Ayoub, J. Toufaily, E. Guénin, G. Enderlin, Metal vs. Metal-Free Catalysts for Oxidation of 5-Hydroxymethylfurfural and Levoglucosenone to Biosourced Chemicals, *ChemSusChem* 2022, e202102606.

Submitted

- N. Ayoub, J. Toufaily, E. Guénin, G. Enderlin, Catalyst-free process for oxidation of furfural to maleic acid by high frequency ultrasonic activation. (Submitted to *Green Chemistry* journal)

Oral communication

- N. Ayoub, J. Toufaily, E. Guénin, G. Enderlin, Metal-free catalysis for gram-scale oxidations of bio-sourced furan derivatives, 5th EuChemS Conference on Green and Sustainable Chemistry, 26 – 29 September 2021, Thessaloniki, Greece.

Annexes

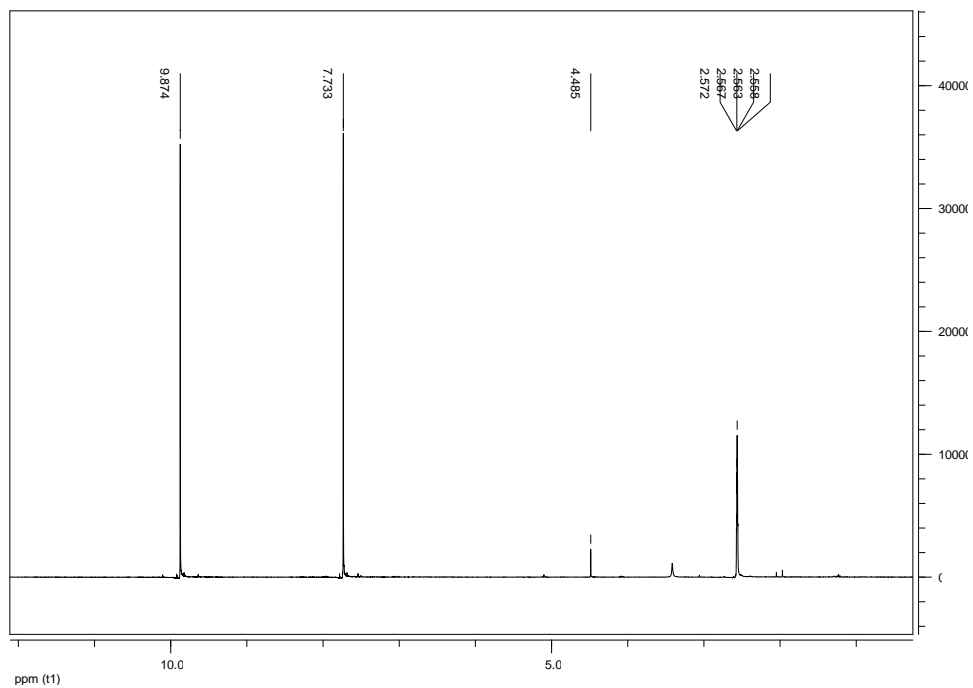
HMF oxidation into DFF

Figure A.1 - 1H spectrum of DFF after filtration and evaporation (DMSO-d6), (4.485 ppm corresponds to nitromethane traces)

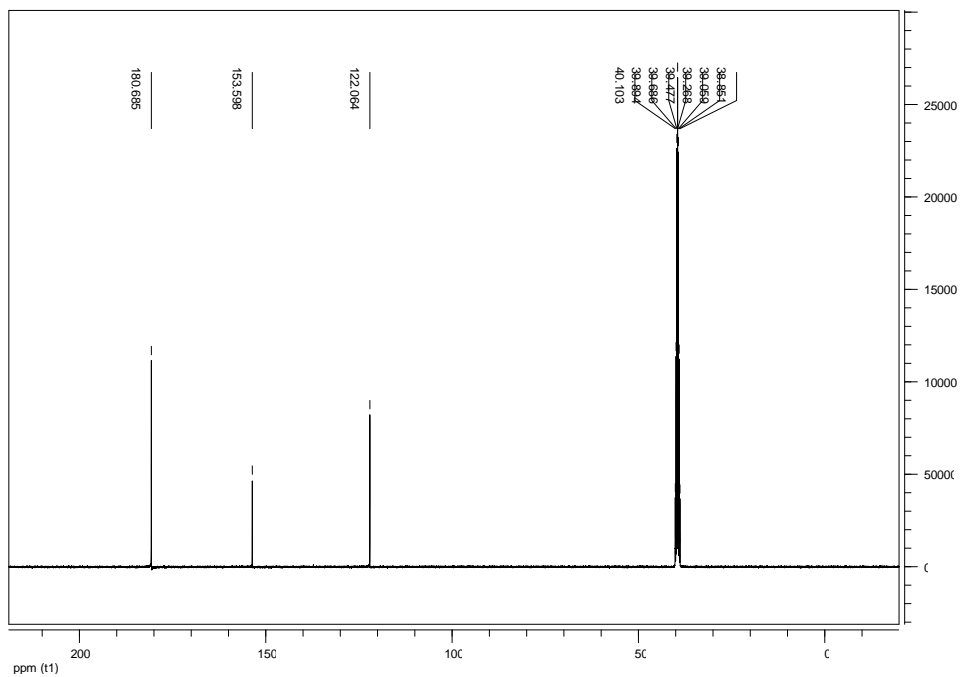


Figure A.2 - 13C spectrum of DFF after filtration and evaporation (DMSO-d6)

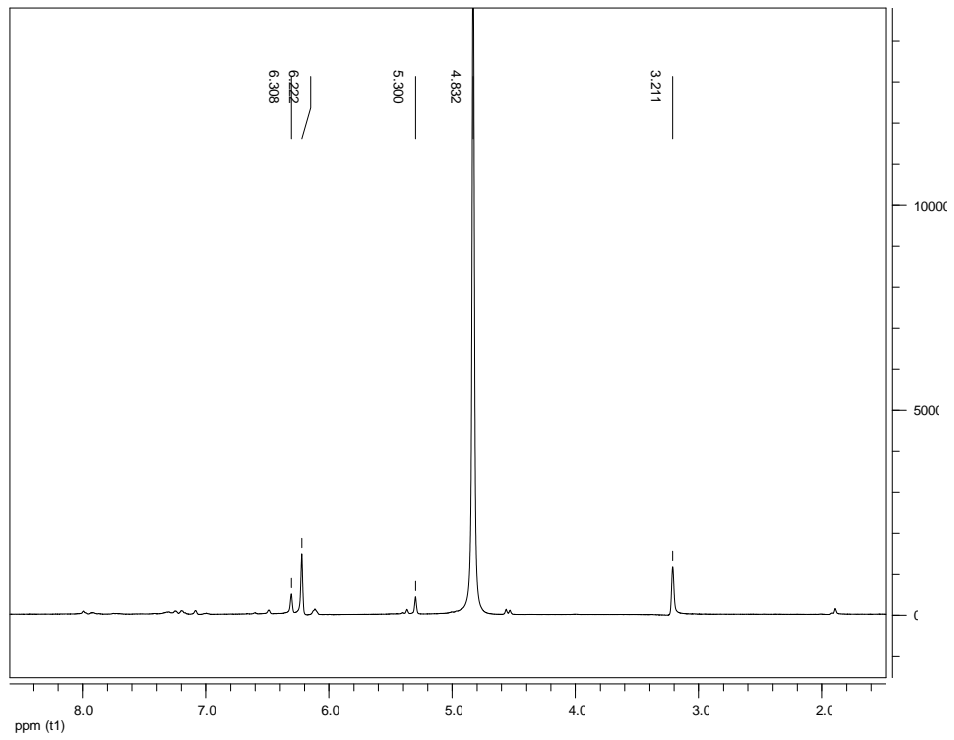


Figure A.3 -1H spectrum of over-oxidation of HMF (CDCl₃)

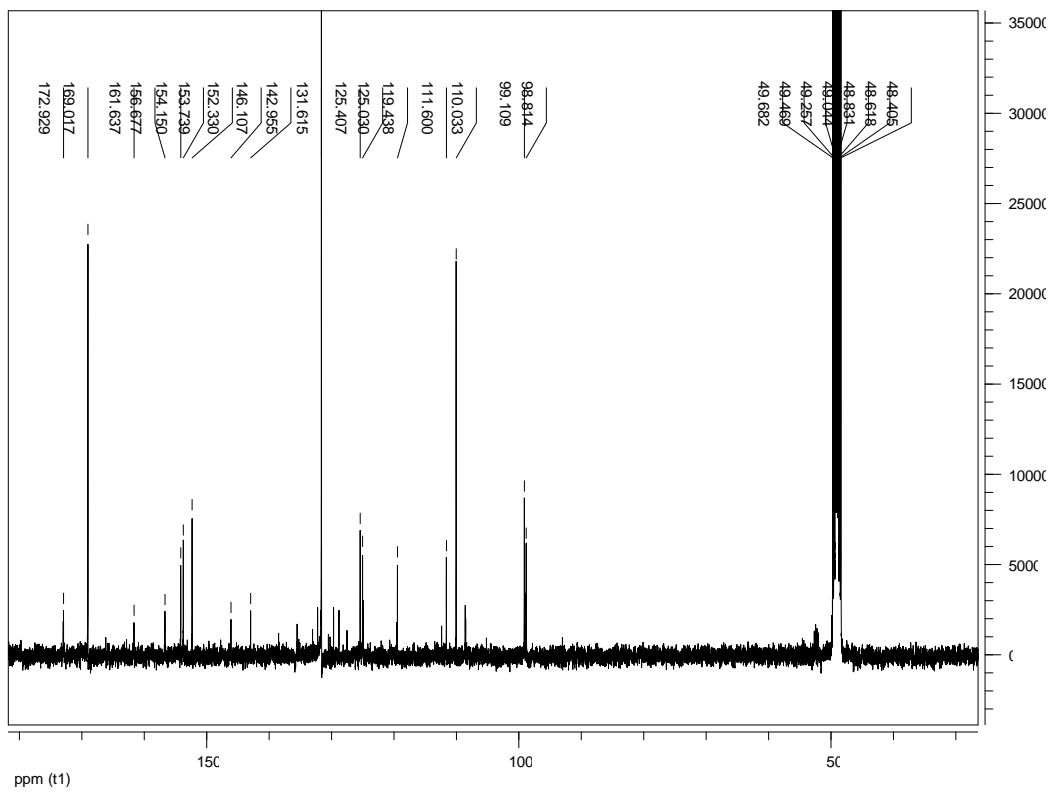
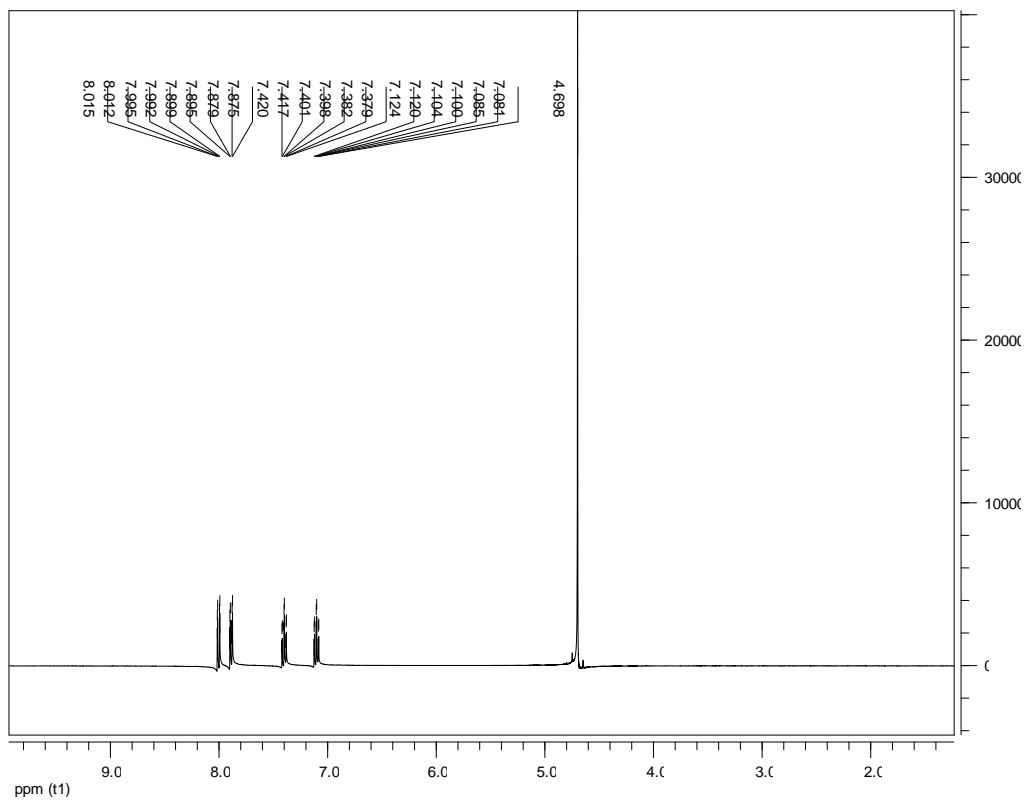
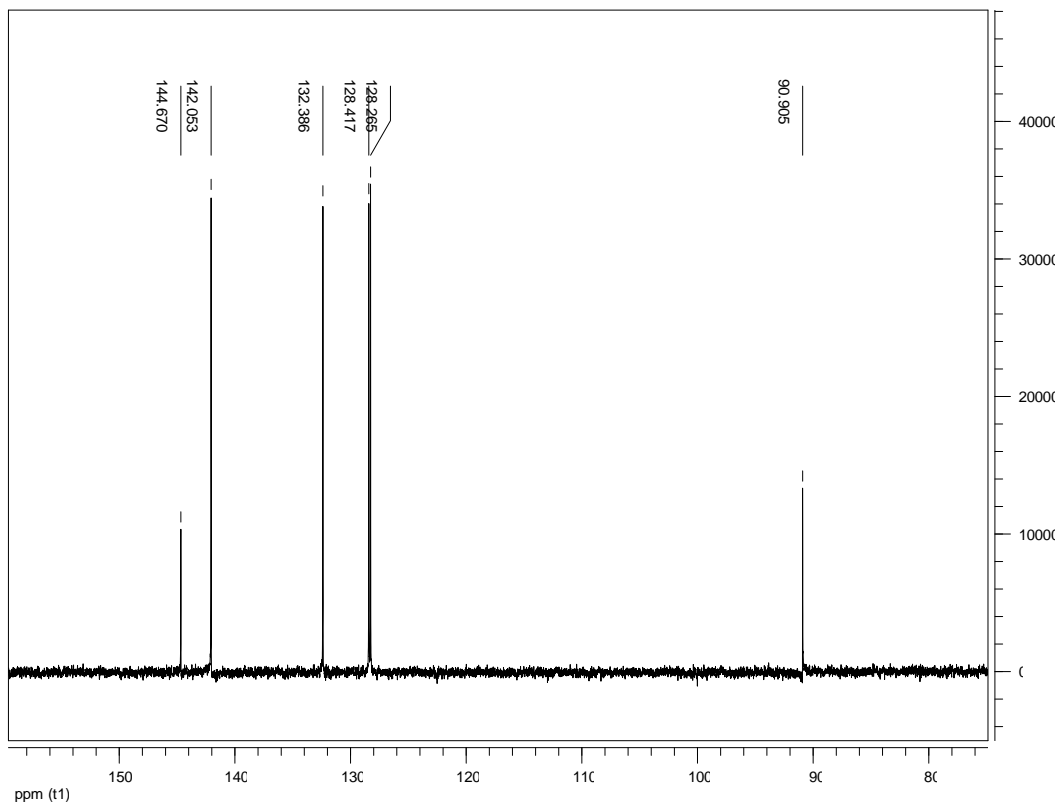


Figure A.4 -13C spectrum of over-oxidation of HMF (CDCl₃)

Figure A.5 - ^1H spectrum of IBS catalyst (CDCl_3)Figure A.6 - ^{13}C spectrum of IBS catalyst (CDCl_3)

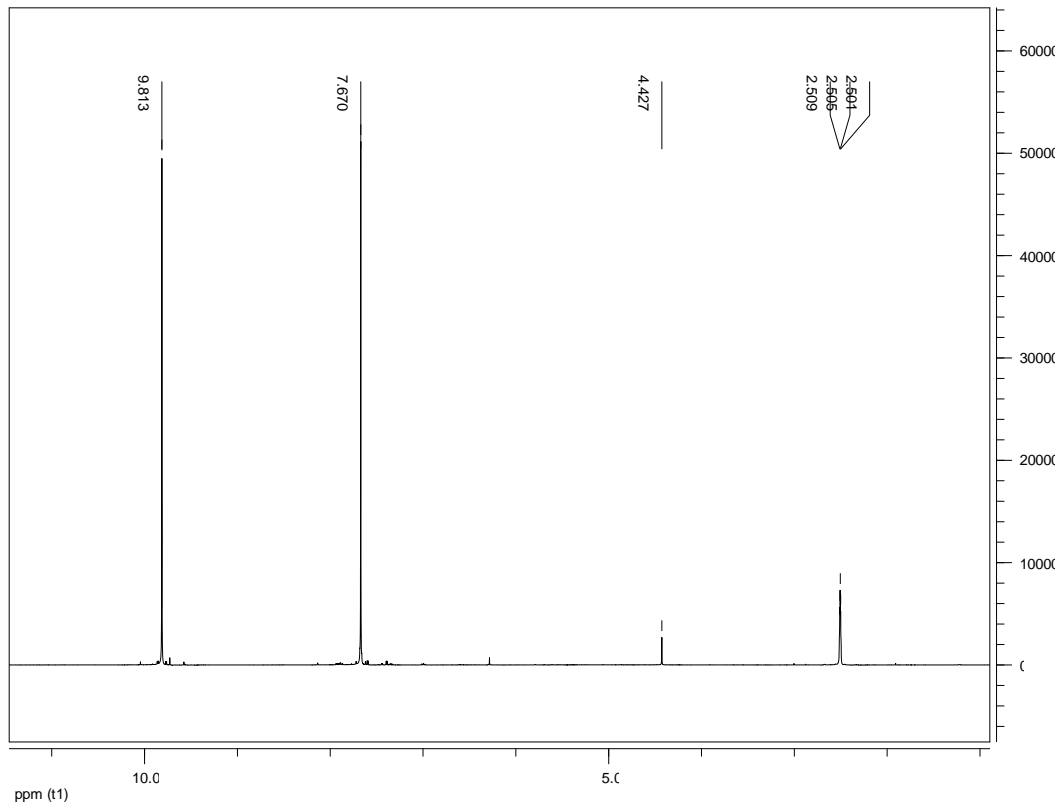


Figure A.7 - 1H spectrum of the gram scale of HMF oxidation (CDCl₃)

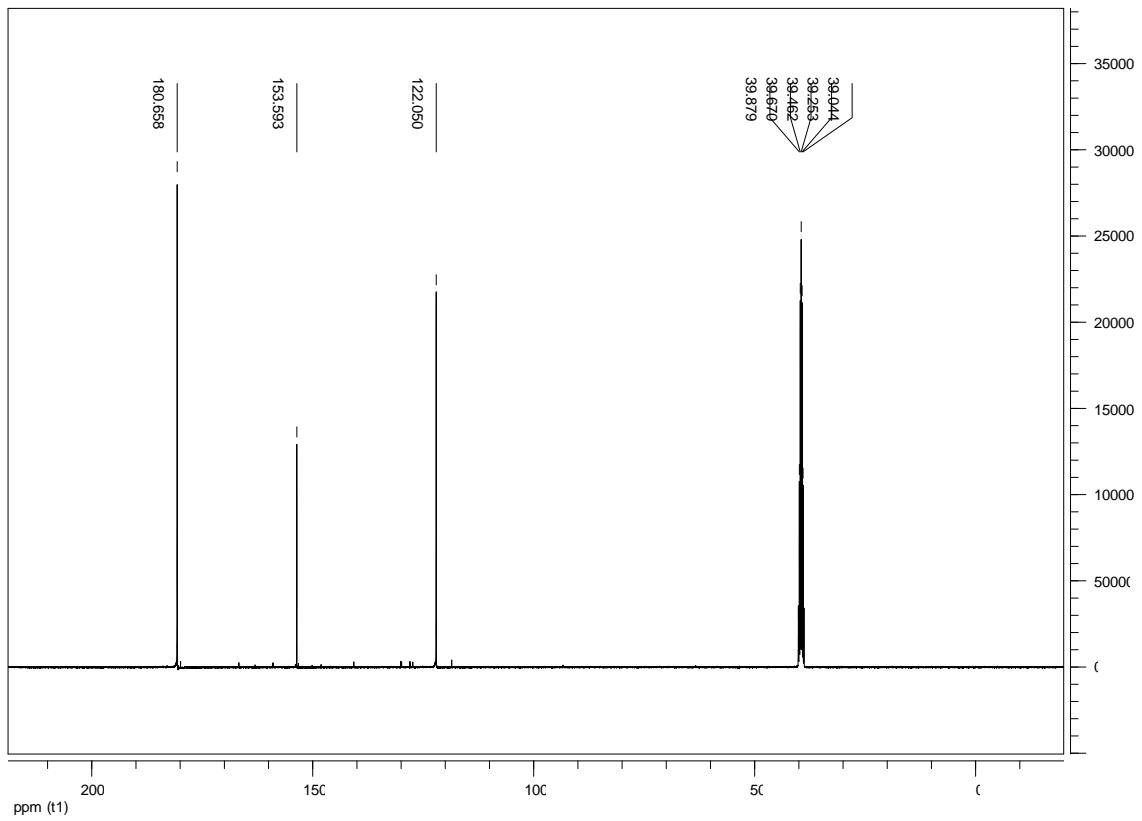


Figure A.8 - 13C spectrum of the gram scale of HMF oxidation (CDCl₃)

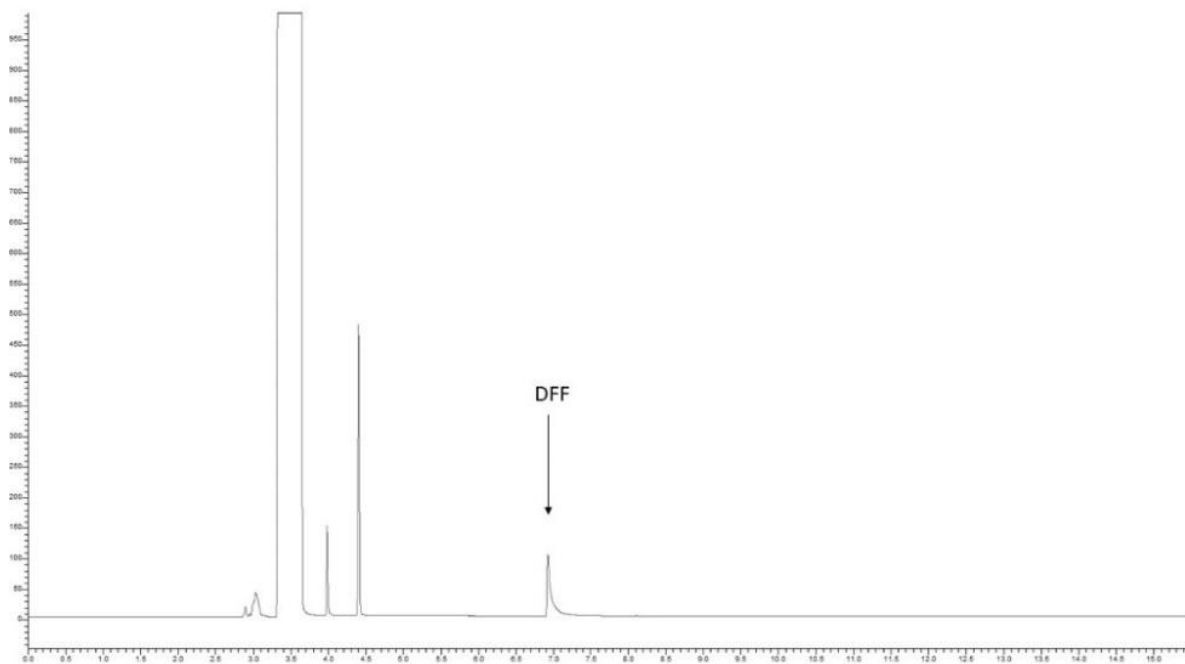


Figure A.9 - Chromatogram of DFF after filtration and evaporation

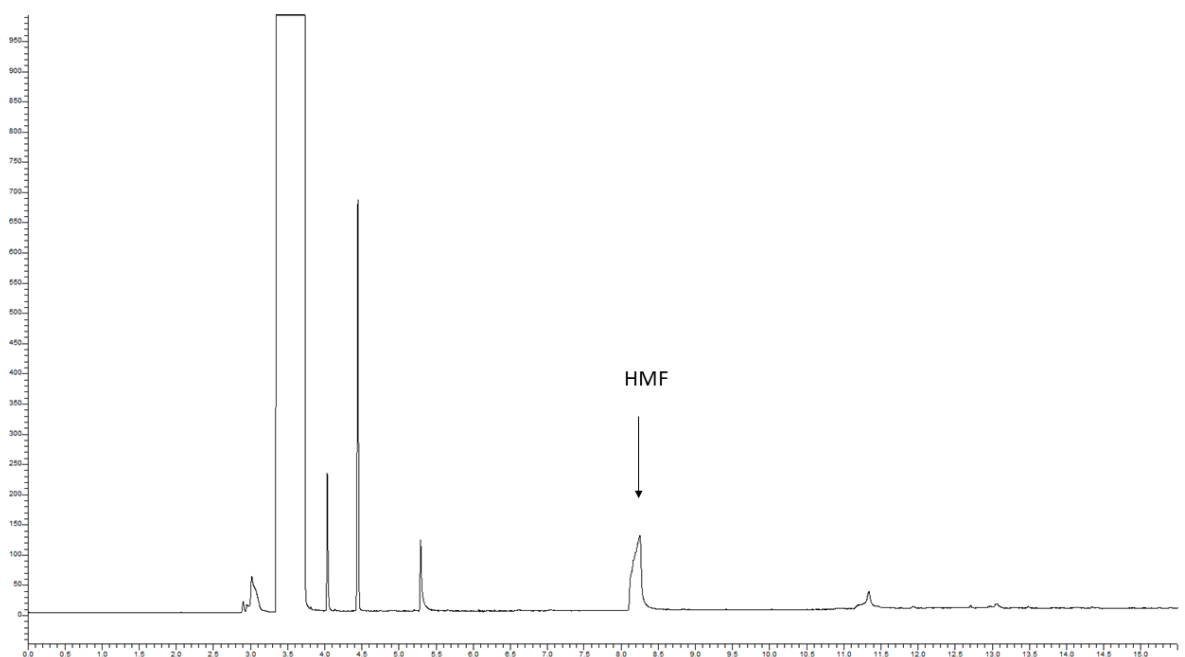


Figure A.10 - chromatogram of HMF oxidation without catalyst

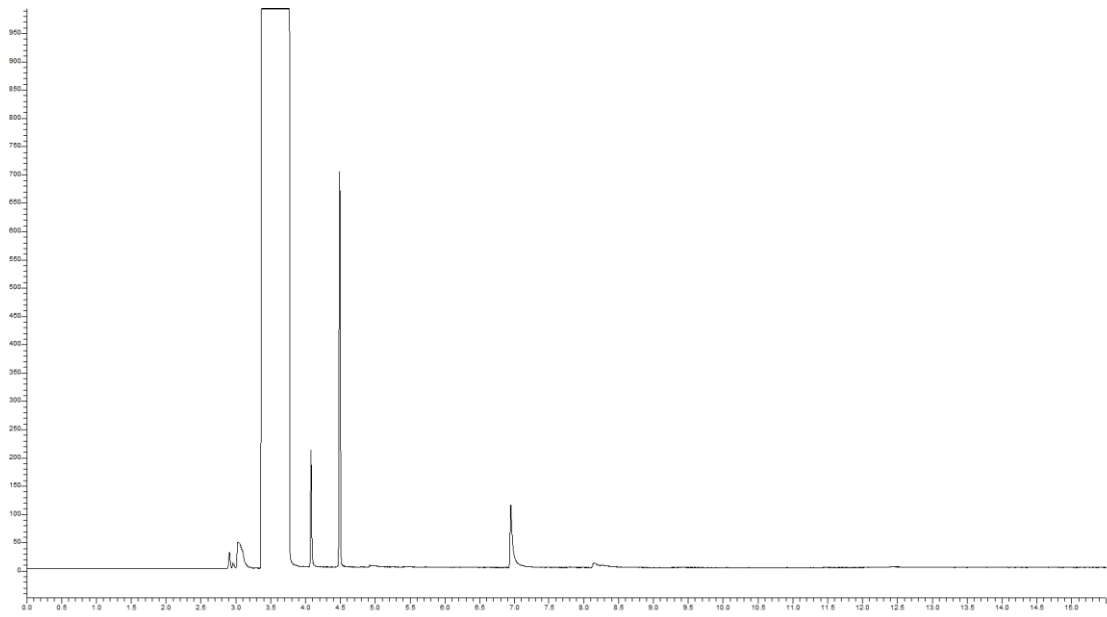


Figure A.11 - chromatogram of HMF oxidation without solvent

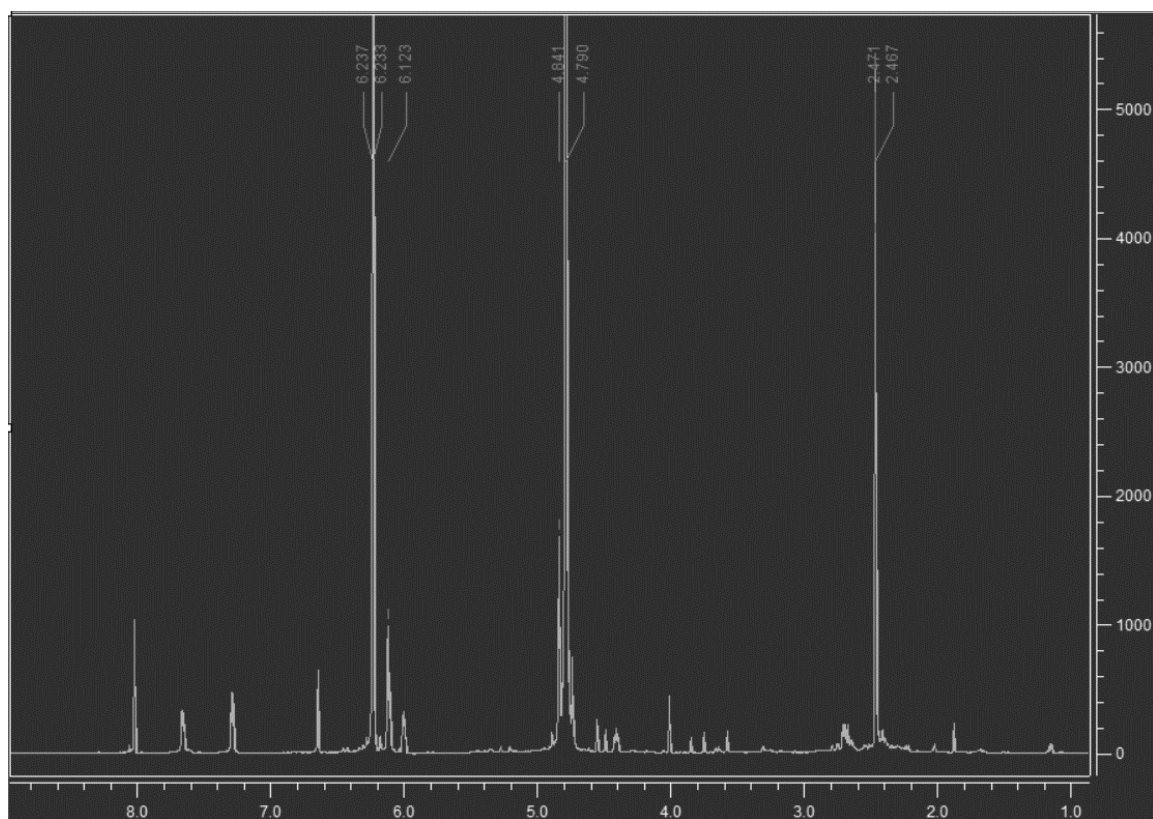
Furfural oxidation using HFUS

Figure A.12 - 1H spectrum; Furfural 10 mL (0.12 mol), H₂O₂ 40 mL (1.7 mol), 42 °C, 2 h, 565 kHz, 80 W (D₂O)

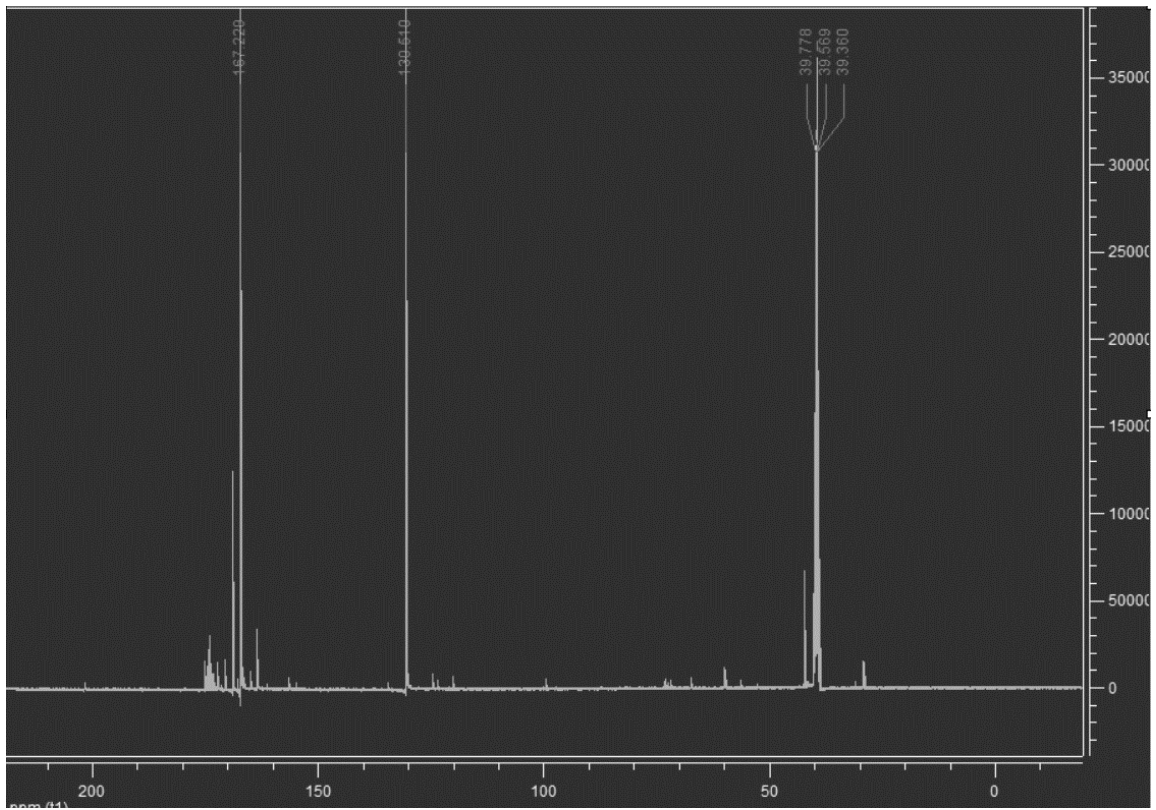


Figure A.13 - ¹³C spectrum; Furfural 10 mL (0.12 mol), H₂O₂ 40 mL (1.7 mol), 42 °C, 2 h, 565 kHz, 80 W (D₂O)

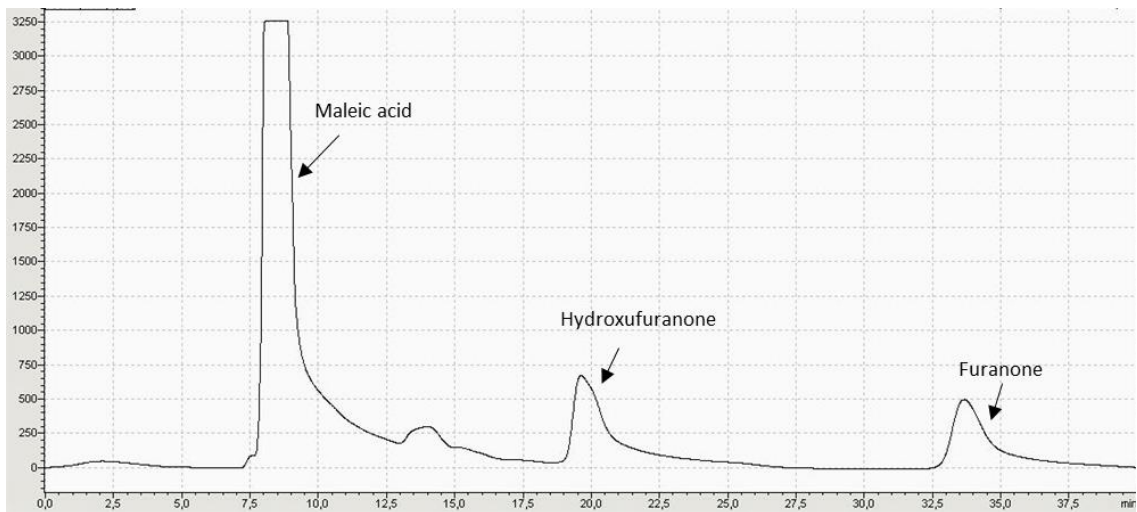


Figure A.14 - HPLC chromatogram; Furfural 10 mL (0.12 mol), H₂O₂ 40 mL (1.7 mol), 42 °C, 2 h, 565 kHz, 80 W

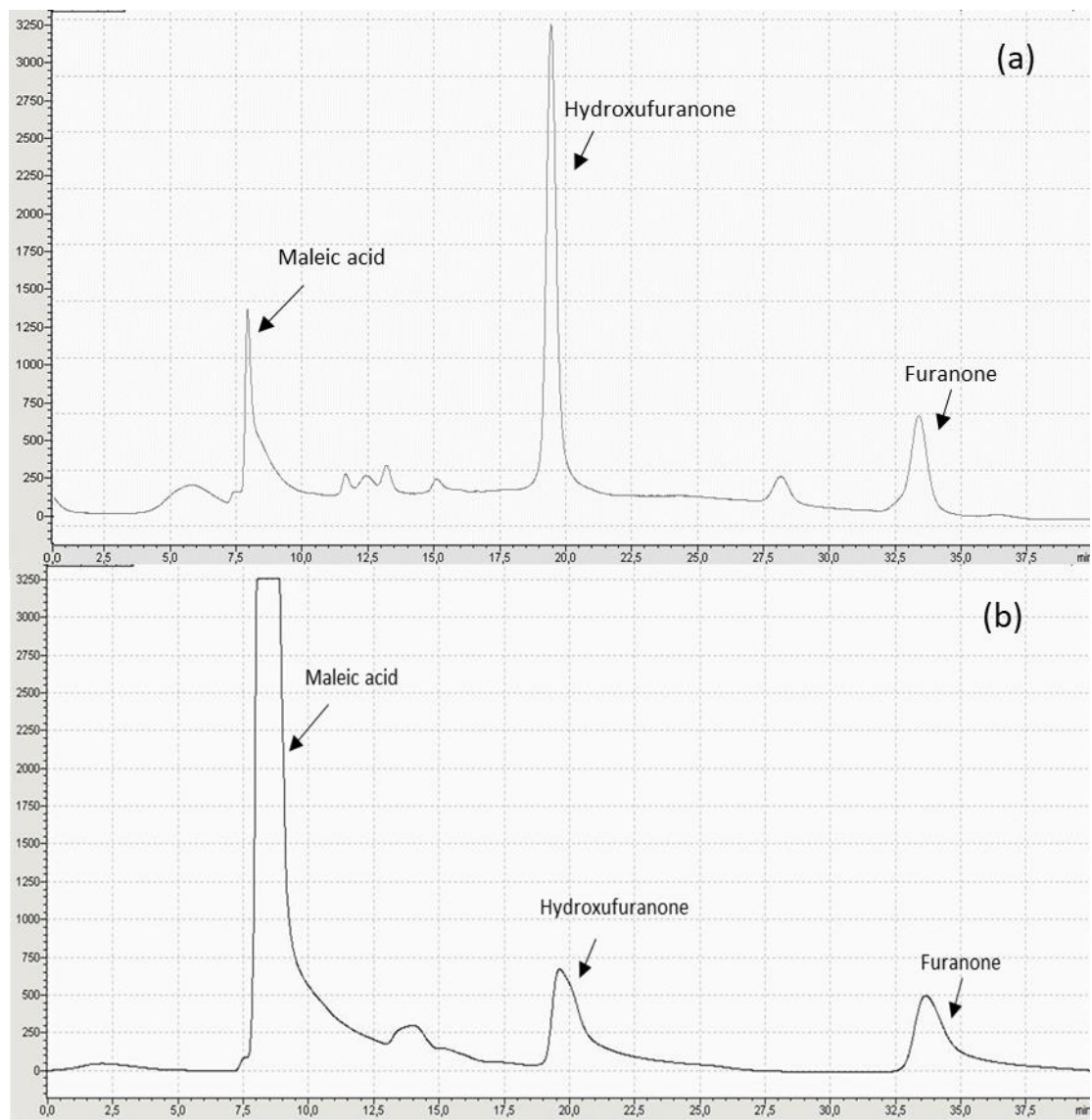


Figure A.15 - HPLC chromatogram before (a) and after (b) boiling at 565 kHz, Furfural 10 mL (0.12 mol); H₂O₂ 40 mL (1.7 mol), 2 h, 42 °C, 80 W.

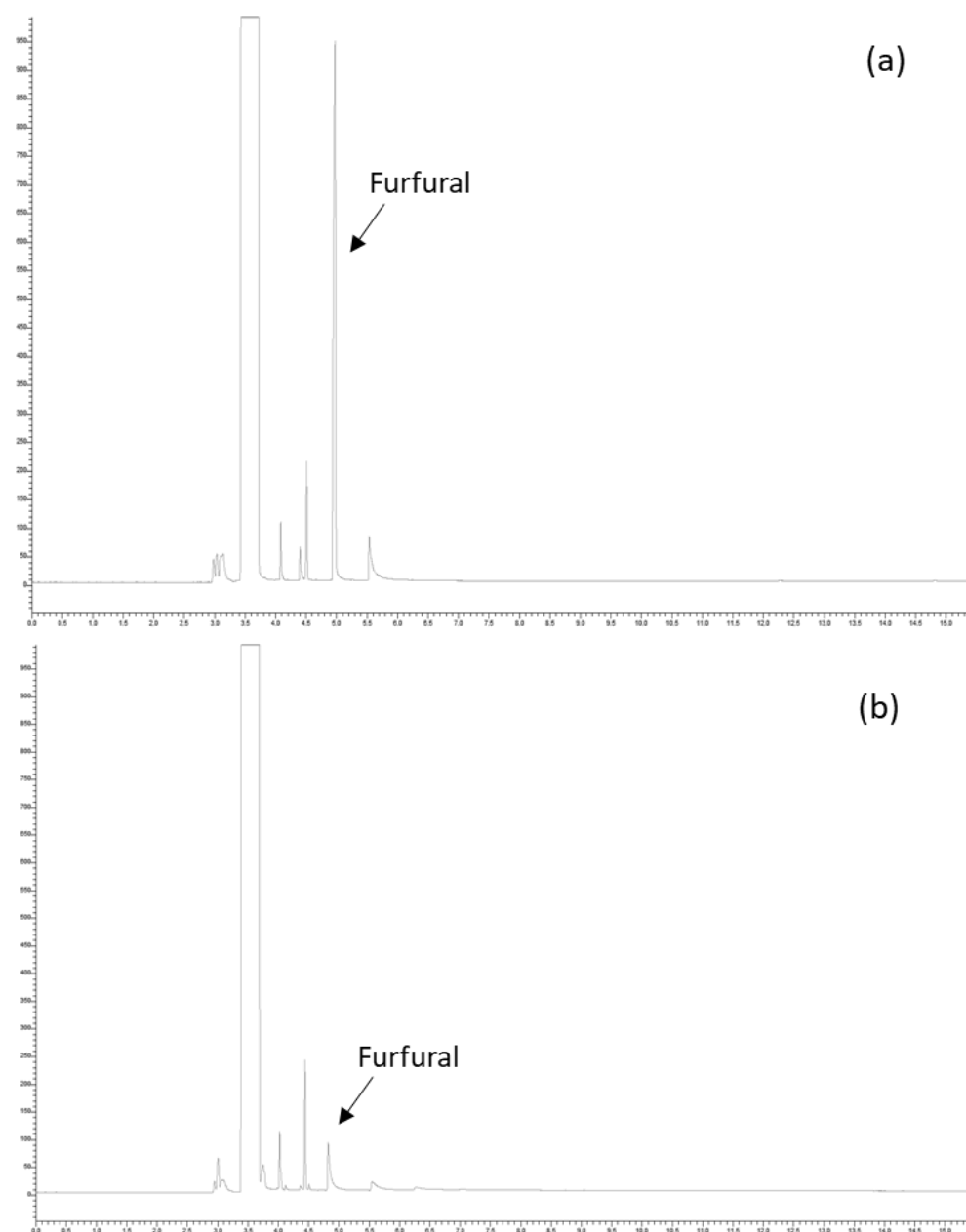
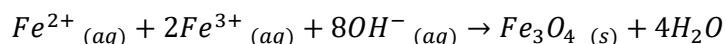


Figure A.16 - GC chromatogram before (a) and after (b) boiling at 565 kHz, Furfural 10 mL (0.12 mol); H₂O₂ 40 mL (1.7 mol), 2 h, 42 °C, 80 W.

Nanoparticles synthesis

Three samples of magnetite nanoparticles were prepared by alkaline co-precipitation. A mixing of iron ions in form of hydrated chloride salts were poured in alkaline medium, in the proportion of Fe^{3+}/Fe^{2+} of 2/1. Initially, 0,01 mol of $FeCl_2 \cdot 4H_2O$ were dissolved in 7,5 mL of HCl $1 \text{ mol} \cdot L^{-1}$ to prevent premature oxidation of Fe^{2+} to Fe^{3+} in aqueous solutions. 0.02 mol of $FeCl_3 \cdot 6H_2O$ were dissolved in 160 mL of water, and mixed with the ferrous solution through an ultrasound bath. Afterwards, the binary solution of Fe^{2+} and Fe^{3+} was added, with a burette of 100 mL, into a solution of $NaOH$ $2 \text{ mol} \cdot L^{-1}$ (84 mL). For 2 h, under constant stirring at 2000 rpm, the solution reacted at constant temperature ($35^\circ C$).

It is important to note that, when $NaOH$ was used, the binary solution of Fe^{2+} and Fe^{3+} was added over the base contained. The resulting black precipitate was isolated by a magnetic field and washed several times with distilled water, reaching a value of pH equal to 7. This process is characterized by the following chemical equation:



To produce nanoparticles of Fe_3O_4 by co-precipitation methodology there are two parameters to be considered in order to obtain nanoparticles with a uniform length (between 9 and 16 nm). The methodology used is the co-precipitation. The first one is to respect concentrations of Fe^{2+} and Fe^{3+} to a proportion 1:2. The second one is to follow the molar relations explained in the table below:

Table A.1 - Molar relations for the different reagents

Molar relations	
Fe^{3+}/Fe^{2+}	2
$NaOH/Fe_{total}$	5.50
H_2O/Fe_{total}	298.60
HCl/Fe^{2+}	0.75

The chemicals reagents used in this experiments were $FeCl_3 \cdot 6H_2O$, $FeCl_2 \cdot 4H_2O$, $NaOH$, distilled water and HCl . Normally when planning these experiments, it is better to fix one component and equilibrate the others with the molar relations (Fe^{2+} for example). If the Fe^{2+} is fixed to 1.5 g, then the other reagents, holding the molar relations, are as follow:

Table A. 2 - Weights and volumes of reagents fixing $\text{FeCl}_2 \cdot 4\text{H}_2\text{O}$ to 1.5 g

	Weight (g)	Volume (mL)	Mol
$\text{FeCl}_2 \cdot 4\text{H}_2\text{O}$	1.5	-	0.007
$\text{FeCl}_3 \cdot 6\text{H}_2\text{O}$	3.78	-	0.014
H_2O	-	112.86	6.27
HCl (1M)	-	5.25	0.00525
NaOH (2M)	-	58	0.11

To prepare the solution of Fe^{3+} , we weigh the powder of $\text{FeCl}_3 \cdot 6\text{H}_2\text{O}$ to follow the relation 1:2 of $\text{Fe}^{2+}/\text{Fe}^{3+}$. To do so, we place it on a beaker and we add water until the relation H_2O is fulfilled. Be aware of the water contained on the Fe^{2+} and Fe^{3+} powders. Homogenize the sample with an ultrasonic-bath for 5 min.

It is better to prepare the solution of Fe^{2+} the same day the reaction is going to take place, to avoid premature oxidation. We weigh the powder of $\text{FeCl}_2 \cdot 4\text{H}_2\text{O}$, and we placed it in a beaker and we add the necessary volume of HCl to reach the relation $\text{HCl}/\text{Fe}^{2+}$. The HCl used for these experiments was 1 M. Homogenize the sample with an ultrasonic-bath for 5 min. Once homogenized, the solutions $\text{Fe}^{3+}/\text{Fe}^{2+}$ should be mixed and stirred on an ultrasonic-bath to achieve the perfect molar relation $\text{Fe}^{3+}/\text{Fe}^{2+}$.

To prepare the solution of NaOH, we weigh the powder on a beaker and we mix it with water to obtain a 2 M concentration solution. Stirred it with a magnetic agitator to homogenize.

The equipment used in the experiments was the following:

- Thermal bath
- 250 mL reactor
- Mechanical stirrer
- Peristaltic pump

The thermal bath is used to maintain the temperature of 30 °C to allow the repeatability of the experiments.

To do so, the bath is connected to the thermal shell of the reactor through plastic pipes. A peristaltic pump is required to do the impulsion. The flow rate was set to 1.5 L/min.

To start the experiment, the bath was heated to 30 °C and the pump was set to 1.5 L/min. Wait 20 minutes to heat and stabilize the temperature inside the reactor. First, the NaOH solution was placed inside the reactor. Then the reactor was sealed and stirred for 1 minute.

Using another peristaltic bomb, at a speed of 400 mL/min the solution of $\text{Fe}^{2+}/\text{Fe}^{3+}$ was poured into the reactor. This procedure is relevant because the speed addition will give uniform diameters and less agglomerations.



Figure A.17 - The used reactor with thermal shell

After adding the ferrous solution, the mix is left for 2 hours with vigorous agitation. If the reaction is well done, the color of the solution inside will be black, indicating the magnetite is formed.

If the nanoparticles precipitate at the bottom of the reactor when the stirring stops, it indicates agglomeration and different diameters of nanoparticles. If the size is uniform, the particles will stay in suspension. The ferrofluid is transferred to a 1 L beaker.



Figure A.18 - The synthesis process

A specific volume of HCl 2.5 M must be added to the solution to neutralize it. This volume depends on the concentration of NaOH remaining in the solution. At this pH 7, MNP lose their surface charges, tend to aggregate themselves, become sensible to the magnetic field, and therefore are easy to be separated through a magnet.

In order to wash the nanoparticles, a magnetic separator was used for the separation of MNP and the solution. The solution inside the beaker was first neutralized with HCl 2.5 M and then divided into 50 mL falcon tubes. Afterwards, the tubes were placed inside the magnetic separator and left for 5 min. After checking that nanoparticles have been attracted by the magnet and the solution has become transparent, pour the solution and rinse it with water. Keep the pH at 7 and repeat the operation 4 times.

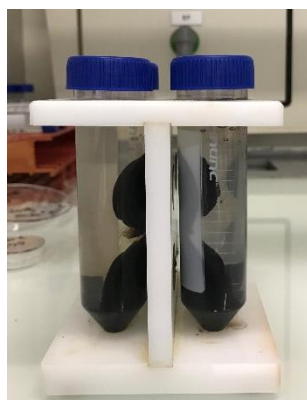


Figure A.19 - The magnetic separator

After washing down the samples, nanoparticles are scattered in water, adjusting the pH to 2 with a known volume of HCl. At the end, a black ferrofluid is obtained. In this state the nanoparticles are stable.

The concentration of Fe₃O₄ nanoparticles is done by spectroscopy UV. The equation used in this case is as follows:

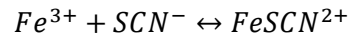
$$[Fe] = \frac{Abs_{480} \times k}{\varepsilon \times L} = \frac{Abs_{480} \times 300}{420 \times 1}$$

The UV is done at a wave length $\lambda=480$ nm, being Abs (absorbance) given by the UV spectroscopy, k (factor of dilution), ε (absorptivity) and L (length of the optical path containing the sample). In this case for Fe₃O₄ nanoparticles k oscillates between 300 and 500 depending on the volume used to wash the nanoparticles. ε equals to 420 L/mol·cm and L to 1 cm. To calculate the concentration of Fe₃O₄ do the conversion as it follows:

$$[Fe] \frac{\text{mol}}{L} \times \frac{1 \text{ mol } Fe_3O_4}{3 \text{ mol } Fe} \times \frac{231.53 \text{ g } Fe_3O_4}{1 \text{ mol } Fe_3O_4} = [Fe_3O_4] \frac{\text{g}}{L}$$

- Concentration determination

To know the exact concentration of nanoparticles, a full oxidation is required. The nanoparticles created of Fe_3O_4 are a mixture of Fe^{2+} and Fe^{3+} . In order to form the complex $FeSCN^{2+}$, and to obtain a solution, which has its band of absorbance at 475nm, all Fe^{2+} must be transformed in Fe^{3+} .



First, the concentration of the nanoparticles solution must be between 2 mM and 20 mM of Fe, which are the detection limits. To do so, we calculate the theoretical concentration of Fe and we dilute it till 15 mM are reached. For example, with 1.5 g of $FeCl_2 \cdot 4H_2O$ and 4.5 g of $FeCl_3 \cdot 6H_2O$ and a volume of 187.6 mL the theoretical concentration of Fe is 0.12 M.

$$1.5 \text{ g } FeCl_2 \cdot 4H_2O \times \frac{1 \text{ mol } FeCl_2 \cdot 4H_2O}{198.83 \text{ g } FeCl_2 \cdot 4H_2O} \times \frac{1 \text{ mol } Fe}{1 \text{ mol } FeCl_2 \cdot 4H_2O} = 0.0075 \text{ mol } Fe$$

$$4.5 \text{ g } FeCl_3 \cdot 6H_2O \times \frac{1 \text{ mol } FeCl_3 \cdot 6H_2O}{270.35 \text{ g } FeCl_3 \cdot 6H_2O} \times \frac{1 \text{ mol } Fe}{1 \text{ mol } FeCl_3 \cdot 6H_2O} = 0.015 \text{ mol } Fe$$

$$\frac{\text{mol } Fe}{\text{Total Volume}} = \frac{0.0075 \text{ mol } Fe + 0.015 \text{ mol } Fe}{0.1876 \text{ L}} = 0.12 \text{ mol/L } Fe$$

To place it to 15 mM, dilute 84 μL of nanoparticles solution in 1 mL of deionized water with a factor 12 dilution.

Once the solution is ready in a Falcon tube of 15 mL, place the next reagents:

1. 10 μL of nanoparticles solution 15 mM [Fe]
2. 100 μL of a H_2O_2 solution 20% m/m
3. 100 μL of a HNO_3 solution 7 M

Heat the falcon tube in a thermal bath for 2-3 hours to destroy the nanoparticles and oxidize Fe^{2+} to Fe^{3+} .

4. Add 1 mL of deionized water
5. 100 μL of a KSCN solution 2 M

Once the KSCN is introduced inside the falcon tube it is important to measure the absorbance immediately. Place the UV to 475 nm and measure the absorbance. The blanc used was water. With the following equation, the concentration of Fe can be found:

$$Abs_{475\text{ nm}} = 0.054 \times [Fe]_{on\text{ mM}} \times Dilution\ factor$$

For a direct measure of nanoparticles concentration, the wave length was 480 nm ($\lambda=480\text{ nm}$), the dilution factor was 1/300, ϵ was $420\text{ L}\cdot\text{mol}^{-1}\cdot\text{cm}^{-1}$ and L being 1 cm. With the following equation, the concentration was determined:

$$[Fe] = \frac{Abs \times Dilution\ factor}{\epsilon \times L}$$

By doing the calculation, we can obtain the concentrations of the three nanoparticles samples, and they are 0.096 M for the first one, 0.153 M for the second and 0.136 M for the third.

La biomasse fait partie des ressources renouvelables qui peuvent répondre durablement à nos besoins de production de carburants, de produits chimiques et de matériaux. En effet, la biomasse non comestible telle que la lignocellulose a attiré l'attention des chercheurs et des scientifiques au cours des dernières décennies en tant qu'alternative renouvelable.

Le furfural et le 5-hydroxyméthylfurfural (HMF), dérivés de la déshydratation des pentoses et des hexoses respectivement, sont produits à plusieurs millions de tonnes par an. Ces derniers composés sont donc des molécules plateformes et représentent un intérêt majeur dans le cadre du développement durable. Ce travail vise à explorer des méthodes nouvelles et vertes pour l'oxydation sélective du furfural et de HMF afin de produire des produits biosourcés à haute valeur ajoutée tels que le 2,5-diformylfurane (DFF), l'acide maléique et l'acide succinique.

Tout d'abord, un système alternatif d'oxydation de HMF a été présenté, sans l'utilisation de catalyseurs de métaux nobles, de hautes pressions et évitant la production de déchets toxiques. Dans ce contexte, l'oxydation à l'échelle du gramme de HMF conduit à la formation de DFF. Cette réaction a été catalysée par l'acide 2-iodobenzènesulfonique en présence d'Oxone®. Dans des conditions expérimentales optimisées, la conversion du HMF s'est avérée être de 100%, tandis que le rendement et la sélectivité du DFF étaient vers 90%.

Par la suite, nous avons démontré un processus sans catalyseur pour la synthèse à l'échelle du gramme de l'acide maléique à partir de furfural en utilisant des irradiations ultrasonores à hautes fréquences. Une sélectivité de 70% en acide maléique avec 92% de conversion du furfural a été obtenue sans aucun catalyseur dans des conditions douces en utilisant H₂O₂ comme oxydant.

Notre approche alternative permet l'utilisation de la biomasse au lieu du pétrole pour synthétiser l'acide maléique à partir du furfural dans un processus écologique et économe en énergie.

Enfin, un nouveau procédé catalytique est développé en utilisant des nanoparticules de magnétite, comme catalyseur métallique bon marché et non noble, et du peroxyde d'hydrogène pour l'oxydation du furfural en acide succinique. La conversion totale du furfural a été obtenue avec 67% de rendement en acide succinique dans des conditions douces.

Mots-clés : furfural, HMF, oxydation, catalyse non-métallique, acide maléique, DFF, acide succinique, nanoparticules, ultrason à haute fréquence.

Abstract

Biomass is one of the renewable and green resources that can sustainably meet our needs for the production of fuels, chemicals and materials. Indeed, nonedible biomass such as lignocellulose has attracted attention of researchers and scientists in the last decades as a renewable alternative.

Furfural and 5-hydroxymethylfurfural (HMF), derived from the dehydration of pentoses and hexoses respectively, are produced in multimillion ton-scale annually. The latter compounds are, therefore, platform molecules and represent a major interest in the context of sustainable development. This work aims to explore novel and green methods for the selective oxidation of furfural and HMF to produce high value-added bio-sourced products such as, 2,5-diformylfuran (DFF), maleic acid and succinic acid.

First, an alternative system of HMF oxidation was presented, without the use of noble metal catalysts, high pressures and avoiding the production of toxic wastes. In this context, the gram-scale oxidation HMF leads to the formation of DFF. This reaction was catalyzed by 2-iodobenzenesulfonic acid in the presence of Oxone[®]. Under optimized experimental conditions, the HMF conversion was found to be 100%, while the DFF yield and selectivity were almost 90%.

Subsequently, we demonstrated a catalyst-free process for the gram-scale synthesis of maleic acid from furfural using high frequency ultrasound irradiations. A 70% selectivity of maleic acid with 92% of furfural conversion were achieved without any catalyst under mild conditions using H₂O₂ as oxidant. Our alternative approach enables the use of biomass instead of petroleum to synthesize maleic acid from furfural in an eco-friendly and energy-efficient process.

At last, a novel catalytic process is developed using magnetite nanoparticles, as a cheap and non-noble metal catalyst, and hydrogen peroxide for the oxidation of furfural into succinic acid. Total conversion of furfural was achieved with 67% of succinic acid yield under mild conditions.

Keywords: furfural, HMF, oxidation, metal-free catalysis, maleic acid, DFF, succinic acid, nanoparticles, high frequency ultra-sound.

